Perceptual stability
during saccadic eye movements

Dissertation

**Zur Erlangung des Doktorgrades
der Naturwissenschaften
(Dr. rer. nat.)**

**dem Fachbereich Physik
der Philipps-Universität Marburg
vorgelegt von**

Steffen Klingenhöfer
aus Rotenburg/Fulda

Marburg/Lahn 2012

Contents

Summary

Humans and other primates perform multiple fast eye movements per second in order to redirect gaze within the visual field. These so called saccades challenge visual perception: During the movement phases the projection of the outside world sweeps rapidly across the photoreceptors altering the retinal positions of objects that are otherwise stable in the environment. Despite this ever-changing sensory input, the brain creates the percept of a continuous, stable visual world. Currently, it is assumed that this perceptual stability is achieved by the synergistic interplay of multiple mechanisms, for example, a reduction of the sensitivity of the visual system around the time of the eye movement ('saccadic suppression') as well as transient reorganizations in the neuronal representations of space ('remapping'). This thesis comprises six studies on trans-saccadic perceptual stability.

It is well known that perceptual stability breaks down for the fraction of a second surrounding the time of a saccade ('perisaccadically') when confronted under laboratory conditions with brief stimuli (∼10 ms duration). When observers are asked to localize such stimuli in the fronto-parallel plane these stimuli are systematically mislocalized. Depending on certain experimental parameters the characteristics of the mislocalization patterns vary between two variants called 'perisaccadic shift' (perceived positions are uniformly shifted in the same direction) and 'perisaccadic compression' (perceived positions gather around the position of the saccade target). In two psychophysical studies we have investigated whether perisaccadic localization errors are confined to localization of visual stimuli in the fronto-parallel plane. In the first study, we demonstrated for the first time systematic errors for perisaccadic depth judgements. The results of the second study showed that localization of auditory targets was only mildly influenced by saccadic eye-movements. In particular, we did not observe the spatio-temporal pattern characteristic for the visual effects. This lack of cross-modal transfer argues against the hypothesis that the brain makes use of a universal modality-independent representation of space for localization purposes. Taken together, these studies show that perisaccadic mislocalization is a phenomenon that occurs when visual but not auditory spatial information has to be integrated with fast-changing eye-position signals.

In a modeling study we demonstrated that perisaccadic mislocalization of briefly flashed visual stimuli can arise because of an erroneous representation of the eye-position signal during the saccade. Remarkably, our model nevertheless maintains perceptual stability for stimuli that are persistently present in the environment; a feature that earlier theoretical accounts had failed to produce.

In the next step we experimentally disrupted the stability of the outside world

using a so called saccade adaptation paradigm. We asked human observers to perform visually guided saccades. During the eye movement we systematically displaced the saccade target to a new position. As expected from earlier studies, the oculomotor system adapted to this situation. Saccade endpoints gradually approached the final, i.e. the displaced, position of the saccade target. During this paradigm we interspersed some trials in which we psychophysically measured the ability of the observers to detect displacements of the saccade target to random positions. We found that during these trials the point of subjective equality of the psychometric curves, i.e. the target position at which the observers likely reported a displacement to the left or to the right at chance level, shifted according to the change in saccade endpoints during saccade adaptation. In other words, perception adapted according to the change in oculomotor behavior. In one condition, when the saccade target was displaced against the direction of the saccade (backward adaptation) and when it was visible immediately after saccade offset, we observed an additional broadening of the psychometric curve. Perceptual stability, in the sense of an insensitivity to detect target displacements, had increased near the position of the target step. This result suggested a change in the neural representation of space near the saccade target during saccade adaptation.

To test this hypothesis directly, we investigated the cortical representation of visual space in area V4 of the macaque monkey by mapping neuronal receptive fields across saccadic eye movements. In line with our psychophysical results we observed deformations in the receptive fields that postsaccadically fell near the position of the adaptation step: the peaks of the receptive fields seemed slightly broadened and were shifted against the direction of the adaptation. Although the shift in receptive field position was small and compensated only for about 30% to 45% of the adaptation induced change in saccade amplitude, it was consistently observable during the complete adaptation process. In the same series of experiments we tested the hypothesis, recently put forward by Zirnsak et al. (Vision Research, 2011), that the perceptual perisaccadic compression effect arises due to a presaccadic reorganization of the receptive field structure in V4. We did not find any evidence for such remapping processes. The measured receptive fields were stable in eye-centered coordinates and did not show any dynamic changes.

Prior to saccade onset this was also true for the amplitude of the stimulus driven neuronal activity; that is, we did not find any evidence for saccadic suppression in area V4. Instead we observed a strong increase in activity that built up after the eye movement. Similar postsaccadic enhancement effects have been observed in multiple areas of the visual system. We demonstrated for the first time that this effect is related to the neuronal response characteristics following stimulation onset. When exposed to continuous stimulation many neurons de-

crease their activity to a lower level compared to their initial onset response, a phenomenon called neuronal adaptation. We could show that the characteristic postsaccadic increase in activity reflects a release from neuronal adaptation. Interestingly, the transient component of the onset response was removed in the postsaccadic activity. This mechanism might contribute to perceptual stability by distinguishing stimuli that are newly presented from those that are brought into the receptive field by a saccade.

Taken together, our results are in line with the notion that transsaccadic perceptual stability is supported by the synergistic interaction of multiple processes that are capable of covering transient distortions of the sensory input to create the percept of a stable visual world.

Zusammenfassung

Menschen und andere Primaten führen pro Sekunde mehrere schnelle Augenbewegungen aus, um ihren Blick im visuellen Feld neu auszurichten. Diese schnellen Augenbewegungen, Sakkaden genannt, stellen eine Herausforderung für die Wahrnehmung dar. Während Sakkaden wird das Bild der Umgebung schnell über die Photorezeptoren bewegt, wodurch sich permanente Positionsänderungen auf der Retina ergeben. Trotz dieser sich ständig ändernden sensorischen Stimulation gelingt es dem Gehirn, den Eindruck einer stabilen Umwelt zu erzeugen. Diese Doktorarbeit umfasst sechs Studien, die sich mit dem Phänomen der perzeptuellen Stabilität während Sakkaden befassen.

Aus früheren Studien ist bekannt, dass die perzeptuelle Stabilität kurzfristig gestört ist, wenn unter Laborbedingungen unmittelbar vor, während oder kurz nach einer Sakkade ("perisakkadisch") visuelle Stimuli von sehr kurzer Dauer (∼10 ms) eingeblendet werden. Versuchpersonen, die solche Stimuli lokalisieren sollen, unterliegen systematischen Fehlwahrnehmungen bezüglich des Ortes der Stimulation. In Abhängigkeit von bestimmten experimentellen Parametern zeigen sich zwei Ausprägungen dieses Effekts: "Perisakkadische Verschiebung" ist dadurch gekennzeichnet, dass die Stimuli unabhängig von ihrer Position alle gleichmäßig verschoben im Raum wahrgenommen werden; bei "perisakkadischer Kompression" werden alle Stimuli um den Endpunkt der Sakkade herum wahrgenommen. In zwei Studien wurde in dieser Arbeit untersucht, ob diese bekannten Fehlwahrnehmungen auf die Lokalisation visueller Stimuli in der fronto-parallelen Ebene beschränkt sind. In einer dieser Studien konnte gezeigt werden, dass auch die Lokalisation in der Tiefenebene charakteristischen Fehlwahrnehmungen unterliegt. In der zweiten Studie zeigte sich, dass die Ortswahrnehmung von auditorischen Stimuli nur in geringerem Maße durch die Augenbewegung beeinflusst wird. Insbesondere traten die für visuelle Stimuli charakteristischen raum-zeitlichen Fehllokalisationsmuster nicht bei auditorischer Stimulation auf. Dieser Befund spricht gegen die Hypothese, dass das Gehirn während Lokalisationsaufgaben auf eine modalitäten-unabhängige, übergeordnete Repräsentation des Raumes zurückgreift. Fehlwahrnehmungen des Ortes treten folglich immer nur dann auf, wenn visuelle Information mit Signalen bezüglich der Augenposition verrechnet werden muss. In einer Modellierungsstudie in dieser Arbeit konnte gezeigt werden, dass perisakkadische Misslokalisationen durch ein fehlerbehaftetes Augenpositionssignal entstehen können. Bemerkenswerterweise zeigte sich in dem Modell zwar eine Fehllokalisation kurzzeitig präsentierter Reize, für dauerhafte Stimuli konnte jedoch perisakkadische räumliche Stabilität erzielt werden. Frühere Modelle beinhalteten diese Eigenschaft nicht.

Im nächsten Schritt dieser Arbeit wurde die räumliche Stabilität der visuellen Umgebung mittels eines sogenannten Sakkaden-Adaptations-Paradigmas aufgehoben. Versuchspersonen führten Sakkaden auf ein visuelles Ziel aus. Während der Bewegungsphase wurde das Sakkadenziel systematisch von seinem ursprünglichen Ort weg versetzt. Wie aufgrund von früheren Studien zu erwarten war, passte sich das okulomotorische System dieser Bedingung an, indem die Amplitude der Sakkaden derart verändert wurde, dass die Augenbewegung immer mehr zu dem veränderten Zielort hin durchgeführt wurde. Während dieses Ablaufes wurde mit psychphysikalischen Methoden die Fähigkeit der Versuchspersonen eine Verschiebung des Sakkadenziels auf eine zufällige Position hin zu detektieren abgefragt. Entsprechend der Änderung der Sakkadenamplituden zeigte sich eine Verschiebung des subjektiven Äquivalenzpunktes (engl: "point of subjective equality", jene Position bei der die Wahrscheinlichkeit einen Versatz nach links oder rechts zu detektieren bei jeweils 50% liegt). In einer Adaptationsbedingung, in der das Sakkadenziel entgegen der Richtung der ursprünglichen Sakkade versetzt wurde, zeigte sich zusätzlich eine Verringerung der Steigung der gemessenen psychometrischen Funktion. In anderen Worten, die räumliche Stabilität bezüglich der Detektion des Versatzes des Sakkadenziels erhöhte sich.

Dieses Ergebnis legte die Vermutung nahe, dass durch Sakkadenadaptation die neuronale Repräsentation des Raumes in der Nähe des Sakkadenziels geändert wird. Wir untersuchten diese Hypothese indem wir die Struktur der sogenannten Rezeptiven Felder im visuellen Areal V4 des Makkaken kartierten. Als Rezeptive Felder werden jene Bereiche des Sehfeldes bezeichnet, innerhalb welcher man durch Stimulation eine Änderung der neuronalen Aktivität auslösen kann. Entsprechend der zugrunde liegenden Hypothese beobachteten wir eine Deformation jener Rezeptiver Felder, welche nach einer Sakkade in der Nähe des Ziels gelegen waren. Die Position des Raumes, an der die stärkste neuronale Aktivierung erzeugt werden konnte, verschob sich leicht in Gegenrichtung des Adaptationssschrittes; zudem schienen die Rezeptiven Felder leicht verbreitert zu sein. Die Verschiebung der Rezeptiven Felder war relativ gering (sie kompensierte zu ungefähr 30% bis 45% von der Änderung der Sakkadenamplitude), jedoch war sie konsistent während des gesamten Adaptationsverlaufs zu erkennen. In entsprechenden neurophysiologischen Experimenten wurde zudem die von Zirnsak et al. (Vision Research, 2011) vorgeschlagene Hypothese untersucht, dass perisakkadische Kompression anhand von Remapping-Mechanismen in V4 zu erklären sei. Wir fanden keine Belege für solche Remapping-Prozesse in V4; die kartierten Rezeptiven Felder zeigten perisakkadisch keine Änderung ihrer räumlichen Eigenschaften.

Vor Sakkadenbeginn galt dies auch für die Amplituden der durch Stimulation ausgelösten neuronalen Antworten, das heißt wir fanden keine Belege für sakkadis-

che Suppression in V4. Es zeigte sich jedoch nach dem Ende einer Sakkade eine starke Erhöhung der neuronalen Aktivität. Ähnliche Antwortmuster wurden bereits in vielen anderen Arealen des visuellen Systems beobachtet. Wir kamen zum ersten Mal dem Ursprung dieses Effekts auf die Spur. Er ist verknüpft mit dem charakteristischen Antwortverhalten nach der Reizpräsentation: Nach einem initialen transienten Anstieg der neuronalen Aktivität reduzieren viele Neurone ihre Aktivität. Dieser Effekt wird neuronale Adaptation genannt. Wir konnten zeigen, dass die Erhöhung der postsakkadischen Aktivität durch eine Aufhebung der neuronalen Adaptation zu erklären ist. Interessanterweise war allerdings die initiale transiente Phase der Reizantwort in der postsakkadischen Aktivität unterdrückt. Dies könnte ein Mechanismus sein, der zur transsakkadischen perzeptuellen Stabilität beiträgt, indem er Reize, die im Rezeptiven Feld neu eingeblendet werden, von solchen unterscheidet, die durch eine Sakkade in das Rezeptive Feld gebracht werden.

Zusammenfassend kann gesagt werden, dass unsere Ergebnisse im Einklang stehen mit der Ansicht, dass mehrere Prozesse gemeinsam für die Wahrnehmung einer stabilen Umwelt sorgen. So können kurzzeitige Störungen des sensorischen Signals abgefangen werden.

1 Introduction

During our waking hours, we perform about three to five saccadic eye movements per second - we move our eyes more often than our hearts beat. Each of these fast movements challenges visual perception in a number of ways. It is the topic of this thesis, how the brain copes with these challenges and creates the percept of a continuous, stable visual world.

The purpose of saccadic eye movements, often just called saccades, is to redirect the center of gaze to different objects or locations within the visual field. Vision in a natural environment is to a large part made up of continual alteration between brief periods during which eye position remains relatively stable, so called fixation periods, and saccades. This behavior was nicely demonstrated in an early study published in 1967 by Yarbus, following the advent of eye tracking technology that allowed a precise measurement of gaze position. A classical result of this study, showing the fixation positions of a human observer while looking at a painting, is reproduced in figure 1A. Based on this illustration one might realize that the way visual information is gathered by the eyes is fundamentally different from our percept of the visual world. In our mind, the image of a stable visual environment, detailed all over the field of view, is formed. Due to the foveal structure of the retina, however, the eyes are only able to deliver high acuity vision in a region limited to a few degrees of visual angle. In figure 1B this is illustrated by a blurring of the image outside of the foveal vision. In addition, the image of the external world that is projected onto the retina sweeps over the photoreceptors at high speeds during every saccade. The sensory input thus consists of a stream of visual snapshots, acquired during fixation periods, interspersed with brief motion stimuli, produced by the eye movements (figure 1C). The problem of perceptual stability across saccades deals with the question how the visual system, in cooperation with the oculomotor system, converts the stream of sensory input to the percept of a spatially congruent, continuous visual world.

Although closely related, the subject can be conceptually divided into two subdivisions. One is concerned with the question why the motion stimulus produced by the eye movement, escapes perception. This effect is usually referred to as 'saccadic omission'; the term summarizes two mechanisms studied in this
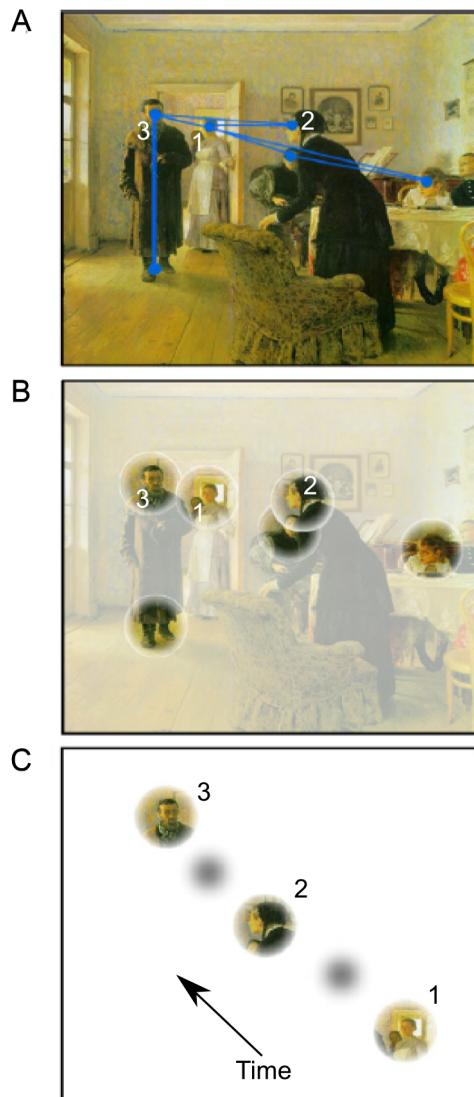
Figure 1: Illustration of eye movement patterns during natural viewing and the problem of perceptual stability across saccades. A) Vision in a natural environment is characterized by continual alternation of fixation periods (dots) and saccadic eye movements (lines), illustrated by the example of a human observer looking at a painting. Numbers mark three consecutive fixation positions. B) Due to the foveal structure of the retina, visual acuity declines as the distance from the fovea increases (illustrated by the shading). C) In contrast to our percept of a detail rich, stable visual environment the input to the visual system consists of a stream of multiple 'snapshots', obtained during the fixation periods, that are interspersed with abrupt motion stimuli generated during the eye movement (illustrated by the grey patches). Modified after (Wurtz, 2008), based on (Yarbus, 1967).

context, 'saccadic suppression' and 'visual masking' caused by the saccade. The second aspect of transsaccadic perceptual stability deals with the spatial problem and is usually referred to as spatial or saccadic 'updating': The brain has to keep track of eye positions across different fixation periods. Directed interactions with the physical world, like pointing at or grasping an object is only possible if the position of the object on the retina is combined with information about the direction of the eye in the orbit. One theory on how perceptual stability is established postulated that eye position information might be used in the brain to create a world centered representation of the visual environment (cf. section 1.4).

The following sections give a concise introduction into the general field of transsaccadic perceptual stability. More specific aspects can be found in the in-

troductory sections of the respective studies in chapter 2.

1.1 Saccadic eye movements

General characteristics

Due to the foveal structure of their retinas, humans and other primates have to redirect gaze to different regions within a visual scene to achieve high resolution vision across a large part of the visual scenery. Under natural viewing condition, such changes in the direction of gaze occur at a rate of about three to five times per second - more often than our heart beats (see e.g. Mazer and Gallant, 2003). During so called fixation periods, typically only a few hundred milliseconds in duration, the eye position remains relatively stable; then, a fast saccadic eye movement, often just referred to as 'saccade', redirects gaze so that a different part of the visual scene is brought to the fovea. Saccade amplitudes (i.e. the rotation angles of the eyes) can reach values of more than $80°$; in everyday life, however, the amplitude distribution is skewed towards values smaller than $15°$ (Carpenter, 1988). Figure 2A illustrates the movement trajectory of a saccade in a typical paradigm used in the laboratory: A fixation target is displaced by $10°$; after a certain reaction time, also called the latency period, the eyes start to move and, after about 40 ms, the center of gaze is brought to the fixation target again. A consequence of the short movement duration of saccades is that their trajectories have to be programmed in advance (ballistic movement); the neuronal latencies of any feedback signal that could be used to adjust the trajectory during the actual movement would be too long. The movement trajectories of saccades are rather stereotyped, i.e. saccades of similar amplitude show an approximately similar velocity profile. Saccades of different amplitude are characterized by an approximately linear relationship that holds between saccade amplitude and duration as well as between saccade amplitude and peak velocity (the 'saccadic main sequence', Bahill et al., 1975).

Saccade adaptation

The saccadic system features a remarkable plasticity that guarantees movement accuracy despite of changes in oculomotor conditions such as fatigue, injury, or growth. When saccades consistently miss their targets, the saccadic gain (saccade amplitude relative to target distance) is gradually adjusted. In the laboratory, this mechanism, usually referred to as saccade adaptation, is typically studied by slightly displacing the saccade target while the eyes are moving (McLaughlin, 1967,
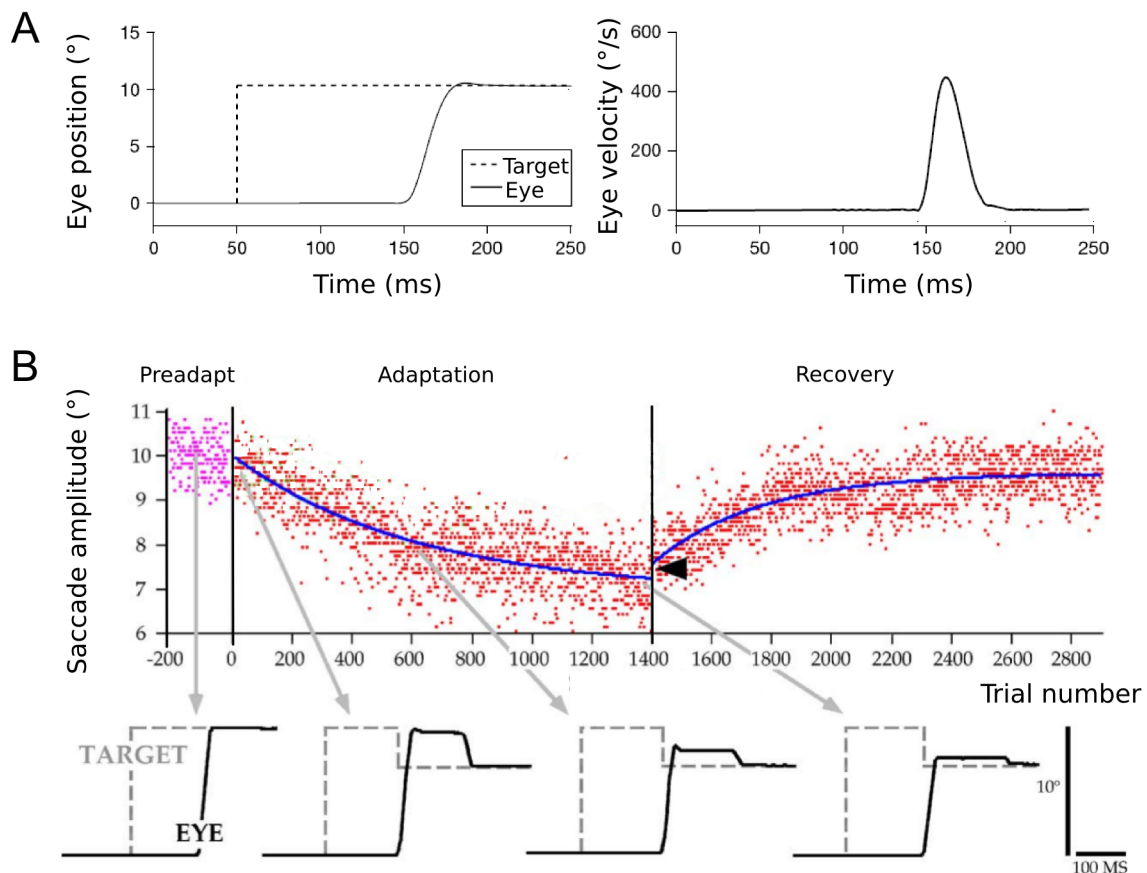
Figure 2: **Examples of saccade and saccade adaptation experiments.** A) Eye and target position as a function of time in a visually guided saccade paradigm (left); the corresponding eye velocity is shown on the right. Typical durations and peak velocities of 10° saccades are 40 ms and 400° /s, respectively. Saccade latencies strongly depend on task difficulty as well as on other factors and range from approximately 80 ms to 300 ms. B) Saccade endpoints (top panels) and single trial examples (bottom panels) during backward saccade adaptation. The initial displacement of the saccade target was always 10° . Prior to adaptation, saccade amplitudes scattered around this value (magenta). In the adaptation phase, the saccade target was stepped backward by 3.3° during the eye movement (red). This led to a gradual reduction in saccade amplitude. Data were obtained from a monkey; human subjects show considerably faster adaptation (within several tens of trials). Modified after (Catz and Thier, 2007, A) and (Hopp and Fuchs, 2004, B).

Fig. 2B, lower panels). If the displacement of the saccade target is smaller than about 30% of the amplitude of the saccade, the step will not come to awareness. The oculomotor system, however, will detect a decalibration and adjust saccade gain accordingly. During the first trials of this paradigm, saccade endpoints will fall close to the initial position of the saccade target. However, there is no target at this position anymore, and a small corrective saccade towards the new target

4

position has to be conducted. If this pattern is repeated over and over again, saccade gain will be gradually adjusted in such a way that the first saccade will land closer and closer to the new target position, although the saccade target is initially always presented at the same original position. Human subjects, typically adapt within a couple of tens of trials; then the gain change reaches a plateau level often slightly smaller than the amplitude of the target step (e.g. 20% target steps might lead to 15% adaptation). For yet unknown reasons, monkeys show similar adaptation courses, but on a timescale that is by a factor of 10 larger than in humans (i.e. adaptation takes a couple of hundreds of trials, Fig. 2B). Adaptation can be elicited in different directions relative to the initial saccade vector: A target step in the same direction will lead to an increase in saccade amplitude, called forward or outward adaptation; target steps in the opposite direction will lead to a decrease in saccade amplitude (backward or inward adaptation). In addition to the described adaptation effect that builds up rather quickly, another form of adaptation that acts on a longer timescale has been described (long-term adaptation, Robinson et al., 2006).

Since McLaughlin has established the adaptation paradigm in the laboratory, many experiments have been conducted on the characteristics of saccade adaptation. A comprehensive review of the literature is given by Hopp and Fuchs (2004).

1.2 Neuroanatomical structures related to saccades and perisaccadic perception

Saccadic circuitry

Saccades are controlled by a distributed network of brain areas that interact and complement each other at multiple levels (Fig. 3). Eye movements are controlled by the synergistic action of three pairs of extraocular muscles. The signals that control these muscles are generated in various local groups of neurons in the brainstem, termed collectively the brainstem burst generator (BBG). This structure receives input from the cerebellum (CER), the frontal eye fields (FEF), and the superior colliculus (SC). The SC is a multilayered structure that contains aligned topographic maps of visual and motor space. Neurons in the intermediate and deeper layers of the SC discharge at their maximum frequency for saccades of a certain vector and increasingly less the more a vector deviates from the preferred one ('movement fields'). The SC receives direct input from the retina as well as from other subcortical and cortical areas including the FEF and the lateral intraparietal area (LIP, sometimes also called the parietal eye field). Similar to
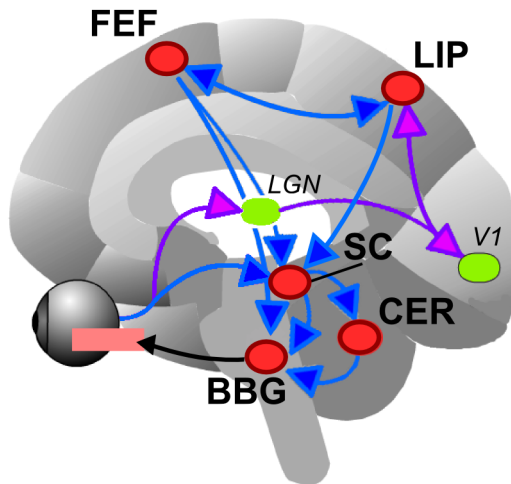
Figure 3: Highly schematic circuit of neuronal structures involved in saccade generation. Visual information about target location enters the superior colliculus (SC) either through a direct projection from the retina or via descending pathways from the frontal eye field (FEF) or the lateral intraparietal area (LIP). Visual information ascents to LIP or FEF, for example, via the lateral geniculate nucleus (LGN), the primary visual cortex (V1), and further processing areas (not shown). The brainstem burst generator (BBG) controls the extra-ocular muscles and receives input from the cerebellum (CER), the SC, and the FEF. Modified after (Vilis, 2012).

the SC, areas FEF and LIP contain neurons that respond to visual stimulation as well as neurons that carry eye movement related signals; electrical stimulation in these regions can elicit saccades. FEF and LIP have strong reciprocal connections; both areas are also involved in spatial attention and saccades towards remembered locations ('memory guided saccades').

The site of saccade adaptation

As mentioned above, the saccadic system can rapidly adapt the amplitude of saccades to retain movement accuracy. Behavioral experiments suggest this adaptation takes place at a level where saccades are still represented as a vector (Phillips et al., 1997; Wallman and Fuchs, 1998); this excludes the BBG as a site of adaptation as its responses correspond to the horizontal and vertical vector components. Melis and van Gisbergen (1996) elicited saccades by electrical stimulation of the SC. By presenting, and perisaccadically displacing, a visual target at the endpoint of the electrically evoked saccades Melis and van Gisbergen could elicit saccade adaptation. This suggests that adaptation takes place at or downstream of the SC. (Frens and Opstal, 1997) did not observe a change in the activity of movement related neurons in the SC during saccade adaptation; they concluded the adaptation site must be downstream of the SC. Although the result of the experiments in the SC are still disputed (Hopp and Fuchs, 2004), there is a general agreement that the cerebellum plays a vital role in the generation and maintenance of accurate saccades. Human patients with cerebellar lesions show saccadic dysmetria that does not resolve with time (Zee et al., 1976). The same holds true for lesions in parts of the monkey cerebellum (Optican and Robinson, 1980;

Figure 4: Structures of the monkey brain potentially contributing to perisaccadic perceptual stability. Approximate anatomical locations of cortical areas are marked on the illustration of a slightly inflated brain of the macaque monkey (adpted after Sugrue et al., 2005. Visually driven neuronal activity is primarily conveyed to the primary visual cortex (V1) via the lateral geniculate nucleus (LGN) along two anatomically and functionally different subcortical pathways (magno- and parvocellular pathway). Following V1, a dorsal processing stream including, amongst others, areas MT, MST, LIP and a ventral stream including area V4 can be distinguished. The frontal eye fields (FEF) are included in the network via strong fronto-parietal connections.
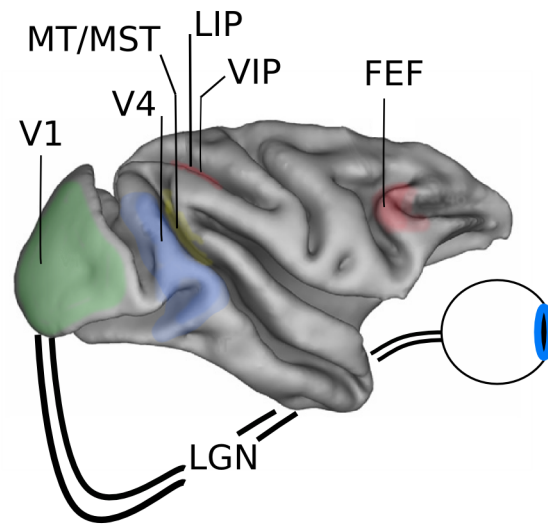
Robinson et al., 2002). In addition, signals have been identified in the cerebellum that seem suitable to drive saccade adaptation (Catz et al., 2005; Fuchs et al., 1993; Kojima et al., 2010).

The visual system

The visual system is formed by a distributed network of multiple structures that are largely interconnected. Characteristic for this network is, on the one hand, a strong parallel processing scheme, on the other hand, a processing hierarchy: Structures of the early visual system code simple features (e.g. oriented edges); higher areas represent complex features with increasing invariance (e.g. faces independent of viewing angle) and integrate signals from different senses.

Fibers from the retina run via the lateral geniculate nucleus (LGN) to the primary visual cortex (V1)(Fig.4). An important organizational principle of this early visual pathway is an anatomical and functional separation in two processing streams, called magno- and parvocellular pathway (M and P pathway). In contrast to neurons of the M pathway, those in the P pathway are sensitive to color but less sensitive to luminance contrast. In addition, the pathways differ in their preferences concerning stimulation of different spatio-temporal frequency (neurons in the M pathway respond stronger to higher temporal and lower spatial frequencies); there is, however, an overlap in the range covered by both pathways (see e.g. Merigan and Maunsell, 1993, for a review). From V1, also called striate cortex, signals are relayed through adjacent areas ('extrastriate areas') along the so called dorsal and ventral streams to the parietal and temporal lobes, re-
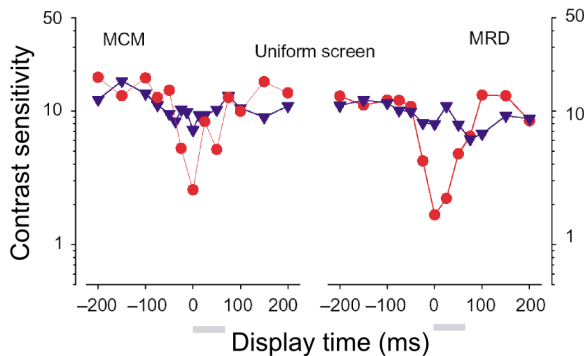
Figure 5: Time course of saccadic suppression. Diamond et al. (2000) measured the time course of the sensitivity to detect brief (8 ms) stimuli presented on an unstructured background around the onset of a saccades (red). Data of two subjects are presented, gray bars indicate saccade duration. When saccades were simulated using a rotating mirror no effect could be observed in the same condition (blue), suggesting saccadic suppression is an active process. Modified after (Diamond et al., 2000).

spectively (Ungerleider and Mishkin, 1982). The dorsal stream includes, amongst others, motion processing areas MT (middle temporal) and MST (medial superior temporal), eye-movement related area LIP, and motion processing and multisensory area VIP (ventral intraparietal). A key area of the ventral stream, involved in form and object representation, is visual area V4. This area is strongly interconnected with many cortical areas including, for example, extrastriate areas, inferior temporal cortex (IT), areas MT, MST, LIP, VIP of the dorsal stream and frontal area FEF (Ungerleider et al., 2008). The functional role of V4 is still debated; recently, it has been suggested to be the extraction of visual features either via figure ground segregation or via attentional feature selection(Roe et al., 2012).

1.3 Perisaccadic perception

Saccadic omission

The question of why we do not perceive the retinal motion caused by saccades has already been posed and investigated over 100 years ago (Dodge, 1900; Holt, 1903). Unlike it was proposed at that time, it is today widely accepted that the visual system is not completely insensitive to stimulation during saccades. Currently, it is assumed that the phenomenon, often referred to as 'saccadic omission', relies mainly on two distinct processes: saccadic suppression, considered to be an active process (i.e. bound the actual motor act), and visual masking, a passive mechanism that can be elicited during fixation by simulating the visual stimulation caused by the eye movement.

The term 'saccadic suppression' itself comprises a number of effects (e.g. saccadic suppression of displacement (Bridgeman et al., 1975), or saccadic suppression of motion perception (Burr et al., 1982)); usually, it refers to a reduction in

the sensitivity to detect transient stimuli that are presented at the time of saccades. Diamond et al. (2000) investigated the sensitivity to detect briefly flashed stimuli (8 ms) as a function of the stimulus presentation time relative to the onset of a saccade (Fig.5). Diamond et al. found that the sensitivity to detect the stimuli started to decrease already 50 ms before the eyes started to move, was minimal at movement onset, and recovered to normal briefly after movement offset. As the obtained sensitivity curves were different for real and simulated saccades (realized by a mirror rotating with a saccadic velocity profile), (Diamond et al., 2000) postulated the existence of an active suppression mechanism. Burr et al. (1994) showed that saccadic suppression is confined to stimuli of certain features: Suppression only affects stimuli containing luminance contrast of low spatial frequencies; equiluminant stimuli (i.e. those modulated only in color, e.g. red-green) and stimuli of high spatial frequency are not actively suppressed. The similarity of these features to the known characteristics of the magno- and parvocellular pathways (cf. section 1.2) made Burr et al. suggest the site of saccadic suppression might be located in these early structures. Later reports have challenged this view (Chahine and Krekelberg, 2009; Watson and Krekelberg, 2009).

Visual masking is a phenomenon not confined to saccades: When a brief stimulus, called the target, is presented shortly before or after the mask, i.e. a second stimulus that is in certain feature (e.g. brightness, contrast) stronger than the first stimulus, both stimuli interact, and the target stimulus might not be detected at all. The case in which the target precedes the mask is called 'forward' masking, the other case 'backward' masking. The blurred image caused by saccades in a well lit, feature rich environment is a weak stimulus in comparison to the pre- and postsaccadic scene and might therefore be 'overwritten' by forward and backward masking. Campbell and Wurtz (1978) demonstrated this by illuminating the laboratory only during the movement phase of a saccade; in this case retinal motion is perceived. If the illumination phase extends to times prior to or after the movement phase, a stable image is perceived. In line with this, Diamond et al. (2000) found a decrease in flash detection sensitivity when saccades were simulated by moving a structured instead of a uniform background.

Perisaccadic localization

A popular experimental 'tool' to study the spatial aspects of perisaccadic perception are localization paradigms. To localize a target in external space, it is not sufficient to know the coordinates of the target's image on the retina, the 'eye-centered', or 'retinal' coordinates. Assuming the head is fixed relative to external space, as is often the case in the laboratory, the position of gaze in the external
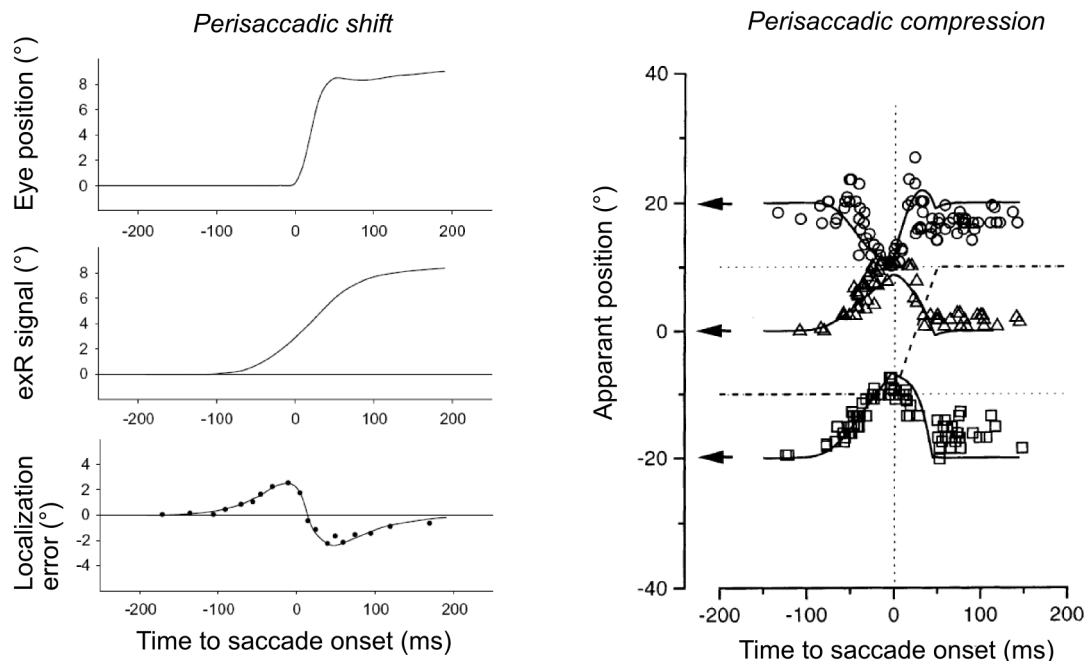
Figure 6: Examples of perisaccadic mislocalization. Briefly presented stimuli are mislocalized perisaccadically (i.e. briefly before, during or after the saccade) Left). When experiments are conducted in a dark environment without visual references, mislocalization shows a characteristic time course as a function of stimulus presentation time relative to saccade onset, but is independent of stimulus position ('perisaccadic shift', lower panel). It has been suggested that this mislocalization might be due to an erroneous neural representation of eye position, called an extra retinal signal (exR, middle panel, Dassonville et al., 1992; Honda, 1991. Modified after (Honda, 1991, left). Right) When experiments are conducted in a lighted environment, perceived perisaccadic stimulus positions are 'compressed' around the position of the saccade target. This effect might be related to a response bias towards the saccade target position, potentially caused by spatial attention directed to this position (Zirnsak et al., 2010). Modified after (Honda, 1991, left) and (Ross et al., 1997, right).

world is also needed. This information is determined by the rotation angle of the eye relative to the head, often just called eye position.

During saccades the eye position changes rapidly. To investigate how the brain keeps track of these changes, experiments have been conducted in which a brief (10 ms) localization target, that was above detection threshold and visible despite of saccadic suppression, was perisaccadically presented (i.e. prior to, during, or briefly after a saccade, typically -100 ms to +100 ms). By varying the target presentation time relative to the saccade in different trials, the time course of perisaccadic localization could be measured: Perisaccadic spatial perception is subject to characteristic mislocalization effects.

By now, two different mislocalization patterns have been observed: perisaccadic 'shift' and 'compression' (Fig. 6). In experiments that are conducted in an otherwise completely dark environment, mislocalization does not depend on the position of the localization stimulus relative to the saccade target. Mislocalization starts about 50 ms to 100 ms prior to the saccade when stimuli appear to be 'shifted' in the direction of the impending eye movement. During the saccade the direction of mislocalization reverses; localization returns to normal about 50 ms after saccade offset (Bischof and Kramer, 1968; Dassonville et al., 1992; Honda, 1991; Matin and Pearce, 1965). Based on these findings it was assumed that the neural representation of eye position was perisaccadically not congruent with the actual eye position, but that it reflects a 'damped' (i.e. a slowly changing but anticipatory) version instead (Dassonville et al., 1992; Honda, 1991, cf. Fig. 6). In a simulation study, (Pola, 2004) pointed out that perisaccadic shift can also be the result of a veridical eye position signal if delays and other characteristics of neural responses are taken into account.

The mislocalization pattern changes, when experiments are conducted in a lighted environment in which visual references are visible (Lappe et al., 2000) and when the stimulus contrast to the background is low (Michels and Lappe, 2004). Under these conditions the direction of mislocalization depends on stimulus position: Stimuli beyond the saccade target are mislocalized against, at other positions in the direction of the saccade. Stimuli are said to be 'compressed' around the saccade target (Ross et al., 1997, cf. Fig. 6). Such a spatially non-uniform mislocalization pattern can not be explained by an erroneous eye-position signal. It has been suggested to be related to a response bias towards the saccade target (Maij et al., 2011), potentially mediated by focal spatial attention (Zirnsak et al., 2010).

Both perisaccadic shift as well as compression are as well discussed to be related to changes in the neural representation of space that take place perisaccadically. These mechanisms will be described in the next section.

1.4 Neural correlates of perisaccadic perception

Potential correlates of saccadic omission

Since Diamond et al. (2000) have published the time course of saccadic suppression (in the sense of a reduction in the sensitivity to detect brief perisaccadic stimuli), a number of physiological studies have investigated the perisaccadic response properties of neurons in different structures of the visual system, aiming at identifying the neural correlate of this phenomenon (see Ibbotson et al., 2008, for a
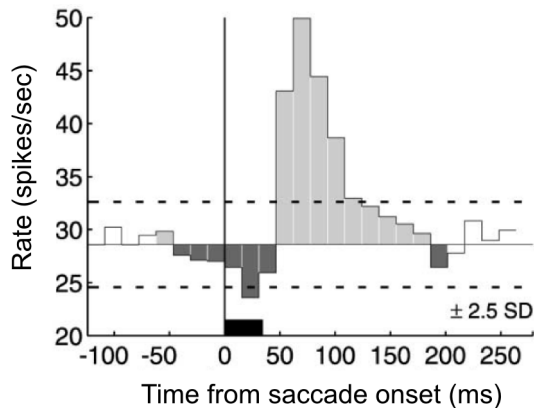
Figure 7: Example of perisaccadic modulation of neuronal responses. Stimulus driven activity of a representative magnocellular neuron of the LGN as function of stimulus presentation time relative to saccade onset. The LGN was considered a potential neural correlate of saccadic suppression (cf. Fig. 5). A typical response pattern found in the LGN and in other visual areas was a small suppression of the neuronal activity followed by a strong increase in postsaccadic activity. Modified after (Reppas et al., 2002).

recent review). The underlying reasoning in most of these studies was the assumption that the reduced perceptual sensitivity to perisaccadic stimulation (compared to fixation) should yield a neural correlate in reduced neuronal activity evoked by a perisaccadic stimulus.

Based on the selectivity of saccadic suppression to stimulus attributes mainly processed by the magnocellular pathway, Burr et al. (1994) suggested suppression might be caused by an 'early' structure of the visual pathway, for example the LGN, where magno- and parvocellular processing is still anatomically separated. As a test of this hypothesis, (Ramcharan et al., 2001; Reppas et al., 2002) recorded the perisaccadic activity of magno- and parvocellular neurons in the LGN. In contrast to the above mentioned reasoning, the most pronounced effect that was found in both studies was not a reduction, but a strong increase in activity that built up shortly after the saccade ('postsaccadic enhancement', Fig. 7). Reppas et al. (2002) also observed a slight reduction in activity during the eye movement; compared to the postsaccadic effect, however, this modulation was minor. Consequently, the search for the site of saccadic suppression was continued in 'higher' areas of the visual system. By now, potential neural correlates of saccadic suppression have been identified primarily in the motion processing areas of the dorsal pathway (MT, MST, VIP): Perisaccadically, these areas show reduced excitability (Ibbotson et al., 2008; Thiele et al., 2002) following a time course that is consistent with the behavioral data (Bremmer et al., 2009). In the ventral pathway, response characteristics consistent with a selective suppression of stimulus features conveyed by the magnocellular pathway have been reported in area V4 of the monkey (Han et al., 2009) as well as in the corresponding area in humans (Kleiser et al., 2004, a functional MRI study).

A potential neural correlate of visual masking, i.e. the reduced visibility of a 'target' stimulus caused by an interaction with a second stimulus ('mask'), has

been observed in a subpopulation of V1 neurons (Judge et al., 1980). When first activated by a stationary stimulus (corresponding to the presaccadic visual stimulation), many neurons did not respond to a following, brief motion stimulus (simulating the retinal motion induced by the saccade, forward masking); importantly, without the preceding stimulation the motion stimulus did well activate the same neuron. Recently, a mechanism of saccadic backward masking has been proposed (Ibbotson and Cloherty, 2009). Without suggesting a specific mechanism, Ibbotson and Cloherty hypothesized that the postsaccadically increased activity, observed in many visual areas, could 'overpower' the activity elicited by the visual stimulation during the saccade.

Neural representations of space

As discussed in section 1.3, spatial orientation in the external world requires the integration of positional information given in the reference frame of the retina ('eye-centered coordinates') and information on the rotation of the eye relative to the head ('eye position'; again under the simplifying assumption the head is fixed relative to the external world). At early processing stages of the visual system, the visual field is represented in cortical maps in eye-centered coordinates: The receptive field (RF) of a neuron, i.e. the region of the visual field in which stimulation can change the neuron's activity, will always be at the same position relative to the fovea ('eye-centered RFs).In contrast, in certain higher cortical areas (e.g. VIP, V6A) neurons with RFs in a head-centered reference frame have been described (Duhamel et al., 1997; Galletti et al., 1993): Those neurons respond to stimulation at the same position in space relative to the head ('head-centered coordinates'), i.e. when eye position changes, the RF position in space remains constant. Intermediate stages between eye- and head-centered reference frames were also observed. Examples of neurons coding space in different reference frames are presented in Fig. 8 . While it is not exactly clear by now, how the observed extra-retinal reference frames actually arise, there is ample evidence that eye position signals are present in many areas of the visual system (Andersen and Mountcastle, 1983; Bremmer, 2000; Bremmer et al., 1997). It is therefore also conceivable that visual space beyond eye-centered coordinates might be coded in a broadly distributed representation using a more implicit coding scheme than the above described head centered(Krekelberg et al., 2003)

Based on the framework of different reference frames in the visual system are two prominent theories on spatial updating across saccades. In one of them it is assumed that perception is based on a space-centered representation of the visual field ('spatiocentric theory'). As the eyes move, the images obtained during each
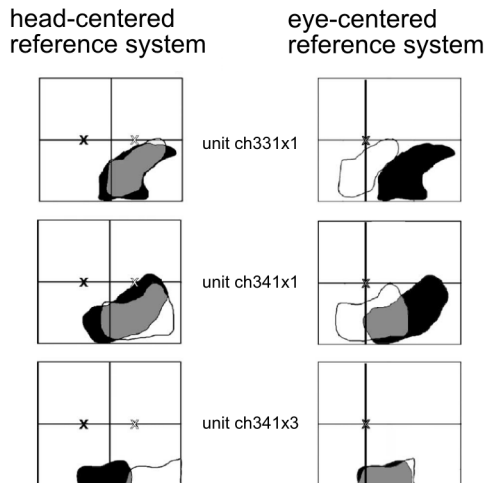
head-centered
reference system

eye-centered
reference system

unit ch331x1

unit ch341x1

unit ch341x3

Figure 8: Receptive fields encoding space in different reference frames Data of three example neurons encoding space in head-centered (top), intermediate (middle), and eye-centered (bottom) reference frames. The receptive field (RF) of a neuron is defined as the region in space in which stimulation can change the neuron's activity. Left row: RFs, plotted in head-centered coordinates, when the monkey was fixating the left (black) or the right (white) fixation target. In the neuron with a head-centered RF, the RF position remains constant in head centered space (top); the position of the eye-centered RF moves according to the change in eye position (bottom). The situation reverses when the RFs are plotted in an eye-centered reference system (right column). The figure presents auditory RFs (i.e. the activity is evoked by auditory stimulation at a certain position in space) recorded in area VIP. Similar characteristics have been observed for visual RFs. Modified after (Schlack et al., 2005).

fixation period are, like pieces of a puzzle, incorporated at the corresponding positions of the perceptual map. In the second theory it is proposed that perception relies on eye-centered representations of visual space. In this notion, perceptual stability might be mediated by mechanisms that reorganize the spatial representation around the time of a saccade ('remapping theory'). The most prominent example of such a remapping mechanism was described by Duhamel et al. (1992) in area LIP of the parietal cortex (Fig. 9A). A subpopulation of the neurons in this area changed their spatial response characteristics before an impending saccade ('predictive' remapping): The neurons started to fire, if a stimulus was presented outside of the current RF but at their 'future' RF, i.e. at the position where the RF would be located at after the saccade. Since the initial description by Duhamel et al., similar effects, though with slightly different temporal characteristics, have been reported in different areas of the visual system (FEF: Umeno and Goldberg, 1997 SC: Walker et al., 1995; they are usually more prominent in higher cortical areas (Nakamura and Colby, 2002). It has been shown in the FEF, that the remapping mechanism relies on an ascending signal from the SC that provides the information about the impending saccade (Sommer and Wurtz, 2006, the signal is usually referred to as 'corollary discharge'). In ventral area V4, a remapping process with different spatial characteristics was observed (Tolias et al., 2001): RFs were not shifted according to the vector of the impending saccade to
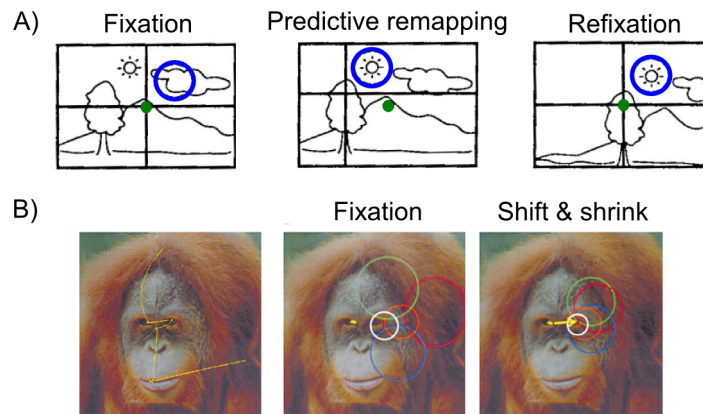
Figure 9: Examples of perisaccadic receptive fields remapping. In certain areas of the visual system, the spatial representation of the visual field (given by the receptive field (RF) structure) is subject to transient reorganisation processes at the time of saccades ('remapping'). A) A subpopulation of LIP neurons show 'predictive remapping': During the saccade preparation phase, when gaze (green dot) is still at the initial fixation point, but a saccade to a different location (cross) is planned, the RFs (blue circle) of some neurons shift to the position were they will be located after the saccade (right panel). B) In area V4 different remapping characteristics have been described: Compared to fixation (middle panel), RFs shift and decrease in size prior to a saccade (right panel, 'shift & shrink remapping'). Modified after (Duhamel et al., 1992, A) and (Tolias et al., 2001, B).

their future RF positions, but towards the position of the saccade target; in addition, it was reported that the RFs shrank in size ('shift & shrink remapping', 9B).

Although, the basic mechanisms for both of the above mentioned theories on saccadic updating have been observed on the neuronal level, the actual contributions of these mechanisms to perceptual stability are not clear by now. Similarly, it still remains elusive if and how these processes are related to the observed perceptual mislocalization effects.

References

Andersen RA, Mountcastle VB (1983) The influence of the angle of gaze upon the excitability of the light-sensitive neurons of the posterior parietal cortex. J Neurosci 3(3):532–548

Bahill A, Clark M, Stark L (1975) The main sequence, a tool for studying human eye movements. Math Biosci 24:191–204

Bischof N, Kramer E (1968) Untersuchungen und "uberlegungen zur richtungswahrnehmung bei willk"uhrlichen sakkadischen augenbewegungen. Psychologische Forschung 32:185–218

Bremmer F (2000) Eye position effects in macaque area v4. Neuroreport 11(6):1277–1283

Bremmer F, Ilg UJ, Thiele A, Distler C, Hoffmann KP (1997) Eye position effects in monkey cortex. i. visual and pursuit-related activity in extrastriate areas mt and mst. JNeurophysiol 77:944–961

Bremmer F, Kubischik M, Hoffmann KP, Krekelberg B (2009) Neural dynamics of saccadic suppression. J Neurosci 29(40):12,374–12,383

Bridgeman B, Hendry D, Stark L (1975) Failure to detect displacement of the visual world during saccadic eye movements. Vision Res 15(6):719–722

Burr DC, Holt J, Johnstone JR, Ross J (1982) Selective depression of motion sensitivity during saccades. JPhysiol 333:1–15

Burr DC, Morrone MC, Ross J (1994) Selective suppression of the magnocellular visual pathway during saccadic eye movements. Nature 371:511–513

Campbell FW, Wurtz RH (1978) Saccadic omission: why we do not see a grey-out during a saccadic eye movement. Vision Res 18:1297–1303

Carpenter R (1988) Movements of the eyes (2nd Edition). Pion

Catz N, Thier P (2007) Neural control of saccadic eye movements. Dev Ophthalmol 40:52–75

Catz N, Dicke PW, Thier P (2005) Cerebellar complex spike firing is suitable to induce as well as to stabilize motor learning. Curr Biol 15(24):2179–2189

Chahine G, Krekelberg B (2009) Cortical contributions to saccadic suppression. PLoS One 4(9):e6900

Dassonville P, Schlag J, Schlag-Rey M (1992) Oculomotor localization relies on a damped representation of saccadic eye displacement in human and nonhuman primates. VisNeurosci 9:261–269

Diamond MR, Ross J, Morrone MC (2000) Extraretinal control of saccadic suppression. JNeurosci 20:3449–3455

Dodge R (1900) Visual perception during eye movement, vol 7, pp 454–465

Duhamel JR, Colby CL, Goldberg ME (1992) The updating of the representation of visual space in parietal cortex by intended eye movements. Science 255:90–92

Duhamel JR, Bremmer F, BenHamed S, Graf W (1997) Spatial invariance of visual receptive fields in parietal cortex neurons. Nature 389:845–848

Frens MA, Opstal AJV (1997) Monkey superior colliculus activity during short-term saccadic adaptation. Brain Res Bull 43(5):473–483

Fuchs AF, Robinson FR, Straube A (1993) Role of the caudal fastigial nucleus in saccade generation. i. neuronal discharge pattern. J Neurophysiol 70(5):1723–1740

Galletti C, Battaglini PP, Fattori P (1993) Parietal neurons encoding spatial locations in craniotopic coordinates. Exp Brain Res 96(2):221–229

Han X, Xian SX, Moore T (2009) Dynamic sensitivity of area v4 neurons during saccade preparation. Proc Natl Acad Sci U S A 106(31):13,046–13,051

Holt EB (1903) Eye movements and central anaesthesia, vol 4, pp 3–45

Honda H (1991) The time courses of visual mislocalization and of extraretinal eye position signals at the time of vertical saccades. Vision Res 31:1915–1921

Hopp JJ, Fuchs AF (2004) The characteristics and neuronal substrate of saccadic eye movement plasticity. Prog Neurobiol 72(1):27–53

Ibbotson MR, Cloherty SL (2009) Visual perception: saccadic omission–suppression or temporal masking? Curr Biol 19(12):R493–R496

Ibbotson MR, Crowder NA, Cloherty SL, Price NSC, Mustari MJ (2008) Saccadic modulation of neural responses: possible roles in saccadic suppression, enhancement, and time compression. J Neurosci 28(43):10,952–10,960

Judge SJ, Wurtz RH, Richmond BJ (1980) Vision during saccadic eye movements. i. visual interactions in striate cortex. J Neurophysiol 43(4):1133–1155

Kleiser R, Seitz RJ, Krekelberg B (2004) Neural correlates of saccadic suppression in humans. CurrBiol 14:386–390

Kojima Y, Soetedjo R, Fuchs AF (2010) Changes in simple spike activity of some purkinje cells in the oculomotor vermis during saccade adaptation are appropriate to participate in motor learning. J Neurosci 30(10):3715–3727

Krekelberg B, Kubischik M, Hoffmann KP, Bremmer F (2003) Neural correlates of visual localization and perisaccadic mislocalization. Neuron 37:537–545

Lappe M, Awater H, Krekelberg B (2000) Postsaccadic visual references generate presaccadic compression of space. Nature 403:892–895

Maij F, Brenner E, Smeets JBJ (2011) Temporal uncertainty separates flashes from their background during saccades. J Neurosci 31(10):3708–3711

Matin L, Pearce DG (1965) Visual perception of direction for stimuli during voluntary saccadic eye movements. Science 148:1485–1488

Mazer JA, Gallant JL (2003) Goal-related activity in v4 during free viewing visual search. evidence for a ventral stream visual salience map. Neuron 40(6):1241–1250

McLaughlin S (1967) Parametric adjustment in saccadic eye movements. Percept Psychophys 2:359–362

Melis BJ, van Gisbergen JA (1996) Short-term adaptation of electrically induced saccades in monkey superior colliculus. J Neurophysiol 76(3):1744–1758

Merigan WH, Maunsell JH (1993) How parallel are the primate visual pathways? Annu Rev Neurosci 16:369–402

Michels L, Lappe M (2004) Contrast dependency of sacadic compression and suppression. Vision Res 44:2327–2336

Nakamura K, Colby CL (2002) Updating of the visual representation in monkey striate and extrastriate cortex during saccades. Proc Natl Acad Sci U S A 99(6):4026–4031

Optican LM, Robinson DA (1980) Cerebellar-dependent adaptive control of primate saccadic system. J Neurophysiol 44(6):1058–1076

Phillips JO, Fuchs AF, Ling L, Iwamoto Y, Votaw S (1997) Gain adaptation of eye and head movement components of simian gaze shifts. J Neurophysiol 78(5):2817–2821

Pola J (2004) Models of the mechanism underlying perceived location of a perisaccadic flash. Vision Res 44:2799–2813

Ramcharan EJ, Gnadt JW, Sherman SM (2001) The effects of saccadic eye movements on the activity of geniculate relay neurons in the monkey. VisNeurosci 18:253–258

Reppas JB, Usrey WM, Reid RC (2002) Saccadic eye movements modulate visual responses in the lateral geniculate nucleus. Neuron 35:961–974

Robinson FR, Fuchs AF, Noto CT (2002) Cerebellar influences on saccade plasticity. Ann N Y Acad Sci 956:155–163

Robinson FR, Soetedjo R, Noto C (2006) Distinct short-term and long-term adaptation to reduce saccade size in monkey. J Neurophysiol 96(3):1030–1041

Roe AW, Chelazzi L, Connor CE, Conway BR, Fujita I, Gallant JL, Lu H, Vanduffel W (2012) Toward a unified theory of visual area v4. Neuron 74(1):12–29

Ross J, Morrone MC, Burr DC (1997) Compression of visual space before saccades. Nature 386:598–601

Schlack A, Sterbing-D'Angelo SJ, Hartung K, Hoffmann KP, Bremmer F (2005) Multisensory space representations in the macaque ventral intraparietal area. J Neurosci 25(18):4616–4625

Sommer MA, Wurtz RH (2006) Influence of the thalamus on spatial visual processing in frontal cortex. Nature 444(7117):374–377

Sugrue LP, Corrado GS, Newsome WT (2005) Choosing the greater of two goods: neural currencies for valuation and decision making. Nat Rev Neurosci 6(5):363–375

Thiele A, Henning P, Kubischik M, Hoffmann KP (2002) Neural mechanisms of saccadic suppression. Science 295:2460–2462

Tolias AS, Moore T, Smirnakis SM, Tehovnik EJ, Siapas AG, Schiller PH (2001) Eye movements modulate visual receptive fields of v4 neurons. Neuron 29:757–767

Umeno MM, Goldberg ME (1997) Spatial processing in the monkey frontal eye field. i. predictive visual responses. JNeurophysiol 78:1373–1383

Ungerleider LG, Mishkin M (1982) Two cortical visual systems, M.I.T. Press

Ungerleider LG, Galkin TW, Desimone R, Gattass R (2008) Cortical connections of area v4 in the macaque. Cereb Cortex 18(3):477–499

Vilis T (2012) The physiology of the senses: Transformations for perception and action

Walker MF, Fitzgibbon EJ, Goldberg ME (1995) Neurons in the monkey superior colliculus predict the visual result of impending saccadic eye movements. JNeurophysiol 73:1988–2003

Wallman J, Fuchs AF (1998) Saccadic gain modification: visual error drives motor adaptation. J Neurophysiol 80(5):2405–2416

Watson TL, Krekelberg B (2009) The relationship between saccadic suppression and perceptual stability. Curr Biol 19(12):1040–1043

Wurtz RH (2008) Neuronal mechanisms of visual stability. Vision Res 48(20):2070–2089

Yarbus AL (1967) Eye movements and vision. New York: Plenum

Zee DS, Yee RD, Cogan DG, Robinson DA, Engel WK (1976) Ocular motor abnormalities in hereditary cerebellar ataxia. Brain 99(2):207–234

Zirnsak M, Lappe M, Hamker FH (2010) The spatial distribution of receptive field changes in a model of peri-saccadic perception: predictive remapping and shifts towards the saccade target. Vision Res 50(14):1328–1337

2 Studies

Study 1:
Perisaccadic localization of auditory stimuli
Klingenhoefer, S.; Bremmer, F.
Experimental Brain Research, 2009

Study 2:
Depth perception during saccades
Teichert, T.; Klingenhoefer S., Wachtler, T; Bremmer, F.
Journal of Vision, 2008

Study 3:
Perisaccadic mislocalization as optimal percept
Teichert, T.; Klingenhoefer S.; Wachtler, T; Bremmer, F.
Journal of Vision, 2010

Study 4:
Saccadic suppression of displacement in face of saccade adaptation
Klingenhoefer, S.; Bremmer, F.
Vision Research, 2011

Study 5:
Perisaccadic response modulations in area V4 of the macaque monkey
Klingenhoefer, S.; Bremmer, F.
in preparation

Study 6:
Perisaccadic receptive field dynamics in area V4 of the macaque monkey during saccade adaptation
Klingenhoefer, S.; Bremmer, F.
in preparation

RESEARCH ARTICLE

Perisaccadic localization of auditory stimuli

Steffen Klingenhoefer · Frank Bremmer

Abstract Interaction with the outside world requires the knowledge about where objects are with respect to one's own body. Such spatial information is represented in various topographic maps in different sensory systems. From a computational point of view, however, a single, modality-invariant map of the incoming sensory signals appears to be a more efficient strategy for spatial representations. If such a single supra-modal map existed and were used for perceptual purposes, localization characteristics should be similar across modalities. Previous studies had shown mislocalization of brief visual stimuli presented in the temporal vicinity of saccadic eye-movements. Here, we tested, if such mislocalizations could also be found for auditory stimuli. We presented brief noise bursts before, during, and after visually guided saccades. Indeed, we found localization errors for these auditory stimuli. The spatio-temporal pattern of this mislocalization, however, clearly differed from the one found for visual stimuli. The spatial error also depended on the exact type of eye-movement (visually guided vs. memory guided saccades). Finally, results obtained in fixational control paradigms under different conditions suggest that auditory localization can be strongly influenced by both static and dynamic visual stimuli. Visual localization on the other hand is not influenced by distracting visual stimuli but can be inaccurate in the temporal vicinity of eye-movements. Taken together, our results argue against a single, modality-independent spatial representation of sensory signals.

Introduction

Interaction with the outside world is based on fast and reliable sensorimotor processes. As part of such processes, sensory signals have to be transformed in order to be used for motor commands. At the neuronal level, spatial information is represented in topographic maps within the different sensory streams. This raises the question about the reference frames used by the different sensors and effectors. In the visual system, incoming information is encoded in retinotopic maps in striate and early extrastriate areas (Wandell et al. 2007). In the tactile domain spatial information is represented in a body map (homunculus) in primary somatosensory cortex (Kaas et al. 1979). In the auditory cortex, spatial information seems to be represented implicitly by a population of neurons (Woods et al. 2006). From a computational point of view, however, a single, modality-independent spatial representation would be preferable as compared to a number of unimodal representations encoding signals in various reference frames. Signals arising from such a map could be directly used in the relevant motor system enhancing fast and precise actions under sensory guidance. Indeed, such supra-modal or amodal representations have been found in the Superior Colliculus (SC) (Jay and Sparks 1984) and in a subregion of posterior–parietal cortex, i.e. in the ventral intraparietal area (VIP) of the macaque monkey (Schlack et al. 2005; Avillac et al. 2005). In the SC, auditory receptive fields were shown to move (to

Electronic supplementary material   The online version of this article (doi:10.1007/s00221-009-1869-3) contains supplementary material, which is available to authorized users.

S. Klingenhoefer (✉) · F. Bremmer
Department of Neurophysics, Philipps-University Marburg, Renthof 7, 35037 Marburg, Germany
e-mail: steffen.klingenhoefer@physik.uni-marburg.de

some extent) with gaze direction. Hence, visual and auditory signals are encoded in retinal coordinates. This is an efficient type of encoding because the SC is involved in the control of saccadic eye-movements. In other words, the sensor's reference frame (retinal) is directly coupled to the effector (eye-ball). Neurons in area VIP respond to visual, tactile, auditory and vestibular stimulation (Colby et al. 1993; Bremmer et al. 2002; Schlack et al. 2002). Surprisingly, about one-third of the cells encode visual information explicitly in head-centered coordinates (Duhamel et al. 1997). On the other hand, about one quarter of the cells encode auditory information in retinal coordinates (Schlack et al. 2005). Cells with visual and auditory responses tend to encode sensory information in the same frame of reference. There is strong evidence that a functional equivalent of macaque area VIP exists also in humans. In a functional imaging study we could show in the depth of the human intraparietal sulcus neural activity related to visual, tactile and auditory motion (Bremmer et al. 2001b). If activity in this part of human PPC was used to establish a supra-modal spatial representation of the environment, one would expect that perceptual effects as described in one sensory domain would also be found for stimuli from the other domains (Bremmer et al. 2001a; Bremmer 2005).

In the visual domain, a number of studies have described localization errors for stimuli presented briefly before, during and after saccades. In darkness, a bimodal error pattern is observed: first, stimuli are perceived as being shifted in the direction of the eye-movement and then into the opposite direction (Shift) (Honda 1989; Cai et al. 1997). In light, stimuli are perceived as being shifted towards the landing point of the eye (Compression) (Ross et al. 1997; Lappe et al. 2000). If localization of perisaccadic stimuli was based on the decoding of neural activity within supra-modal representations of the environment (e.g. area VIP or the SC), we would expect similar errors also for the spatial perception of auditory stimuli. Accordingly, in our present study we asked subjects to localize brief auditory stimuli that were presented during both, visually guided and memory guided saccades. Performance was compared to a number of control conditions in which subjects were fixating different targets in otherwise darkness. Part of this work has been presented as conference proceedings (Klingenhoefer and Bremmer 2004).

Experiment 1

In experiment 1, we investigated the influence of visually guided eye-movements (fixation and saccades) on the localization of auditory stimuli. To reproduce data from previous experiments on visual localization (Honda 1989, van der Heijden et al. 1999), two subjects were also tested in corresponding visual localization conditions.

Materials and methods

Participants

Six right-handed human subjects (two females, average age: 27 years) participated in these experiments. All subjects had normal or corrected-to-normal vision and normal hearing and were experienced in psychophysical experiments. Except for one participant, who was one of the authors, all subjects were naïve as to the purpose of the study. The experiments were performed in accordance with the ethical standards of the 1964 Declaration of Helsinki. All subjects had given informed written consent prior to the study.

Experimental setup

Experiments were performed in a light-tight, sound-attenuated experimental chamber. Subjects were seated comfortably in a chair with their head supported by a chin rest. Eye-movements were monitored using an infrared camera system running at 500 Hz (EyeLink2, SR Research). Visual stimuli were presented on a 19″ CRT-monitor (100 Hz refresh rate) that was placed at eye level, 57 cm in front of the subjects covering a visual area of $40° \times 30°$. Auditory stimuli were controlled by a sound board (Audigy2, Sound-Blaster) and presented via a moveable speaker (Visaton, SC 8) that was placed just in front of the monitor, 7.5 cm below eye level. Using the ASIO drivers of the soundcard with a buffer size of 64 byte, the delay for the sound presentation was (6 ± 1) ms. To avoid acoustic reflections from the surface of the monitor, anechoic foam was placed between the loudspeaker and the lower half of the monitor. The complete acoustic setup was hidden behind opaque but acoustically permeable cloth. The horizontal position of the loudspeaker could be varied in a range of 40 cm by the stimulus PC with a precision of about 1 mm.

Stimuli and localization method

All stimuli were presented on a black background (luminance < 0.1 cd/m^2). To achieve a dark background and minimize stimulus persistence due to phosphor afterglow, a neutral density filter was placed right in front of the monitor. Eye-movements were guided by two small targets, F1 and F2, located at $-7.5°$ (left) and $+7.5°$ (right) from straight ahead. The targets were white circles (luminance: 20 cd/m^2) with a diameter of 0.5° surrounding a tiny black center (luminance: < 0.1 cd/m^2, diameter: 0.1°). In the visual localization conditions stimuli were vertical white bars (ranging from the top of the visible monitor area to the vertical midline, luminance 20 cd/m^2) that were flashed for 10 ms. Auditory stimuli were brief bursts of white noise
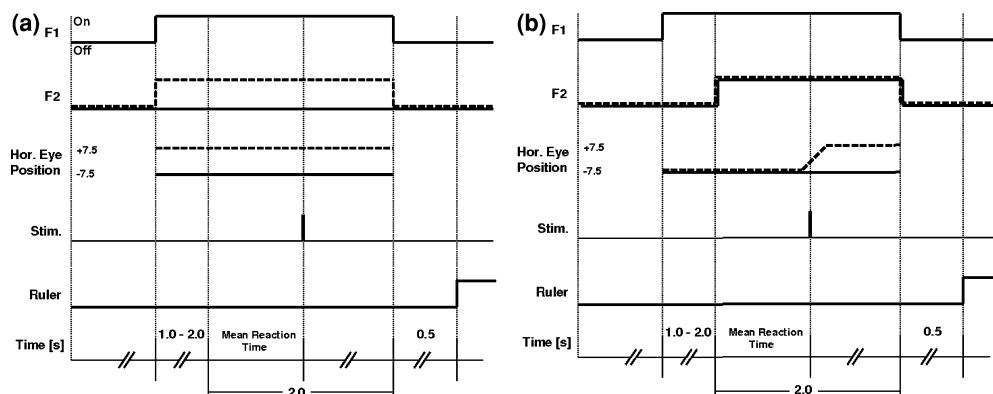
413

Fig. 1 Time course for different paradigms of experiment 1. **a** Fixation conditions F1 (*solid line*) and F2 (*dashed line*). **b** Fixation condition CAP (*solid line*) and saccade condition SAC (*dashed line*). Note that in all conditions the ruler, which was used to judge the perceived position, was presented not before the end of the trials. Except for the presence of the two fixation points no stimuli were visible during the trials

(5 ms, 75 dB SPL). Both auditory and visual localization targets could be presented at one of four possible positions (+2.5°, +5.5°, +9.5° and +12.5° right from straight ahead), which were symmetrically distributed around F2.

As mentioned above, all experiments were performed in a light-tight chamber. Accordingly, all experiments were performed in complete darkness except for the fixation points. These experimental conditions, therefore, more likely induce a shift-like (Honda 1989; Cai et al. 1997) rather than a compression-like (Ross et al. 1997; Lappe et al. 2000) mislocalization of visual stimuli presented perisaccadically. A ruler (spatial resolution 0.5°), which served as a localization device was displayed at least 500 ms after the offset of the fixation (or saccade) targets. In order to avoid habituation effects, random tick marks were generated for each trial. Subjects reported the perceived position of the localization target by entering the number of the tickmark closest to the target flash. Subjects received no feedback on their performance.

Experimental paradigms

Localization performance for both sensory modalities, vision and audition, was investigated in a blocked design with counterbalanced presentation order in four different paradigms: one saccade condition and three fixational controls. The control conditions were designed to represent the different temporal epochs of the saccade trials. Time course and stimulus parameters were identical for auditory and visual tasks and are shown schematically in Fig. 1.

Fixation at F1 (F1) In this condition subjects were instructed to fixate the left fixation target (F1). After the beginning of each trial a localization target was presented

after a random time varying between 1.2 and 2.2 s. The subjects were allowed to move their eyes freely after the disappearance of F1, i.e. 3.5–4.0 s after the beginning of the trial (Fig. 1a, solid line).

Fixation at F2 (F2) In this condition both fixation targets, F1 and F2, were visible throughout the trial and subjects had to fixate F2. Otherwise, experimental conditions were identical with F1 (Fig. 1a, dashed line).

Capture task (CAP) As in F1-trials, the subjects were asked to fixate the left fixation target throughout the trial. However, in this task the second fixation target F2 appeared 100–400 ms prior to the localization stimulus (Fig. 1b, solid line).

Saccade task (SAC) In this condition, stimulation was identical to the Capture Task but subjects received a different instruction: after the appearance of F2 the subjects had to saccade to this target and keep fixation until the end of the trial. The afore mentioned onset asynchrony of 100–400 ms between F2 and the localization stimulus in the Capture Task was chosen such that in the saccade paradigm the stimulus fell in the perisaccadic period of 100 ms prior to 100 ms after the saccade (Fig. 1b, dashed line). The exact timing of stimulus presentation depended on the mean reaction time of each subject, which varied for the different subjects between 185 and 280 ms.

All subjects completed 120 trials for each fixational paradigm (i.e. F1-, F2- and CAP-trials). As we were especially interested in the time course of perisaccadic localization, a subset of the participants ($n = 2$ for visual, $n = 4$ for auditory stimuli) was tested more frequently in the saccade condition (∼400 trials) than in the fixational controls to ensure a reasonable data density for the time-resolved analysis.

In all four conditions the beginning of a trial was preceded by a period in which the stimulus speaker could be repositioned. To mask the sound of the moving speaker during this procedure, white noise was presented by another speaker positioned 30 cm below eye level in straight ahead direction for 2-s. Subjects were thus unaware of any possible movement of the target speaker. After this 2-s period the subjects started the trial by fixation of the particular fixation point and a key press with their right hand.

Data analysis

Data were analyzed offline using in-house software based on Matlab (The MathWorks, R2007b) in combination with the corresponding statistics toolbox. Eye-movement data were analyzed concerning subjects' correct behavior in the four different paradigms. Fixational trials in which fixation was broken or saccade trials including inaccurate saccades (i.e. reaction times <100 ms or >500 ms or amplitude <10° or >20°) were discarded. This was the case in about 3% of the trials in experiment 1.

To analyze the time course of localization performance in the perisaccadic epoch, both running averages and running standard errors were calculated using a windowed Gaussian filter (window size 50 ms, $\sigma = 25$ ms). Saccade onset time was defined based on the built-in detection algorithm of the eye-tracker using a combined velocity and acceleration criterion. For population analysis, data from different subjects were pooled for each of the four possible stimulus positions. To calculate the population average across all stimulus positions, the four population data vectors were normalized by subtraction of the corresponding mean value calculated for the perisaccadic epoch. Afterwards, the data vectors were pooled again so that a running average and standard error could be computed. To test for any significant perisaccadic modulation of localization performance, we used a bootstrapping technique to determine a confidence interval to check for any significant perisaccadic modulation in localization compared to pre- and postsaccadic periods. In order to calculate this interval, response values from epochs in which localization was stationary ($t < -100$ ms or $t > 100$ ms relative to saccade onset) were re-sampled to form data vectors of the same configuration as the measured data vectors. Running averages of localization data lying beyond the 95% confidence intervals of the running average were considered to show a statistically significant modulation of performance.

To compare localization performance between different conditions, we computed two measures: a compression index (CI) and a shift index (SI). For this purpose, linear regression functions were fitted through the data for each condition individually. In the SAC-condition only data points from the perisaccadic epoch (i.e. $t > -50$ ms

and $t < +50$) entered the analysis. The compression index served as a measure of spatial gain, i.e. the extent of the perceptual space in comparison with the physical stimulus space.[1] It was computed as $CI = 1 - m$, with m being the slope of the fitted linear function. Therefore, a compression index which equals 0 implies the perceptual space has the same spatial extent as the physical stimulus space. Positive CI-values denote a compressed space perception; negative values indicate an expansion of perceptual space. In order to calculate the shift index, the center of the perceptual space was calculated using the fitted regression function. The shift index is a measure of how much the center of the perceived space deviates from the center of the physical stimulus space (i.e. 7.5° in experiment 1, 10.0° in experiment 2). Consequently, the reference system for the shift index is the physical stimulus space—not the fovea. The shift index was computed by subtracting the center of the physical stimulus space from the center of the perceptual space. Hence, a shift index which equals -1 indicates the center of the perceived space to be shifted by 1° to the left compared to its physical position. Standard errors for the compression and shift index were calculated using a standard bootstrap procedure. The shift and compression indices of the four different conditions were statistically analyzed using one-way ANOVAs for repeated measures. In case significant differences were found, post hoc pairwise comparisons between all different conditions were made using Holm–Sidaks t tests. For all statistical procedures we used an alpha level of 0.05.

Results

Time course of perisaccadic localization of visual and auditory stimuli

The perceived stimulus position as a function of stimulus presentation time relative to saccade onset is shown in Fig. 2. As expected from the literature (Honda 1989; Cai et al. 1997), in the visual localization condition (Fig. 2a, b) large systematic errors were observed. About 70 ms prior to saccade onset, perceived stimulus locations were significantly shifted in the direction of the saccade. Mislocalization peaked around saccade onset (peak modulation +3.1°). In contrast to the results in the visual domain, localization

---

[1] It should be noted that the compression index is only an indirect measure of spatial extent as it is derived from localization data of singular stimuli—subjects perception of spatial extend was not explicitly retrieved. Recently, Reeve et al. (2008) presented evidence that measures of spatial extend that are derived from single stimuli localization data may differ from direct measurements of spatial extend.
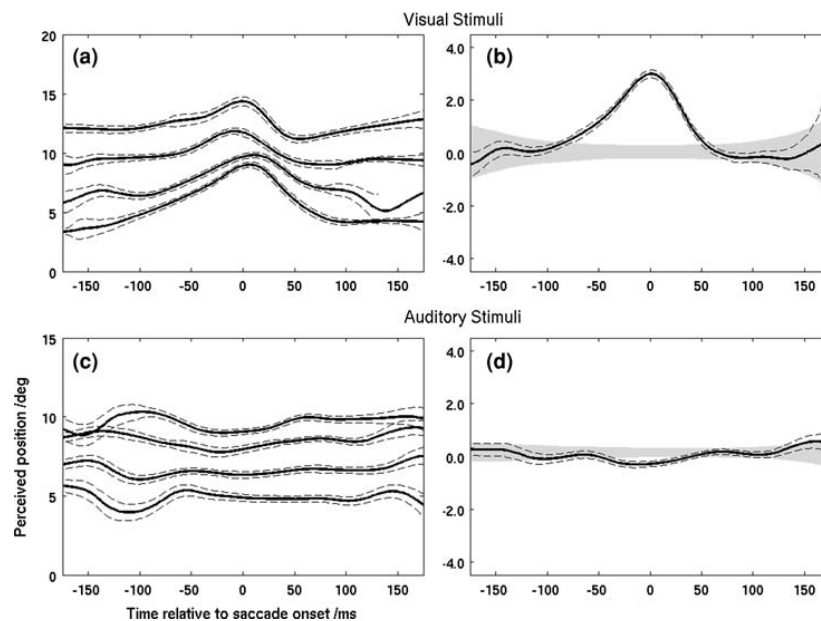
Fig. 2 Temporal modulation of perisaccadic localization. Running averages (*thick lines*) and standard error (*dashed lines*) of localization data are plotted for visual stimuli (**a**, **b**) and auditory stimuli (**c**, **d**). All panels show population data. In b,d all stimulus positions were pooled. Grey areas represent 95% confidence intervals derived from pre- and postsaccadic data (t < −100 ms or t > 100 ms relative to saccade onset) in which. All perceived position data points were centered on the val-ues observed in this non perisaccadic epoch by subtraction of the mean perceived position of this epoch. Visual stimuli were strongly mislocalized in the direction of the saccade with peak error at saccade onset. Localization of auditory stimuli revealed only a slight misperception opposite to saccade direction around saccade onset. 382 × 273 mm (85 × 85 DPI)

of auditory stimuli was rather stationary during the perisaccadic period (Fig. 2c, d). As subjects could clearly discriminate all four stimulus positions, this perceptual stationarity was certainly not due to a general inability to localize the auditory stimuli. In comparison to pre- and postsaccadic epochs (cf. Data analysis) the pooled data in Fig. 2d reveal a marginally significant perisaccadic modulation around saccade onset (peak modulation −0.4°). The perceived positions appear slightly shifted against the saccade direction during this time.

Localization of auditory targets in different experimental conditions

Mean perceived positions and corresponding standard errors for the auditory stimuli in all four conditions (F1, F2, CAP, and SAC) are shown in Fig. 3a, b. A comparison of the F1- and F2-condition, in which the subjects fixated either the left or the right fixation target, shows a clear effect of eye-position on auditory localization: perceived positions were shifted in the direction of gaze (Fig. 3a). The appearance of F2 in the CAP-condition induced a compression of perceptual space. Likewise, a compression of auditory space was observed in the saccade condition.

Compared to the CAP-condition the observed compression in the SAC-condition was more pronounced, additionally perceived positions were shifted in the direction of the saccade.

For a quantitative comparison of the different conditions shift- and compression indices were calculated for the results of the auditory localization experiments (Fig. 4a, b). Statistical analysis revealed a significant effect of the factor condition for both the shift indices ($P = 0.008$) and the compression indices ($P = 0.003$) (ANOVA for repeated measures). Post hoc pairwise comparisons between all conditions using Holm–Sidak t tests revealed significant differences in shift indices between the F1- and F2- ($P = 0.01$) as well as between F1- and CAP-conditions ($P = 0.04$). Compression indices were significantly different between F1- and SAC-conditions ($P < 0.001$).

Localization of visual targets in different conditions

Mean perceived positions and corresponding standard errors for the visual stimuli in all four conditions (F1, F2, CAP, and SAC) are shown in Fig. 3c, d. The corresponding shift and compression indices obtained from the visual localization data are presented in Fig. 4c, d.
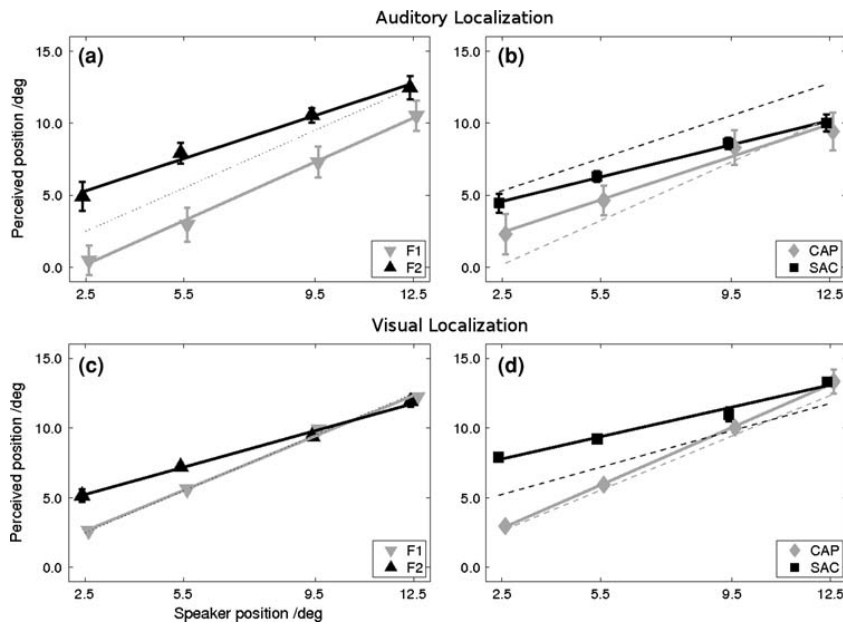
🖉 Springer

27

Fig. 3 Localization in saccade and fixation conditions (**a**, **b** auditory stimuli; **c**, **d** visual stimuli). Mean perceived positions and standard errors for the four target positions in the four tasks (F1, F2, SAC, and CAP. For details see main body text) are shown. Solid lines show the respective regression functions. Values of the SAC-condition are based on data from the perisaccadic epoch only ($t > -50$ ms and $t < +50$ ms) a, A comparison of the F1- and F2-conditions reveals a strong eye-position effect: perceived space is shifted along with the direction of gaze. The dotted line represents ideal localization. **b** In both, the CAP- and the SAC-condition the perceptual space is compressed as indicated by the smaller slope of the regression functions. This effect is more pronounced in the SAC-condition. For better comparison, the dashed lines depict the regression lines of the F1- and F2-data. **c** Visual localization in fixation conditions tended to be biased towards the fovea. **d** Visual distractor stimuli do not influence visual localization (compare CAP- and F1-conditions). Perisaccadically, perceived locations were strongly shifted in the direction of the saccade. Additionally, a slight compression effect, probably due to the presence of the fixation points during the trial, was observed

Statistical analysis revealed a significant effect of the factor condition for the shift ($P = 0.01$) as well as for the compression indices ($P = 0.01$) (ANOVA for repeated measures). Post hoc pairwise comparisons between all conditions using Holm–Sidak t tests revealed a significant difference in shift index between the SAC condition and the three fixation conditions (F1: $P = 0.02$, F2: $P = 0.04$, CAP: $P = 0.04$). The shift indices did not differ significantly between the fixation conditions. Compression indices were significantly different between SAC- and F1- ($P = 0.04$) as well as between SAC- and CAP-conditions ($P = 0.03$). Further comparisons did not reveal significant differences.

Discussion

In this first experiment, we investigated perisaccadic localization of visual and auditory stimuli during visually guided saccades. Our results for perisaccadic visual localization are in perfect agreement with earlier studies demonstrating apparent position shifts in the direction of the impending eye-movement (Matin and Pearce 1965; Bischof and Kramer 1968; Honda 1989; Cai et al. 1997). Although, in our data this perceptual effect was found for all stimulus positions, it was strongest for stimuli in a spatial range between the initial fixation point and the saccade target. This difference in effect size results in a positive compression index for this condition. This was probably due to the presence of the fixation target throughout the trial, which might cause a small compression effect (Ross et al. 1997) as it constitutes a visual reference (Lappe et al. 2000). In line with Binda et al. (2007), we found that auditory localization was quite accurate during saccades. Most importantly, perisaccadic localization of auditory stimuli did not reveal the same spatio-temporal mislocalization pattern that was observed for visual stimuli.

Notably, in comparison to fixational controls auditory localization was altered in this saccade condition. Perceptual space was clearly compressed towards the endpoint of the saccade. However, this perceptual compression was different from the 'Compression' described for the visual domain (Ross et al. 1997; Kaiser and Lappe 2004). Perisaccadic auditory compression did not reveal a substantial temporal modulation. Furthermore, this compression
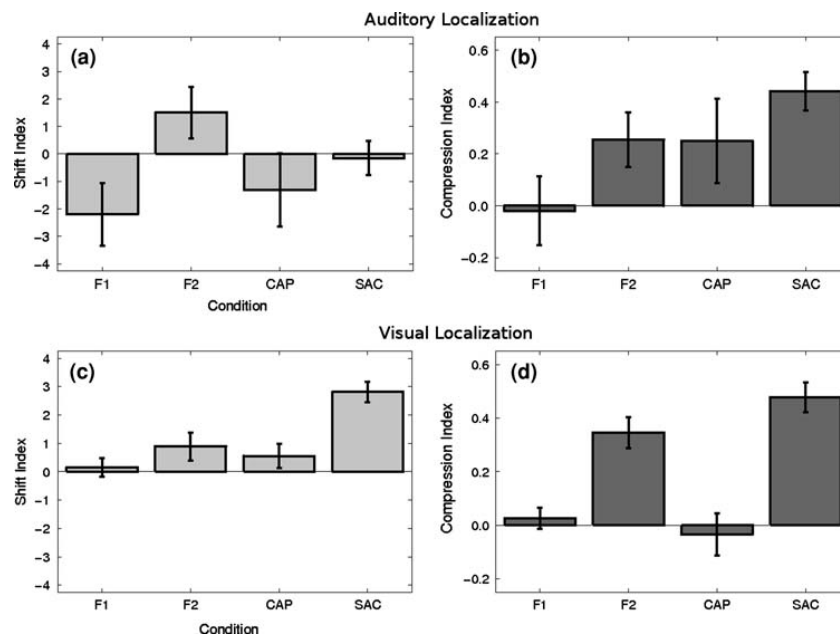
Fig. 4 Population mean and corresponding standard errors of the shift and compression indices (**a**, **b** auditory stimuli; **c**, **d** visual stimuli). **a**, **b** For auditory localization we found significantly different shift and compression indices between conditions (ANOVA for repeated measures, $P < 0.05$). **a** Post hoc Holm–Sidak t tests revealed significant differences between shift indices in F1- and F2- as well as in F1- and SAC-conditions ($P < 0.05$). **b** Compression indices were significantly different between the F1- and SAC-condition. **c**, **d** For visual localization we found significantly different shift and compression indices between conditions (ANOVA for repeated measures, $P < 0.05$). **c** The shift index of the SAC-condition differed significantly from all three control conditions (Holm–Sidak t tests, $P < 0.05$). Other differences were not significant. **d** Compression indices were significantly different between SAC- and F1- and between SAC- and CAPconditions

occurred under experimental conditions evoking a 'Shift' pattern for visual stimuli.

A compression of perceptual auditory space, less pronounced though, was also observed in the Capture Task (CAP). It is well known that salient visual events can bias auditory localization in an attractive way—an effect known as 'auditory capture' or 'ventriloquism effect' (Bertelson and Aschersleben 1998; Alais and Burr 2004). Thus, it is more than plausible, that the perceptual compression in both tasks, SAC and CAP, was induced, at least in part, by this effect. Although statistically not significant, behavioral performance in the SAC and the CAP condition was not identical. The stronger compression and slight shift towards the saccade target in the SAC-condition therefore must be due to the different behavioral states in the two conditions. In the SAC-condition, the visual stimulus served as a saccade target. In the CAP-condition, however, it served as a distracter and a reflexive eye-movement towards this distracter had to be suppressed. From neurophysiological studies in monkeys as well as from behavioral studies on humans we know that suddenly appearing visual stimuli attract attention (Bisley and Goldberg 2003; Carrasco et al. 2004). In case of the saccades, the intention to make a

saccade spatially coincides with the focus of attention. The more pronounced effects in the SAC condition might thus be due to the spatial coincidence of the intended saccade-goal and the attentional spotlight induced by the appearance of the saccade target. There is one critical issue, however, that needs to be considered. In the SAC condition, the visual target, which was presented in the retinal periphery earlier in the trial, became a new foveal stimulus at the time the eye landed at the new position. This 'additional' visual stimulation hence could amplify the ventriloquism effect and, hence, amplify the perceptual compression of auditory space. At first glance, the notion of a 'new' stimulus appearing in the fovea after a saccade seems incompatible with the literature on object continuity across saccades (Deubel 2004). Nevertheless, it is conceivable, that such a stimulus elicits a transient response in cortical areas where object correspondence is not established but which might contribute to multisensory integration. As a consequence of this account, no compression should be observed if saccades were made in the absence of a visual target as is the case for memory guided saccades.

In line with other studies (Lewald and Ehrenstein 1996; Lewald 1998; Getzmann 2002; Razavi et al. 2007) we

29

found auditory localization to be influenced by the direction of gaze. In our case perceived positions were shifted by about one quarter of the underlying shift in eye position. As perceptual auditory space differs between the F1- and the F2-condition—the question arises as to when the transition from one state to the other takes place given that a saccade is made from F1 to F2. We found no evidence for such a transition in the brief perisaccadic period, suggesting that this effect is not a quick, instantaneous rearrangement of auditory space but happens at a larger time scale. Indeed, Razavi et al. (2007) have demonstrated, that a realignment of auditory space with changing eye position takes place within several minutes, following an exponential time course. In contrast to auditory localization, we did not find any significant differences between the three fixational conditions in the visual localization experiments. However, as a comparison of the compression indices between the F1- and F2-condition reveals, there was a strong tendency for visual localization to be biased towards the fovea ($P = 0.06$). Such a localization bias is in line with results reported by van der Heijden et al. (1999).

So far, our experiments [as well as earlier studies (e.g. Lewald and Ehrenstein 1996; Lewald 1998; Getzmann 2002; Razavi et al. 2007)] did not investigate the role of the visual stimuli used as fixation points or to guide eye-movements in detail. To address this issue we performed a second set of experiments using memory guided saccades as well as 'memory guided fixations' (i.e. conditions in which subjects were asked to fixate the position of a former visual stimulus in a complete dark environment).

Experiment 2

In experiment 1, we had studied localization during visually guided eye-movements. Given the potential interference of the visual fixation points with auditory localization, in experiment 2, subjects were tested in the same behavioral auditory localization paradigms, but in the absence of visual stimulation.

Materials and methods

Participants

Six right-handed human subjects (three female, average age: 24 years), who all had given written informed consent, participated in this experiment. All subjects were naïve as to the purpose of this study except for one of the authors. All subjects had previous experience in psychophysical studies but had not participated in experiment 1.

Experimental setup

The experimental setup used in this experiment was similar but not identical to the one used in Experiment 1. Visual stimuli were presented by means of a CRT-projector (150 Hz refresh rate) on a tangent screen covering the central $80° × 60°$ of the visual field at a distance of 1.14 m in front of the subject's head. Fixation positions were at $-10°$ left and at $+10°$ right from straight ahead. Possible target locations for the auditory stimuli were $+2.5°$, $+7.5°$, $+12.5°$ and $+17.5°$. Auditory stimuli were presented via the same moveable speaker as used in experiment 1. In this setup, the speaker was placed 1 cm behind the visually opaque but acoustically transparent projection screen. Again the movement sound of the speaker during the repositioning period at the beginning of each trial was masked by 2-s of white noise presented from a second speaker 1.3 m below the center of the screen. A ruler was presented after each trial to indicate the perceived location of the stimuli. In this experiment, a brief tactile stimulus was applied to the subjects' left index finger in the Saccade- (SAC) and in the Capture-Condition (CAP). This stimulation served as go-signal (SAC) and distractor (CAP), respectively. Tactile stimulation was generated using a vibration device that produced brief (20 ms) low frequency (∼200 Hz) stimulation. To obstruct any residual auditory stimulation by the vibration device it was placed in a small sound proof box, in which the subjects had to insert their left hand during the experiments. Again the right hand was used to control the response keyboard. Prior to each experiment, the positions of the vibration device and response keyboard were fixed in a way that subjects sat comfortably and arm posture was symmetrical relative to the body's midline.

Experimental paradigms

The experimental paradigms were similar to those tested in experiment 1, i.e. subjects were tested under the four conditions F1, F2, CAP and SAC. However, conditions were modified in such a way, that no visual stimuli were visible during the stimulus presentation phase (see Fig. 5). At the beginning of each trial the two fixation points F1 and F2 were both visible. Subjects fixated either the left fixation point (F1-, CAP- and SAC-condition) or the right fixation point (F2-condition) and started the trial by a key press. After 200 ms both points disappeared. The subjects were instructed to keep fixation at the same position until the end of the trial (F1-, F2- and CAP-condition). Alternatively, they had to keep fixation until a tactile go-signal had been given, then saccade towards the remembered position of F2 (SAC-condition). In both the CAP- and the SAC-condition a brief tactile stimulus was applied 750–1500 ms after trial start. In all conditions, times were chosen in such a way that the auditory stimuli fell into the perisaccadic period in the
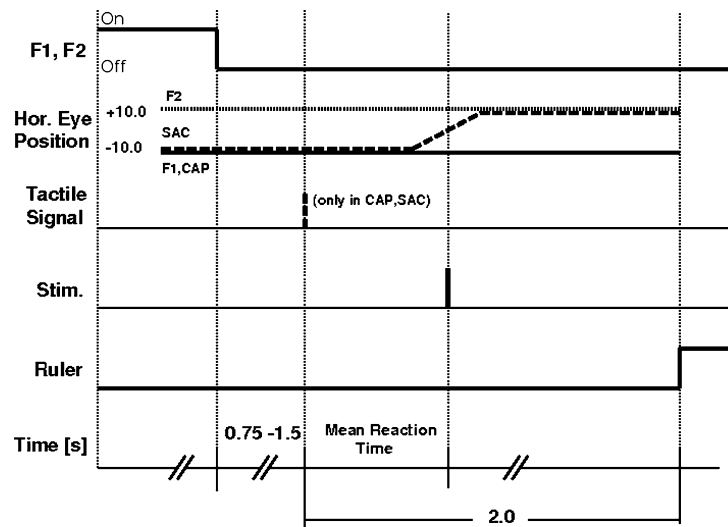
Fig. 5 Time course for the different paradigms of Experiment 2. Experiments were conducted in total darkness, during the trials no visual stimuli were visible. In the fixation conditions F1 (*solid line*) and CAP (*solid line*) subjects fixated in the dark at the position were the left fixation point had been presented before the beginning of the trial (i.e. at −10.0°). In F2-trials (*dashed line*) fixation in the dark was required at position +10.0°. In the SAC-condition (dotted line) subjects performed memory guided saccades from −10.0° to +10.0°. In this condition the saccade was triggered by a tactile stimulus on their left index finger. In the CAP-condition the same tactile stimulus served as a distractor
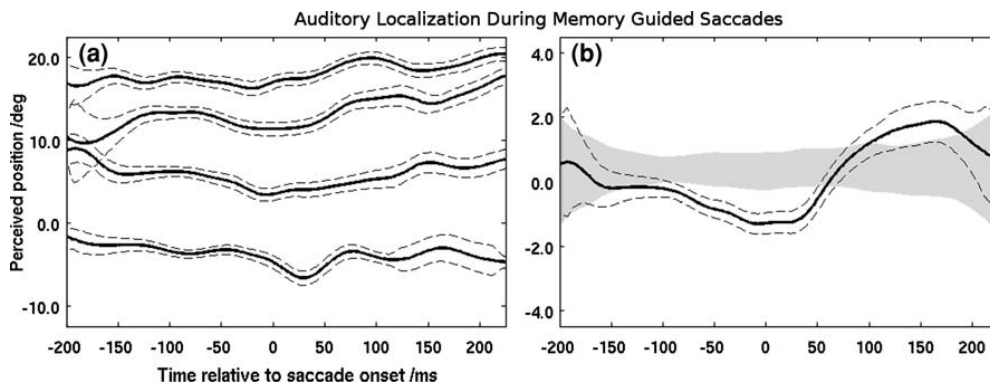

Auditory Localization During Memory Guided Saccades

Fig. 6 Localization of auditory stimuli during memory guided saccades. Conventions as in Fig. 2. Localization of auditory stimuli was modulated perisaccadically. Near saccade onset targets were mislocal-ized against the direction of the saccade. Briefly thereafter, there was a tendency for mislocalization in the opposite direction

saccade condition. To this end, stimuli were presented 200–350 ms after the tactile go-signal (CAP- and SAC condition) and 950–1,850 ms after trial begin (F1- and F2-condition), respectively. Before the start of the experiment, all subjects underwent a brief training session consisting of about 50 trials (half of which were saccade trials, the other half fixation trials). After training all subjects were able to keep fixation in the dark and generate appropriate memory guided saccades (see Supplementary Material, Fig. S1).

Data analysis

Data analysis was identical to experiment 1. To calculate the perisaccadic confidence interval, which allows to test for significant perisaccadic modulations in localization, data from an early presaccadic ($t < −100$ ms relative to saccade onset) and a late postsaccadic epoch ($t > 200$ ms after saccade onset) were used, as localization was stationary in these temporal epochs.

Fig. 7 Localization of auditory stimuli in saccade and fixation conditions in the absence of visual stimulation. Conventions as in Fig. 3. **a** In the fixation tasks (F1, F2) there was no evidence for an influence of gaze on localization. **b** Again perceptual space was compressed in the CAP and in the SAC-condition
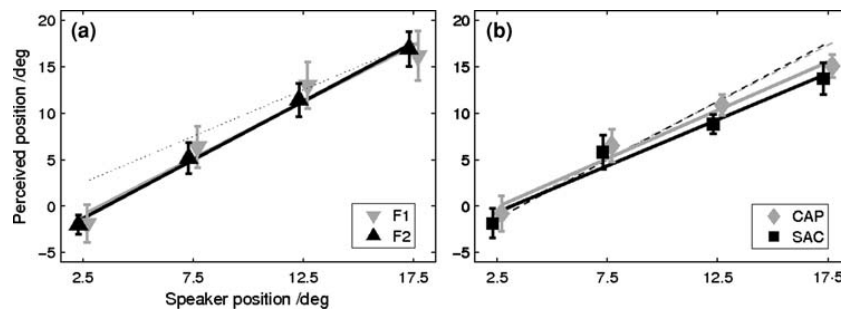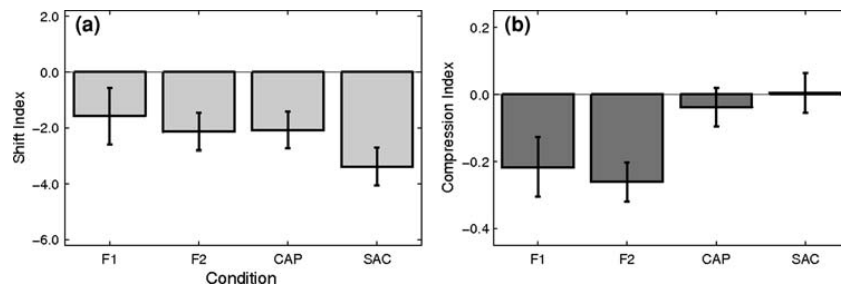
Fig. 8 Shift (**a**) and compression indices (**b**) for data from Experiment 2. Neither the shift nor the compression indices differed significantly between conditions (ANOVA for repeated measures). As in the first experiment, there was a tendency for the largest compression index to be observed in the saccade condition

Results

Time course of perisaccadic localization

Memory guided saccade durations were slightly longer (mean duration: 80 ms, SE: 11 ms) than comparable visually guided saccades (mean duration: 62 ms, SE 4 ms) and their endpoints were more variable (mean: 10.3°, SE: 1.0° vs. 9.0°, SE: 0.5°, see Supplementary Material, Fig. S1). Six percent of the trials had to be excluded because of movement inaccuracies. The time course for localization of auditory stimuli during memory guided saccades is shown in Fig. 6. Similar to the first experiment, we did not find any evidence for a crossmodal transfer of the well known mislocalization effect from the visual to the auditory domain. Again, for the auditory domain we found a significant modulation of perceived target position against the direction of the saccade for times close to saccade onset. For memory guided saccades, however, this effect was much stronger than for visually guided saccades. However, compared to the visual mislocalization effect it was rather small (3.1° peak modulation for visual stimuli as compared to −1.2° for auditory stimuli). After the end of the saccade, the stimuli were mislocalized against the direction of the saccade. Localization returned to a steady state level 200 ms after saccade onset.

Comparison of saccade and fixation conditions

Mean perceived positions in the different experimental conditions are shown in Fig. 7; the corresponding shift and

compression indices in Fig. 8. Perceived positions in all three fixational control conditions were shifted towards negative values compared to the actual stimulus positions—probably reflecting a response bias in this particular experimental setup. This shift was even more pronounced in the saccade condition. Notably, the clear difference in localization between conditions F1- and F2 as observed in the experiment was not present when the subjects were fixating in the dark. In the saccade condition perceptual space was again compressed as compared to the F1- and F2-conditions. Surprisingly, this was also the case in the CAP-condition. A statistical analysis of the compression indices of all four conditions (Fig. 8) did not reveal a significant effect ($P = 0.25$) (ANOVA for repeated measures). The same holds true for an analysis of the shift indices ($P = 0.66$) (ANOVA for repeated measures).

Discussion

In this second experiment perisaccadic localization of auditory stimuli differed from the well known (mis-)localization of visual stimuli[2] (e.g. Honda 1989; Cai et al. 1997; Lappe et al. 2000). Similar to the results of the first experiment, we observed a modulation of auditory localization: near saccade onset, perceived positions were shifted opposite to

---

[2] We did not study visual localization during memeory guided saccades in our setup. However, Awater and Lappe (2004) have demonstrated that the mislocalization pattern is independent of a visual saccade target.

32

421

the direction of the eye-movement. Thereafter, perceived locations were shifted in the direction of the eye-movement. 200 ms after saccade onset localization returned back to normal.

Similar to the results from our first experiment, we observed a compression effect in the saccade condition in comparison to the fixational control conditions F1 and F2. Surprisingly, we found the compression not only in the SAC but also in the CAP condition. Based on the available data, two mechanisms might explain this observation. First, the compression might have been caused by the tactile stimulation that has been applied in both conditions. Evidence for this hypothesis comes from a study by Caclin et al. (2002). These authors showed that auditory localization can be influenced by synchronous tactile stimulation in an attractive manner, similar to the capture of audition by vision in ventriloquism. However, given the stimulus arrangement in our study one would have expected either a complete shift of perceptual space towards the tactile stimulation (left hand), or an expansion of space [assuming an attraction effect, that loosens strength with increasing distance as reported by (Bolognini et al. 2007)]. Second, the observed compression might have been due to overt and covert processes involved in saccade preparation (and/or shifts of attention). All subjects underwent a training session in the saccade condition, prior to the actual experiment. It is conceivable that they have build up a strong association between the tactile signal and saccade execution. So, covert saccade related preparatory processes might have also been at work in the CAP-condition (Bracewell et al. 1996). Certainly, further experiments are needed to clarify this issue.

In the first experiment we found, in line with a number of earlier studies (Lewald and Ehrenstein 1996; Lewald 1998; Getzmann 2002; Razavi et al. 2007), a difference in sound localization between conditions in which subjects were fixating either a visual target on the left or on the right. In our second experiment we found no such effect of gaze direction in the absence of visual stimulation. This finding highlights the importance of the visual fixation target and suggests the presence of such a target to be an integral part of the described 'eye position' effect to evolve. This point has only received minor attention in the relevant literature so far and thus might, amongst others, explain part of the discrepancies in effect size and direction of an influence of eye position on auditory localization as reported in the literature. The question arises whether or not the 'eye position effect' is similar to or even identical with the ventriloquism effect. Typically, the ventriloquism effect has been studied using salient events, like flashing stimuli. Certainly, a persistent visual stimulus in an otherwise dark environment constitutes a salient feature per se. However, from our point of view both effects differ in a decisive

point: the ventriloquism effect compresses space around the location of the visual event (cf. Fig. 3b). The 'eye-position effect' rather shifts the complete perceptual space along with the eyes [cf. Fig. 3a or e.g. (Razavi et al. 2007)].

Nevertheless, the role of static visual stimuli should be further elaborated for a better understanding of both the 'eye-position effect' as well as the ventriloquism effect.

In summary, by using paradigms free of visual stimulation, we intended to explore the influence of visual stimulation on auditory localization. In the visually guided conditions in experiment 1 we observed two major effects: a strong influence of eye position and a perisaccadic compression of perceptual space. In the absence of visual stimulation in experiment 2, we did not observe a statistical difference between the shift indices or the compression indices between different behavioral conditions. We thus conclude visual stimulation (even if it is static) has a profound influence on auditory localization. Besides, our results include some evidence of a modulation of auditory spatial perception by eye-movements or related attentional mechanisms. Compared to the potential impact of the visual system these factors seem to be rather small. On the other hand, as the results of the CAP-condition in our visual localization experiment reveal, dynamic visual distractor stimuli do not seem to have a strong influence on visual localization performance. However, visual localization is readily susceptible to influences induced by dynamic changes in eye-position. This argument is not only supported by our and others results on perisaccadic localization (Honda 1989; Cai et al. 1997; Ross et al. 1997), but also by other studies on the influence of different types of eye-movements on visual localization (e.g. van Beers et al. 2001; Kaminiarz et al. 2007).

General discussion

In this study, we asked whether the well-known effect of perisaccadic mislocalization of visual stimuli generalizes to the auditory domain. Our results clearly show that this is not the case. In the visual control condition, we found a strong shift-like mislocalization effect. This finding is in accordance with a number of previous reports (e.g. Honda 1989; Cai et al. 1997; Lappe et al. 2000). In contrast, perisaccadic localization of auditory stimuli was rather stationary. A comparably small modulation of perceived location against the direction of the saccade was observed for both visually guided and memory guided saccades. However, as both direction and effect size diverged for the visual and the auditory stimulus modalities, those phenomena are clearly independent. Our results suggest that, perisaccadically, localization of visual and auditory stimuli relies on different cortical representations. When tested under laboratory

33

conditions, the visual spatial representation reveals gross distortions. On the other side, the auditory representation is rather unaffected by the rapid change in eye position. This observation suggests that—at least perisaccadically—part of the spatial auditory processing stream is only mildly influenced by eye position. In line with this conclusion are results from macaque inferior colliculus and auditory cortex (Groh et al. 2001; Werner-Reiss et al. 2003; Woods et al. 2006). These studies clearly show that in relevant areas (IC and auditory cortex) eye position modulates neuronal activity but keeps spatial tuning unaffected.

Above, we had introduced the idea of a supra-modal representation of space that might be advantageous to guide behavior based on multisensory input. Our results do not support this notion for perisaccadic perception. However, they should not be considered as evidence against supra-modal multisensory representations and their benefits in general. Preferably, they should be seen in line with numerous studies which discuss multisensory integration in the framework of optimal signal integration (e.g. Binda et al. 2007; Rowland et al. 2007; Reeve et al. 2008). In this framework, our psychophysical findings can be explained without the assumption of separate neural populations and thus it holds the potentiality to conjoin them with the above-mentioned physiological results on the representation of multisensory space in parietal cortex (Schlack et al. 2005).

References

Alais D, Burr D (2004) The ventriloquist effect results from near-optimal bimodal integration. Curr Biol 14:257–262

Avillac M, Deneve S, Olivier E, Pouget A, Duhamel JR (2005) Reference frames for representing visual and tactile locations in parietal cortex. Nat Neurosci 8:941–949

Awater H, Lappe M (2004) Perception of visual space at the time of pro- and anti-saccades. JNeurophysiol 91:2457–2464

Bertelson P, Aschersleben G (1998) Automatic visual bias of perceived auditory location. Psychon Bull Rev 5:482–489

Binda P, Bruno A, Burr DC, Morrone MC (2007) Fusion of visual and auditory stimuli during saccades: a Bayesian explanation for peri-saccadic distortions. J Neurosci 27:8525–8532

Bischof N, Kramer E (1968) Investigations and considerations of directional perception during voluntary saccadic eye movements. Psychol Forsch 32:185–218

Bisley JW, Goldberg ME (2003) Neuronal activity in the lateral intraparietal area and spatial attention. Science 299:81–86

Bolognini N, Leo F, Passamonti C, Stein BE, Ladavas E (2007) Multisensory-mediated auditory localization. Perception 36:1477–1485

Bracewell RM, Mazzoni P, Barash S, Andersen RA (1996) Motor intention activity in the macaque's lateral intraparietal area. II. Changes of motor plan. J Neurophysiol 76:1457–1464

Bremmer F (2005) Navigation in space—the role of the macaque ventral intraparietal area. J Physiol 566:29–35

Bremmer F, Schlack A, Duhamel JR, Graf W, Fink GR (2001a) Space coding in primate posterior parietal cortex. Neuroimage 14:S46–S51

Bremmer F, Schlack A, Shah NJ, Zafiris O, Kubischik M, Hoffmann K-P, Zilles K, Fink GR (2001b) Polymodal motion processing in posterior parietal and premotor cortex: a human fMRI study strongly implies equivalencies between humans and monkeys. Neuron 29:287–296

Bremmer F, Klam F, Duhamel J-R, Ben Hamed S, Graf W (2002) Visual-vestibular interactive responses in the macaque ventral intraparietal area (VIP). Eur J Neurosci 16:1569–1586

Caclin A, Soto-Faraco S, Kingstone A, Spence C (2002) Tactile "capture" of audition. Percept Psychophys 64:616–630

Cai RH, Pouget A, Schlag-Rey M, Schlag J (1997) Perceived geometrical relationships affected by eye-movement signals. Nature 386:601–604

Carrasco M, Ling S, Read S (2004) Attention alters appearance. Nat Neurosci 7:308–313

Colby CL, Duhamel JR, Goldberg ME (1993) Ventral intraparietal area of the macaque: anatomic location and visual response properties. J Neurophysiol 69:902–914

Deubel H (2004) Localization of targets across saccades: Role of landmark objects. Vis Cogn 11:173–202

Duhamel JR, Bremmer F, BenHamed S, Graf W (1997) Spatial invariance of visual receptive fields in parietal cortex neurons. Nature 389:845–848

Getzmann S (2002) The effect of eye position and background noise on vertical sound localization. Hear Res 169:130–139

Groh JM, Trause AS, Underhill AM, Clark KR, Inati S (2001) Eye position influences auditory responses in primate inferior colliculus. Neuron 29:509–518

Honda H (1989) Perceptual localization of visual stimuli flashed during saccades. Percept Psychophys 45:162–174

Jay MF, Sparks DL (1984) Auditory receptive fields in primate superior colliculus shift with changes in eye position. Nature 309:345–347

Kaas JH, Nelson RJ, Sur M, Lin CS, Merzenich MM (1979) Multiple representations of the body within the primary somatosensory cortex of primates. Science 204:521–523

Kaiser M, Lappe M (2004) Perisaccadic mislocalization orthogonal to saccade direction. Neuron 41:293–300

Kaminiarz A, Krekelberg B, Bremmer F (2007) Localization of visual targets during optokinetic eye movements. Vision Res 47:869–878

Klingenhoefer S, Bremmer F (2004) Perisaccadic mislocalization of auditory targets. In: Ilg UJ, Bülthoff HH, Mallot HA (eds) Dynamic perception. AKA Akad Verlag, Berlin, pp 65–70

Lappe M, Awater H, Krekelberg B (2000) Postsaccadic visual references generate presaccadic compression of space. Nature 403:892–895

Lewald J (1998) The effect of gaze eccentricity on perceived sound direction and its relation to visual localization. Hear Res 115:206–216

Lewald J, Ehrenstein WH (1996) The effect of eye position on auditory lateralization. Exp Brain Res 108:473–485

Matin L, Pearce DG (1965) Visual perception of direction for stimuli flashed during voluntary saccadic eye movements. Science 148:1485–1488

Razavi B, O'Neill WE, Paige GD (2007) Auditory spatial perception dynamically realigns with changing eye position. J Neurosci 27:10249–10258

Reeve P, Clark JJ, O'Regan JK (2008) Convergent localization near saccades without equivalent compression of perceived separation. J Vis 8:1–19

34

Ross J, Morrone MC, Burr DC (1997) Compression of visual space before saccades. Nature 386:598–601

Rowland B, Stanford T, Stein B (2007) A Bayesian model unifies multisensory spatial localization with the physiological properties of the superior colliculus. Exp Brain Res 180:153–161

Schlack A, Hoffmann KP, Bremmer F (2002) Interaction of linear vestibular and visual stimulation in the macaque ventral intraparietal area (VIP). Eur J Neurosci 16:1877–1886

Schlack A, Sterbing-D'Angelo SJ, Hartung K, Hoffmann KP, Bremmer F (2005) Multisensory space representations in the macaque ventral intraparietal area. J Neurosci 25:4616–4625

van Beers RJ, Wolpert DM, Haggard P (2001) Sensorimotor integration compensates for visual localization errors during smooth pursuit eye movements. J Neurophysiol 85:1914–1922

van der Heijden AH, van der Geest JN, de Leeuw F, Krikke K, Müsseler J (1999) Sources of position-perception error for small isolated targets. Psychol Res 62:20–35

Wandell BA, Dumoulin SO, Brewer AA (2007) Visual field maps in human cortex. Neuron 56:366–383

Werner-Reiss U, Kelly KA, Trause AS, Underhill AM, Groh JM (2003) Eye-position affects activity in primary auditory cortex of primates. Curr Biol 13:554–562

Woods TM, Lopez SE, Long JH, Rahman JE, Recanzone GH (2006) Effects of stimulus azimuth and intensity on the single-neuron activity in the auditory cortex of the alert macaque monkey. J Neurophysiol 96:3323–3337

Depth perception during saccades

Tobias Teichert NeuroPhysics Group, Department of Physics, Philipps University, Marburg, Germany

Steffen Klingenhoefer NeuroPhysics Group, Department of Physics, Philipps University, Marburg, Germany

Thomas Wachtler NeuroPhysics Group, Department of Physics, Philipps University, Marburg, Germany

Frank Bremmer NeuroPhysics Group, Department of Physics, Philipps University, Marburg, Germany

A number of studies have investigated the localization of briefly flashed targets during saccades to understand how the brain perceptually compensates for changes in gaze direction. Typical version saccades, i.e., saccades between two points of the horopter, are not only associated with changes in gaze direction, but also with large transient changes of ocular vergence. These transient changes in vergence have to be compensated for just as changes in gaze direction. We investigated depth judgments of perisaccadically flashed stimuli relative to continuously present references and report several novel findings. First, disparity thresholds increased around saccade onset. Second, for horizontal saccades, depth judgments were prone to systematic errors: Stimuli flashed around saccade onset were perceived in a closer depth plane than persistently shown references with the same retinal disparity. Briefly before and after this period, flashed stimuli tended to be perceived in a farther depth plane. Third, depth judgments for upward and downward saccades differed substantially: For upward, but not for downward saccades we observed the same pattern of mislocalization as for horizontal saccades. Finally, unlike localization in the fronto-parallel plane, depth judgments did not critically depend on the presence of visual references. Current models fail to account for the observed pattern of mislocalization in depth.

Introduction

Humans and other primates perform fast ballistic eye movements (saccades) on average three times a second. These saccades are accompanied by large changes in direction of gaze and ocular vergence. Even pure version saccades, i.e., saccades from one point of the horopter to another, induce transient changes in vergence caused by slight differences in the velocity profiles between the two eyes (Collewijn, Erkelens, & Steinman, 1988a). A typical horizontal saccade is accompanied by a brief divergent and a subsequent convergent component. Upward saccades show the same pattern, while downward saccades show an inverted pattern, i.e., an initial convergent and a subsequent divergent component (Collewijn, Erkelens, & Steinman, 1988b).

A large number of studies have investigated the localization of perisaccadically flashed stimuli to test how the visual system accounts perceptually for the large changes in gaze direction (e.g., Cai, Pouget, Schlag-Rey, & Schlag, 1997; Honda, 1989, 1991; Lappe, Awater, &

Krekelberg, 2000; Morrone, Ross, & Burr, 1997; Ross, Morrone, & Burr, 1997). Two distinct patterns of mislocalization in the fronto-parallel plane were observed which seem to depend on the presence of visual references and/or the ambient lighting conditions (Lappe et al., 2000; Morrone, Ma-Wyatt, & Ross, 2005a). In the dark, i.e., in the absence of visual references, perisaccadically flashed stimuli are uniformly mislocalized in the direction of the saccade vector when flashed prior to saccade onset, and in the opposite direction shortly thereafter (perisaccadic shift: Cai et al., 1997; Honda, 1989, 1991). In ambient light conditions and in the presence of visual references, perisaccadically flashed stimuli are mislocalized toward the endpoint of the saccade (perisaccadic compression: Morrone et al., 1997; Ross et al., 1997).

So far, it is not known whether depth judgments are affected perisaccadically in a way similar to judgments about the location in the fronto-parallel plane. In the present study we examined perisaccadic depth judgments of stimuli flashed around the onset of horizontal and vertical saccades—both in the dark and in ambient light conditions. Our experiments were designed to test whether

explanations put forward to explain the mislocalization in the fronto-parallel plane also apply to localization in depth.

Methods

Experimental setup

Stimuli were presented binocularly on a Wheatstone stereoscope. Subjects were seated in front of a mirror system, head movements were restricted with a chin rest. The mirrors of the stereoscope were positioned 5 cm in front of the subjects' eyes. A PC with a 100 Hz dual head graphics card was used to present the stimuli on two identical 15″ monitors with a resolution of 1024 × 768 pixels each. Monitors were positioned 75 cm left and right of the mirror system, amounting to a total viewing distance of 80 cm. Pixel size was 1.3′. Positions of both eyes were measured with an infrared eye tracker (EyeLink2, SR Research Inc.) with a temporal resolution of 2 ms.

Stimuli

Subjects initialized a trial by pressing a key on the computer keyboard. A fixation target which consisted of a long vertical bar (size 13′ × 90′) and a short horizontal bar (30′ × 13′) appeared either 3.25° to the left or to the right of the center of the display on the horizontal meridian (Figure 1). After a fixed temporal interval ($t = 500$ ms) an identical saccade target appeared at the opposite side with respect to the vertical meridian. The fixation cross remained on the screen and subjects were required to maintain fixation for a variable temporal interval ($t = 1000$ ms–2000 ms). The subject's 6.5° right- or leftward saccade was induced by the disappearance of the small horizontal bar of the fixation target.

At 8 different times relative to this go-signal a small vertical bar (13′ × 90′) was flashed for a single frame (10 ms)
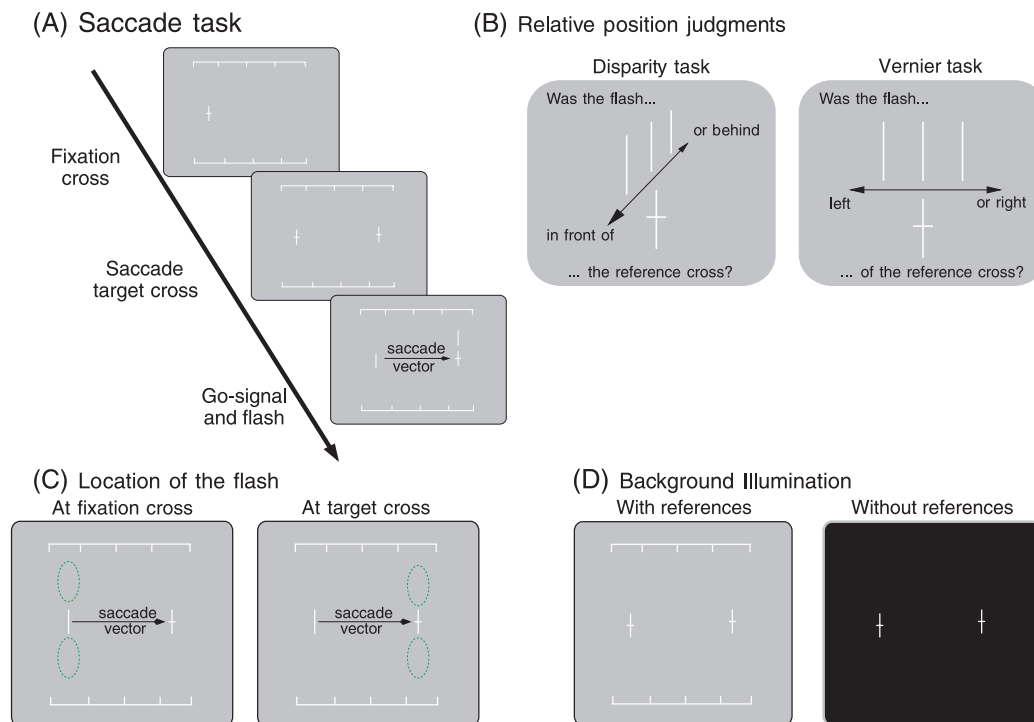
Figure 1. Methods. Subjects performed 6.5° left and rightward saccades (A) while performing a disparity or a vernier task (B) of a briefly flashed bar. The bar was in front of, in the same depth, or behind the reference in the depth task. In the vernier task the bar was left, right, or at the same lateral position as the reference. The flashed bar could appear either above or below the fixation or the saccade target (C) which served as reference for the tasks in the corresponding trials. The experiment was performed either in presence or absence of additional visual references (D). Stimuli were presented on a Wheatstone stereoscope.

either above or below the fixation or the saccade target. Depending on the position of the flash, either the fixation or the saccade target served as reference for the relative position task (see below). On any given trial, either the fixation or saccade target was pseudo-randomly chosen to serve as the reference. The choice of the reference did not depend on the timing of the flash relative to the saccade go signal. Similarly, the vertical position of the flash either above or below the reference was chosen pseudo-randomly. In different blocks of trials either the horizontal position or the depth of the flashed bar had to be judged relative to the reference.

Vertical saccades

Conditions in experiments with vertical saccades were kept as similar as possible to those for horizontal saccades. However, a few changes were inevitable. The fixation target appeared either 3.25° above or below the center of the display. The flash appeared either to the left or to the right of the fixation or the saccade target, respectively. The flashed bar was slightly larger ($45' \times 90'$) than in the experiments with horizontal saccades.

Depth judgments

In the blocks of trials which required depth judgments, the bar was flashed with either crossed, uncrossed or zero disparity. In a two-alternative forced-choice (2AFC) procedure subjects judged whether the flashed bar was in front of or behind the reference which defined the plane of fixation, i.e., zero disparity. The disparity offsets were chosen well above each subject's individual threshold as determined during steady fixation. For the horizontal saccades, disparity values of ± 2.6 and $0'$ were used for two subjects. For one subject with slightly larger disparity thresholds we presented disparity values of ± 5.2 and $0'$. A larger range of disparity values of ± 7.8, ± 2.6, and $0'$ was used for the vertical saccades (see Results).

To avoid subjects from being able to solve the task monocularly, the horizontal position of the flash was given a random lateral offset. The amount of this jitter was in the same order of magnitude as the horizontal disparity value. Accordingly, the horizontal position of the flash relative to the reference in one eye alone could not be mapped to a given horizontal disparity.

Vernier judgments

In the blocks of trials which required horizontal vernier judgments, the bar was flashed either to the left, to the right or at the same horizontal position as the reference. In a 2AFC-procedure subjects judged whether the flashed bar was to the left or to the right of the reference. The magnitude of the lateral shift

(± 21 minutes of arc) was chosen well above each subject's individual threshold.

Background illumination

Experiments 1 and 2 were performed under two different lighting conditions. Experiment 1 was performed in a completely dark room with a black monitor background that lacked any visual references. In order to minimize phosphor persistence effects and to reduce the background luminance below detection threshold, tinted panes were placed in front of the monitors in this condition. Under such conditions, perisaccadic shift can be observed reliably (Cai et al., 1997; Honda, 1989, 1991; Lappe et al., 2000). In Experiment 2, a gray background and two white horizontal rulers were permanently visible 4.3° above and below the fixation and saccade target. Under these conditions, perisaccadic compression can be induced reliably (Lappe et al., 2000; Ross et al., 1997).

Luminance and phosphor decay in the two conditions were measured using a photometer (Photoresearch Spectraspot SPRD) and a fast photo diode (Siemens BPX63). Background luminance was 130 and 0.1 cd/m^2 in the compression and shift condition, respectively. Stimulus luminance was 280 and 25 cd/m^2, respectively. Phosphor decay times were measured as the decay time to 10% of the peak value after presentation of a stimulus. From this data we calculated the time it took for the stimulus luminance to drop below the luminance of the uniform background as 4 ms and 3 ms for the compression and shift condition, respectively.

Data processing

Times of saccade onset were calculated offline with in-house software. Saccades were defined as contiguous epochs with a velocity above 54 degree per second and the maximum velocity surpassing a threshold of 162 degrees per second. Saccade amplitude was defined as the displacement in the relevant direction during the saccade. Only trials with saccades of an amplitude larger than 3.2 degrees were used for the analysis. The delay between stimulus presentation and eye-position signal was estimated to be below 5 ms.

Responses of the subjects were coded as plus or minus one, corresponding to the right and left mouse-button, respectively. A moving average of the responses with respect to the time between flash and saccade onset was calculated offline for each stimulus condition separately. Moving averages were calculated using a Gaussian kernel with a standard deviation of 8 ms. In a bootstrap-procedure 100 identical moving averages were calculated, using re-sampled responses randomly drawn from the pool of responses acquired more than 50 ms before or after saccade onset. The boot-strapped moving averages were based on identical trial-times as the original moving averages. Only the responses for each trial were randomized. Time-resolved

5% and 95% quantiles of the 100 bootstrapped moving averages were used as lower and upper bounds to determine epochs during which subjects' responses were significantly different from what would be expected if depth judgments were not affected perisaccadically. The width of the confidence interval is mainly a function of the number of trials in a certain time bin. Time bins with many trials will yield a narrow confidence interval.

Whenever five different relative disparity values were presented, time-resolved psychometric functions were determined. At each time point, cumulative Gaussians with two parameters were fit to the five moving averages. The same process was repeated 100 times for the 100 bootstrapped moving averages which were calculated as described above. This procedure rendered confidence intervals for the parameters of the psychometric function under the assumption that depth judgments were not affected perisaccadically. As for the individual moving averages, the width of the confidence intervals for the

psychometric parameters decreases with the number of trials in that time bin.

Results

Experiment 1: Depth and vernier judgments in the absence of visual references

In Experiment 1, we tested depth perception during left and rightward horizontal saccades in the absence of visual references. Such conditions have previously been shown to elicit a shift-like pattern of mislocalization in the fronto-parallel plane (Cai et al., 1997; Honda, 1989, 1991; Lappe et al., 2000). Three human observers performed vernier and depth judgments of flashed stimuli relative
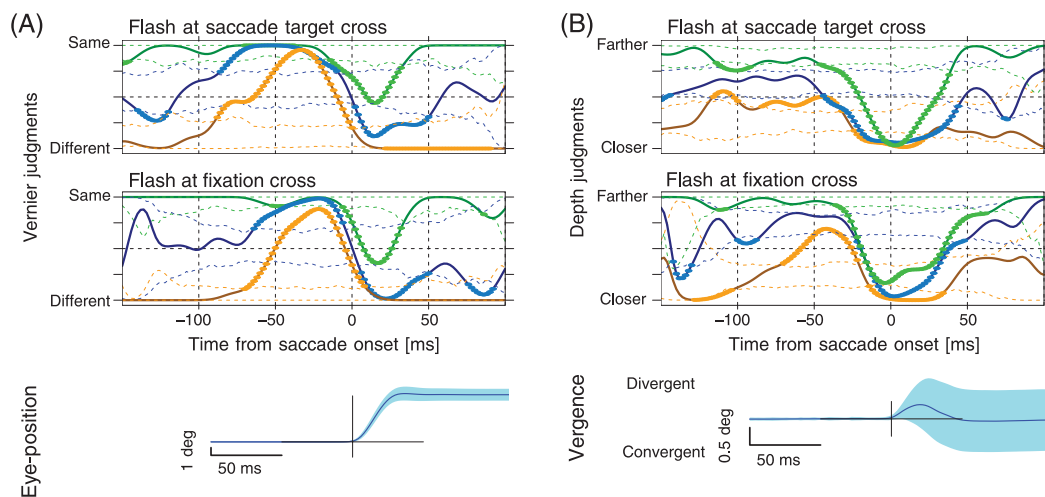

Figure 2. Vernier (A) and depth judgments (B) in the absence of visual references. Moving averages of the results of the 2AFC vernier (A) and depth (B) judgments as a function of time relative to saccade onset at *t* = 0 ms. Both panels show moving averages with data pooled across all subjects. Individual subjects show similar results (data not shown). Different colors correspond to different stimuli. In the vernier task, the blue color represents stimuli with the same horizontal position as the reference. The green and orange color corresponds to stimuli, which are positioned relative to the reference in the opposite and the same direction of the saccade vector, respectively. For example, for rightward saccades, the green color corresponds to stimuli right of the reference. For leftward saccades, the green color corresponds to stimuli left of the reference. In the depth task, orange corresponds to crossed disparity, blue to zero disparity, and green to uncrossed disparity. Dotted lines demarcate the confidence limits (see Methods). Bright dots on the solid lines denote periods when the moving averages were outside of these confidence limits. In the lower panel, mean and standard deviation of perisaccadic changes in gaze-direction (A) and ocular vergence (B) are depicted by the blue line and blue shaded area, respectively. (A) In the vernier task, subjects judged the flashed stimulus as being either left or right of the reference. For the analysis, these judgments were coded as being either in the same or opposite direction of the saccade vector. For example, during rightward saccades a 'right'-response corresponded to a 'same'-judgment. Vernier judgments reveal the expected bi-phasic pattern of mislocalization in direction of the saccade vector before saccade onset (orange and blue line from −50 to 0 ms relative to saccade onset) and contrary to its direction after saccade onset (green and blue line from 0 to 30 ms after saccade onset). (B) Depth judgments reveal a distinct pattern of mislocalization in depth. Stimuli flashed from −20 to 30 ms relative to saccade onset were mislocalized to a closer depth plane (green and blue line), while stimuli shortly before and after this period tended to be mislocalized to a farther depth plane (orange and blue line).

to a continuously present reference, while performing 6.5 degree left- and rightward saccades. Figures 2A and 2B show the results of the vernier and depth task, respectively. Responses pooled over subjects and saccade directions are shown as a function of time relative to saccade onset. In the case of correct performance, the green and the orange data lines would run at the bottom and the top of the panel, respectively. However, differing from veridical perception and confirming previous results (Cai et al., 1997; Honda, 1989, 1991; Lappe et al., 2000) vernier judgments revealed a biphasic shift pattern (see Figure 2A). Prior to saccade onset, stimuli were mislocalized in direction of the saccade vector (orange and blue line in Figure 2A, −50 to 0 ms relative to saccade onset). In contrast, stimuli were mislocalized in direction opposite to the saccade direction when flashed after saccade onset (green and blue line in Figure 2A, 0 to 30 ms after saccade onset). The timing of the shift pattern is slightly earlier than has been reported in previous studies (Cai et al., 1997; Honda, 1989, 1991; Lappe et al., 2000).

Figure 2B shows the results of the 2AFC depth judgments. Stimuli flashed more than 100 ms before or more than 50 ms after saccade onset were correctly perceived to be in front of the reference cross when presented with crossed disparity (orange line in Figure 2B). In the same time interval, stimuli with uncrossed disparity were reliably judged as being behind the reference (green line). However, almost all stimuli flashed from −20 to +30 ms relative to saccade onset were perceived to be in front of the reference, even if they were presented in the same or a farther depth plane (blue and green lines in Figure 2B). In contrast, stimuli flashed around 100 to 50 ms before or 30 to 70 ms after saccade onset had a tendency to be mislocalized to a farther depth plane (blue and orange line).

For vernier as well as the depth judgments we observe a decrease in the width of the confidence interval toward the time of saccade onset. Time bins long before or long after saccade onset typically have wider confidence intervals. This is accompanied by a general increase in variability of the moving averages which is especially evident for the zero shift and zero disparity condition. Both effects are due to differences in sampling density in different time-bins. The higher sampling density in the time window from −50 to 50 ms after saccade onset decreases the variability of the moving averages which in turn leads to the narrower confidence intervals. This effect is especially evident in the zero-shift and zero-disparity conditions because the variance of a binomial distribution peaks at a probability p of 0.5 which is close to the response probability for these conditions.

Experiment 2: Depth and vernier judgments in the presence of visual references

Localization in the fronto-parallel plane depends critically on the presence of visual references and/or the background lighting conditions (Lappe et al., 2000; Morrone et al., 2005a). In the second experiment we tested whether localization in depth shows a similar dependency. Three observers performed 2AFC vernier and depth judgments in conditions known to elicit perisaccadic compression (Lappe et al. 2000; Morrone et al., 1997; Ross et al., 1997). Figures 3A and 3B show the results of the vernier and depth task, respectively.

The vernier judgments no longer showed the biphasic shift pattern observed in the data of Experiment 1. Instead, they revealed a pattern, which was compatible with perisaccadic compression. Stimuli flashed beyond the
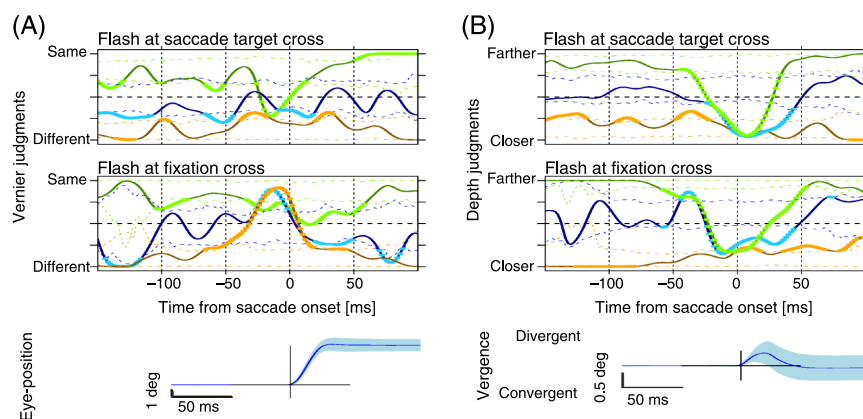
Figure 3. Vernier (A) and depth judgments (B) in the presence of visual references. Conventions as in Figure 2. (A) Vernier judgments provide evidence for mislocalization of flashed stimuli towards a point close to the saccade target (saccadic compression). (B) Depth judgments reveal a similar pattern of mislocalization in depth as observed in the absence of visual references. In this case, however, the flanking regions, i.e., the periods with mislocalization to a farther depth plane, are less prominent.

saccade target cross were mislocalized opposite to the direction of the saccade when flashed around saccade onset (green line, upper panel of Figure 3A). All other stimuli were mislocalized in direction of the saccade (blue and orange lines). Compression occurred slightly earlier than would be expected from previous studies (Lappe et al., 2000; Morrone et al., 1997; Ross et al., 1997). Overall, this pattern is consistent with compression toward a point in space close to the saccade target.

Figure 3B shows the results of the depth judgments during conditions which cause perisaccadic compression. A similar pattern of mislocalization in depth could be observed as in the condition without visual references. Further, there was no apparent difference between stimuli flashed at fixation and saccade target. However, while the effect of mislocalization to a closer depth plane around saccade onset was equally pronounced, the temporal flanking periods with mislocalization toward a farther depth plane seemed less pronounced than in the condition without visual references. Finally, strongest mislocalization was observed at saccade onset, i.e. at the same time as in Experiment 1.

Timing of mislocalization towards a closer depth plane

So far, our results suggest that mislocalization toward a closer depth plane starts well before saccade onset. It is critical to rule out that phosphor decay or temporal smoothing used to calculate the moving averages are responsible for the early onset (see Methods). We measured phosphor decay times in the range of 4 ms (see Methods). Thus, it seems unlikely that phosphor decay might account for the early onset of the mislocalization which starts about 25 ms before saccade onset.

In our previous analyses we had used a symmetric Gaussian kernel with a standard deviation of 8 ms to smooth the data in time. This smoothing might have contributed to the early onset of the effect. To rule out this possibility we repeated the analyses using a Gaussian with a smaller standard deviation (3 ms), a rectangular kernel with a total width of 10 ms as well as an asymmetric exponential kernel with a half-height decay time of 3.5 ms. Using the bootstrap method described above we determined time points where the moving average deviated from what would have been expected based on the distribution of responses to stimuli flashed more than 50 ms before saccade onset.

Pooling all responses to uncrossed stimuli from Experiments 1 and 2, we found evidence for mislocalization toward a closer depth plane as early as 25, 22, and 19 ms before saccade onset for the three kernels, respectively. For the zero disparity stimuli the values were 20, 19, and 16 ms, respectively. Thus, our results clearly support the notion that the effect of mislocalization toward a closer depth plane starts well before saccade onset.

Similarly, we estimated the end of the period of mislocalization to a closer depth plane. In this case, the asymmetric exponential kernel was inverted in time. For the stimuli with crossed disparity we found values of 29, 25, and 23 ms, respectively, for the three kernels. For the zero disparity stimuli we found values of 37, 32, and 30 ms, respectively. Given an average saccade duration of 33 ms, our data suggest that the effect of mislocalization probably does not persist beyond saccade offset.

As mentioned previously, perisaccadic compression and perisaccadic shift appeared earlier than would be expected from the literature. If this discrepancy were to be caused by delays in the system this would also affect our estimate of the time of onset of mislocalization toward a closer depth plane. However, the delay was estimated to be below 5 ms and hence does not change our interpretation that the effect starts before saccade onset.

Experiment 3: Depth judgments during vertical saccades

The mislocalization in depth observed in Experiments 1 and 2 might have been caused by perisaccadic suppression or changes in attentional load imposed by saccade planning and execution. From these experiments it is not clear whether the transient changes of ocular vergence contribute to the mislocalization. To investigate this possibility we tested whether the pattern of mislocalization depends on the sign of the vergence changes during saccades. To that end subjects performed up- and downward saccades which have been shown to give rise to inverted pattern of vergence changes (Collewijn et al., 1988b): upward saccades are accompanied by an initial divergent and a subsequent convergent component, much like horizontal saccades. Downward saccades, in contrast, are accompanied by an initial convergent and a subsequent divergent component.

Two observers performed 2AFC depth judgments of flashed stimuli relative to a continuously present reference while performing 6.5 degree up- and downward saccades. Judgments were performed in the presence of visual references. Vernier judgments were not measured for vertical saccades, because it had been shown previously that there are no differences in mislocalization in the fronto-parallel plane between horizontal and vertical saccades (Honda, 1991).

Pilot experiments had revealed strong effects of perisaccadic suppression during vertical saccades. A considerable fraction of perisaccadic flashes were not seen during vertical saccades, while during horizontal saccades subjects had detected almost all flashed stimuli. To account for this difference, the width of the flashed bars was increased (see Methods). Further, we used a wider range of disparity values in order to fit time-resolved psychometric functions to the data.

42

The results of the depth judgments during vertical saccades are presented in Figure 4. The pattern of mislocalization during upward saccades was similar to that observed for horizontal saccades. Stimuli flashed around saccade onset tended to be perceived in a closer depth plane, while stimuli flashed shortly before or after this period tended to be mislocalized to a farther depth plane. However, for downward saccades, a clearly different pattern emerged. Although perisaccadic depth judgments were impaired, there was no tendency to perceive perisaccadically flashed bars in front of the reference. Additional analyses revealed that for downward saccades, perisaccadic performance for large crossed and uncrossed disparities was significantly above chance-level.

Experiment 4: Comparison of depth judgments during horizontal and vertical saccades

In Experiments 1 and 2, only a single very small disparity offset was used. Hence, we performed an additional experiment with horizontal saccades using the same stimuli and range of disparities as for the vertical saccades in Experiment 3. This enabled us to directly compare psychometric functions for upward, downward, and horizontal saccades. Figure 5 shows the results for the left- and rightward saccades separately. The results are consistent with Experiments 1 and 2.

We separately fit time-resolved psychometric functions to the data for rightward, leftward, upward and downward saccades (see Methods for details). Furthermore, the data were split according to the position of the flash at the fixation or saccade target. Figures 6A and 6B show the estimated parameters for flashes at the fixation and saccade target, respectively. The panels in Figure 6A show the mean of the fitted cumulative Gaussian (point of subjective equality, PSE). PSE values above 7.8 min or below −7.8 min arc depend on extrapolation, as the largest disparity offsets were ±7.8 min arc. Thus, the precise values of parameter estimates close to or outside this range are uncertain. The panels in Figure 6B display the width of the fitted Gaussian (just noticeable difference, JND) as a function of time of the flash relative to saccade onset. Data are displayed separately for rightward (blue), leftward (green), upward (orange), and downward (red) saccades. Time points at which the parameter estimate is outside the confidence interval (see Methods) are indicated by a bright dot in the corresponding color.

We observe a significant increase in JND around saccade onset. The increase starts between 50 and 40 ms before saccade onset and lasts until 30 to 40 ms after saccade onset. In most cases the PSE shifts beyond the range of displayed disparity values (see below). In those time-bins, both the PSE and JND depend mainly on extrapolation and the precise values should be interpreted with caution.

The main effect of mislocalization toward a closer depth plane around saccade onset is reflected as a shift of the PSE toward positive disparity values (farther depth plane) for the horizontal and upward saccades. For these cases,
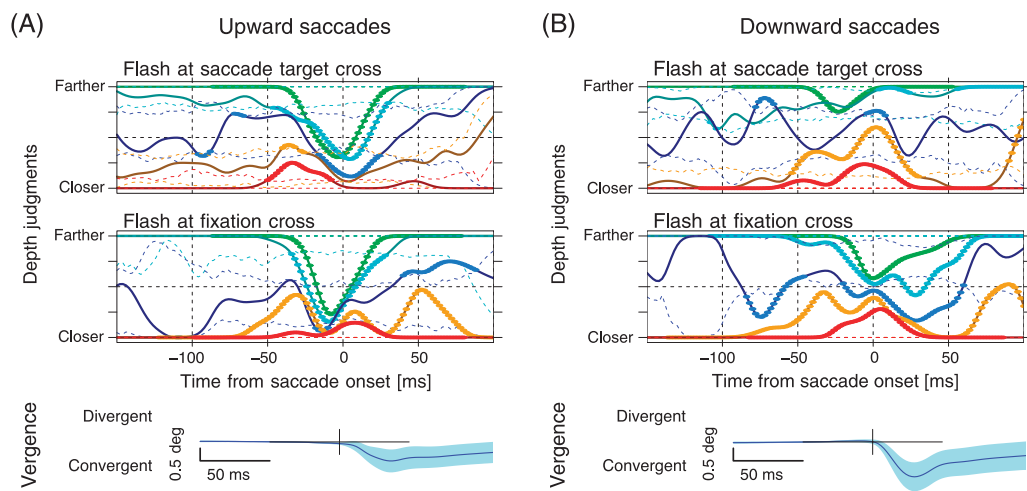
Figure 4. Depth judgments during vertical saccades. (A) Conventions similar to Figure 2B. However, green and cyan colors correspond to large and small uncrossed disparities, blue corresponds to zero disparity, and red and orange correspond to large and small crossed disparities. (A) During upward saccades, a similar tri-phasic pattern of mislocalization in depth can be observed as for the horizontal saccades. (B) Depth judgments during the downward saccades reveal a different pattern. Depth judgments appear to be slightly impaired during saccades but show no clear indication of a shift in depth.

Figure 5. Depth judgments during horizontal saccades. Conventions as in Figure 4. Background lighting conditions as in Experiments 2 and 3. Results with 5 different disparity values are similar to the ones reported with 3 disparity values in Figures 2B and 3B. Furthermore, leftward (A) and rightward (B) saccades reveal a similar pattern of mislocalization in depth.
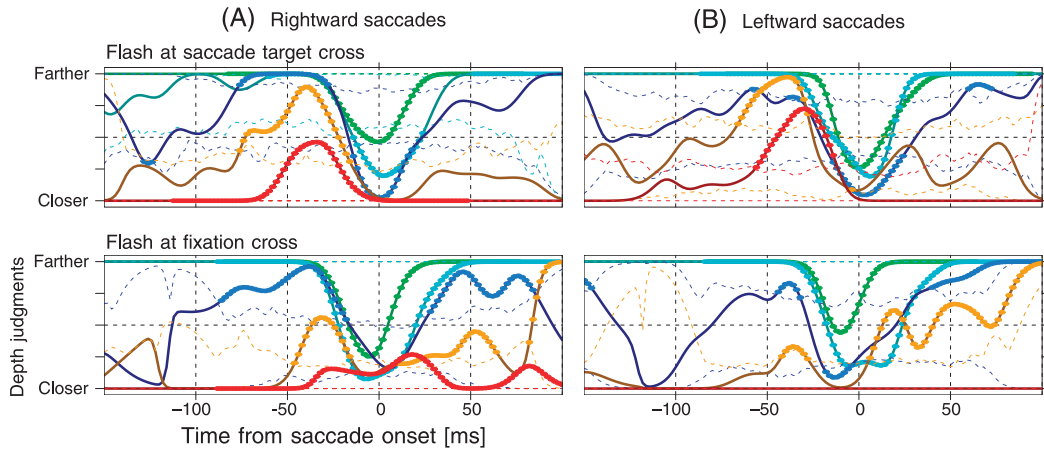
the PSE reaches or exceeds the critical value of 7.8 min arc. In contrast, a clearly different pattern is observed for downward saccades: for stimuli flashed at the fixation target, the amplitude of the effect is greatly reduced and the timing is less precise. For stimuli flashed at the saccade target, the direction of the shift in PSE is even reversed: perisaccadic flashes are perceived in a farther depth plane.

The analysis further reveals that for horizontal and upward saccades, the PSE is often significantly smaller than zero shortly before and after the period of mislocalization toward a closer depth plane. This effect is not quite as consistent as the main effect and seems to be stronger at larger eccentricities: the effect is larger for stimuli flashed at the saccade target before saccade onset and for stimuli flashed at the fixation cross after the saccade. For flashes
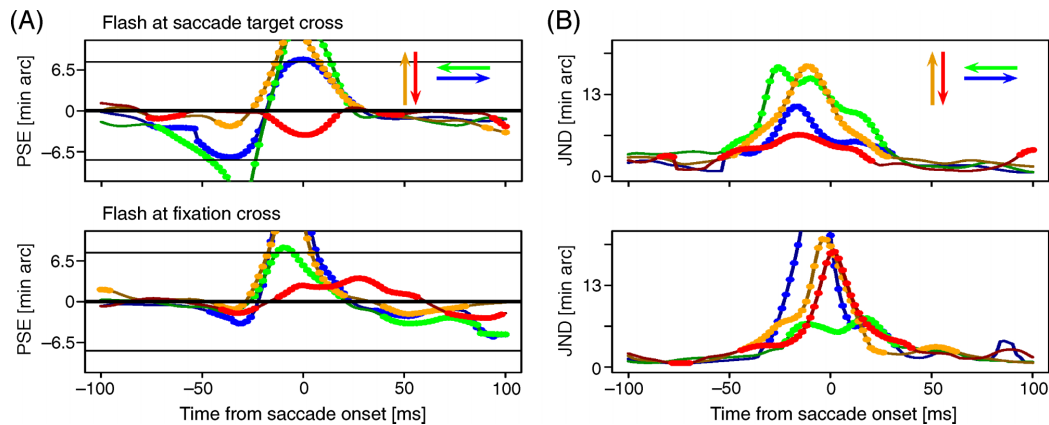
Figure 6. Time-resolved psychometric functions for stimuli flashed during leftward (green), rightward (blue), upward (orange), and downward (red) saccades. (A) For horizontal and upward saccades PSE shifts toward uncrossed disparities around saccade onset. In all cases the PSE shifts beyond the range of displayed disparities (±7.8 min arc) and hence depend on extrapolation. Further, shortly before and after this period the PSE shifts toward crossed disparities. Mislocalization for the downward saccades (red line) shows a clearly different pattern. First, the amplitude is much smaller and the pattern differs for stimuli presented near the fixation and the saccade target. (B) Estimates of the JND are significantly elevated from about 40 ms before saccade onset at the fixation cross and 50 ms before saccade onset at saccade target. The JND returns to values within the confidence limit about 30 to 40 ms after saccade onset.

at the fixation target a significant shift in PSE toward negative disparities can be observed prior to and after the mislocalization toward a closer depth plane. Also, a significant shift toward a farther depth plane can be observed for stimuli flashed at the saccade target before saccade onset. Only for stimuli flashed at saccade target after the saccade the effect does not reach significance. Overall, the analysis of the moving psychometric functions supports the notion of three distinct phases of mislocalization (farther–closer–farther) for stimuli flashed during horizontal and upward saccades.

Eye-movement analysis

The most important characteristics of the eye movements, i.e., time-resolved mean version and vergence in the conditions, which require vernier and depth judgments, respectively, are plotted in the lower panels of Figures 2, 3, and 4. Figures 2A and 3A show that the average amplitude of horizontal saccades was in the expected range (6.2 ± 0.8 degrees), confirming that subjects performed the saccades as instructed. Saccades had slightly longer amplitudes in the shift condition as compared to the compression condition (6.22 ± 0.78 degrees versus 6.08 ± 0.73 degrees). Average saccade duration was 32 ± 4 ms. In line with the larger amplitude, we also found a slightly longer duration for the saccades in the shift condition (33.5 ± 3.8 ms versus 32.3 ± 4.1 ms). Despite the small size of the effects they reached significance in a linear model with the factors 'Subject' and 'Background condition'.

Figures 2B and 3B show the typical biphasic pattern of transient vergence responses with an initial divergent and a subsequent convergent component. Consistent with reports in the literature (Collewijn et al., 1988a), the amplitude of the vergence movement was in the range of 0.5 degrees visual angle (mean cumulative divergent eye movements in the first 20 ms after saccade onset: 0.67 ± 0.44 degrees). Figures 4A and 4B show that this pattern is reversed for both upward and downward saccades. Here we observed an initial convergent movement followed by a subsequent divergent movement. The amplitude of this pattern was larger for the downward saccades.

The results of Experiment 3 have revealed striking differences between upward and downward saccades. Some of these differences might be due to differences in saccade parameters such as amplitude, duration, peak velocity, and amount of vergence. Thus, we performed a more detailed analysis of the upward and downward saccades, which might help to understand the different mislocalization patterns in the two conditions. A linear model with the factors 'Subject', 'Saccade Direction' and their interaction term was fit to the data. We found a significant effect of saccade direction on amplitude, duration, peak velocity and amount of convergence. As we were only interested in effects which were uniform across subjects, we performed post-hoc *t*-tests within

subjects and screened for significant effects with identical sign for both subjects. This reduced the potential candidate parameters to saccade duration and amount of convergence. In order to account for the large qualitative differences in mislocalization between the upward and downward saccades the effects should not only be significant, but also substantial in size. Saccade duration was 3.5 ms longer for downward as compared to upward saccades. Given the mean duration of 36.8 ms, this amounts to a modulation of 9%. Amount of cumulative convergence in the first 20 ms after saccade onset was 0.6 degrees larger for the downward as compared to the upward saccades. Given a mean cumulative convergence of 0.6 degrees, this amounts to a modulation of 90%.

Discussion

We examined depth judgments for stimuli flashed around the onset of horizontal and vertical saccades relative to continuously present references. For all saccade directions we observed an increase in disparity thresholds beginning about 30 ms before saccade onset and lasting until saccade offset.

Stimuli flashed ±25 ms around the onset of horizontal saccades were systematically mislocalized to a closer depth plane. In contrast, stimuli flashed shortly before or after this period tended to be mislocalized to a farther depth plane. While a similar pattern was observed during upward saccades we found a clearly different pattern of mislocalization during downward saccades.

Perisaccadic suppression and depth perception

In the following we discuss three different mechanisms which might contribute to the observed threshold elevations. Image smear caused by the fast changes in gaze direction may account in part for the observed threshold elevations. However, two observations back the assumption that other mechanisms might be involved. First, image smear is perpendicular to the relevant dimension for the vertical saccades and parallel for the horizontal saccades. Thus, we might expect a bigger effect of image smear for horizontal saccades. However, thresholds were similar during horizontal and upward saccades. Second, the early onset of the effect prior to saccade onset clearly indicates that other factors such as perisaccadic suppression are likely to play a role. This assumption is backed by the similar time courses for increases in depth thresholds and perisaccadic suppression (Diamond, Ross, & Morrone, 2000; Michels & Lappe, 2004).

Further, shifts of attention associated with saccade execution might also affect disparity thresholds. If such

shifts of attention are involved, we might expect differences between fixation and saccade target as attention shifts from the fixation point toward the saccade target shortly before saccade onset (Castet, Jeanjean, Montagnini, Laugier, & Masson, 2006; Gersch, Kowler, & Dosher, 2004). For horizontal and upward saccades, estimates of JNDs were very variable, and consequently such an effect could not be detected. The large variability might be due to the large shifts of the PSE, which cause the estimates of JND to rely on extrapolation. For downward saccades, however, the shift in PSE was considerably smaller, and thus estimates of disparity thresholds were much more reliable. For the downward saccades we indeed found smaller perisaccadic disparity thresholds at the saccade target, which might be caused by shifts of attention. We conclude that the perisaccadic increases in depth thresholds are likely to be caused by a combination of perisaccadic suppression, high attentional load, and image smear.

While increases in disparity thresholds can not explain the systematic error in depth judgments, they might do so in combination with a perceptual bias to perceive stimuli closer than their retinal disparity would suggest. Regardless of how such a prior probability might be implemented neuronally, we would expect it to gain influence over depth estimates in conditions when estimates of retinal disparity are noisy. As this is likely to be the case perisaccadically, we would expect a tendency to perceive perisaccadic flashes in a closer depth plane.

We conclude that a depth bias in combination with additional mechanisms such as perisaccadic suppression or high attentional load during saccade preparation and execution can explain part of our results. This is especially true for the early onset of the mislocalization toward a closer depth plane. However, this explanation fails to account the clear differences between upward and downward saccades, as well as the flanking phases of mislocalization toward a farther depth-plane.

Damped disparity and persistent flash hypothesis

In the following we discuss two mechanisms which are conceivable to understand the flanking phases with mislocalization toward a closer depth plane as well as the differences between upward and downward saccades.

Persistent flash hypothesis

Compared to brisk response onsets, neuronal responses due to stimulus offset decay only slowly over time. Consequently, a briefly flashed stimulus will elicit neuronal activity for a period which is clearly longer than the actual stimulus presentation (Pola, 2004). Pola has argued convincingly that during this decay period, encoded

features like retinal position or disparity are expected to stay constant, regardless of changes in gaze direction or ocular vergence. Thus, while a flashed stimulus may coincide with a continuously present stimulus for only a single monitor frame, their corresponding neuronal activities will overlap for a considerably longer time in the visual system. Due to the ensuing temporal uncertainty, relative disparity judgments may have a unique solution in the outside world but not in visual system (Figure 7A). Such a situation is expected to arise if the disparity of the continuously present stimulus rapidly changes, as is the case during saccades.

Damped disparity hypothesis

The study by Nienborg, Bridge, Perker, and Cummings (2005) suggests that neuronal responses in V1 do not track rapid changes in retinal disparity. These authors found that disparity-selective neurons in primary visual cortex (V1) do not follow fast oscillations in retinal disparity (10 Hz high-frequency cutoff measured at half peak height). Thus, while neurons in area V1 are expected to signal the correct disparity of a flashed stimulus, they might fail to do so for a continuously present stimulus when its retinal disparity is subject to rapid changes as for example during brisk changes in ocular vergence. Consequently, we might expect systematic errors of relative depth judgments in such situations (Figure 7B).

For horizontal saccades, the persistent flash hypothesis predicts a period with mislocalization toward a farther depth plane for stimuli flashed just prior to saccade onset and toward a closer depth plane for stimuli flashed later during the saccade (black line in Figure 7A). Under the same conditions, the damped disparity hypothesis predicts mislocalization toward a farther depth plane for stimuli flashed just after saccade offset and toward a closer depth plane for stimuli flashed later during the saccade (black line in Figure 7B). For horizontal saccades the two hypotheses predict a central period with mislocalization toward a closer depth plane as well as two flanking periods with mislocalization toward a farther depth plane (black line in Figure 7C). Further, the sign of the mislocalization predicted by these two hypotheses depends on the sign of the disparity/vergence changes. Thus, they would predict an inverted pattern of mislocalization for downward saccades which show an inverted pattern of vergence changes compared to horizontal saccades.

There are three points, however, which argue against the idea that the damped disparity and persistent flash hypothesis alone can account for the observed pattern of mislocalization. First, both hypotheses would predict mislocalization toward a closer depth plane only for stimuli flashed after saccade onset. However, we observe mislocalization toward a closer depth plane for stimuli flashed well before saccade onset. Second, while the pattern of mislocalization in depth during downward saccades is clearly different from the one

observed for horizontal and upward saccades, it is not the predicted inverted version. Third, contrary to our expectations (Collewijn et al., 1988b), we found vergence changes during upward saccades to be very similar to the ones observed during downward saccades, but with smaller amplitude. Thus, both hypotheses would predict a similar pattern of mislocalization in depth for upward and downward saccades. However, the pattern of mislocalization in depth during upward saccades is more similar to the one observed for horizontal saccades.

Relation to mislocalization in the fronto-parallel plane

In the following we will briefly relate our findings of mislocalization in depth to three mechanisms which can explain mislocalization in the fronto-parallel plane: the damped eye-position model (Honda, 1989; Matin, 1976), Pola's model (Pola, 2004) and the compressed time model which to our knowledge has not been described in the literature.

Damped eye-position model

This model assumes that the mislocalization of flashed stimuli is exclusively due to an erroneous estimate of

(A) Persisten flash hypothesis

(B) Damped disparity hypothesis

(C) Combination of both hypothesis

Time from saccade onset

current eye-position. Under this assumption, it is possible to infer the brain's estimate of eye-position as the sum of actual eye-position and the localization error (see, for example, Honda, 1989; Matin, 1976). The observed pattern of mislocalization was taken to suggest that the brain's estimate of eye-position is a damped version of the actual eye-position.

Pola's model

This model explains mislocalization as a combination of two mechanisms (Pola, 2004). First, it exploits the mechanisms of neuronal persistence (cf. above, the persistent flash hypothesis). Second, it assumes an erroneous estimate of eye-position. However, due to the interaction with the first mechanism, the erroneous eye-position estimate has a different form than the one predicted from the damped eye-position model.
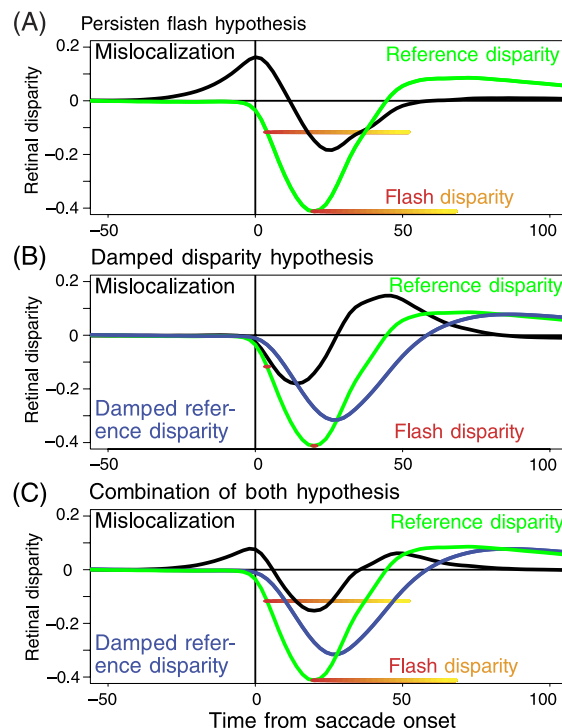
Figure 7. Two hypotheses for systematic errors in relative depth judgments between flashed and continuously present stimuli during fast vergence changes. Typical horizontal version saccades are accompanied by transient changes in vergence. Retinal disparity of a continuously present reference (green line) is plotted as a function of time from saccade onset. (A) Persistent flash hypothesis. Following an idea proposed by Pola (2004), we assume that neuronal activity elicited by flashed stimuli slowly decays and lasts for a considerably longer period than the stimulus was actually present on the screen (red-orange lines). During the entire period of slow decay, the neuronally signaled disparity is expected to stay constant. Thus, relative disparity comparisons (difference between blue and red/orange/yellow line) give rise to different results at different time points during the decay period. It was suggested that the final depth judgment might be an average over the entire decay period weighted with the corresponding strength of the decaying neuronal activity. The persistent flash hypothesis would give rise to two distinct periods of mislocalization, one toward a farther depth plane for stimuli flashed prior to divergent eye movements and one toward a closer depth plane for stimuli flashed prior to convergent eye movements (black line). (B) Damped disparity hypothesis. Based on the results of Nienborg et al. (2005), we hypothesize that neurons in primary visual cortex cannot follow fast changes in disparity. Hence they do not signal the correct retinal disparity (green line), but a low-pass filtered version thereof (blue line). For reasons of simplicity neuronal delays were disregarded. If we further assume that neurons correctly signal disparity of flashed stimuli (red dots), we would expect mislocalization in depth when the blue and green lines do not match. The damped disparity hypothesis predicts one epoch of mislocalization towards a closer depth plane for stimuli flashed during the first part of the saccade, and one epoch with mislocalization toward a farther depth plane in the second half and extending for a short while after saccade completion (black line). (C) Taken together the two hypotheses predict three epochs of mislocalization, first toward a farther depth plane, then toward a closer depth plane and finally toward a farther depth plane again (black line).

Compressed time model

This model is based on similar simplified assumption as the damped eye-position model. However, it assumes that the time assigned to the flash is erroneous while estimated eye-position is accurate. The model assumes that the correct retinal position estimate is assigned the wrong time and consequently paired with the correct eye-position estimate for the wrong time. The pattern of distortion in time which would replicate the empirical results corresponds to a compression of time around the midpoint of the saccade. In the light of recent experiments reporting perisaccadic compression of time this might not seem entirely unrealistic (Morrone, Ross, & Burr, 2005b).

If we substitute ocular vergence for eye-position all three models can be extrapolated to predict mislocalization in depth. For horizontal saccades, the damped eye-position model as well as Pola's model predict the same tri-phasic pattern of mislocalization as the combination of the persistent flash and damped vergence hypothesis (see above). Thus, they fail to account for the observed data in the same points as outlined in the previous paragraph.

The compressed time model would predict a different pattern of mislocalization in depth. For horizontal saccades it would predict two distinct epochs of mislocalization toward a farther depth plane with a short period of veridical depth perception about halfway into the saccade. However, the observed pattern of mislocalization in depth does not match this prediction.

In summary, none of the three explanations of mislocalization in the fronto-parallel plane generalizes to predict the precise pattern of mislocalization in depth.

Conclusions

Our study provides new insight into depth perception during saccadic eye movements. We show that, despite retinal slip, perisaccadic suppression, and large retinal eccentricities, depth perception is not abolished during saccades. The accuracy of depth judgments seems to depend on saccade direction. The best results were observed during downward saccades. For horizontal and upward saccades, we found a pronounced pattern of mislocalization in depth: stimuli flashed ±25 ms around saccade onset were systematically mislocalized to a closer depth plane. Further, stimuli flashed just before and after this period were mislocalized toward a farther depth plane. None of the mechanisms considered so far gives a completely satisfactory account of the data.

Acknowledgments

References

Cai, R. H., Pouget, A., Schlag-Rey, M., & Schlag, J. (1997). Perceived geometrical relationships affected by eye-movements. *Nature, 386,* 601–604. [PubMed]

Castet, E., Jeanjean, S., Montagnini, A., Laugier, D., & Masson, G. S. (2006). Dynamics of attentional deployment during saccadic programming. *Journal of Vision, 6*(3):2, 196–212, http://journalofvision.org/6/3/2/, doi:10.1167/6.3.2. [PubMed] [Article]

Collewijn, H., Erkelens, C. J., & Steinman, R. M. (1988a). Binocular co-ordination of human horizontal saccadic eye movements. *The Journal of Physiology, 404,* 157–182. [PubMed] [Article]

Collewijn, H., Erkelens, C. J., & Steinman, R. M. (1988b). Binocular co-ordination of human vertical saccadic eye movements. *The Journal of Physiology, 404,* 183–197. [PubMed] [Article]

Diamond, M. R., Ross, J., & Morrone, M. C. (2000). Extraretinal control of saccadic suppression. *Journal of Neuroscience, 20,* 3449–3455. [PubMed] [Article]

Gersch, T. M., Kowler, E., & Dosher, B. (2004). Dynamic allocation of visual attention during the execution of sequences of saccades. *Vision Research, 44,* 1469–1483. [PubMed]

Honda, H. (1989). Perceptual localization of visual stimuli flashed during saccades. *Perceptual Psychophysics, 45,* 162–174. [PubMed]

Honda, H. (1991). The time courses of visual mislocalization and of extraretinal eye position signals at the time of vertical saccades. *Vision Research, 31,* 1915–1921. [PubMed]

Lappe, M., Awater, H., & Krekelberg, B. (2000). Postsaccadic visual references generate presaccadic compression of space. *Nature, 403,* 892–895. [PubMed]

Matin, L. (1976). Saccades and extraretinal signals for visual direction. In A. Monty & J. W. Senders (Eds.), *Eye movements and psychological processes* (pp. 205–219).

Michels, L., & Lappe, M. (2004). Contrast dependency of saccadic compression and suppression. *Vision Research, 44,* 2327–2336. [PubMed]

Morrone, M. C., Ma-Wyatt, A., & Ross, J. (2005a). Seeing and ballistic pointing at perisaccadic targets. *Journal*

of Vision, 5(9):7, 741–754, http://journalofvision.org/ 5/9/7/, doi:10.1167/5.9.7. [PubMed] [Article]

Morrone, M. C., Ross, J., & Burr, D. (2005b). Saccadic eye movements cause compression of time as well space. *Nature Neuroscience, 8,* 950–954. [PubMed]

Morrone, M. C., Ross, J., & Burr, D. C. (1997). Apparent position of visual targets during real and simulated saccadic eye movements. *Journal of Neuroscience, 17,* 7941–7953. [PubMed] [Article]

Nienborg, H., Bridge, H., Perker, A. J., & Cummings, B. G. (2005). Neuronal computation of disparity in V1 limits temporal resolution for detecting disparity modulation. *Journal of Neuroscience, 25,* 10207–10219. [PubMed] [Article]

Pola, J. (2004). Models of the mechanism underlying perceived location of a perisaccadic flash. *Vision Research, 44,* 2799–2813. [PubMed]

Ross, J., Morrone, M. C., & Burr, D. C. (1997). Compression of visual space before saccades. *Nature, 386,* 598–601. [PubMed]

Perisaccadic mislocalization as optimal percept

Tobias Teichert
Columbia University, Department of Neuroscience, New York, NY, USA, & Philipps University, Department of Physics, NeuroPhysics Group, Marburg, Germany

Steffen Klingenhoefer
Philipps University, Department of Physics, NeuroPhysics Group, Marburg, Germany

Thomas Wachtler
Ludwig-Maximilians-Universität München, Department of Biology, Martinsried, Germany, & Philipps University, Department of Physics, NeuroPhysics Group, Marburg, Germany

Frank Bremmer
Philipps University, Department of Physics, NeuroPhysics Group, Marburg, Germany

The spatially uniform mislocalization of stimuli flashed around the onset of fast eye-movements (perisaccadic shift) has previously been explained by an inaccurate internal representation of current eye position. However, this hypothesis does not account for the observation that continuously presented stimuli are correctly localized during saccades. Here we show that the two findings are not mutually exclusive. The novelty of our approach lies in our interpretation of the extraretinal signal which, in contrast to other models, is **not** considered an (erroneous) estimate of current eye-position. Based on the reafference principle, our model assumes that the extraretinal signal is optimal in that it accurately predicts the neural representation of the retinal position of a continuously present stimulus. Perisaccadic shift arises as a consequence of maintaining stable perisaccadic position estimates for continuously present stimuli under the physiologically plausible assumption of temporal low-pass filtering in the afferent visual pathway. Consequently, our model reconciles the reafference principle with the finding of perisaccadic shift.

Introduction

Eye movements challenge visual perception (Bremmer & Krekelberg, 2003). Changes in the direction of gaze dramatically change the afferent flow to early visual areas. Nevertheless, we perceive the visual environment as being stable during eye movements. This is generally taken to be the result of an internally generated signal, the so-called extra-retinal signal (*exR*). The *exR* is assumed to account for changes in afferent flow which are caused by the movement of the eyes (reafference principle, e.g., von Holst & Mittelstaedt, 1950).

In contrast to this subjective observation of perceptual stability during eye movements in general and saccades in particular, several studies have reported systematic mislocalization of stimuli flashed around the onset of saccades (perisaccadic shift: Cai, Pouget, Schlag-Rey, & Schlag, 1997; Honda, 1989; Lappe, Awater, & Krekelberg, 2000). In the dark, the spatial perception of perisaccadically

flashed stimuli shows a biphasic error pattern. Stimuli flashed prior to saccade onset or during the first half of the saccade are mislocalized in the direction of the saccade. Stimuli flashed during the second half of the saccade or shortly after saccade offset are mislocalized in the direction opposite to the saccade.

Perisaccadic shift is generally taken as evidence that the reafference principle is violated perisaccadically. Consequently, it is assumed that alternative mechanisms, such as saccadic suppression, visual masking or the remapping of receptive fields, mediate perceptual stability during saccades (reviewed e.g., by Wurtz, 2008). While these mechanisms certainly play an important role, we show here that the original argument, namely that perisaccadic shift implies a breakdown of the reafference principle, is not compelling. We present a model that, based on the reafference principle, explains both, perisaccadic stability for continuously present stimuli and perisaccadic mislocalization for flashed stimuli.

Review of current models of perisaccadic shift

Our model is the logical next step in a series of models which have so far been put forward to explain perisaccadic shift. We will briefly outline these models to motivate the current work. The first and still widely accepted model of perisaccadic shift explains the mislocalization of flashed stimuli by an erroneous internal estimate of the current eye-position (Matin, 1976; Ross, Morrone, Goldberg, & Burr, 2001; Schlag & Schlag-Rey, 2002). This idea is quantified by Equation 1:

$$E_f(t) = exR(t) - h(t). \qquad (1)$$

Here, $E_f(t)$ corresponds to the observed localization error of a stimulus flashed at time t after saccade onset. Further, $h(t)$ corresponds to the direction of gaze at the time of the flash and $exR(t)$ denotes the extraretinal signal at the time of the flash. In this context it is assumed that in order to guarantee perceptual stability exR needs to be equal to eye-position: $exR(t) = h(t)$. Hence, it is assumed that $exR(t)$ is the visual system's estimated direction of gaze. The observed pattern of mislocalization can be predicted under the assumption that $exR(t)$ is a damped version of the actual eye-position (see Honda, 1989, Figure 4, or Pola, 2004, Figure 1). Hence, this model is often referred to as the damped eye position model.

While this elegant approach provides a mechanism of perisaccadic shift, it leaves several issues open. First and foremost, it does not provide a compelling reason as to why the visual system would choose exR in a way that solves Equation 1. One tentative explanation is that a damped version of eye-position is the visual system's best guess of actual eye-position under the assumption that it is not able to produce signals that change in time as rapidly as eye position. However, it seems unlikely that the same system which controls eye-position by sending out highly time-variant neuronal signals to a sluggish eye-plant should not be able to produce signals that describe these very same changes in eye position.

Second, it was pointed out that the damped eye position model might be overly simplistic as it relies on physiologically implausible assumptions (Pola, 2004). In particular, the damped eye-position model assumes that the neuronal representation of the flashed stimulus may be modeled as having virtually no extension in time, i.e., as a Dirac delta function. However, while this is a reasonable simplification for the retinal projection of the stimulus, it is certainly not for its neuronal representation (for a similar argument see Schlag & Schlag-Rey, 1995). The temporal low-pass properties of neurons in the afferent visual pathway, also referred to as persistence, complicate Equation 1. A mathematical formulation of

this view is given by Equation 2 (for more details see Pola, 2004):

$$E_f(t) = \int [R_{f,t}(\tau) - exR(\tau)]\xi_0(\tau - t)d\tau. \qquad (2)$$

In this model, the localization error arises as the weighted average of the instantaneous mislocalization error over a period of time τ. The duration and weight of this epoch is described by ξ_0 which represents the persistence of sensory preprocessing in afferent neurons. ξ_0 is normalized such that $\int \xi_0(\tau)d\tau = 1$. $R_{f,t}(\tau)$ corresponds to the time-resolved retinal signal of a stimulus flashed at time t after saccade onset (see Equation 5 for details). Pola has argued convincingly that $R_{f,t}(\tau)$ is constant and corresponds to the inverse of direction of gaze at the time of the flash: $R_{f,t}(\tau) = -h(t)$. For example, a flash at 0 deg in craniocentric coordinates presented while gaze is directed 5 degrees towards the right, will drive neurons with receptive fields 5 deg to the left of the fovea. We can rewrite $R_{f,t}(\tau)$ as $R_f(t)$ and remove it from the integral. For more details on the use of functions, their arguments and subscripts, refer to Appendix A. Thus, we can reformulate Equation 2:

$$E_f(t) = R_f(t) - exR * \xi_0(t). \qquad (2')$$

Here * corresponds to the convolution operator (see Appendix A for a definition). We see that Equation 1 is a special case of Equation 2′ by setting ξ_0 equal to a Dirac delta function (see Appendix A for details). For a wide range of choices of ξ_0 we can find an entire family of functions exR which solve the equation. In other words, Equation 2′ describes an infinite number of models of perisaccadic shift, including the damped eye-position model. In order to come up with a unique solution, Equation 2′ needs to be restricted. One way to do so is to measure the persistence of the afferent neurons in question and hence determine ξ_0 explicitly. However, it is not obvious which neurons at what level of the visual hierarchy should be considered. Alternatively, ξ_0 may be estimated from psychophysical data as has been done by Pola (2004). Following this approach, it is possible to identify a family of models of perisaccadic shift all of which use physiologically plausible temporal dynamics.

A final criticism of the damped eye position model is that it predicts perisaccadic mislocalization also for continuously present stimuli (Pola, 2004). Hence, it fails to account for the finding that flashed stimuli are mislocalized relative to continuously present stimuli (Cai et al., 1997). It is not immediately obvious whether the family of models described by Equation 2′ predict mislocalization for continuously present stimuli or not. Based on the assumption of linearity (see below) we show

that in general, these models do predict mislocalization for continuously present stimuli. However, we show that some of the models of this kind come very close to predicting visual stability for continuously present stimuli.

Reafference principle: A model of perisaccadic shift?

In the current manuscript we take a novel approach which at the same time resolves the issues of current models of perisaccadic shift which were raised above and imposes restrictions on the family of models described by Equation 2′. The novelty and power of our approach lies in the idea of deriving restrictions for *exR* from a setting that is independent from the one used to measure perisaccadic shift. In particular, we start with the following assumption: visual processing is based on and optimized for continuously present stimuli. Thus, assuming that the reafference principle is valid during saccades, we choose *exR* such that continuously present stimuli are **not** mislocalized. This restriction is described by Equation 3:

$$E_c(\tau) \equiv 0. \qquad (3)$$

In Equation 3, E_c corresponds to the localization error of a continuously present stimulus at time τ after saccade onset. Whenever Equation 3 holds, continuously present stimuli are not mislocalized perisaccadically and the visual world appears stable during saccades. It is essential to point out the difference to previous models which choose *exR* in order to predict the previously measured perisaccadic shift. Such an approach will usually lead to a violation of the reafference principle, i.e., these models will not be able to explain perisaccadic stability for continuously present stimuli. Here we invert the problem

in order to determine the properties of the sensory preprocessing, i.e., ξ_0, which are necessary to produce perisaccadic shift. In contrast to other models, our approach does **not** necessarily guarantee a solution.

In the current paper, we show that it is possible to find preprocessing parameters ξ_0 which reconcile the reafference principle with perisaccadic shift, i.e., simultaneously solve Equations 2′ and 3. Hence, perceptual stability for continuously present stimuli, i.e., Equation 3, on the one hand and perisaccadic shift, i.e., Equation 2′, on the other hand are not mutually exclusive. Further, we show that the preprocessing parameters ξ_0 which simultaneously solve Equations 2′ and 3 have physiologically plausible low-pass filter properties. In contrast, we show that for a wide range of un-physiological choices of ξ_0, our model does **not** predict perisaccadic shift of realistic amplitude. In particular, we can rule out the case that ξ_0 equals a Dirac delta function which underlies the damped eye position model. In summary, we argue that the visual system chooses *exR* in order to guarantee perisaccadic stability, and in doing so causes perisaccadic shift under the assumption of physiologically plausible temporal low-pass filtering in the afferent visual pathway. In addition, our analysis reduces the dimensionality of the family of potential models of perisaccadic shift described by Equation 2′.

Model

We simulate neuronal activity in a retinocentric visual area around the time of a saccade. From the resulting population activity we derive a scalar estimate of retinocentric position (the so-called retinal signal, R). R is converted to a craniocentric position estimate W by subtracting the extraretinal signal *exR*.
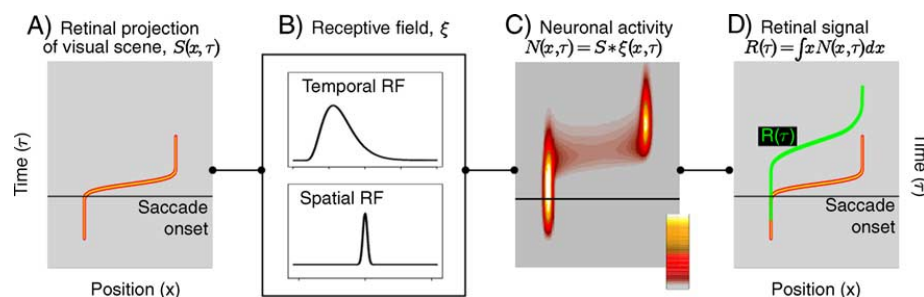
Figure 1. The model simulates neuronal activity in a one-dimensional retino-centric layer around the time of saccade onset while presenting a stimulus at 0 deg cranio-centric position (see Methods for details). Neuronal activity $N(x, \tau)$ (panel C) is simulated as the convolution of the retinal projection of the visual stimulus $S(x, \tau)$ (panel A) with the spatio-temporal receptive field ξ (panel B). The time-resolved retinal signal $R(\tau)$ is calculated as the center of gravity of neuronal activity at any given time (green line in panel D). Due to the properties of the temporal receptive field the retinal signal only begins to reflect the eye-movement well after saccade onset.

Preprocessing in early visual areas was simulated in a layer of 201 rate-coding neurons in a one-dimensional retinocentric area spanning roughly 10° of visual space. Neuronal activity was simulated around the onset of a simulated 6° leftward saccade (from x = +3° to x = −3°, craniocentric coordinates) while presenting stimuli of variable duration at x = 0° in craniocentric coordinates. The saccade was simulated with a Gaussian velocity profile over time with a standard deviation of 8 ms. This setting corresponded to a saccade duration of 40 ms (using a speed criterion of 15 deg/sec) and a peak velocity of 300 deg/sec (Carpenter, 1988).

The neurons were modeled as linear filters, yielding a spatio-temporal neural activity profile $N(x, \tau)$ that corresponded to the linear convolution of the retinal stimulus S with a spatio-temporal receptive field ξ. The activity of the neurons is described by Equation 4 (see Figure 1D):

$$N(x, \tau) = S * \xi(x, \tau). \tag{4}$$

Here x corresponds to the receptive field position in retinal coordinates and τ indicates time relative to saccade onset. The input S corresponds to the retinal projection of the visual scene coded as zeros and ones, depending on the presence of a stimulus. Note that the temporal kernel ξ_0 in Equation 2′ is identical to the temporal aspect of the spatio-temporal kernel ξ in Equation 4, i.e., $\xi_0(\tau) = \xi(0, \tau)$. The spatial receptive field was modeled as a Gaussian with a standard deviation of 0.15°, normalized to a maximum amplitude of 1 (see Figure 1B, upper panel). The temporal impulse response was described as a Gamma distribution with various scale and shape parameters (see Figure 1B, lower panel). A gamma distribution can be described as the convolution of n exponential distributions. The shape parameter of the gamma distribution corresponds to the number n; the scale parameter corresponds to the time constant λ of the underlying exponential distributions. Hence, the entire temporal receptive field is determined by the shape parameter n and the scale parameter λ. Unless mentioned otherwise, the n was set to 5. The resulting kernel is a low-pass filter of order n and cutoff wavelength $2\pi\lambda$. The extent of the kernel in time can be quantified by its standard deviation which is given as $\sqrt{n\lambda^2}$. Kernels with large standard deviation give rise to a system with slow temporal dynamics. Vice verse, small standard deviation is an indicator of fast temporal dynamics. In addition, a delay of 15 ms was added to the kernel to account for conduction delays caused by preprocessing in the afferent visual pathway.

Whenever the maximum firing rate was above zero, an object was deemed to be present in the scene and its retinal signal $R(\tau)$ was derived as the center of gravity of the neuronal activity at time τ in question (see Figure 1D):

$$R(\tau) = \int x N(x, \tau) dx. \tag{5}$$

This instantaneous retinal position estimate was converted to instantaneous craniocentric coordinates $W(\tau)$, by subtracting $exR(\tau)$:

$$W(\tau) = R(\tau) - exR(\tau). \tag{6}$$

Note, that $R(\tau)$ is only defined when an object is present in the scene. Hence, the same restrictions apply to $W(\tau)$. Finally, the time-resolved craniocentric position estimate was converted into a global position estimate $\overline{W}$ as the weighted mean of the instantaneous craniocentric position estimate:

$$\overline{W} = \int W(\tau) g(\tau) d\tau. \tag{7}$$

Here the weights $g(\tau)$ were calculated as the maximum of the neuronal activity at time τ. In addition, the weights were normalized to a sum of one: $g(\tau) = \max[N(x, \tau)]/\int \max[N(x, \tau)]d\tau$. For stimuli flashed at time t after saccade onset, the weights g are defined by the temporal impulse response function: $g(\tau) = \xi_0(\tau - t)$.

The actual position of the stimulus was always fixed at 0°. Hence, $\overline{W}$ also corresponds to the localization error $\overline{E}$. By substituting $\overline{W}$ for $\overline{E}$, $exR(\tau) - R_{f,t}(\tau)$ for $W(\tau)$ and $g(\tau)$ for $\xi_0(\tau - t)$ we see that for flashed stimuli, Equation 7 corresponds to Equation 2.

Optimization of the extraretinal signal

In the context of our model, the reafference principle holds if continuously present stimuli are not mislocalized during saccades as described in Equation 3. Thus, for stationary stimuli presented continuously at 0 deg in craniocentric coordinates, the extraretinal signal has to be identical to the retinal signal:

$$exR(\tau) \equiv R_c(\tau). \tag{8}$$

This is achieved by a simple calibration procedure. The model is run while presenting a stimulus continuously at 0° in craniocentric coordinates (see Figure 1 or Supplementary movie). R_c is determined and for all subsequent runs exR is set to R_c, regardless of whether presenting flashed or continuously present stimuli. In a

real system that performs saccades of variable direction and amplitude, such a simple mapping is not feasible. Instead, *exR* actually has to be trained with a number of different saccade vectors.

Results

Veridical localization of continuously present stimuli

Figures 2A through 2D show the response of the model for a continuously present stimulus for four different choices of ξ with increasingly slower temporal dynamics, i.e., longer time constants λ (see Methods). Prior to saccade onset the eye is fixating 3° to the right of the stimulus which consequently drives neurons with receptive fields 3° to the left of the fovea. At time 0 the eye starts to move to the left and finally reaches a position 3° to the left of the stimulus which consequently drives neurons with receptive fields 3° to the right of the fovea. Between 25 and 50 ms after saccade onset, the neuronal representation of the stimulus begins to reflect this change in eye-position as the center of gravity of the neuronal activity, i.e., R_c, moves from −3° to +3° (green lines in Figure 2, see also Supplementary movie). Note that for slower temporal dynamics, described by increases in the scale parameter λ (panels A through D), R_c begins to move later and at lower speeds. Accordingly, each of the four models will use different extraretinal signals which, according to Equation 8, are set to R_c.

As a consequence of this calibration, all models will meet the requirements of Equation 3, i.e., the craniocentric representation of the stimulus $W_c(\tau)$ (blue line in Figure 2) accurately remains at 0° during the entire perisaccadic time period. Hence, continuously present stimuli are not mislocalized, regardless of the receptive field properties defined by ξ. In the following we will explore the predictions of the models for flashed stimuli.

Shift-like mislocalization of flashed stimuli

Based on ξ and *exR* we can derive the mislocalization of flashed stimuli by solving Equation 2′. Alternatively, we can run the model multiple times and simulate flashes at various times relative to saccade onset. Figures 3A–3D show the responses of the model from Figure 2B to stimuli flashed at four different times relative to saccade onset. Stimuli flashed before saccade onset or in the first half of the saccade are mislocalized in the direction of the saccade (Figures 3A and 3B). Stimuli flashed in the second half of the saccade and briefly after saccade completion are mislocalized in direction opposite to the saccade (Figure 3D). Figure 3E depicts a summary of mislocalization as a function of flash onset relative to saccade onset. It verifies that the model indeed predicts the biphasic pattern of mislocalization that is typically referred to as perisaccadic shift. It is important to note that the mislocalization starts well before saccade onset and that the maximal amplitude is observed for stimuli flashed around saccade onset. At the same time it is important to note again that the model does not predict mislocalization for continuously present stimuli. Figure 4 shows the
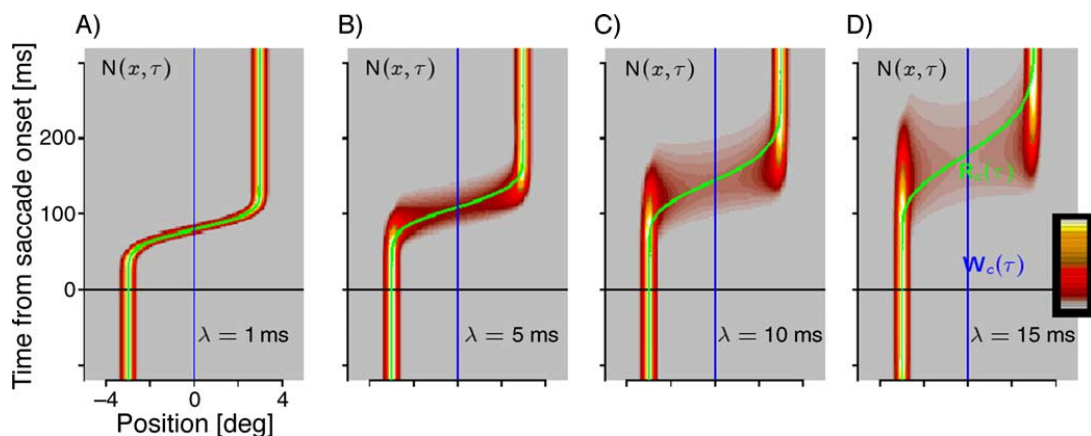
Figure 2. No mislocalization for continuously present stimuli. The behavior of the model depends mainly on the spatio-temporal receptive field ξ. Panels A through D show responses of the model for increasingly slower temporal dynamics, i.e., a longer scale parameter λ for the temporal receptive fields (see Methods for details). As the temporal dynamics get slower, the retinal signal $R_c(\tau)$ (green line) starts moving later and at lower speeds. The instantaneous cranio-centric position $R_c(\tau)$, (blue line) remains constant 0 deg. This indicates that regardless of the choice of ξ, the model predicts stable and accurate cranio-centric position estimates for continuously present stimuli.

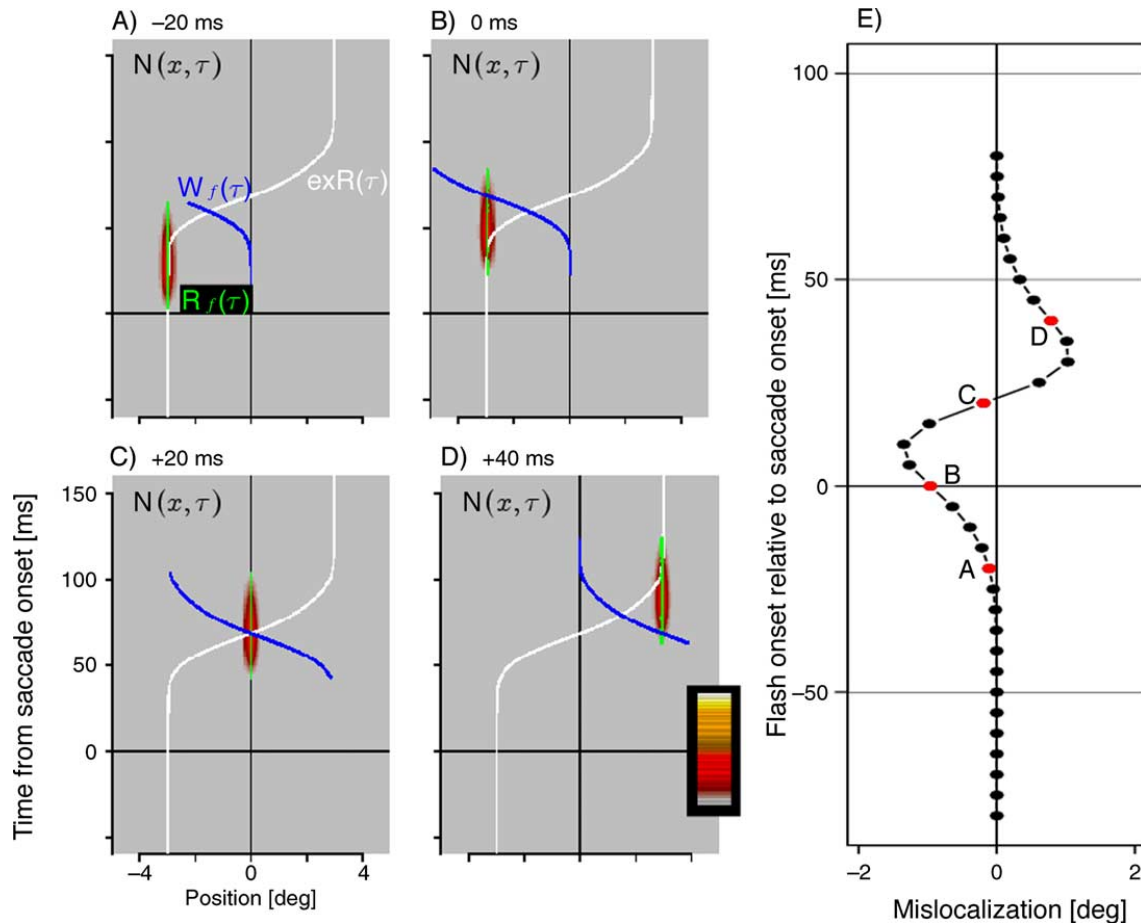Figure 3. The localization of flashed stimuli: Perisaccadic shift. Panels A to D show the neuronal responses of the model from Figure 2C to stimuli flashed at various times relative to saccade onset. The white line corresponds to the extraretinal signal *exR*. The green and blue lines correspond to $R_f(\tau)$ and $W_f(\tau)$. Note that $W_f(\tau)$ deviates from 0 deg indicating that stimuli are mislocalized. Panel E summarizes the resulting mislocalization as a function of the flash onset relative to saccade onset. Negative values indicate mislocalization in direction of the saccade. From bottom to top, the four red dots correspond to the panels A to D.

predicted perisaccadic shift for the four choices of λ which were used in Figures 2A through 2D. Note that it is only in the conditions with slower temporal dynamics, i.e., conditions with longer time constants, that the predicted mislocalization error reaches an amplitude that is comparable to experimental findings (see below for a quantitative analysis).

Read-out of population activity

The retinal signal can be derived from the population activity $N(x, \tau)$ in a number of different ways. In the simulations above, we assumed that R corresponds to the center of gravity (CG) of the neuronal activity (see Methods). Alternatively, R may, for example, be defined as the retinal location with the strongest activity (MAX) or be derived by a maximum likelihood method (ML). Several recent studies have provided neuronal mechanisms for ML calculations (Deneve, Latham, & Pouget, 2001) as well as evidence in favor of the brain using ML-like methods (e.g., Knill & Pouget, 2004). Hence, it is important to test how our model is affected by using the MAX or the ML method instead of the CG method to estimate the retinal signal.

Figure 5 shows the results of the MAX method (results for the ML method are virtually identical). There are two remarkable points. First, the retinal signals derived with
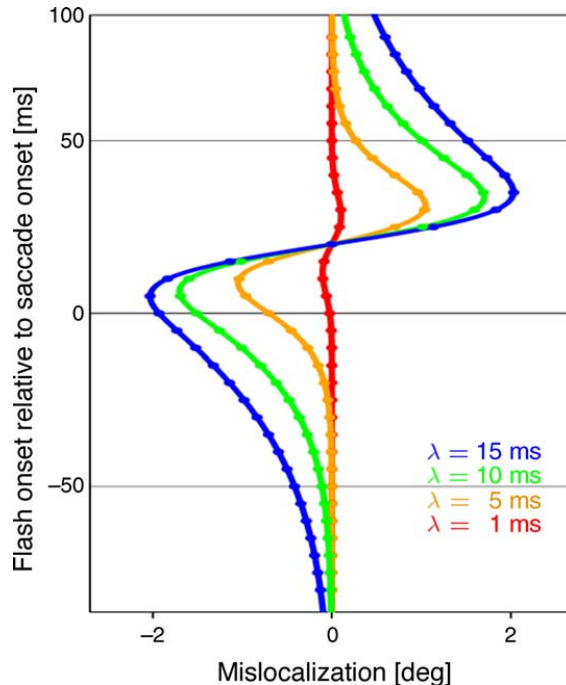
Figure 4. Perisaccadic shift occurs only with slow temporal dynamics. Perisaccadic shift as predicted for the model with four different temporal dynamics as depicted in Figure 2. Mislocalization amplitude increases with slower temporal dynamics, i.e., longer scale parameters λ. Mislocalization with a realistic amplitude is only seen when λ is between 10 and 15 ms.

the MAX method differ substantially from the ones calculated with the CG method. This difference is most obvious for the two slowest conditions. For the CG method, the retinal signal changes smoothly as a function of time. In contrast, the retinal signal derived with the MAX method is essentially a step function. From one time point to the next, the retinal signal jumps from the pre- to the post-saccadic value. Second, despite these differences, the main effect, i.e., the biphasic mislocalization of the flashed stimuli can still be observed. Finally, we find the same dependence of the amplitude of the perisaccadic shift on the time constant as previously observed for the CG method.

Slow dynamics are necessary for perisaccadic shift

In the previous simulations we held the shape of the temporal impulse response constant. In the following simulations we systematically vary the shape of this

temporal kernel. As it is impossible to explore all possible shapes we settled for the subspace of kernels described by the two-dimensional Gamma distribution family (see Methods). Our simulations show that the amplitude of the predicted mislocalization increases both with the shape parameter *n,* as well as the scale parameter λ (see Figures 6A and 6D for results of the CG and MAX method, respectively). Closer investigation revealed that the mislocalization amplitude could be described reasonably well as a function of the standard deviation of the kernel which is given by $\sqrt{n\lambda^2}$ (see inset Figures 6A and 6D).

To quantify the fit of the predictions to actual data we compared it to the mislocalization error reported by Honda (1989). As we did not have access to the actual data we emulated these previous results by estimating the parameters of the damped eye-position model which best fit the mislocalization amplitude reported in his paper. For saccades of 8° amplitude mislocalization ranging from −2.4° to +2.4° was reported. The range of this mislocalization corresponds to 0.6 times the saccade amplitude.

A number of models accurately predicted the emulated data reasonably well (see Figures 6B and 6E). The family of models that fits Honda's data best can be described as having temporal receptive fields with a standard deviation around 24 ms and 35 ms for the CG and MAX method, respectively. For example, using a shape parameter *n* of 5, we can find a good model for the CG method by setting λ equal to 10.6 ms, as the standard deviation of the temporal receptive field, i.e., a gamma-distribution with shape parameter 5 and scale parameter 10.6 ms, will be close to 24 ms: $\sqrt{n\lambda^2} = \sqrt{5 \times (10.7 \text{ ms})^2} = 23.9$ ms. Similarly, by setting λ to 15.7 ms we will find a good model for the MAX method. Despite having different temporal receptive fields, and consequently different extraretinal signals, these models predict almost identical mislocalization profiles (three examples each are plotted in Figures 6C and 6F).

Relative position judgments

Intuitively, relative position judgments should be unaffected by changes in direction of gaze. Nevertheless, errors of relative position judgments around saccades have been reported both between a flashed and a continuously present stimulus (e.g., Cai et al., 1997) and between two flashed stimuli (e.g. Schlag & Schlag-Rey, 1995). Hence, it is of special importance to elaborate how our model deals with relative position judgments.

In the context of our model, relative position judgments could be defined either as 1) the comparison of the two global craniocentric position estimates, 2) the time-averaged comparison of the two instantaneous craniocentric position estimates or 3) the time-averaged comparison of the two retinal signals.
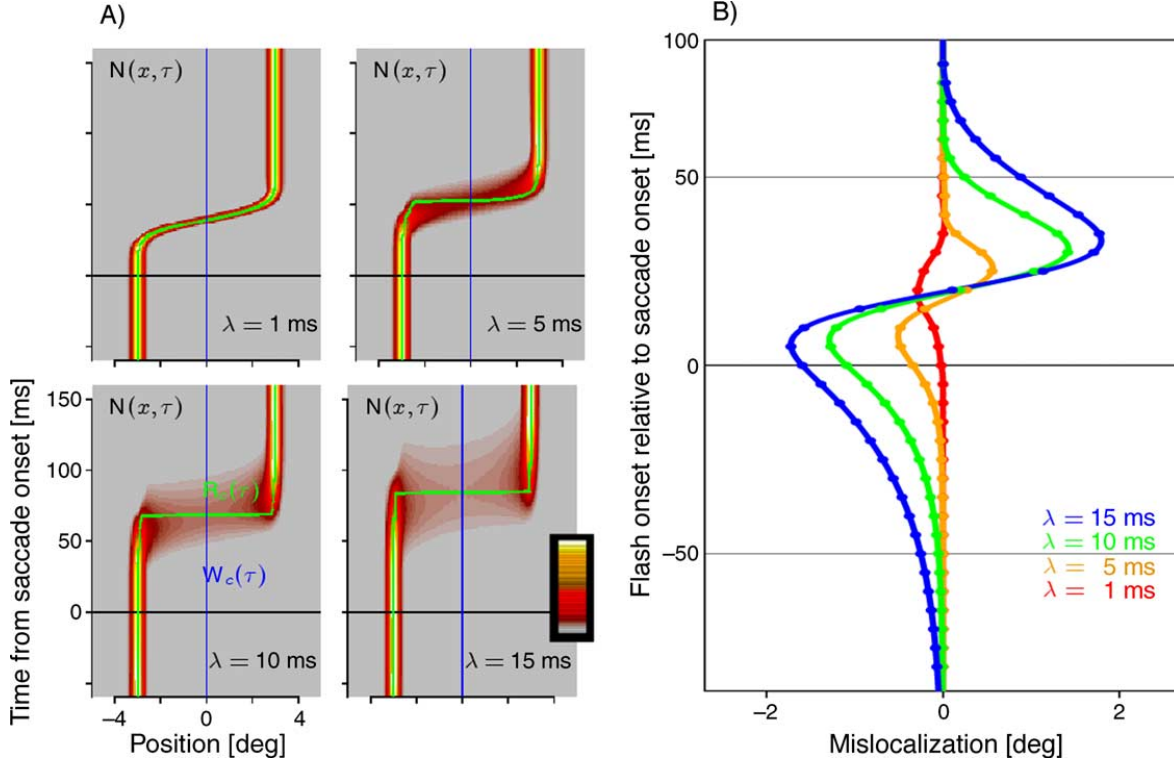
Figure 5. Perisaccadic shift with a fast retinal signal. (A) Neuronal responses for the model with four different temporal dynamics, as in Figure 2. In contrast to Figure 2, the retinal signal is defined as the location with the strongest activity (MAX method, see text for details). Note that the retinal signals differ substantially from the ones observed with the center of gravity method (CG) in Figure 2. Instead of becoming slower with increasing λ they are fastest for the slowest dynamics where they resemble a step function. B) Predicted mislocalization for flashed stimuli with the MAX method. As observed for the CG method in Figure 4, mislocalization amplitude increases with slower temporal dynamics λ.

First, we will elaborate the predictions of the three methods for the comparison of a flashed and a continuously present stimulus. The mathematical description of the three relative position methods is given by the Equations D1, D2 and D3 below:

$$\overline{\Delta}_{f,c}^{\overline{W}}(t) = \overline{W}_c - \overline{W}_f(t), \tag{D1}$$

$$\overline{\Delta}_{f,c}^{W}(t) = \int[W_c(\tau) - W_{f,t}(\tau)]g(\tau)d\tau, \tag{D2}$$

$$\overline{\Delta}_{f,c}^{R}(t) = \int[R_c(\tau) - R_{f,t}(\tau)]g(\tau)d\tau. \tag{D3}$$

Using Equation 8, it becomes obvious that all three estimates of relative position $\Delta_{f,c}(t)$ are identical and equal to $E_f(t)$. Hence, the relative error between the flashed and the continuously present stimulus is identical to the absolute error of the flashed stimulus. Further, it is clear from Equation D3 that the relative mislocalization does not depend on the execution of an eye-movement: as the extraretinal signal does not figure into Equation D3, the same pattern of relative mislocalization will be observed if the continuously present stimulus is actively moved across the retina by a saccade or is moved across the retina due to stimulus motion. Consequently, our model makes identical predictions for relative position judgments during real and simulated saccades.

Now we will turn to the relative localization of two stimuli flashed at times u and v, respectively. In analogy to Equations D1, D2 and D3, we define the Equations D1′,
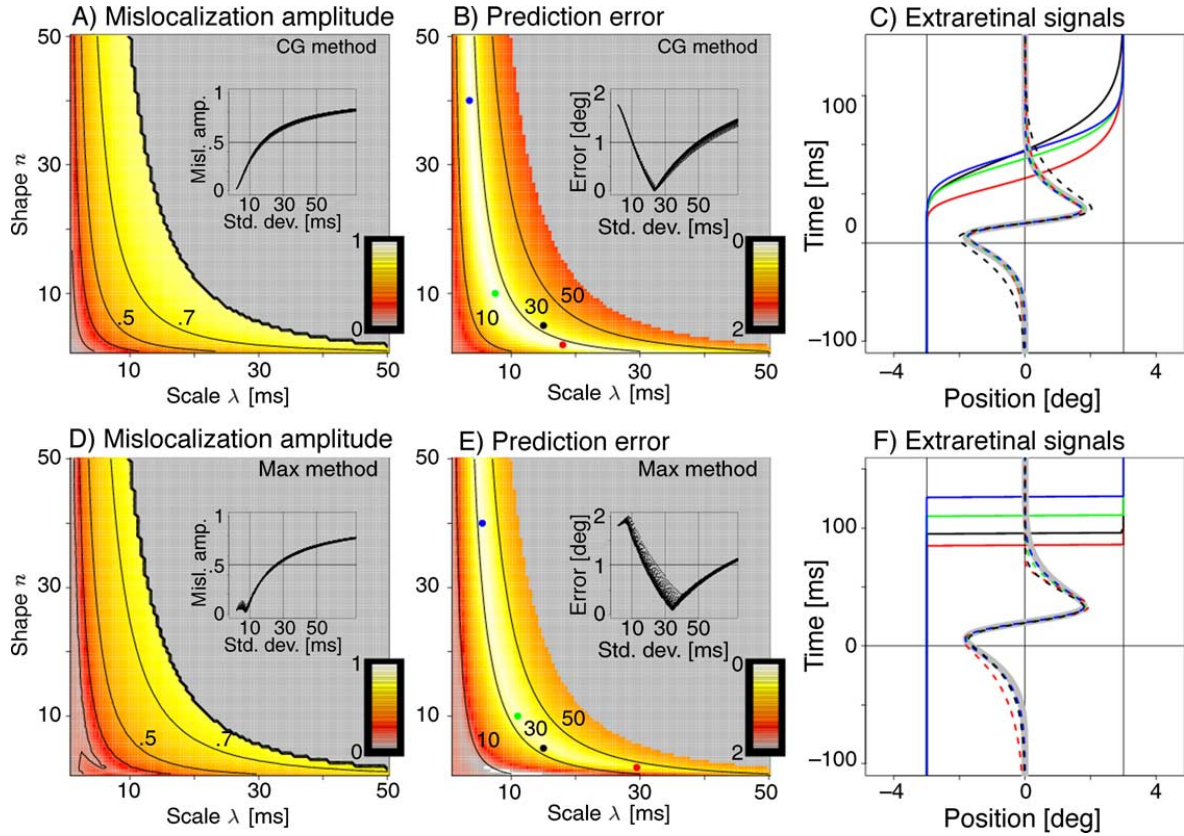
Figure 6. Possible models of perisaccadic shift. Mislocalization as a function of the temporal receptive fields which were modeled as gamma distributions with different scale and shape parameters (λ and n plotted on the x and y axis, respectively). Upper and lower row illustrate results for the CG method and the MAX method, respectively. (A),(D) Magnitude of the mislocalization defined as the range of mislocalization values (max–min) normalized to saccade amplitude as a function of shape and scale parameter. Across all models, mislocalization amplitude can be predicted reasonably well by the standard deviation of the temporal receptive fields alone (see methods and inset). (B),(E) Similarity between model predictions and data from Honda (1989) was quantified as the maximum difference. The black lines are iso-standard deviation curves of the temporal receptive fields. Across all models, the error can be predicted reasonably well by the standard deviation of the temporal receptive fields alone (see inset). Models that provide a good fit (i.e., error close to zero) have a standard deviation around 24 and 35 ms for the CG and MAX method, respectively. (C),(F) Extraretinal signal (solid lines) and predicted mislocalization (dashed lines) for the four models indicated by the red, green, blue and black dots in (B) and (E), respectively. The red, green and blue models were selected randomly from the family of models which provide a good fit to the data (thick gray line, see text for details). Note that despite the variability between the extraretinal signals, predicted mislocalization is very similar for all models. The black model uses the temporal receptive field selected by Pola (2004) on the basis of flicker fusion thresholds. Despite the fact that it was not selected based on its fit to the data it matches it quite well.

D2′ and D3′. Within the framework of our model, these formulas provide a mathematical description of the relative localization for two stimuli flashed at times u and v, respectively:

$$\overline{\Delta}_{f,f}^{\overline{W}}(u,v) = \overline{W}_f(u) - \overline{W}_f(v), \tag{D1′}$$

$$\overline{\Delta}_{f,f}^{W}(u,v) = \int [W_{f,u}(\tau) - W_{f,v}(\tau)] g(\tau) d\tau, \tag{D2′}$$

$$\overline{\Delta}_{f,f}^{R}(u,v) = \int [R_{f,u}(\tau) - R_{f,v}(\tau)] g(\tau) d\tau. \tag{D3′}$$

In contrast to the relative position judgments between a flashed and a continuously present stimulus, here the three equations yield different results. From Equation D3′ the relative position difference between the two flashed stimuli is equal to the difference in the direction of gaze at the time of the flash: $\overline{\Delta}_{f,f}^{R}(u, v) = R_f(u) - R_f(v)$. In particular, if both stimuli are flashed before saccade onset, the two stimuli will not be mislocalized relative to each other. This is not in keeping with experimental findings. If we use the fact that $W_f(\tau) = R_f(\tau) - exR(\tau)$ we see that Equation D2′ yields the same results as Equation D3′. In contrast, Equation D1′ describes the relative mislocalization as the difference in the global craniocentric position estimates. Hence, in line with experimental findings, two stimuli flashed before saccade onset will be mislocalized relative to each other.

Discussion

For almost 200 years, the reafference principle has been one of the most widely accepted theories in sensory-motor research in general, and oculomotor control in particular (e.g., Helmholtz, 1866; Purkinje, 1825; Steinbuch, 1811; von Holst & Mittelstaedt, 1950; for a thorough historical review see Gruesser, 1995). For many years, the finding of perisaccadic shift was interpreted as evidence **against** the reafference principle. We argue that this interpretation was based on disregarding slow temporal dynamics in afferent visual neurons, which in turn, led to the faulty assumption that the extraretinal signal should represent eye position. Recent modeling work has acknowledged temporal low-pass filtering (Pola, 2004) and considerably changed our interpretation of perisaccadic shift. However, the implications of this low-pass filtering for the retinal signal of continuously present stimuli had not been acknowledged so far. Our model closes this link and hence provides a stringent implementation of the reafference principle. As required by the reafference principle, our model views the extraretinal signal not as an erroneous estimate of eye-position, but rather as an accurate estimation of the retinal signal of continuously present stimulus. By inverting this model we can deduce the preprocessing parameters that predict perisaccadic shift in the framework of the reafference principle. Our results show that for physiologically plausible preprocessing parameters, the reafference model does indeed predict perisaccadic shift. Hence, the reafference principle provides a very simple and elegant account of both, perisaccadic shift **and** perisaccadic stability.

In addition to the reafference principle, our model is indebted to a number previous approaches such as an informal suggestion by MacKay (1970) to account for mislocalization during simulated saccades, a model by Krekelberg and Lappe (2000) to account for the flash lag effect and the models by Pola (2004, 2007, 2008) to account for mislocalization during real saccades. Our new model provides five main advances to the field.

(1) Our model provides a novel and compelling explanation as to **why** perisaccadic shift occurs. While previous models could accurately model perisaccadic shift, they did not convincingly answer the question why the extraretinal signal would happen to be chosen in a way that is necessary to predict perisaccadic shift. In our framework, perisaccadic shift follows from two simple principles: perisaccadic visual stability and physiologically plausible temporal dynamics in the afferent visual pathway. The former principle can easily be verified by introspection: the world does appear stable during saccades; the latter has been documented extensively in electrophysiological and psychophysical studies.

In the context of our model the extraretinal signal is optimal in that it guarantees perisaccadic visual stability for continuously present stimuli. This interpretation removes perisaccadic shift from the list of mislocalization phenomena such as the Filehne Illusion and the phenomenon of autokinesis which are thought to be caused by an inadequate extraretinal signal. Note, that our explanation of perisaccadic shift by an accurate extraretinal signal does not imply that the extraretinal signal would have to be accurate in other conditions as well which give rise, for example, to the Filehne Illusion.

(2) Our model demonstrates that mislocalization of flashed stimuli and correct localization of continuously present stimuli are **not** mutually exclusive. Hence, to our best knowledge, it provides the first account for erroneous perisaccadic **relative** position judgments between flashed and continuously present stimuli (Cai et al., 1997; Teichert, Klingenhoefer, Wachtler, & Bremmer, 2008).

(3) Our model provides a link between two of the three frameworks of visual stability during eye movements: efferent (e.g., Helmholtz, 1866; von Holst & Mittelstaedt, 1950) and reafferent theories (Murakami & Cavanagh, 1998, 2001). The former theory holds that the efference copy provides a means to correct afferent signals for changes of the position of the retinae in space, the latter assumes that changes of direction of gaze can be estimated from the afferent visual signals themselves without knowledge of either motor efference or proprioceptive afference. For the absolute localization of flashed stimuli in the dark our model depends exclusively on the efferent theory of visual stability. In contrast, the relative mislocalization during simulated saccades depends exclusively on the reafferent theory. The link between the two theories can best be appreciated for relative position judgments during real saccades: if the extraretinal signal accurately predicts the retinal signal of the continuously present stimulus, both theories make exactly the same predictions.

(4) The model predicts relative mislocalization of a flashed relative to a continuously present stimulus during simulated saccades. This visual stimulus configuration is

very similar to the one in which the flash lag effect is typically observed. Hence, we establish a common ground between models of perisaccadic shift and the flash lag effect (e.g., Krekelberg & Lappe, 2000). The field of perisaccadic mislocalization may benefit from certain ideas which have been brought up in the flash lag literature. For example, the mechanism of motion extrapolation (Nijhawan, 1994) by lateral connections as well as subtle latency differences between flashed and continuously present stimuli (e.g., Purushothaman, Patel, Bedell, & Ogmen, 1998) may play an important role in the fine-tuning of more sophisticated versions of our model (see also below).

(5) Our approach imposes novel restrictions on the family of possible models described by Equation 2′. Realistic patterns of perisaccadic mislocalization can **only** be observed with slow temporal dynamics. Our simulations suggest that the standard deviation of the temporal kernels needs to be on the order of 24 and 35 ms for the CG and MAX method, respectively. Thus, we can definitely rule out the damped eye-position model which relies on the assumption that the temporal kernel is a Dirac delta function.

Relation to previous models

Our approach supports and complements Pola's work. First, independent of the flicker-fusion experiments that motivated Pola's choice of a slow temporal kernel, we find that **only** such slow temporal kernels may produce perisaccadic shift in the context of our model. This converging evidence should considerably strengthen the case in favor of the slow temporal kernels. Second, the restrictions imposed by Pola on the set of solutions of Equation 2′, are orthogonal to the restrictions we can impose. While he identifies a single temporal receptive field with the associated family of extraretinal signals, we identify a family of temporal receptive fields each with its unique extraretinal signal derived via Equation 8. These restrictions may be combined to yield a unique model of perisaccadic shift, i.e., we can use the temporal receptive field identified by Pola in our model. Using the CG and the MAX method, respectively, we identify two unique models of perisaccadic shift. For the CG method the predicted mislocalization amplitude exceeds the one observed by Honda (1989), for the MAX method it matches it pretty closely (see Figures 6C and 6E, black dotted line). As there is considerable variability in reported mislocalization amplitude, we do not consider this a definite argument against the CG method. Further, the estimation of the temporal receptive field properties from flicker fusion data is certainly subject to variability. Hence, we regard both of these models are feasible candidates. Note that the two models have very different extraretinal signals. The CG model features a slow exR, while the MAX/ML model features a very fast one.

Note that for both of these models which lie at the intersection of Pola's and our restrictions, the extraretinal signal starts moving only well after saccade onset. Furthermore, within the framework of our simulations there is not a single plausible model (i.e., a model with causal receptive fields) with an *exR* that starts moving before saccade onset. This provides further evidence against the common assumption that the mislocalization of stimuli flashed before saccade onset can only be explained by an anticipatory extraretinal signal. This argument certainly does not deny the existence of anticipatory signals that may help to prepare visual areas for upcoming saccades. It merely argues against the involvement of such signals in perisaccadic shift.

Effect of stimulus duration

Our model predicts no mislocalization for continuously present stimuli, and shift-like mislocalization for flashed stimuli. Therefore, it seems well suited to make predictions regarding the transition between these two extremes. We simulated the localization of flashes with different durations from 1 to 80 ms (data not shown). As expected, the maximal mislocalization amplitude drops gradually to about a quarter of its original value as stimulus duration is increased from 1 to 80 ms. For longer stimuli, a small effect of saccades on mislocalization in saccade direction is predicted when stimulus offset occurs around saccade onset. Conversely, mislocalization opposite to saccade direction is predicted when stimulus onset occurs around saccade offset.

Assumption of linearity

In the context of the current model we assumed that the visual system processes information linearly and strictly feed-forward. Rational for this assumption was to keep the model both easy to understand and mathematically tractable. However, we acknowledge that the assumption of linearity is a simplification that almost certainly will be violated especially when using very short visual stimuli. Several studies have shown that responses to very brief visual stimuli are stronger and last longer than responses predicted from linear models (Duysens, Orban, Cremieux, & Maers, 1985; Kratz & May, 1990; Levick & Zacks, 1970). Other studies suggest different nonlinearities that may lead to latency differences between responses to the flashed and moving present stimuli (e.g., Orban, Hoffman, & Duysens, 1985). Similarly, there may be nonlinearities present in the responses to the continuously present stimuli. These nonlinearities may be mediated by lateral or feedback projections (Matin, Clymer, & Matin, 1972).

Naturally, our idea of calibrating the extraretinal signal to cancel out the retinal signal of a continuously present stimulus can be applied to models that incorporate such

nonlinearities. We do expect that the inclusion of these nonlinearities will provide an even better understanding of the precise mechanisms at work.

Within the current computational context it is easy to investigate the effects of the nonlinearities associated with the flashed stimuli. We discuss two types of nonlinearities, which affect (1) response amplitude and (2) shape of the temporal impulse response for flashed stimuli. Interestingly, increasing response amplitude of the flashed stimuli has no effect on the observed mislocalization (data not shown). The reason for this can be understood from Equation 7: the time-resolved world-centered position estimate, $W(t)$, is independent of response amplitude. In addition, the weights $g(t)$ are independent of response amplitude because of the normalization step that sets the integral of $g(t)$ equal to one.

Nonlinearities that change the shape of the temporal impulse response function will change the mislocalization profile. These changes will introduce asymmetries favoring either mislocalization in the direction of the saccade prior to saccade onset or mislocalization in the direction opposite to saccade direction in the second half of the saccade. Which of the two effects occurs can, to a first approximation, be predicted from the center of gravity of the temporal impulse response function. If the center of gravity shifts towards later times, it will increase the mislocalization amplitude in saccade direction. If it shifts towards earlier times, it will decrease the mislocalization amplitude in saccade direction. An example of the latter case could be a reduction of response latency for flashed stimuli that would shift the entire neuronal response to earlier times and consequently attenuate the mislocalization amplitude in saccade direction (data not shown). An example of the second case could be a prolongation of the neuronal response of flashed stimuli that would shift the center of gravity of the impulse response function towards later times.

Active eye-movement versus passive image motion

Flashed stimuli are not only mislocalized during real but also during simulated saccades. Stimuli flashed around the onset of fast uniform background motion will be mislocalized in direction opposite to the background motion, i.e., in the direction of the simulated saccade. The pattern of mislocalization during simulated saccades is quite similar to the one observed during real saccades (Honda, 1995; MacKay, 1970; Morrone, Ross, & Burr, 1997, see however, Ostendorf, Fischer, Gaymard, & Ploner, 2006). Despite these similarities, no common mechanism has been suggested for mislocalization during real saccades in the dark and simulated saccades in ambient lighting conditions. In the following we want to relate the predictions of our model to the observation of mislocalization during simulated saccades.

We begin our discussion of the matter by noting that our model by itself does not predict the observed mislocalization of stimuli flashed during simulated saccades: the extraretinal signal stays constant and hence flashed stimuli are not mislocalized in craniocentric coordinates. However, as noted above, our model does predict relative mislocalization between the flashed stimulus and the continuously present background. In other words, the flashed stimulus is mislocalized relative to the coordinate system defined by the visual references in the background.

We speculate that the empirically observed absolute mislocalization of the flashed stimulus may be causally related to this mislocalization relative to the visually defined coordinate system. To that aim we assume that in the presence of visual references, the visual system estimates the craniocentric position of the flashed stimulus indirectly, i.e., relative to the visual references:

$$\overline{W}_f = \overline{W}_c + \Delta. \tag{9}$$

Here $\overline{W}_c$ corresponds to the craniocentric position of the continuous stimulus and Δ is given by our model as calculated by Equations D1′/2′/3′. In the context of our model, $\overline{W}_c$ does not correspond to the true location of the continuously present stimulus. Consequently, Equation 9 does not predict the empirically observed mislocalization. However, if we assume that the visual system has an independent way to correctly estimate $\overline{W}_c$, Equation 9 would predict the observed mislocalization during simulated saccades. We will not speculate in detail about the mechanisms that may give rise to an accurate estimate of $\overline{W}_c$. However, we assume that it would involve neurons with inherently faster temporal dynamics, i.e., the magnocellular pathway, in combination with cross-validation by other sensory-motor systems.

It is important to note that for simulated saccades the reported effect of mislocalization in the direction opposite to the simulated saccade tended to be weaker or even absent (Morrone et al., 1997). Assuming that our model provides an accurate prediction of the relative position error, this implies that in the second half of the simulated saccade part of the error is actually carried by an absolute mislocalization of the continuously present stimulus, i.e., an error in $\overline{W}_c$. Further, it needs to be mentioned that one recent study (Ostendorf et al., 2006) reported compression of space around the onset of simulated saccades. Our model does not predict such behavior (see next paragraph).

Relation to perisaccadic compression

Depending on the presence of visual references and/or background luminance, different patterns of perisaccadic mislocalization have been reported (Lappe et al., 2000).

Perisaccadic shift is generally observed in the dark and in the absence of (postsaccadic) visual references. With ambient light and in the presence of visual references a different pattern of mislocalization is observed, the so-called perisaccadic compression (e.g., Morrone et al., 1997). So far, no model of perisaccadic mislocalization, including ours, has been able to accurately predict perisaccadic shift and compression as a function of the visual references and/or background luminance.

However, it is important to note that our model accurately predicts relative mislocalization during simulated saccades, which are necessarily conducted with visual references (see above). Such conditions typically lead to perisaccadic compression if measured with real, not simulated saccades. Our tentative explanation of this finding is the following. We assume that perisaccadic compression depends in one way or another on the remapping of receptive fields. Hence we do not expect perisaccadic compression during simulated saccades independent of the presence or absence of visual references. Further, we suggest that receptive fields are remapped during real saccades *only if* visual stimuli are present in the scene. In the dark, the remapping of receptive fields which is thought to link the pre- and postsaccadic neuronal representation in retinocentric visual areas seems pointless. Under this assumption we would predict no perisaccadic compression during real saccades in the absence of visual references.

Conclusions

For almost 200 years, the reafference principle was thought to mediate perceptual stability during eye-movements. Several experiments used brief perisaccadically presented stimuli to test the validity of the reafference principle around the occurrence of fast eye-movements; the finding of perisaccadic shift was interpreted as evidence against the reafference principle. Consequently, perisaccadic visual stability was attributed other mechanisms such as a general decrease of visual sensitivity (saccadic suppression), the remapping of visual receptive fields and visual masking. Our modeling efforts show that the reafference principle actually provides a very simple and elegant account of perisaccadic shift, if slow temporal dynamics in the afferent visual pathway are acknowledged: instead of interpreting the extraretinal signal as a faulty estimate of eye position, we interpret it as an accurate estimate of the neuronal representation of a continuously present stimulus. Hence, the model solves the apparent paradox of why mislocalization occurs for flashed, but not for continuously present stimuli. Rather than being mutually exclusive, we argue that mislocalization of flashed stimuli arises as a consequence of providing accurate craniocentric position estimates for

continuously present stimuli under the assumption temporal low-pass filtering the afferent visual pathway.

Appendix A

Function arguments and subscripts:

To specify the input to the functions (see below) we use a number of different arguments. The main argument(s) is (are) presented in parenthesis following the function symbol. Additional qualifying arguments are represented as subscripts.

c/f—qualifies a function as pertaining either to conditions with a **f**lashed or a **c**ontinuously present stimulus.

τ—denotes time within a trial relative to saccade onset. For example: $R_c(\tau)$ denotes the retinal signal of a continuously present stimulus as a function of time τ after saccade onset.

t—specifies a condition in which the flash was present at time t relative to saccade onset. For example: $E_f(t)$ denotes the craniocentric localization error of a stimulus flashed at time t relative to saccade onset. Note the subtle but important difference between the two arguments t and τ: $exR(\tau)$ describes the extraretinal signal as a function of time from saccade onset. In contrast, $exR(t)$ denotes the value of the extraretinal signal at the time the flash was presented.

x—indexes a particular neuron. As the neurons are arranged retinotopically, x indicates a particular retinocentric position.

Constants and Operators

n—**shape parameter** of the Gamma distribution.

λ—**scale parameter** of the Gamma distribution. Corresponds to the time constant of the underlying exponential distribution.

$*$—**convolution operator**. The spatio-temporal convolution operator was defined by:

$$S * \xi(x, \tau) = \iint S(u, v)\xi(u-x, v-\tau)dudv. \qquad \text{(A1)}$$

Functions

$h(\tau)$—**direction of gaze** as a function of time from saccade onset.

$S(x, \tau)$—**retinal projection** of the visual scene as a function of one-dimensional space x and time τ after saccade onset.

$\xi(x, \tau)$—**(spatio-) temporal receptive field**. A kernel which describes the neuronal processing of the retinal

stimulus. $\xi(0, \tau)$ describes the one-dimensional temporal receptive field (spatial position x is being held constant at zero). To simplify the notation we use $\xi_0(\tau)$ or simply ξ_0 to refer to the same expression, i.e., the temporal receptive field.

$N(x, \tau)$—**neuronal activity** in the retinocentric visual area as a function of position x and time τ after saccade onset. In Equation 4 $N(x, \tau)$ is described as the convolution of S with ξ.

$R_{c/f,t}(\tau)$—**retinal signal** defined in Equation 5 as the retinocentric position of a stimulus as estimated from the neuronal activity. For example, $R_{f,t}(\tau)$ denotes the retinal signal of a stimulus flashed at time t after saccade onset as a function of time τ after saccade onset. As $R_{f,t}(\tau)$ does not vary as a function of τ, we will at times rewrite the same expression as $R_f(t)$. Note that $R_f(t)$ is the inverse of direction of gaze at the time of the flash $R_f(t) = -h(t)$.

$exR(\tau)$—**extraretinal signal**. In the context of the damped eye-position model, exR is interpreted as the visual system's (erroneous) estimate of eye-position. In the current manuscript exR is defined as the retinal signal of a continuously present stimulus (see Equation 8). Hence exR is not an (erroneous) estimate of eye-position, but an accurate estimate of R_c. exR can be thought of as the output of the forward model (e.g., Kalveram, 1993) which explicitly predicts the reafference as a function of the efference and the neuronal preprocessing (reafference Principle: von Holst & Mittelstaedt, 1950). If ξ_0 is a Dirac impulse our definition and the definition used in the damped eye-position model are identical (except for the sign).

$W_{c/f,t}(\tau)$—**instantaneous craniocentric position**. Is derived by subtracting exR from R (see Equation 6). Additional subscripts may specify the instantaneous craniocentric position of the continuous or the flashed stimulus. If the flashed stimulus is specified, a second subscript t may indicate the time of the flash relative to saccade onset.

$\overline{W}_{f/c}(t)$—**global craniocentric position**. For clarity, the second subscript indicating the time t of the flash after saccade onset is now the explicit argument. $\overline{W}_f(t)$ represents the craniocentric position estimate of a stimulus flashed at time t after saccade onset. Notice the difference to the instantaneous craniocentric position which is expressed as a function of τ, i.e. time after saccade onset.

$\overline{E}_f(t)$—**global craniocentric position error**. Because the actual stimulus position was always 0° in craniocentric coordinates, it is identical to the global craniocentric position: $\overline{E}_f(t) = \overline{W}_f(t)$.

References

Bremmer, F., & Krekelberg, B. (2003). Seeing and acting at the same time: Challenges for brain (and) research. *Neuron, 38,* 367–370. [PubMed]

Cai, R. H., Pouget, A., Schlag-Rey, M., & Schlag, J. (1997). Perceived geometrical relationships affected by eye-movements. *Nature, 386,* 601–604. [PubMed]

Carpenter, R. H. S. (1988). *Movements of the eyes*. London: Pion Ltd.

Deneve, S., Latham, P. E., & Pouget, A. (2001). Efficient computation and cue integration with noisy population codes. *Nature, 4,* 826–831. [PubMed]

Duysens, J., Orban, G. A., Cremieux, J., & Maers, H. (1985). Visual cortical correlates of visible persistence. *Vision Research, 25,* 171–178. [PubMed]

Gruesser, O. J. (1995). On the history of the ideas of efference copy and reafference. In C. Debru (Ed.), *Essays in the history of the physiological sciences*. Amsterdam–Atlanta, GA: Rodopi-Clio medica.

Helmholtz, H. v. (1866). *Handbuch der physiologischen Optik*. Leipzig: Voss.

Honda, H. (1989). Perceptual localization of visual stimuli flashed during saccades. *Perception & Psychophysics, 45,* 162–174. [PubMed]

Honda, H. (1995). Visual mislocalization produced by a rapid image displacement on the retina: Examination by means of dichoptic presentation of a target and its background scene. *Vision Research, 35,* 3021–3028. [PubMed]

Kalveram, K. T. (1993). A neural-network model enabling sensorimotor learning: Application to the control of arm movements and some implications for speech-motor control and stuttering. *Psychological Research, 55,* 299–314. [PubMed]

Knill, D. C., & Pouget, A. (2004). The Bayesian brain: The role of uncertainty in neural coding and computation. *Trends in Neurosciences, 27,* 712–719. [PubMed]

Kratz, K. E., & May, J. G. (1990). Response persistence of cat retinal ganglion cells to the temporarily discrete

presentation of sinewave gratings. *International Journal of Neuroscience, 9,* 435–444. [PubMed]

Krekelberg, B., & Lappe, M. (2000). A model of perceived relative positions of moving objects based upon a slow averaging process. *Vision Research, 40,* 201–215. [PubMed]

Lappe, M., Awater, H., & Krekelberg, B. (2000). Postsaccadic visual references generate presaccadic compression of space. *Nature, 386,* 892–895. [PubMed]

Levick, W. R., & Zacks, L. (1970). Responses of cat retinal ganglion cells to brief flashes of light. *The Journal of Physiology, 206,* 677–700. [PubMed]

MacKay, D. M. (1970). Mislocation of test flashes during saccadic image displacements. *Nature, 227,* 731–733. [PubMed]

Matin, E., Clymer, A. B., & Matin, L. (1972). Metacontrast and saccadic suppression. *Science, 178,* 179–182. [PubMed]

Matin, L. (1976). Saccades and extraretinal signals for visual direction. In R. A. Monty & J. W. Senders (Eds.), *Eye movements and psychological processes* (pp. 205–219). New York: John Wiley.

Morrone, M. C., Ross, J., & Burr, D. C. (1997). Apparent position of visual targets during real and simulated saccadic eye movements. *Journal of Neuroscience, 17,* 17941–17953. [PubMed]

Murakami, I., & Cavanagh, P. (1998). A jitter after-effect reveals motion-based stabilization of vision. *Nature, 395,* 798–801. [PubMed]

Murakami, I., & Cavanagh, P. (2001). Visual jitter: Evidence for visual-motion based compensation of retinal slip due to small eye movements. *Vision Research, 41,* 798–801. [PubMed]

Nijhawan, R. (1994). Motion extrapolation in catching. *Nature, 370,* 256–257. [PubMed]

Orban, G. A., Hoffman, K. P., & Duysens, J. (1985). Velocity selectivity in the cat visual system: I. Responses of LGN cells to moving bar stimuli: A comparison with cortical areas 17 and 18. *Journal of Neurophysiology, 54,* 1026–1049. [PubMed]

Ostendorf, F., Fischer, C., Gaymard, B., & Ploner, C. J. (2006). Perisaccadic mislocalization without saccadic eye movements. *Journal of Neuroscience, 137,* 737–745. [PubMed]

Pola, J. (2004). Models of the mechanism underlying perceived location of a perisaccadic flash. *Vision Research, 44,* 2799–2813. [PubMed]

Pola, J. (2007). A model for the mechanisms for the perceived location of a single flash and two successive flashes presented around the time of a saccade. *Vision Research, 47,* 2798–2813. [PubMed]

Pola, J. (2008). An explanation of perisaccadic compression of visual space. *Society for Neuroscience,* 165.27/II10.

Purkinje, J. E. (1825). Ueber die Scheinbewegungen, welche in subjectiven Umfange des Gesichtssinnes vorkommen. *4. Bulletin der Naturwisssenschaftlichen Sektion der Schlesischen Gesellschaft.*

Purushothaman, G., Patel, S., Bedell, H. E., & Ogmen, H. (1998). Moving ahead through different visual latency. *Nature, 396,* 424. [PubMed]

Ross, J., Morrone, M. C., Goldberg, M. E., & Burr, D. C. (2001). Changes in visual perception at the time of saccades. *Trends in Neurosciences, 24,* 113–121. [PubMed]

Schlag, J., & Schlag-Rey, M. (1995). Illusory localization of stimuli flashed in the dark before saccades. *Vision Research, 3,* 2347–2357. [PubMed]

Schlag, J., & Schlag-Rey, M. (2002). Through the eye, slowly: Delays and localization errors in the visual system. *Nature Reviews, Neuroscience, 3,* 191–215. [PubMed]

Steinbuch, J. G. (1811). *Beytrag zur Physiologie der Sinne.* Nuernberg: Schrag.

Teichert, T., Klingenhoefer, S., Wachtler, T., & Bremmer, F. (2008). Depth perception during saccades. *Journal of Vision, 8*(14):27, 1–13, http://www.journalofvision.org/content/8/14/27, doi:10.1167/8.14.27. [PubMed] [Article]

Von Holst, E., & Mittelstaedt, H. (1950). Das Reafferenzprinzip. *Naturwissenschaften, 37,* 464–476.

Wurtz, R. H. (2008). Neuronal mechanisms of visual stability. *Vision Research, 48,* 2070–2089. [PubMed]

Saccadic suppression of displacement in face of saccade adaptation

S. Klingenhoefer *, F. Bremmer

Dept. Neurophysics, Philipps-University Marburg, Germany

A B S T R A C T

Saccades challenge visual perception since they induce large shifts of the image on the retina. Nevertheless, we perceive the outer world as being stable. The saccadic system also can rapidly adapt to changes in the environment (saccadic adaptation). In such case, a dissociation is introduced between a driving visual signal (the original saccade target) and a motor output (the adapted saccade vector). The question arises, how saccadic adaptation interferes with perceptual visual stability. In order to answer this question, we engaged human subjects in a saccade adaptation paradigm and interspersed trials in which the saccade target was displaced perisaccadically to a random position. In these trials subjects had to report on their perception of displacements of the saccade target. Subjects were tested in two conditions. In the 'blank' condition, the saccade target was briefly blanked after the end of the saccade. In the 'no-blank' condition the target was permanently visible. Confirming previous findings, the visual system was rather insensitive to displacements of the saccade target in an unadapted state, an effect termed saccadic suppression of displacement (SSD). In all adaptation conditions, we found spatial perception to correlate with the adaptive changes in saccade landing site. In contrast, small changes in saccade amplitude that occurred on a trial by trial basis did not correlate with perception. In the 'no-blank' condition we observed a prominent increase in suppression strength during backward adaptation. We discuss our findings in the context of existing theories on transsaccadic perceptual stability and its neural basis.

© 2010 Elsevier Ltd. All rights reserved.

1. Introduction

It is well known that the oculomotor system is able to retain its accuracy in case of changes in oculomotor conditions (e.g. muscle weakness or neural damage) that otherwise would lead to movement inaccuracy and poor vision. In the laboratory this effect, termed saccade adaptation, is typically studied by repetitive displacements of the saccade target while the eyes are moving. When the targets are shifted systematically in saccade direction, this process is called forward adaptation, for shifts against saccade direction it is called backward adaptation (McLaughlin (1967), Miller, Anstis, and Templeton (1981) and others, see Hopp and Fuchs (2004) for a review). During the first trials of an adaptation experiment, the motor error as induced by the target shift is corrected by secondary saccades. After a few tens of trials, however, human subjects adjust the gain of their first saccade until the displaced target position is reached with a single saccade.

The adaptation effect is not only relevant in the context of oculomotor learning. The investigation of saccade adaptation might also contribute to the understanding of the mechanisms that guarantee transsaccadic perceptual stability. Saccades in general

challenge visual perception (Bremmer & Krekelberg, 2003). Saccade adaptation specifically challenges perceptual stability as it interferes with the established mapping between pre- and post-saccadic perceptual space. Parts of the presaccadic visual field that were 'bound' to certain post-saccadic positions prior to adaptation will fall onto different spatial locations afterwards.

In the present study we aimed to investigate how the visual system would retain perceptual stability in the presence of motor distortions as induced by saccade adaptation. It is known that transsaccadic perceptual stability is supported by different mechanisms. On the one hand, specific aspects of visual perception are suppressed during saccades ((Bremmer, Kubischik, Hoffmann, & Krekelberg, 2009; Burr, Morrone, & Ross, 1994), see Ross, Morrone, Goldberg, and Burr (2001) for a review). On the other hand, mechanisms that guarantee space congruency across fixations are involved (see Wurtz (2008) for a review). Existing theories of transsaccadic stability can be grossly divided into those that emphasize post-saccadic (and in some notions rather 'passive') effects and others that focus on the contribution of active preparatory processes that operate prior to the saccade (see Wurtz (2008) for a review).

Evidence for the latter originates from physiological findings that were first made by single cell recordings in area LIP of the rhesus monkey while the animal performed a saccade task (Colby, Duhamel, & Goldberg, 1995; Duhamel, Colby, & Goldberg, 1992). In

---

* Corresponding author. Address: Department of Neurophysics, Philipps-University Marburg, Karl-v-Frisch-Str. 8a, D-35032 Marburg, Germany.

E-mail address: steffen.klingenhoefer@physik.uni-marburg.de (S. Klingenhoefer).

this study, some of the observed neurons showed a remarkable spatial response profile prior to the eye movements: they shifted their receptive fields (RFs) from their current position to their designated post-saccadic position thereby anticipating the spatial consequences of the upcoming saccade. Since the discovery of this effect, usually termed saccadic 'remapping' or 'updating', it has been replicated in slightly different variations in multiple other areas of the monkey brain including the FEF (Umeno & Goldberg, 1997), the SC (Walker, Fitzgibbon, & Goldberg, 1995) and earlier extrastriate visual areas (Nakamura & Colby, 2002) as well as in humans (Merriam, Genovese, & Colby, 2003). For the monkey, it has been demonstrated that the anticipatory shifting of the RFs in the FEF is caused by an internal copy of the motor command, termed corollary discharge or efference copy (Sperry, 1950; von Holst & Mittelstaedt, 1950), that represents the metrics of the upcoming saccades (Sommer & Wurtz, 2006). It is currently unknown, however, if and how RFs shift in case of saccade adaptation, i.e. if the shift would be based on the adapted or rather on an unadapted efference copy.

An alternative hypothesis concerning perceptual stability is mainly based on results obtained in human psychophysical experiments. One classical paradigm to study transsaccadic perceptual stability in humans is the so called 'saccadic suppression of displacement' paradigm (SSD) (Bridgeman, Hendry, & Stark, 1975). In this paradigm subjects perform a visually guided saccade. While the eyes are in flight, the saccade target is slightly displaced to a random position. Subjects report if (or alternatively in which direction) they have perceived a displacement of the target. Usually, displacement detection thresholds increase dramatically during saccades compared to fixation conditions (Bridgeman et al., 1975; Deubel, Schneider, & Bridgeman, 1996; Li & Matin, 1990). In other words, the visual system is rather tolerant against transsaccadic discrepancies in object positions. This tolerance, which typically is considered as evidence for perisaccadic perceptual stability, can be easily disrupted, though, using a simple manipulation termed blanking effect. In such case, the saccade target is briefly blanked (typically 200 ms) at the time the eyes land (Deubel et al., 1996). This cancels perceptual stability and subjects regain a remarkable precision in a displacement discrimination task. Based on these and other findings (Deubel, Bridgeman, & Schneider, 1998), Deubel and colleagues have proposed that re-afferent visual information (i.e. the post-saccadic visual scene) and in particular the presence of reference objects like the saccade target itself might play an important role in the preservation of transsaccadic perceptual stability (Bridgeman, 1995; Deubel, 2004; Deubel et al., 1998).

Following a slightly different approach, a couple of recent studies have found adaptation specific distortions in perceptual localization of stimuli that are presented before, during or after a saccade (Awater, Burr, Lappe, Morrone, & Goldberg, 2005; Bahcall & Kowler, 1999; Collins, Dore-Mazars, & Lappe, 2007; Collins, Rolfs, Deubel, and Cavanagh, 2009).

Bahcall and Kowler (1999) and Collins et al. (2009) asked subjects to indicate the position of a visual target that was used to elicit an (adapted) saccade in a blanking paradigm. Judgments were made by comparing the remembered target position to that of a probe stimulus, that was presented some time (200 ms) after the saccade had ended. In these experiments, the original saccade target was blanked before (Bahcall & Kowler, 1999) or during (Collins et al., 2009) the saccade. In non-adaptive control trials, localization of the saccade target was almost veridical. In adaptation trials, however, the probe stimuli had to be shifted in the direction of adaptation to match the remembered position of the saccade target.

In our present study we aimed at extending the existing literature on localization during saccade adaptation by investigating SSD in face of saccade adaptation. In contrast to Bahcall and Kowler

(1999) and Collins et al. (2009) we conducted our main experiments under conditions in which perceptual stability was not disrupted by the target blanking effect. Further, we did not only concentrate on the spatial aspect of SSD, but did also quantify suppression strength. We engaged subjects in saccade adaptation paradigms. Once adaptation was established, we interspersed trials in which perception of saccade target displacements was tested in a discrimination task (left/right), and, supplementary to former studies, also in a detection (yes/no) task. In addition to a *blank* condition we tested a *no-blank* condition in which the saccade target was not blanked when perceptual judgments were acquired. To avoid positional judgments with respect to external visual references, all our experiments were conducted in a completely dark environment.

2. Materials and methods

2.1. Subjects

Five subjects (three female and two male, mean age 26 years) gave written consent to participate in the experiments. All of them were experienced in psychophysical experiments, but were, except for one of the authors, naïve as to the goals of this study. The experiments were performed in accordance with the ethical standards of the 1964 Declaration of Helsinki.

2.2. Apparatus

Experiments were performed in a light and sound proof experimental chamber. Subjects were comfortably seated with their head supported by a chin rest. Eye position was monitored at 500 Hz using an infra-red eye tracker system (EyeLink II, SR-Research). Subjects were facing a large screen ($80° \times 60°$ of visual angle) on which stimuli were projected by a CRT projector (Marquee 8000, running at 150 Hz). Background luminance of the screen and its surroundings was below 0.1 cd/m², i.e. there were no visual references available during the trials. Saccade onset detection that triggered target displacements in the adaptation conditions and target disappearance in the *blank* trials (cf. below) was based on a pure position criterion: eye position had to deviate from the initial fixation position by more than 2° in the direction of the intended saccade for more than two samples.

2.3. Task

Subjects always had to make a saccade from left to right in response to a jump of a fixation target. In some trials ('probe trials') they were prompted to report their perception of perisaccadic target displacements. In such case we collected two responses: the direction of the target displacement (left/right) and whether or not subjects had perceived such a displacement (yes/no). In the following, we will refer to the results of the yes/no task as the detection data, to those of the left/right task as the discrimination data. The detection data are dependent on the response criteria of the subjects ('subjective data'), while the left/right response is bias free ('objective data'). To give a response, subjects pressed one of four possible response keys on the number pad of the keyboard according to the following coding scheme: 7 – 'left, yes', 9 – 'right, yes', 1 – 'left, no', 3 – 'right, no'. The given response was visible to the subject and could be corrected without temporal constraints.

2.4. Experimental conditions

Each subject was tested in the six conditions resulting from the combination of three adaptation conditions (*backward*, *forward* and *no-adaptation*) with two manipulations on the reappearance of the

68

saccade target after displacement (*no-blank* and *blank*) in probe trials. All subjects completed two sessions per condition.

2.4.1. Adaptation conditions

In *forward* and *backward* adaptation trials the saccade target was repositioned upon saccade onset by an amount of 20% of the saccade amplitude either in (*forward*) or against the direction (*backward*) of the eye movement, respectively. The saccade target remained at its original position in the *no-adaptation* control condition. In the following, the *forward* and *backward* adaptation conditions will be marked in figures and indices as 'F' and 'B', respectively; the control condition as 'C'.

2.4.2. Target blanking conditions

In probe trials, a brief blanking of the saccade target (250 ms) upon saccade onset distinguished *blank* trials from *no-blank* trials. In other words, in *no-blank* trials the saccade target was immediately displaced to its final position, in *blank* trials this was only the case after a brief period without any visual stimulation. Note, that the target was only blanked in trials in which the subjects were asked to give perceptual report. All other trials, i.e. pure saccade and pure saccade adaptation trials, were similar in *blank* and *no-blank* sessions.

At most two sessions were completed by an individual subject per day. After having completed an adaptation session, subjects were never tested in another session on the same day. Given these constraints, all conditions were tested in pseudo-randomized order.

2.5. Paradigm

2.5.1. General spatial layout

In all trials and conditions, saccades were triggered by a target jump of 25° amplitude from left to right. Mean positions of the pre- and post-saccadic targets were located on the horizontal meridian at −12.5° and +12.5°, respectively. In order to avoid habituation to particular eye positions, the spatial layout was jittered on a trial by trial basis by a random amount (±5°) around these mean positions. Fixation and saccade targets were white circles, 0.3° in diameter, and had a luminance of 10 cd/m².

2.5.2. Time course

A brief period without any stimulation (250 ms) preceded each trial and then a fixation target appeared on the left side of the screen. Subjects fixated this target and started each trial by button press. After a random time of 500 ms–750 ms the fixation point jumped to the right side of the screen, where it remained visible for another 800 ms. The end of a trial was marked by the disappearance of the fixation target. To prevent dark adaptation each trial was preceded by a luminance stimulus covering the area of the whole screen (12 cd/m², 175 ms).

Each session consisted of 300 trials. In case of adaptation trials, the session started with 15 initial trials and was followed by an adaptation phase of 85 trials. These 100 trials were followed by 200 intermixed adaptation and probe trials. For trials 100–200, probe trials had a probability of 25%. Thereafter, probe probability increased to 35%. Initial trials were pure saccade trials without perisaccadic modification of the saccade target's position. In probe trials the final target position was not determined by the adaptation condition but chosen from a set of positions that allowed an effective assessment of displacement detection performance. For this purpose, target position was drawn from a normal distribution (sigma = 4° in the *no-blank* condition, sigma = 2.6° in the *blank* condition). In order to prevent biasing the measurements by the choice of probe positions, the center of this distribution was determined adaptively during the initial probing phase using two staircase pro-

cedures. Perisaccadic target displacements in adaptation and probe trials were triggered by saccade onset, which was determined by a pure position criterion as described above.

In case of *no-adaptation* trials, the first 100 trials were standard trials without target displacements. In the following 200 trials, standard trials were interspersed with probe trials as described above.

2.6. Data analysis

Data were analyzed using Matlab (The Mathworks, Inc.). In all conditions, the data of the discrimination and the detection task were analyzed separately. In both cases we characterized the spatial aspect of the SSD effect as well as the suppression strength by calculating two indices: a position index (PI) and a suppression index (SI). The indices were defined differently for the two tasks (see below).

2.6.1. Analysis of discrimination data

To determine subjects' discrimination performance, probabilities of 'right' responses were plotted as a function of probe position. Using least squares fitting, logistic psychometric functions with two free parameters (slope and position) were fitted to the data. We defined the position index PI as the point of subjective equality (PSE) of the psychometric function. This determines the probe position where subjects reported 'right' in 50% of the cases, i.e. where discrimination performance was at chance level. To calculate the suppression index (SI) we first determined the precision of the discrimination judgments, i.e. the just noticeable difference (JND) of the psychometric function (measured at 20% and 80% 'right' judgments). The JND was then divided by the value of the *no-blank, no-adaptation* condition and defined the suppression index SI.

2.6.2. Analysis of detection data

When displacement detection responses were plotted as function of target displacement (yes = 1, no = 0), they exhibited a trough at the position with the smallest displacement detection probability. In order to quantify these perceptual data, we fitted asymmetric gaussian functions through the data (Ψ_{det}). The free parameters of the fits were the amplitude (A) of the trough, the halfwidth of the falling (s_{left}) and the rising part (s_{right}) of the curve, as well as the position of the minimum. In order to fit the experimental data of all conditions well, we had to allow for elongated, flat minima. For this reason the position of the fitted curve was defined by two parameters (x_{left} and x_{right}) representing the left and the right border of the minimum separately. All values between these borders were fitted with the same amplitude value (A). To quantify suppression strength, we computed the area between a constant function with detection probability of 90% and that part of the function Ψ_{det} that fell below this probability. This value was divided by the value of the control condition (i.e. the *no-blank, no-adaptation* condition) and defined the suppression index SI. The position index PI was defined as the *x*-component of the centroid of the area of the trough.

2.7. Statistics

To quantify the population data, all measurements from single subjects were pooled prior to the analysis. In all statistical tests, the *no-adaptation* control was compared to both the *backward* and the *forward* condition using an α-level of 5%. Below, adaptation conditions will be indicated in the superscripts of the respective measures; differences will be marked by a delta symbol. For example ΔPI^{B-C} represents the difference in PI between *backward* and *no-adaptation* control condition, i.e. $\Delta PI^{B-C} = PI^B - PI^C$. To establish

significance, 1-α confidence intervals were determined for all test statistics using a resampling bootstrap method. In each test $n = 1000$ bootstrap samples of the respective experimental data were created. Significant difference between adaptation conditions was established by testing if zero was included in the confidence interval of the mean.

3. Results

3.1. Oculomotor behavior

Behavioral data for the different adaptation conditions are presented in Fig. 1. Results of all subjects and of both *blank* and *no-blank* conditions were pooled. No differences in oculomotor behavior could be observed in the data of the *blank* and *no-blank* experiments. As expected and documented in many studies before, targeting saccades of the *no-adaptation* control trials fell slightly short of the saccade target (undershoot). In this condition the gain (gain = saccade amplitude/target amplitude) was constant during the experiment ($g = 0.95$). The adaptation paradigm, on the other hand, induced rapid changes in saccade gain. In both conditions, *forward* and *backward* adaptation, the target position changed by 5°, i.e. 20% of the amplitude in the *non-adaptation* condition (25°). Asymptotic differences in amplitude of $-3.7°$ and 2.2° between control and *backward* and *forward* condition were found, respectively. The corresponding gain values were $g^B = 0.852$ and $g^F = 1.088$ (as compared to the target values $g^B = 0.800$ and $g^F = 1.200$). Confirming results from many previous studies backward adaptation was more complete than forward adaptation. Importantly, during the probe phase saccade gain had already reached an asymptotic level and was thus rather stable.

3.2. Perception (I): SSD in face of saccade adaptation

Saccade landing positions and psychometric functions of the *no-blank* condition are presented in Fig. 2. Functional values resulting
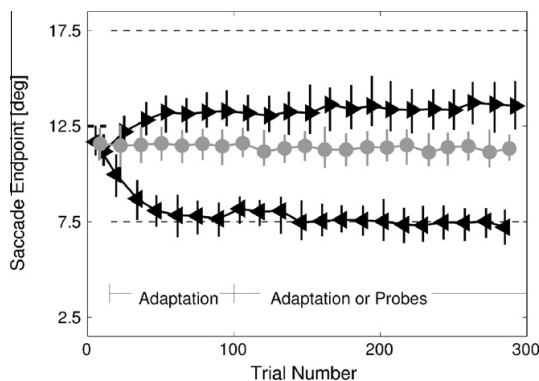

Fig. 1. *Amplitude change during saccade adaptation.* Median horizontal landing positions of targeting saccades are shown as a function of trial number (average data from all subjects and conditions; error bars indicate the first and the third quartile). The position of the initial saccade target on the screen was +12.5°. Target steps during adaptation were ±5°, corresponding to 20% of the intended saccade amplitude. Dashed lines indicate the position of the saccade target after the target step in the adaptation trials. Both adaptation conditions induced a change in saccade gain. Forward adaptation (right-facing triangles), was less complete than backward adaptation (left-facing triangles). Saccade endpoints during the non-adaptive control condition (circles) revealed a typical small saccadic undershoot. After an initial pure adaptation phase, probe trials were interspersed randomly in order to collect responses on the perception of target displacements.

from these behavioral data (the position index (PI) and the suppression index (SI)) are shown in Fig. 3.

As expected, the distributions of the saccade landing sites were different in the adapted as compared to the control condition (left column of Fig. 2). During backward adaptation the endpoint distribution was slightly narrower (3.2° half width at half height (HWHH)) than in the control condition (3.6° HWHH), the peak value increased by 18% as compared to the control condition. During forward adaptation the endpoint distribution was slightly broader (4.0° HWHH) while the peak value decreased by 4% as compared to the control condition.

The middle and right column of Fig. 2 present the psychometric curves of the population data. On average those curves were based on $n = 476$ (min. 469, max. 499) data points. During control saccades, the target positions with the smallest displacement detection probability were $PI_{dis} = 12.7°$ in the discrimination task and $PI_{det} = 12.8°$ in the detection task, i.e. they fell almost exactly on the original target position (12.5°). During adaptation, target stimuli that remained undisplaced at their initial position were likely to be perceived as displaced. Differences in PI between adaptation and control conditions were: $\Delta PI_{dis}^{B-C} = PI_{dis}^B - PI_{dis}^C = -3.8°$ and $\Delta PI_{det}^{B-C} = PI_{det}^B - PI_{det}^C = -3.0°$ in the *backward* condition, as well as $\Delta PI_{dis}^{F-C} = 3.0°$ and $\Delta PI_{det}^{F-C} = 2.7°$ in the *forward* condition. As a consequence of the shifting PIs, the amount of 'perceptual overshoot', i.e. the difference between PI and median saccade landing site (EYE) was rather constant across conditions (cf. dark, inset bars in Fig. 3A) and C)). Compared to the changes of the PIs, the changes in 'perceptual overshoot' were small but significant for the *forward* conditions ($\Delta(EYE - PI)_{dis}^{F-C} = 0.8°$ and $\Delta(PI - EYE)_{det}^{F-C} = 0.6°$) and the *backward* condition of the detection task $\Delta(PI - EYE)_{det}^{B-C} = 0.8°$.

In addition to the shifting of the PIs during adaptation, both the discrimination as well as the detection performance during *backward* adaptation decreased. This was reflected by a significant increase of the SI ($\Delta SI_{dis}^{B-C} = 0.67$ and $\Delta SI_{det}^{B-C} = 0.30$). A more detailed analysis of the detection data during backward adaptation showed that the increase in SI was mainly due to changes in response behavior in the region between the adapted and the unadapted target position (represented by the rising part of the psychometric curve). To quantify this observation, we compared the halfwidths (s) of the falling and the rising components of the asymmetric gauss fit functions. The halfwidth of the rising component (s_{right}) of the psychometric function showed a significant increase in the *backward* adaptation condition when compared to the *no-adaptation* condition ($\Delta s_{right}^{B-C} = 3.8°$). The halfwidth of the falling component did not change significantly ($\Delta s_{left}^{B-C} = -0.6°$).

In addition to the population analysis, we also fitted psychometric curves through the responses of individual subjects (cf. Supplementary Fig. S1). On average single subjects' psychometric curves were based on $n = 95$ responses (min. 89, max. 103). Fig. 4 presents scatter plots of single subjects' PIs and SIs as a function of saccade end position. In both tasks, PIs were highly correlated to changes in saccade endpoint induced by the adaptation paradigms ($R^2 = 0.78$ in the discrimination and $R^2 = 0.92$ in the detection task).

3.3. Perception (II): the influence of target blanking

In the *blank* condition the saccade target was blanked for 200 ms upon saccade onset. Here, saccade endpoint distributions were comparable to those of the control condition (left column of Fig. 5). Both adaptation distributions were slightly lowered with peak reductions of 5% and 16%. The half-widths at half-height increased by 0.1° and 0.8° in the *backward* and *forward* adaptation condition, respectively.

The PIs of the *blank* condition ($PI_{dis}^B = 8.5°$, $PI_{dis}^N = 12.5°$, $PI_{dis}^F = 15.5°$ and $PI_{det}^B = 8.6°$, $PI_{det}^N = 12.4°$, $PI_{det}^F = 14.6°$) were
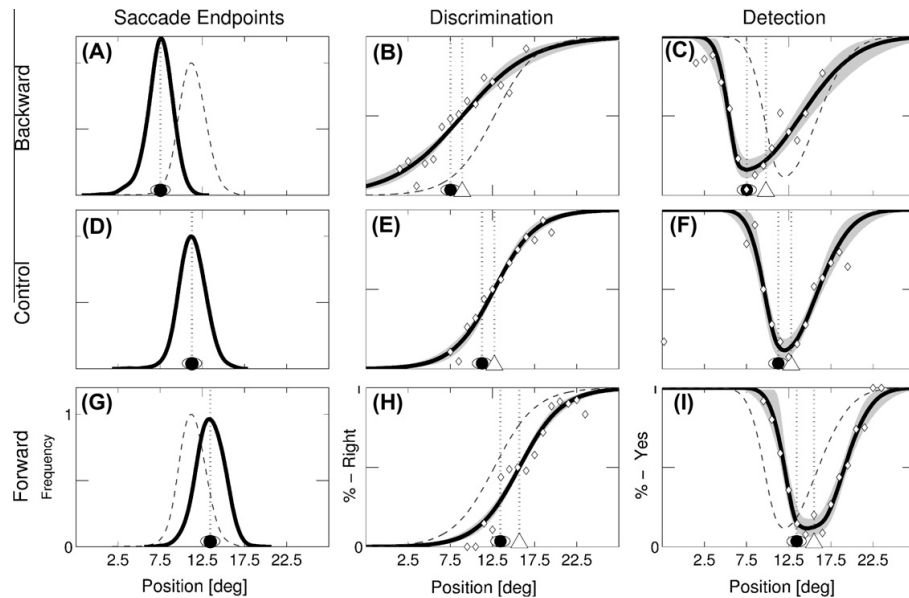
Fig. 2. *Behavioral and perceptual results of the 'no-blank' condition.* Saccade endpoint distributions (left column) as well as the psychometric functions of the discrimination and the detection task (middle and right column, respectively) are shown for different adaptation conditions (population data). Black lines represent the mean fitted curve, grey regions 95% confidence intervals of the mean. To allow for an estimation of the quality of the fit functions, binned response probabilities are presented as diamonds. Results of the control condition are presented in the middle row. Results from backward and forward adaptation are shown in the top and bottom row, respectively. In all panels horizontal screen position is plotted on the abscissa. The ordinates of endpoint distribution graphs represent frequency of occurrence (normalized by the peak value of the control condition); otherwise, response probability is shown. For better comparability between conditions (rows), results from the control condition are shown as dashed lines in all adaptation panels. To simplify comparisons between columns, eye icons on the bottom and vertical dash-dotted lines mark the median saccade endpoint of the corresponding adaptation condition in each panel. Triangles and vertical dotted lines indicate the position index (PI, see Section 2 for details). Psychometric functions shift almost in parallel to the adaptive changes in saccade endpoints (B and C, and H and I). C: In addition, the psychometric functions of the backward condition are flatter than the controls and thus reflect an increase in suppression strength (SI, see Section 2 for details).
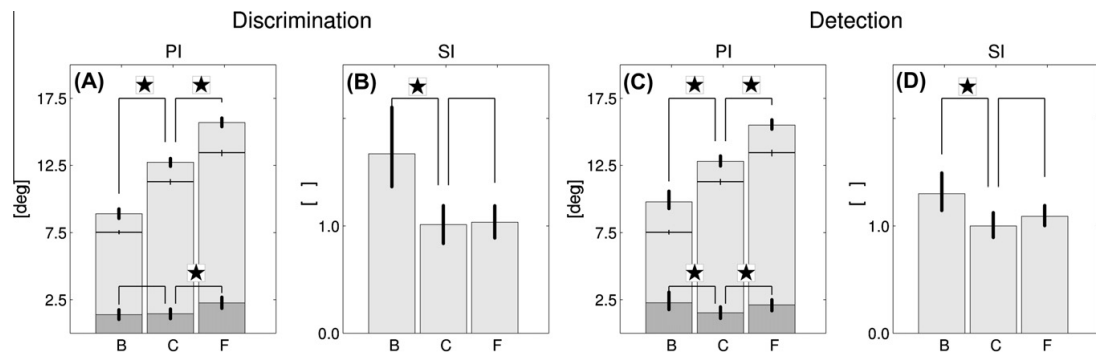

Fig. 3. *Position indices (PI) and suppression indices (SI) of the 'no-blank' condition.* The center column in each panel presents data from the control condition, left and right columns show data from backward and forward adaptation, respectively. Error bars denote 95% confidence intervals of the mean. Significant differences between control and either backward or forward adaptation are marked by asterisks. A and C: Light grey bars represent the position indices (PI). For comparisons, median saccade endpoints are plotted as inset horizontal lines. The adaptation induced changes of the PIs were strong and highly significant. The distances between saccade endpoints and the PIs are shown as dark grey bars. B and D: During backward adaptation the SI increased significantly in both the discrimination and the detection task.

comparable to those of the *no-blank* condition (Fig. 6). The differences in PI between adaptation conditions were highly significant and almost paralleled the adaptation induced changes in saccade landing site. The differences between the PIs and the median saccade landing positions (the 'perceptual overshoot') were rather constant across adaptation conditions again. The modulation of the value of the *forward* adaptation condition in the discrimination task, however, reached significance $\left(\Delta(\mathrm{PI} - \mathrm{EYE})_{\mathrm{dis}}^{\mathrm{B-C}} = 0.7^\circ\right)$. Sin-

gle subjects' PIs were highly correlated to changes in saccade end position ($R^2 = 0.78$ in the discrimination and $R^2 = 0.92$ in the detection task, cf. Supplementary Fig. S2).

In all cases, we found weaker SSD in the *blank* than in the *no-blank* condition. For example, in the population data of the *no-adaptation*, *blank* experiments, the suppression index (SI) dropped to 40% of its level in the *no-blank* condition, in the detection task it dropped to 11%. In the *no-blank* experiments, we found
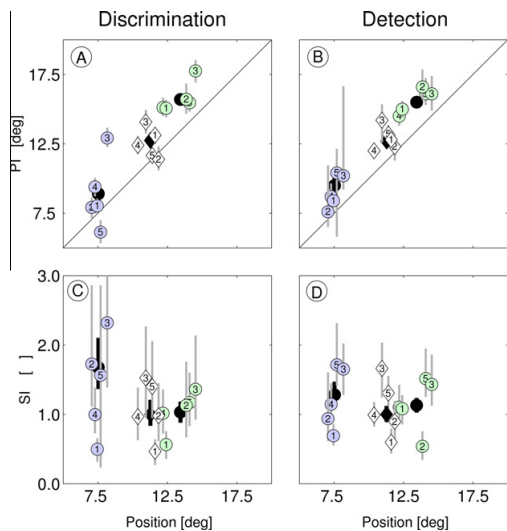
71

Fig. 4. *Comparison of single subject data and population results ('no-blank' condition).* The position indices (PI) and suppression indices (SI) calculated for individual subjects are plotted as a function of mean saccade landing position. Error bars correspond to 95% confidence intervals of the mean. In each panel, diamonds mark data from the no-adaptation condition, circles represent data from the adaptation conditions (blue: backward, green: forward). Numbers on the symbols correspond to subject IDs. For comparison, the results of the population analysis are plotted as black symbols in the background. A and B: Correlations between adaptation induced changes in saccade landing position and PI were high in both tasks ($R^2 = 0.78$ and $R^2 = 0.92$ for the discrimination and detection task, respectively). C and D: All SIs were normalized by the population value of the no-adaptation condition. (For interpretation of the references to colours in this figure legend, the reader is referred to the web version of this paper.)

a prominent increase in the SI of the discrimination data during backward adaptation. This was not the case in the discrimination data of the *blank* condition where the SI did not change significantly ($\Delta SI_{dis}^{B-C} = -0.1°$). The detection data of the *blank* condition, however, showed a significant increase in suppression strength in the *forward* adaptation condition ($\Delta SI_{det}^{B-C} = 0.18$).

3.4. Saccade endpoint variability

Visually guided saccades are a prototypical sensorimotor process. Such processes have to be performed within a certain frame of reference. So far, all perceptual data have been analyzed in a spatiocentric reference frame, namely in screen coordinates. The above described results have clearly shown that the perceptual effects (modulation of the position index PI with adaptation state) have paralleled oculomotor behavior (adaptation induced change of saccadic landing site). This might suggest that these perceptual effects might be best explained in oculocentric (retinal) coordinates. In order to test this hypothesis we transformed the perceptual data to oculocentric coordinates and calculated the corresponding psychometric functions. To compare perception within the two reference frames, we then contrasted the JNDs of the oculocentric psychometric functions with those of the spatiocentric analysis. Smaller JNDs in an oculocentric reference frame are indicative of a rather oculocentric coding. Similarly, a spatiocentric effect will have the smallest variance (which is reflected by the JND) when analyzed in spatiocentric coordinates. The reason for this is, that trial-by-trial saccade endpoint variability is added when an effect is not analyzed in its native coordinate system (see Supplementary material for a detailed explanation). Fig. 7 presents the JNDs as obtained in an oculocentric and in a spatiocentric analysis. In all conditions, the JNDs were consistently larger in the oculocentric analysis. For example, in the *no-adaptation, no-blank* control condition the JND increased by 2.0° in the oculocentric analysis. In the *no-blank* adaptation conditions the increase
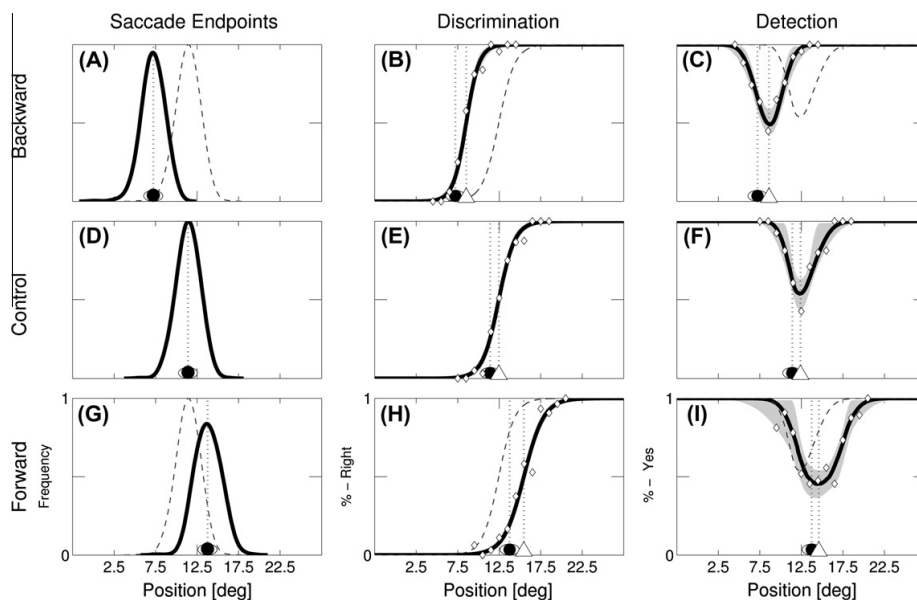
Fig. 5. *Behavioral and perceptual results of the 'blank' condition.* Graphical conventions are the same as in Fig. 2. Similar to the 'no-blank' condition, the psychometric curves shift in parallel to the changes in saccade landing position. The shapes of the curves of the discrimination data are similar across adaptation conditions, those of the detection data show a slight broadening in the forward adaptation condition. In general, the psychometric curves are steeper than those of the 'no-blank' condition (cf. Fig. 2).

887

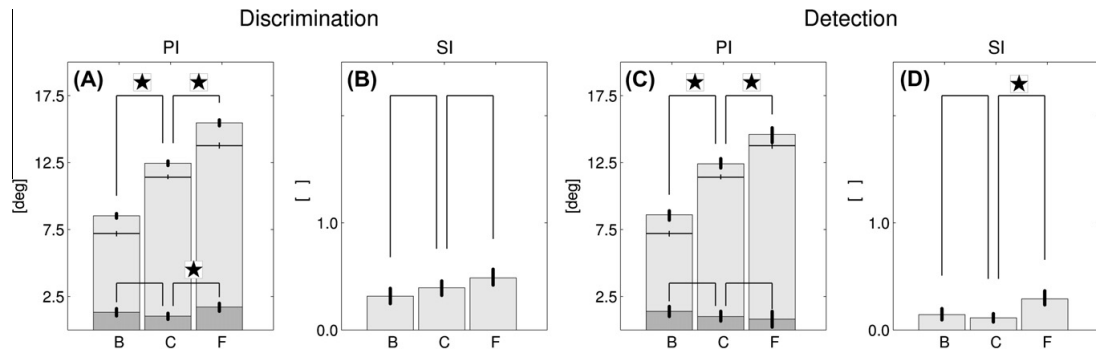**Fig. 6.** *Position indices (PI) and suppression indices (SI) of the 'blank' condition.* Graphical conventions are the same as in Fig. 3. A and C: Spatial characteristics of the results were similar to the 'no-blank' results. The PI changed significantly in the adaptation conditions in response to oculomotor adaptation. The difference between saccade endpoints and PIs, presented as dark grey bars, was constant in almost all conditions (in the forward adaptation condition of the discrimination task a small but significant modulations was observed). B and D: The SIs of the 'blank' condition, normalized by the value of the control condition of the 'no-blank' paradigm are presented. In general, SSD was weak compared to the 'no-blank' condition. The results of the detection task showed a significant increase in the SIs of the forward adaptation condition.
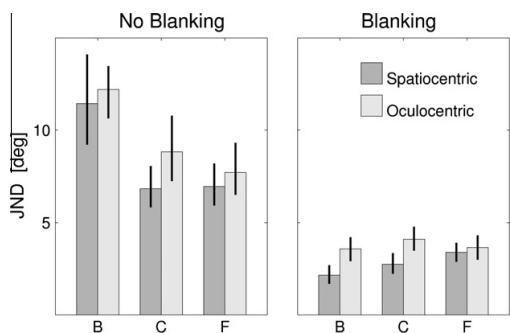

Fig. 7. *Comparison of oculocentric and spatiocentric data analysis.* The just noticeable differences (JNDs) of the psychometric functions of the discrimination task are presented for an analysis in oculo- and in spatiocentric coordinates. Assuming SSD is an oculocentric effect that is analyzed in a spatiocentric reference frame, response variability as reflected by the JNDs will be increased compared to the situation in which the effect is studied in its native coordinate system (due to the additive variability caused by saccade endpoint jitter, cf. Supplementary material). Experimental results, however, show consistently smaller spreads for the spatiocentric analysis.

was smaller 0.8° (*backward*) and 0.7° (*forward*), respectively. As described above, the increase in variance in the oculocentric analysis implies that part of saccade endpoint variability was compensated for in the perceptual judgments and thus the data can be better explained in a spatiocentric reference frame. It is important to note, however, that this is only true for trial by trial endpoint variability that is NOT caused by saccade adaptation. Our earlier results clearly show that changes in saccade endpoints caused by saccade adaptation were NOT compensated for in the perceptual judgments. Therefore, our results dissociate changes in saccade end position caused by saccade adaptation from those induced by trial by trial endpoint variability. Interestingly, the former remained obscured to the perceptual system – even though they were larger in size – whereas the latter were taken into account in the perceptual judgements.

4. Discussion

The goal of this study was to investigate how the visual system would deal with interferences with the established mapping between pre- and post-saccadic space. To this end we studied saccadic suppression of displacement (SSD) during saccade adaptation. We asked subjects to report on their perception of perisaccadic target displacements in two different conditions, known to either retain (*no-blank*) or to disrupt (*blank*) transsaccadic perceptual stability (Deubel et al., 1996).

Our main results can be summarized as follows. Psychometric functions shifted in the adaptation conditions such that the perisaccadic target displacements ceased to be perceived. These perceptual shifts were strongly coupled to the adaptive changes in saccade end position. Suppression strength increased under certain adaptation conditions. Most prominently this was the case during backward adaptation given that the saccade target was not extinguished perisaccadically (*no-blank* condition). If the target was blanked during the saccade, subjects were more likely to report displacements. Discrimination data showed higher precision in displacement detection. Accuracy, however, was not veridical in the adaptation conditions; the results were again biased towards the saccade landing. Finally, our results are consistent with the idea that, unlike information about changes in saccade landing site caused by saccade adaptation, information about trial by trial endpoint variability is included in the perceptual judgments. Below, we will discuss these results in the context of recent findings on perisaccadic localization and existing theories of transsaccadic perceptual stability.

4.1. Comparison to localization studies

In the last years, several studies have investigated the influence of saccade adaptation on perisaccadic localization (Awater et al., 2005; Bahcall & Kowler, 1999; Collins et al., 2007, 2009). Bahcall and Kowler (1999) asked subject to localize the former position of the saccade target relative to a brief post-saccadic stimulus during backward and forward adaptation. Recently, Collins et al. (2009) published a more detailed report for the backward adaptation case using a similar paradigm. In both studies, the saccade target was briefly blanked at the end of the saccade in an effort to avoid saccadic suppression of displacement (SSD). These results are thus comparable to the *blank* condition of our experiments. Both studies showed consistently that the saccade target was not localized at its original position but was perceptually shifted in the direction of adaptation. The spatial results from our current study are in line with these findings, both qualitatively and quantitatively. Neither Bahcall and Kowler (1999) nor Collins et al.

73

(2009), however, reported quantitative data on the strength of SSD under different adaptation conditions.

4.2. Pre- and post-saccadic mechanisms contributing to perceptual stability

A central question in the context of transsaccadic stability is how pre- and post-saccadic information are combined. Two important approaches have emerged: theories that emphasize post-saccadic (and in some notions rather 'passive') effects on the one hand (Bridgeman, 1995; Deubel, 2004; Deubel et al., 1998). On the other hand, active preparatory processes are discussed that operate prior to the saccade (Duhamel et al., 1992; Nakamura & Colby, 2002; Umeno & Goldberg, 1997; Walker et al., 1995). In the following, we will discuss our results within these frameworks.

Some of the aforementioned mislocalization effects observed during saccade adaptation have been interpreted in the context of extraretinal signals conveying information about changes in eye position. Bahcall and Kowler (1999) for example pointed out that the observed mislocalization of the saccade target in the direction of adaptation could be explained, if a signal representing the intended (i.e. the unadapted) rather than the actual saccade amplitude was used. This reasoning assumes that the veridical presaccadic eccentricity of the saccade target is stored in transsaccadic memory. After the saccade, this value is compared to the efference copy signal of the intended saccade in combination with the post-saccadic eccentricity of the target. For example, let's assume a 25° saccade is induced: due to backward adaptation, however, a saccade of only 20° amplitude is performed and brings the displaced saccade target to the fovea (thus canceling out the visual post-saccadic error). If the system knew the actual saccade was only 20° in amplitude, it would signal a 5° target undershoot in comparison with the stored excentricity of the saccade target (25°). This is certainly not what has been observed in the experiments. For this reason it has been inferred that the efference copy reflected the intended 25° saccade rather than the conducted 20° saccade. The same logic can also be applied to our results, leading to the conclusion that in the adaptation paradigm the efference copy carries information about the intended and not the actual saccade.

However, if our results are considered from a different perspective, namely that perceptual stability is mediated by shifts of RFs of neurons in visual cortex based on an efference copy signal, a different conclusion would have to be drawn: the results would have to be explained by RF shifts that are directed to the adapted position as this is the position were no target displacement is perceived. If these RF shifts are driven by an efference copy signal, then this signal has to reflect the actual and NOT the intended saccade amplitude.

Up to now, both lines of arguments are still speculative, because neither the efference copy signal nor the RF shifting have been investigated under adaptation conditions in physiological studies. Recent behavioral studies in humans and monkeys, however, have challenged the use of an 'intended efference' rather than an 'actual efference' copy signal (Collins et al., 2007; Tanaka, 2003).

Our results as well as those of others (Bahcall & Kowler, 1999; Collins et al., 2009) can indeed be explained in a setting consistent with an efference copy reflecting the actual rather than the intended saccade amplitude. In this scenario, it has to be assumed, that the position of the saccade target (25° as in the example above) is first transferred to the adapted motor space (20°) prior to storage in transsaccadic memory. When this position is compared to an efference copy signal reflecting the actual saccade amplitude (20°), no spatial discrepancies will be detected; spatial stability will be established at the landing site of the saccade as observed in our current experiments.

A theory, that incorporates a veridical efference copy is appealing because it would keep coordinate systems aligned between different effector systems and could thus be used to guide behavior without the need of further adaptation processes. In line with this, Bruno and Morrone (2007) have found that during saccade adaptation open loop pointing movements to visual targets are subject to similar spatial distortions as visual localization judgements. In addition, a veridical efference copy theory could be easily integrated into the frameworks that focus on post-saccadic mechanisms to explain transsaccadic perceptual stability (Bridgeman, 1995; Deubel, 2004; Deubel et al., 1998). The decisive point herein is that there is actually no need for an explicit storage of the presaccadic target coordinates within this framework – this information is implicit in the motor act. In other words, the saccade itself could be used as storage device for the presaccadic target position; perceptual stability could be established simply by testing if the saccade target appears in or near the fovea when the eye movement is completed. This strategy relies on two reasonable assumptions, namely that (i) the visual scene does not change during the saccade (Deubel, 2004; Teichert, Klingenhoefer, Wachtler, & Bremmer, 2010) and that (ii) the saccade will bring the target onto the fovea. This hypothesis is compatible with our results and provides probably the most intuitive explanation for them.

4.3. The 'blanking' effect

The remarkable performance subjects showed in the 'blank' condition gave rise to the hypothesis that '…high quality information about presaccadic target position and a precise extraretinal signal are indeed available…' (Deubel, 2004). It has been proposed that in case no visual references are present after the saccade this information is used, otherwise it is overwritten by post-saccadic re-afferent visual input (Deubel, 2004). Our results refine this interpretation inasmuch as they show that during saccade adaptation high precision judgments were indeed accomplished (reflected by the steeper psychometric functions in the *blank* condition). Accuracy, however, was not improved in the *blank* condition – psychometric functions were not centered on the actual target position but rather shifted in the adaptation conditions. Concerning the neural basis of these judgments, the same arguments as discussed above hold true. In particular the observed results can also be explained in a framework that uses an implicit representation of target position (by the motor act) and thus supersedes the use of any explicit extraretinal information.

5. Endpoint variability

Our results showed a clear dissociation between changes in saccade end position caused by saccade adaptation and those resulting from trial by trial endpoint variability. Unlike adaptive changes in end position, those that were caused by trial by trial endpoint variability were compensated for in the perceptual judgements. In case of a slightly undershooting rightward saccade for example, a post-saccadic target that was presented in the fovea would have been correctly judged to be left to the actual saccade target. This is in line with earlier results obtained in a no-adaptation SSD experiment (Deubel et al., 1996) and in backward adaptation experiments in which subjects localized the saccade target in a blank paradigm (Collins et al., 2009). These results suggest the existence of information about saccade endpoint variability that is not caused by saccade adaptation.

On the other hand, Niemeier, Crawford, and Tweed (2003) reported a correlation between eye position scatter and SSD strength between individual subjects. From our point of view, the different results are not mutually exclusive as it might be that

multiple signal sources contribute to saccade endpoint variability (caused by e.g. either 'high level' planning or 'low level' effector noise); only some of them, however, might be included in an efference copy signal.

Certainly, the behavioral results raise the question about the neural representation of the observed behavior. Sommer and Wurtz (2002, 2004) have shown a signal that is sent from the SC via the mediodorsal thalamus (MD) to the FEF carries information about saccade endpoint variability. After inactivation of the MD relay neurons, monkeys did not compensate completely for variations in amplitude of a first saccade in a double step paradigm – with the MD intact, they did. This could be taken as evidence that high precision extraretinal information about saccade amplitude is actually represented in the brain.

5.1. Conclusion

To conclude, our results suggest that transsaccadic spatial memory is sacrificed in order to maintain perceptual stability. It has been suggested that the visual system makes use of the fact that the outside world does not change during saccades (Deubel, 2004; Teichert et al., 2010). Our results reveal that, if the outside world does change perisaccadically, it is not only the oculomotor system that adapts to the new situation – perception also does. We think an important factor in the interplay between the oculomotor and the visual system might be the directive that saccades bring their targets near to the fovea. To finally resolve the mechanisms of transsaccadic perceptual stability (and their neural implementations), however, more experiments will certainly have to be conducted.

Acknowledgment

Appendix A. Supplementary material

Supplementary data associated with this article can be found, in the online version, at doi:10.1016/j.visres.2010.12.006.

References

Awater, H., Burr, D., Lappe, M., Morrone, M. C., & Goldberg, M. E. (2005). Effect of saccadic adaptation on localization of visual targets. *Journal of Neurophysiology, 93*(6), 3605–3614.

Bahcall, D. O., & Kowler, E. (1999). Illusory shifts in visual direction accompany adaptation of saccadic eye movements. *Nature, 400*(6747), 864–866.

Bremmer, F., & Krekelberg, B. (2003). Seeing and acting at the same time: Challenges for brain (and) research. *Neuron, 38*, 367–370.

Bremmer, F., Kubischik, M., Hoffmann, K. P., & Krekelberg, B. (2009). Neural dynamics of saccadic suppression. *Journal of Neuroscience, 29*, 12374–12383.

Bridgeman, B. (1995). Extraretinal signals in visual orientation. *Handbook of Perception and Action, 1*, 191–223.

Bridgeman, B., Hendry, D., & Stark, L. (1975). Failure to detect displacement of the visual world during saccadic eye movements. *Vision Research, 15*(6), 719–722.

Bruno, A., & Morrone, M. C. (2007). Influence of saccadic adaptation on spatial localization: Comparison of verbal and pointing reports. *Journal of Vision, 7*(5), 1–13. 16.

Burr, D. C., Morrone, M. C., & Ross, J. (1994). Selective suppression of the magnocellular visual pathway during saccadic eye movements. *Nature, 371*, 511–513.

Colby, C. L., Duhamel, J. R., & Goldberg, M. E. (1995). Oculocentric spatial representation in parietal cortex. *Cerebral Cortex, 5*(5), 470–481.

Collins, T., Dore-Mazars, K., & Lappe, M. (2007). Motor space structures perceptual space: Evidence from human saccadic adaptation. *Brain Research, 1172*, 32–39.

Collins, T., Rolfs, M., Deubel, H., & Cavanagh, P. (2009). Post-saccadic location judgments reveal remapping of saccade targets to non-foveal locations. *Journal of Vision, 9*(5). 29, 1–9.

Deubel, H. (2004). Localization of targets across saccades: Role of landmark objects. *Visual Cognition, 11*, 173–202.

Deubel, H., Schneider, W. X., & Bridgeman, B. (1996). Postsaccadic target blanking prevents saccadic suppression of image displacement. *Vision Research, 36*, 985–996.

Deubel, H., Bridgeman, B., & Schneider, W. X. (1998). Immediate post-saccadic information mediates space constancy. *Vision Research, 38*, 3147–3159.

Duhamel, J. R., Colby, C. L., & Goldberg, M. E. (1992). The updating of the representation of visual space in parietal cortex by intended eye movements. *Science, 255*, 90–92.

von Holst, H., & Mittelstaedt, E. (1950). Das Reafferenzprinzip. Wechselwirkungen zwischen Zentralnervensystem und Peripherie. *Naturwissenschaften, 37*, 464–476.

Hopp, J. J., & Fuchs, A. F. (2004). The characteristics and neuronal substrate of saccadic eye movement plasticity. *Progress in Neurobiology, 72*(1), 27–53.

Li, W. X., & Matin, L. (1990). Saccadic suppression of displacement: influence of postsaccadic exposure duration and of saccadic stimulus elimination. *Vision Research, 30*(6), 945–955.

McLaughlin, S. (1967). Parametric adjustment in saccadic eye movements. *Perception & Psychophysics, 2*, 359–362.

Merriam, E. P., Genovese, C. R., & Colby, C. L. (2003). Spatial updating in human parietal cortex. *Neuron, 39*, 361–373.

Miller, J. M., Anstis, T., & Templeton, W. B. (1981). Saccadic plasticity: Parametric adaptive control by retinal feedback. *Journal of Experimental Psychology-Human Perception and Performance, 7*(2), 356–366.

Nakamura, K., & Colby, C. L. (2002). Updating of the visual representation in monkey striate and extrastriate cortex during saccades. *Proceedings of the National Academy of Sciences of the United States of America, 99*(6), 4026–4031.

Niemeier, M., Crawford, J. D., & Tweed, D. B. (2003). Optimal transsaccadic integration explains distorted spatial perception. *Nature, 422*, 76–80.

Ross, J., Morrone, M. C., Goldberg, M. E., & Burr, D. C. (2001). Changes in visual perception at the time of saccades. *Trends in Neurosciences, 24*, 113–121.

Sommer, M. A., & Wurtz, R. H. (2002). A pathway in primate brain for internal monitoring of movements. *Science, 296*(5572), 1480–1482.

Sommer, M. A., & Wurtz, R. H. (2004). What the brain stem tells the frontal cortex. I. Oculomotor signals sent from superior colliculus to frontal eye field via mediodorsal thalamus. *Journal of Neurophysiology, 91*(3), :1381–1402.

Sommer, M. A., & Wurtz, R. H. (2006). Influence of the thalamus on spatial visual processing in frontal cortex. *Nature, 444*(7117), 374–377.

Sperry, R. W. (1950). Neural basis of the spontaneous optokinetic response produced by visual inversion. *Journal of Comparative and Physiological Psychology, 43*(6), 482–489.

Tanaka, M. (2003). Contribution of signals downstream from adaptation to saccade programming. *Journal of Neurophysiology, 90*(3), 2080–2086.

Teichert, T., Klingenhoefer, S., Wachtler, T., & Bremmer, F. (2010). Perisaccadic shift as optimal percept. *Journal of Vision, 10*(8). 19, 1–15.

Umeno, M. M., & Goldberg, M. E. (1997). Spatial processing in the monkey frontal eye field. I. Predictive visual responses. *Journal of Neurophysiology, 78*, 1373–1383.

Walker, M. F., Fitzgibbon, E. J., & Goldberg, M. E. (1995). Neurons in the monkey superior colliculus predict the visual result of impending saccadic eye movements. *Journal of Neurophysiology, 73*, 1988–2003.

Wurtz, R. H. (2008). Neuronal mechanisms of visual stability. *Vision Research, 48*(20), 2070–2089.

2.5 Perisaccadic response modulations in area V4 of the macaque monkey

Abstract

Changes in a visual scene, caused by suddenly appearing or moving stimuli, are salient events. In contrast, alterations of the visual input that are a consequence of saccadic eye movements usually go perceptually unnoticed. The effect of apparent perceptual stability during saccades is typically attributed to saccadic suppression and visual masking effects. It was the purpose of this study to further investigate the neural basis of these phenomena. To this end, we recorded multi-unit activity (MUA) in area V4 of two macaque monkeys evoked by visual random noise stimulation. We analyzed the activity following stimulation onset during fixation as well as the stimulus driven activity prior to, during, and shortly after visually guided saccades. After stimulation onset, the MUA showed a transient response which was followed by a decline in activity until a constant level of sustained activity was reached, a phenomenon called neuronal adaptation. The sustained activity did not decrease perisaccadically, i.e., we did not find any evidence for saccadic suppression. Instead, we typically observed a slight pre- and a pronounced postsaccadic increase in activity. The postsaccadic activity reached almost the same level and closely paralleled the time course of the response after stimulus onset. However, there was a notable modification to this: postsaccadic activity lacked the initial transient phase of the stimulus onset response observed during steady fixation. We conclude that saccades can release neuronal adaptation in area V4, even if the receptive fields are continuously stimulated during the eye movement. In this case, the absence of transient response components distinguishes stable from newly appearing stimuli, a mechanism that might contribute to perceptual stability across saccadic eye movements

Introduction

Vision in a natural environment is characterized by continual alternations between fixation periods and saccadic eye movements that redirect gaze to different locations within the visual field. Unlike externally induced changes in a visual scene, which are perceptually salient events (e.g. suddenly appearing or moving stimulus), the retinal changes caused by eye movements usually remain perceptually unnoticed. The apparent perceptual stability despite saccades, often referred to as 'saccadic omission', is mainly attributed to two mechanisms: a reduction in visual sensitivity at the time of the eye movement (saccadic suppression) and visual masking induced by pre- and postsaccadic visual stimulation (see Ross et al. (2001); Wurtz (2008) for reviews). On the search for neural correlates of these mechanisms, various studies have investigated the perisaccadic response properties of neurons in different areas along the hierarchy of the primate visual system. Potential correlates of saccadic suppression have been identified primarily in the motion processing areas of the dorsal stream (Bremmer et al., 2009; Ibbotson et al., 2008; Thiele et al., 2002); these areas show a perisaccadic reduction in activity that matches the time course of similar psychophysical experiments (Diamond et al., 2000). Paradoxically, though, the most prominent observation, reported in almost all of the physiological studies, was not a suppression, but an increase in postsaccadic activity. To date, the origin and functional role of this 'postsaccadic enhancement' remains largely unknown, but the time course of the effect is suggestive of behavioral relevance: it peaks in the middle of a fixation period (i.e. ∼100-150 ms after saccade offset).

Despite the brevity of the fixation periods in natural vision, the visual processing during these periods is subject to adaptation effects. In the visual system, adaptation has been observed in many different areas and at timescales ranging from tens of milliseconds to many seconds (see e.g. Clifford et al. (2007); Kohn (2007); Krekelberg et al. (2006) for reviews). Adaptation on the brief timescale relevant during natural vision is called short-term adaptation or rapid adaptation. It can be elicited by constant or repetitive stimulation and serves to adjust the responsivity of a sensory system and increase its coding efficiency (Müller et al., 1999; Vinje and Gallant, 2000). At the neuronal level, this effect is characterized by a transient-sustained firing pattern that follows stimulation onset (Glasser et al., 2011; Lisberger and Movshon, 1999; Motter, 2006; Müller et al., 1999; Priebe and Lisberger, 2002).

It was the purpose of this study to further investigate the neural basis of perisaccadic perceptual stability. To this end, we recorded visually evoked multi-unit activity (MUA) in ventral area V4 during fixation as well as prior to, during,

and briefly after visually guided saccades. Similar to what has been found in other areas of the visual system, the most pronounced effect we observed was a prominent increase in postsaccadic activity. We present evidence that this postsaccadic enhancement is linked to rapid neuronal adaptation: it reflects a release from adaptation built up during the previous fixation period. The release from adaptation was not complete, though; the initial transient component, present in the onset response during fixation, was absent in the postsaccadic activity. We discuss a potential role of the increased postsaccadic activity in the maintenance of perceptual stability as well as in guiding upcoming saccades by means of a saliency map.

Materials and methods

Experiments were performed in two male macaque monkeys (Macaca mulatta, weight 8.5 kg and 9.5 kg) referred to as M and B in the following. All experimental procedures as well as animal care and housing were in accordance with national German and international published guidelines on the use of animals in research (European Communities Council Directive 86/609/ECC and National Institutes of Health Guide for the Care and Use of Laboratory Animals).

Animal preparation and data acquisition

The animals were prepared for the recordings in an aseptic surgical environment under general anesthesia; post surgery the animals were provided with analgesics and antibiotics. Head fixation during the experiments was accomplished using three small titanium bolts affixed to the skull. The recordings were performed in area V4 which was accessed through the intact dura mata via a recording chamber (10 mm diameter) implanted onto the skull. Area V4 was targeted by its talairach coordinates and identified later on by its topological and functional properties.

We recorded multi-unit activity (MUA) from the upper layers of V4 in the left hemispheres of the animals using the Eckhorn system microdrive (Thomas Recording GmbH, Germany). This system allows individual positioning of up to 16 quartz-isolated platinum-tungsten electrodes (impedance 6-8 MΩ at 135 kHz) in parallel (Eckhorn et al., 1993). To obtain the MUA signal the measured voltage was amplified, band-pass filtered (1 kHz to 10 kHz), full-wave rectified, and low-pass filtered (140 Hz). The resulting signal was recorded at a sampling rate of 500 Hz.

Setup

During the experiments the animals were seated in a dimly lit room 62 cm in front of a CRT monitor subtending 36° x 27° of the visual field (resolution 800x600 pixels running at 100 Hz). Gaze position of the left eye was monitored with an infrared eye-tracker running at a sampling frequency of 240 Hz (Thomas Recording GmbH, Germany). The initial horizontal and vertical calibration of the eye-tracker was established prior to each recording session. During offline analysis the horizontal calibration was refined by minimizing the fixation error (averaged over all trials) during early and late fixation periods at the pre- and postsaccadic target positions.

Behavioral paradigms and visual stimulation

The animals were trained to fixate green circular targets (0.3° diameter) presented on a gray background (25 cd/m^2) at eye level while touching a lever. Fixation had to be maintained until the target dimmed. A liquid reward was given if the animal released the lever within 400 ms after dimming. Trials were aborted if gaze position deviated by more than 1.5° from the target position. In saccade conditions the animal was required to break the initial fixation within 300 ms after the displacement of the target and refixate at the new position within 375 ms. Typically, four paradigms, of which three are relevant for this report, were run in each recording session: a two-dimensional receptive field (RF) mapping (50 trials), a control saccade task without deliberate visual stimulation (*control* condition, 50 trials), and the actual saccade task with stimulation of the RFs by a sparse noise stimulus (*stimulation* condition, 150 trials) (Fig. 1).In addition, the animals performed a saccade adaptation paradigm afterwards; the results of this condition will be presented in a separate report. In some cases, the control condition was skipped due to time constraints. These sessions were only included in such analysis that did not require the data of the *control* condition. In the initial two-dimensional RF mapping the monkey fixated in the center of the screen for 3.0 s. During this period colored bar stimuli of different orientations were presented in rapid sequence at various horizontal and vertical positions near the expected position of the RFs. The stimulus features changed with each refresh cycle of the monitor and were drawn pseudo-randomly from predefined sets (color: red, green, blue, yellow; orientation: 0°, 45°, 90°, 135°; position: centers of a 4x4 square array). Stimulus size was adapted to match the expected RF dimensions; typical values were 2.0° (length) and 0.4° (width). In saccade conditions the target was repositioned by an amplitude of 12.5° after an initial fixation period of variable length (between 700 ms to 1000 ms in monkey M and 200 ms to 500 ms in monkey

B (Fig. 1). Due to saccadic undershoot, the primary saccade brought some of the RFs close to the position of the saccade target (Fig. 2). In order to distinguish artifactual stimulation by the saccade target from pristine perisaccadic response modulations, we blanked the saccade target for 100 ms in the next screen refresh cycle following the detection of a saccade; this was on average 10 ms before saccade offset, the target reappearance 90 ms after saccade offset. While the behavioral task was identical in the *control* and *stimulation* conditions, visual stimulation was different (Fig. 1B). In the *control* condition, saccades were performed on a uniform gray background (25 cd/m^2). In the *stimulation* condition, a random noise stimulus was presented in a predefined stimulation area of the screen on top of the gray background (Fig. 1A). Stimulation started 310 ms after trial begin and was present until trial end. Every single frame of the stimulus consisted of two vertical white bars (75 cd/m^2, typical size: 4.5° (height) and 0.4° (width)) that changed position with every refresh cycle of the monitor, i.e. every 10 ms. The positioning of the two bars was independent from each other and pseudo-randomly distributed within two laterally adjacent but non-overlapping parts of the screen. In total, the two divisions formed one continuous area covering the bigger part of the lower half of the screen; in this way the RFs were permanently stimulated prior to, during, and after the saccades. The exact geometrical stimulation parameters were adjusted on a daily basis to match the RFs of the respective recordings. The RF positions in monkey B required an extension of the stimulation area above the vertical midline. In order to prevent the fixation target of being covered in this case, the flicker stimulus was presented in a graphical layer behind the fixation targets.

Data analysis and statistics

We included data of n=134 recording sites (102 monkey M, 32 monkey B) in our analysis; the inclusion criterion was that the trial averaged activity, evoked by the onset of the stimulus in the *stimulation* condition, yielded a peak signal-to-noise ratio bigger than 5 (z-score).

Unless otherwise stated, all time values relating neuronal activity to an external event (e.g. saccade onset) will consider the latency of the neuronal signal, i.e. the time axis of the recorded activity will be shifted by subtracting the neuronal latency ('shifted time'). The latency was definded as the time between stimulation onset and the time when the following response reached half of its peak activity. For example, assuming a neuronal latency of 60 ms and a saccade of 40 ms duration, the activity, as evoked by a stimulus presented 10 ms before saccade onset, will be measured 50 ms after saccade onset or, respectively, 10 ms after saccade

offset. We will take the latency into account and nevertheless refer to such activity as presaccadic as it was evoked by a presaccadic stimulus. We will use the term postsaccadic only to refer to activity evoked by a stimulus presented after saccade offset. Prior to visualization, the averaged MUA signals were lowpass filtered by convolution with a rectangular kernel of 26 ms duration. Saccades were detected using velocity criteria.

In order to control for artifactual activity in the *stimulation* condition (e.g. potentially caused by RF stimulation induced by the fixation target or the edges of the monitor), we subtracted the averaged activity of the *control* condition from the respective signal of the *stimulation* condition. We will refer to the resulting signal as 'differential activity' (represented by blue lines in the figures).

To analyze the general response characteristics of the population of the recorded signals, we averaged the signals of the individual recording sites.Prior to the calculation of the population average, all signals were normalized by the peak amplitude of the stimulation onset response and, as we were mainly interested in perisaccadic modulations, then mean centered on the average activity of the period 275 ms to 175 ms prior to saccade onset (by subtraction of the mean).

We used the same time window as a reference against which perisaccadic effects were tested in significance testing. Unless otherwise stated, all statistics are based on considering 95% confidence intervals (CI) of the mean. Confidence intervals were obtained by percentile bootstrap procedures using 10000 resamples (Efron, 1979). Statistical difference between two conditions was assessed by calculating the CI for the mean difference; the result was defined as statistically significant if zero was not included in the CI. For the analysis of the time courses of two signals, data points at corresponding times were first compared; to account for multiple testing, the difference between the signals was only considered significant if at least five consecutive samples differed significantly.

Assignment to groups of different postsaccadic response characteristics

The signals of the individual recording sites showed diverse postsaccadic response characteristics. To illustrate this diversity in a systematic way, we identified four different response types and accordingly assigned the signals to four different groups. The grouping was done by visual inspection by an author based on the criteria described below. It is important to note that the transitions between the different groups were gradual. The classification scheme should therefore only be considered as a coarse guideline and not to reflect strictly separate response modes.

After having established an analogy between the postsaccadic activity and the stimulation onset response on the population level, we compared the respective signals of the different recording sites individually. Prior to this comparison, the signals were aligned such that the stimulation onset trigger matched the saccade offset trigger. The postsaccadic activity was then judged relative to the onset response (suppression, match, or enhancement).

We identified four different types of postsaccadic responses; one author accordingly assigned the recording sites to one of the following groups: 1: early-suppression, late match, 2: early-suppression, late enhancement, 3: early match, and 4: early enhancement. 'Early' in this terminology was defined to include times ranging from 0 ms to 75 ms after saccade offset; the 'late' postsaccadic period ranged from 125 ms to 200 ms. In cases where the postsaccadic signal of the *stimulation* condition showed activity that was likely driven by the fixation target, the classification of the early period was done based on the 50 ms period prior to the reappearance response. These cases fell always in the match or enhancement group and thus never required a judgement of the late period. As the classification process was based on the results of the *stimulation* condition only, those data for which the *control* condition had not been measured due to temporal reasons were also included. This was, however, only done when counting the number of the group members. We also plotted the differential activity between the *stimulation* and *control* condition, but only once the classification was completed (only sites with complete *stimulation* and *control* data sets were used in such cases); this was done to verify that the corrected group average showed the same properties as the uncorrected individual signals.

Results

We recorded multi-unit activity (MUA) in area V4 of two macaque monkeys (M and B) in two conditions: In the *stimulation* condition, vertical luminance bars were presented randomly that stimulated the receptive fields (RFs) during fixation and while the animal performed horizontal saccades; in the *control* condition the behavioural paradigm was similar, but deliberate stimulation was absent (cf. Materials and methods).

Due to the random nature of the stimulation, the activity of individual sites could be quite distinct in different trials (Fig. 3). When averaged across trials, however, the signals showed clear stimulus driven activity and, in many cases, a decrease in activity following an initial transient onset response. Due to the phenomenological similarity of this effect to other reports (Müller et al., 1999;

Priebe and Lisberger, 2002), we refer to it as rapid neuronal adaptation. In addition, we often observed pronounced perisaccadic response modulations in the *stimulation* but not in the *control* condition (Fig. 3C). In the following, we will analyze the effects in more detail. We start by reporting population averages; results of individual sites will be discussed thereafter.

Perisaccadic modulations of the population MUA

In psychophysical experiments, it has been demonstrated that perisaccadic perceptual changes, like saccadic suppression, can already be observed for stimuli presented about 50 ms before saccade onset and that they peak at the beginning of the eye movement (Diamond et al., 2000). When neuronal correlates of such effects are to be identified, it has to be kept in mind that, due to the finite transmission velocities of the nervous system, sensory activity is delayed in time relative to its evoking stimulus. To account for this, we used the latency of the stimulation onset response at half-maximum to relate external events, such as saccade onset, to the neuronal activity. In our population of V4 neurons, we found an average neuronal latency of 68 ms with a 95%-confidence interval (CI) of 66 ms to 72 ms (Fig. 4A). Unless otherwise noted, all following results will be reported in 'shifted' time, that is, the neuronal latency will be taken into account (cf. Fig. 4A: bottom axis represents shifted, top axis non-shifted time). To investigate the perisaccadic activity, we aligned all single trial data on saccade onset and calculated the population average thereafter (Fig. 4B). The mean saccadic reaction time was 192 ms.During the reference period, 300 ms to 200 ms prior to saccade onset, the population MUA was almost constant and had an average value of 0.0 units in the *stimulation* condition due to our normalization procedure (see Materials and methods). In the 50 ms period prior to saccade onset, the population MUA was significantly enhanced compared to the reference period (difference: 0.08 units, CI: (0.06 to 0.11) units; bootstrap test, cf. Materials and methods). This increase became significant 132 ms prior to saccade onset (non-shifted time: 64 ms; sliding window bootstrap test, window size: 20 ms) and reached a plateau at a mean level of 0.1 units. We also examined the activity at individual recording sites for presaccadic modulations (using their respective latencies to calculate the shifted time); in 30 out of 90 sites the MUA was significantly enhanced in the 50 ms period prior to saccade onset. It has to be mentioned, however, that some of the signals had not reached a constant activity level during the reference period, but still showed decreasing activity following the stimulation onset response. This might have occluded an enhancement effect from our analysis in a few cases.

The most prominent effect we observed in the perisaccadic data was a strong

increase in postsaccadic activity (Fig. 4B). This effect started to build up imme-
diately after saccade offset and peaked 140 ms thereafter at a level of 0.6 units,
comparable to that of the stimulation onset response (0.5 units). The correspond-
ing data of the *control* condition, however, also showed a peak at the same time
as in the *stimulation* condition and, in addition, an earlier peak at saccade offset.
These peaks resulted from activity obtained at recording sites with RFs near the
fovea that were visually driven, when the fixation target hit their neurons' RFs
at the end of the saccade (i.e. briefly before the target was blanked) and when
it reappeared after the blanking period (90 ms after saccade offset). In order to
test the individual sites for postsaccadic modulations in activity, we analyzed the
period 40 ms to 90 ms after saccade offset, i.e. the activity during the blanking
period, prior to a potential visual response to the fixation target. More than 90
percent (84/90) of the recording sites showed a significant increase in postsaccadic
activity.

To analyze the time course of the postsaccadic activity in the population aver-
aged MUA, we accounted for the non-stimulus driven activity by subtracting the
activity of the *control* condition from the corresponding data of the *stimulation*
condition (Fig. 4C; the data centering was done after the subtraction). The post-
saccadic time course of the resulting signal, which we will refer to as 'differential
activity' in the following, revealed a strong congruency with the response following
stimulation onset. To analyze this systematically, we first aligned the stimulation
onset trigger to match the saccade offset trigger and then compared the two re-
sponse profiles (Fig. 4C). The postsaccadic signal was significantly smaller than
the onset response during the first 48 ms, but subsequently the signals did not
differ significantly. The primary saccades frequently undershot the target (75 per-
cent of the trials; monkey M: 80 percent, monkey B: 65 percent) and were followed
by subsequent secondary saccades. These corrective saccades had a mean ampli-
tude of 0.5° (monkey M: 0.4°, monkey B: 0.6°) and mean latencies after saccade
offset of 260 ms (i.e. 150 ms after reappearance of the fixation target) (monkey
M: 243 ms, monkey B: 301 ms). In order to investigate whether the observed
activity increase following the primary saccades was indeed a postsaccadic effect
or whether it was rather an enhancement preceeding the corrective saccades, we
analyzed the data separately for trials in which corrective saccades had or had not
occurred (Fig. 5). The activity in trials with corrective saccades was significantly
higher at postsaccadic times from 94 ms to 210 ms and 290 ms to 368 ms than
in trials without corrective saccades. The results of the same analysis using the
differential activity were comparable (corresponding times: 148 ms to 210 ms and
280 to 360 ms, data not shown). Effect size was 0.08 units for the uncorrected as
well as the corrected MUA (averaged from -100 ms to + 100 ms around the onset

of the corrective saccade).

Characteristics of individual MUAs

In the next step, we will analyzed the postsaccadic response characteristics of the individual recording sites. Based on the results of the previous sections, we here take the view that the congruently aligned onset response is the reference against which the postsaccadic activity is to be compared. We adapt our terminology accordingly: We call an effect suppressive, if the postsaccadic activity was smaller than the activity of the onset signal at corresponding times. For example, the most prominent effect in the population averaged MUA was an increase in postsaccdic activity compared to the presaccadic signal level. However, as the postsaccadic activity was smaller than the onset response during the first 48 ms, this effect will be referred to as postsaccadic suppression. Following the initial postsaccadic suppression, the population MUA matched the time course of the onset response closely. This result, however, became only evident when the non-stimulus driven activity that was also present in the *control* condition was removed by subtraction of the signals. In order to test whether the population response was representative, we inspected the signals of the individual recording sites. The majority of them showed the same response characteristics as described for the population response, and, importantly, the effect was often obvious in the uncorrected signals of the *stimulation* condition (Fig. 6A).

The signals of the individual sites revealed more diverse response patterns as evident from the population average, though. To describe this diversity in a systematic way, we classified the individual MUAs in groups of similar postsaccadic response characteristics. The assignment to the groups was done by visual inspection by an author and was based on the comparison of the postsaccadic activity in relation to the onset response (suppressed, matching, or enhanced postsaccadic activity, cf. Materials and methods). It should be noted that the transitions between the response groups were rather gradual; the groups thus do not reflect strictly separate response modes, but should rather be considered as exemplification of the different response characteristics that were observed.

We included the data of 134 recording sites in this analysis (monkey M: 102, monkey B: 32). We identified four different groups, depending on the time course of the 'early' (0 ms to 75 ms) and 'late' (125 ms to 200 ms) postsaccadic activity (cf. Materials and methods). The first of the four groups comprised the majority of the recorded sites (68/134; monkey M: 61/102, monkey B: 6/32). These showed the same response characteristics as observed in the population average, i.e. an early suppression and a late match in activity (Fig. 6A). The group average

showed a significant reduction in postsaccadic activity during the first 68 ms and peaked at t=75 ms; thereafter, the signals did not differ significantly. In total 23/134 sites (monkey M: 22/102, monkey B: 1/32) showed an early suppression (average duration 50 ms) but their subsequent activity exceeded the amount of the onset response at the corresponding times (peak time: t=84 ms, Fig. 6B). We also observed recording sites that did not manifest an early postsaccadic suppression. In one of these groups the postsaccadic activity matched the onset response closely (early match group: 32/134 sites; monkey M: 17/102, monkey B: 15/32; Fig. 6C). This group contained signals that did not show a significant increase in postsaccadic activity at all. In these cases, the match in activity was due to the fact that the onset response showed no neuronal adaptation; instead, the signal rose to a certain level after stimulation onset and then the sustained activity remained constant throughout the trial (e.g. middle panel, Fig. 6C). We also observed sites which showed a clear enhancement in the early postsaccadic period (11/134 sites; monkey M: 1/102; monkey B: 10/32; Fig. 6D). The majority of the sites in this group were postsaccadically also driven by the fixation target. The inclusion criterion in this case was an enhancement during the last 50 ms of the postsaccadic blanking period in which no fixation target was present (cf. Materials and methods). The early postsaccadic enhancement effect was confirmed in the group average of the differential activity of the *stimulation* and *control* condition: this signal was enhanced during the complete postsaccadic period compared to the onset response; the effect was significant from 18 ms after saccade offset onwards.

Postsaccadic activity of sites with transient and sustained onset responses

The prevailing response characteristic which we observed in our data was a suppression of the early postsaccadic activity compared to the onset response. It was the goal of the analysis in this section to determine whether this effect was due to a general postsaccadic suppression of activity, or whether the effect was selective to response transients. This approach was inspired by a study that reported differences in the release from neuronal adaptation in area V4 depending on the transiency of the onset responses (Motter, 2006). To quantify the transiency of the onset responses, we calculated a transiency index (TI), defined as the ratio between the peak amplitude of the onset response and the average response amplitude 200 ms to 300 ms after response onset. By this definition, more transient responses are marked by higher, more sustained responses by lower TI-values, respectively. We then followed a strategy comparable to the one used by Motter (2006). Motter analyzed the release from adaptation in two subpopulations that

were obtained by a median split of the population according to the transiency index. Similar to Motter's results, we did not find a clear-cut separation between a transient and a sustained subpopulation; instead, the distribution of TIs was rather gradual (data not shown); It became apparent, however, that the onset responses of monkey M were significantly more transient than those of monkey B (monkey M, TI: 2.8, CI: 2.5 to 3.0; monkey B, TI: 1.8, CI: 1.6 to 2.1; difference in TI: 1.0, CI: 0.6 to 1.3) and had only few overlap in their distributions of TIs. We presumed that this effect might be due to the retinal eccentricity of the RFs, which were, according to the positions of the recording chambers, more eccentric in monkey M than in monkey B (mean eccentricity, monkey M: $4.5°$, monkey B: $1.8°$, Fig. 2). In line with this hypothesis we found a significant correlation between the TI and the eccentricity of the corresponding RF (R^2=0.11, CI:0.02 to 0.30). We therefore decided to not separate the population by a median split according to the TIs but analyzed the data of the two animals separately. In our case, this corresponded to a split by retinal eccentricity of the RF positions and thus yielded more explanatory power than an arbitrary median split.

The averaged time courses of the onset responses of the two animals confirmed the analysis of the transiency indices: following the response peak after stimulation onset, the averaged activity declined faster in monkey B than in monkey M (Fig. 7A). We then compared the averaged onset responses to the aligned postsaccadic time course of the *stimulation* condition as well as the differential activity as described above (Fig. 7B,C, respectively). In monkey M, the postsaccadic time course showed a significant suppression during the first 52 ms after saccade offset and then matched the onset response closely. This was true for both the activity of the *stimulation* condition (Fig. 7B, left) as well as the differential activity (Fig. 7C, left). In monkey B, no early postsaccadic suppression was evident. There were clear contributions to the postsaccadic signal by the fixation target. During the blanking period, which encompassed the time suppression was found in monkey M, the activity level was not significantly suppressed though, neither in the uncorrected (Fig. 7B, right) nor in the differential signal (Fig. 7C, right).

Discussion

Visual adaptation and its underlying neuronal correlates are considered a keystone of visual processing. In this work we investigated the interplay between neuronal adaptation and its functional counterpart: saccadic eye movements. We used random noise stimulation and foundthat it could elicit neuronal adaptation in area V4. Similar to what has been observed in other areas of the visual system,

we observed a prominent increase in postsaccadic activity that closely matched the time course of the onset response; we interpret this as a release from neuronal adaptation. Interestingly, this release from adaptation was not complete, though; the transient component that typically marks the response following the onset of a stimulus was suppressed in the postsaccadic activity.

Attentional modulations in V4

The primary function attributed to area V4 is visual processing. As an intermediate stage in the hierarchy of the visual system, it has no direct anatomical connections to the oculomotor system. It is known, however, that area V4 carries eye-position signals (Bremmer, 2000) and that the activity (Fischer and Boch, 1981a,b; Moore et al., 1998) and receptive field (RF) structure of this area can be modulated prior to saccades (Tolias et al., 2001). Our results are in line with previous studies that have reported an increase in activity prior to saccades in V4 (Fischer and Boch, 1981a,b; Mazer and Gallant, 2003; Moore et al., 1998). This effect is presumably caused by top-down signals from the frontal-eye field (FEF; Armstrong and Moore (2007); Hamker (2005); Moore and Armstrong (2003) or the lateral intraparietal area (LIP; Gee et al. (2010) and is believed to reflect focal attention linked to the saccade target. In our experimental design the RF stimulation was behaviorally irrelevant and the RF positions were spatially well separated from the saccade target; this might be the reason why we found only moderate increases in presaccadic activity. Following the primary saccades, however, the more foveal of the recorded RF potentially marked the target of corrective eye movements due to saccadic undershoot. In this situation we observed enhanced postsaccadic activity that exceeded the amount expected by a release of neuronal adaptation in about 30 percent of the cases (Fig. 6D). This enhancement probably reflects an attentional modulation caused by the behavioural relevance of the saccade target in our task.

Saccade induced release from adaptation. A general mechanism of the visual system?

While presaccadic, attentional modulations have been investigated in area V4 in a number of studies, peri- and postsaccadic effects have received less attention so far. The most prominent effect in our data, however, was a postsaccadic increase in neuronal activity which reflected a release from neuronal adaptation following the saccade. Interestingly, the majority of the neurophysiological experiments on perisaccadic response modulations have reported increases in postsaccadic activ-

ity, even though they have investigated different stages of the visual hierarchy and have used a wide variety of behavioral paradigms and stimuli. We think it is likely that release from adaptation has contributed to the observed effects in studies which have used repetitive or continuously present stimuli capable of eliciting adaptation (e.g. LGN: Ramcharan et al. (2001); Reppas et al. (2002), V1: Gallant et al. (1998); Ito et al. (2011); Yu and Lee (2000)); the time courses reported in these studies seem to be consistent with this view. There are also studies, however, which have found a postsaccadic enhancement, but under conditions where a contribution of neuronal adaptation is more elusive, e.g. when saccades were performed in the dark (Ibbotson et al., 2008; Kagan et al., 2008; Lee and Malpeli, 1998; Royal et al., 2006), or when only one brief stimulus per trial was presented (Bremmer et al., 2009; Ibbotson et al., 2008). Given the current experimental evidence, it is hard to speculate whether all these results might indeed be somehow linked by a common mechanism and whether this mechanism might be neuronal adaptation and its release; certainly more studies will be needed to answer this question adequately.

Related to this consideration is another important question: What triggers the release from adaptation, retinal blur or an extra-retinal signal? Relevant in this context are the results reported by Motter (2006), who investigated neuronal adaptation in V4 during fixation. Motter simulated the visual stimulation during free viewing by presenting sequences of static stimuli with the same timing as typically observed for fixation and saccade periods. Neurons responded to the initial presentation of a stimulus by a transient response that was followed by sustained activity, the characteristic pattern of rapid neuronal adaptation. The stimulus was then replaced by a gray background for 55 ms, imitating the retinal smear caused by the fast eye movement. This blank period released neuronal adaptation, i.e. a stimulus, similar to the one presented before the blank period, elicited a response that exceeded the level of the sustained activity again. Motter analyzed the transiency of the onset responses and noted a preferential loss of the initial transient component in the activity following the blanking phase.These findings, as obtained in a fixation paradigm, are in perfect agreement with the postsaccadic effect we observed: a suppression that predominately affected transients, whereas sustained activity was not suppressed (cf. Fig. 7). Our results thus provide strong evidence for the hypothesis that the postsaccadic increase in activity is not dependent on an extraretinal signal but is predominantly a visual effect.

However, on closer inspection there remain some details that deserve further attention. In the experiments of Motter (2006) the release from adaptation was triggered by the absence of the stimulus during the simulated saccade. In our experiments, in contrast, the stimulation was continuously present during the eye

movement, and, due to the brevity of the single stimuli (¡10 ms), it is debatable how much the retinal smear during the saccades actually blurred them. A similar point can be made by taking the results of some of the above mentioned studies, likely affected by rapid neuronal adaptation, into consideration: In some of the experiments large, spatially uniform stimuli that did not cause any perisaccadic retinal blur were used (Ramcharan et al., 2001; Reppas et al., 2002). It would be interesting to see, if the postsaccadic activity reported in these studies was indeed related to neuronal adaptation. A reanalysis of the data might provide further insight into the release mechanism.

The topography of transient and sustained responses in V4

In the retina and the LGN, transient responses of short latency are a signature of the magnocellular pathway. Parvocellular cells, on the other hand, are chromatic-selective, but less sensitive to luminance contrast, and show more sustained activity which has longer onset latencies (Gouras (1968); Schiller and Malpeli (1978), see Merigan and Maunsell (1993) for a review). In striate cortex the strict anatomical separation of the two pathways dissolves to some extent (Hubel and Livingstone, 1990; Maunsell and Gibson, 1992), and in area V4, neurons have been shown to receive convergent input from both pathways (Ferrera et al., 1992, 1994).

In line with previous studies, which have shown that the clear-cut separation between the magno- and parvocellular response properties is only barely preserved at the cortical level (Maunsell and Gibson, 1992), we found continuous distributions of response latency and transiency that did not permit an unequivocal classification of the sites as receiving either clear magno- or parvocellular input. At the population level, however, the responses to the luminance stimulation that we observed were more transient in recording sites with more peripheral RFs. This might be explained by a higher proportion of magnocellular input at these sites. This account corresponds well to the known topography of the two pathways at the early stages of the visual system: the magnocellular pathway is known to contribute primarily to peripheral vision, parvocellular activity is more prominent in the central part of the visual field (Azzopardi et al., 1999; Gouras, 1968). We therefore speculate that the topography of the relative contributions of the M and P pathways across the visual field might, in principle, be preserved at the level of V4.

Potential functional roles of increased postsaccadic activity

Increased postsaccadic activity is a well known phenomenon in the neurophysiological literature. Yet, there is little experimental work concerning the functional role of the effect by now (but see Ibbotson et al. (2007); Lisberger (1998)). First of all, our results highlight the role of saccades as a counterpart of rapid neuronal adaptation. Neuronal adaptation following prolonged exposure to a continuous stimulus can lead to perceptual visual fading (Ditchburn and Ginsborg, 1952; Riggs, 1952). It is known that microsaccades can counteract this effect (Martinez-Conde et al., 2006). Leopold and Logothetis (1998) reported an increase in activity in V4 following microsaccades that could not be explained by a change in visual stimulation due to the eye movement (a small stimulus was shifted by the microsaccades within a large RF). Given the close correspondence between the time course reported by Leopold and Logothetis (1998) and our results, it is conceivable that the reported post-microsaccadic activity was also due to a release from adaptation.

The release from adaptation that we observed was not complete, though. The initial transient phase of the onset response was absent in the postsaccadic activity. During fixation, transient activity is a characteristic response pattern following abrupt changes in visual stimulation (e.g. the onset of a stimulus). The suppression of this component in the activity elicited by the postsaccadic scene might therefore help to distinguish self-generated from external stimulation and thus to support perceptual stability.

At the perceptual level, saccadic suppression and saccade induced visual masking, which we will refer to as 'saccadic masking' below, have been identified to support perisaccadic visual stability (see Wurtz (2008) for a recent review). From psychophysical studies it is known that one of the characteristics of these effects is their selectivity concerning the magno- and parvocellular streams: only the processing of stimuli that are conveyed by the magnocellular pathway is affected(Diamond et al., 2000). Han et al. (2009) have recently described dynamic changes in the sensitivity of V4 neurons preceding the onset of a saccade. The net result of this study was a reduction in sensitivity that was more pronounced for luminance than for color contrast. Further evidence for selective saccadic suppression in V4 comes from a human fMRI experiment (Kleiser et al., 2004). In contrast, we did not observe a genuine reduction in perisaccadic activity. We can not resolve this discrepancy, but speculate that it might be explained by the differences in stimulation: the former studies flashed one single stimulus per trial; we used continuous random noise stimulation that induced neuronal adaptation. It is conceivable that saccadic suppression and rapid adaptation rely to some extend on the same neural machinery. In this notion, neuronal adaptation would already

have reduced the responsiveness in our experiments and 'blocked' the pathway, so that no further effect due to saccadic suppression could be observed in our experiments. Certainly, more experiments are necessary to clarify this issue.

While we did not find any evidence for saccadic suppression, our results might be related to saccadic masking. It has recently been proposed that saccadic masking results from a combination of a suppression and a subsequent enhancement of neuronal activity: Increased postsaccadic activity might 'overpower' the activity elicited during the eye movement (Ibbotson and Cloherty, 2009). Our results add to this hypothesis by explaining why saccadic masking is, similar to saccadic suppression, selective to stimuli conveyed by the magnocellular pathway (Diamond et al., 2000): The sustained activity of the parvocellular pathway shows, in contrast to the transient responses of the magnocellular pathway, no or only few rapid neuronal adaptation and thus no or only weak increases in postsaccadic activity. Studies in the LGN confirm such a selectivity of postsaccadically increased activity to the magnocellular pathway (Ramcharan et al., 2001; Reppas et al., 2002).

Relevance for natural vision

It is important to note that the results reported here reflect a general mechanism that is not confined to the laboratory. The particular stimulus that we have used in this study is certainly not to be encountered in a natural environment. Yet, the effect which it induced, i.e. rapid neuronal adaptation, is a common phenomenon in natural vision. It can be elicited within a few hundred milliseconds by the exposure to a stationary visual scene, a typical situation during the fixation periods in free viewing. The experimental paradigm of our study corresponds to the situation where the RF stimulation is the same prior to and after the saccade. During free viewing such a situation might arise, for example, while searching for fruits in a tree, when peripheral RFs are moved across similar parts of the foliage or the sky. In cases where pre- and postsaccadic stimulation are different, it is important to note that rapid neuronal adaptation is feature selective, i.e. adaptation to a specific adaptor does not, or only partially, transfer to a different stimulus (Gawne and Woods, 2003; Motter, 2006; Müller et al., 1999). As a consequence of this, the postsaccadic activity of a neuron does not only depend on its feature selectivity and the respective stimulus, but also on the dissimilarity, and accordingly the novelty, of the stimulus to the presaccadic adaptor. A dissimilar postsaccadic stimulus can, for example, elicit a response that exceeds the increased postsaccadic activity due to the adaptation release (Gawne and Woods, 2003; Motter, 2006). The notion that novelty or 'surprise' attracts attention is

well established experimentally (see Ranganath and Rainer (2003) for a review) and is fundamental to many models of dynamic saliency (Einhäuser et al., 2007; Itti and Baldi, 2005; Seo and Milanfar, 2009). It is known that neuronal activity in V4 can act as a saliency map that guides saccades during free viewing visual search: Increased activity of a neuron during a fixation period is likely followed by a saccade towards the RF of the neuron (Bichot et al., 2005; Mazer and Gallant, 2003). Interestingly, the reported time courses of such activity are similar to the postsaccadic effect we observed. This finding suggests another potential role of the postsaccadic activity in V4: It might contribute to a dynamic saliency map that guides subsequent oculomotor behavior.

To summarize, our results have revealed a relationship between increased post-saccadic activity and rapid neuronal adaptation. This 'simple' observation might be relevant in a number of cases, including the interpretation of published data obtained under similar conditions in laboratory settings but also to explain some fundamental aspects of natural vision.

A   Spatial layout

B   Time course

Stimulation

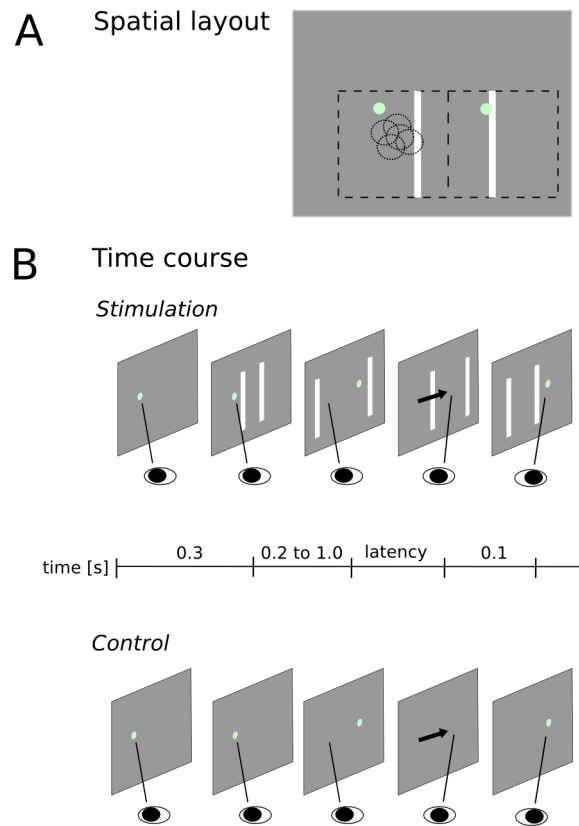time [s]   0.3   0.2 to 1.0   latency   0.1

Control

Figure 1. Experimental design. A) Spatial layout (illustration not drawn to scale). After an initial two-dimensional receptive field mapping (cf. Materials and methods), the animals performed visually guided saccades of 12.5° amplitude on a gray background in two conditions. In the *stimulation* condition the receptive fields (RFs, dotted circles) were stimulated continuously during fixation and perisaccadically by a sparse noise stimulus. The stimulus consisted of two luminance bars, which were independently and randomly repositioned every 10 ms within two subdivisions of a continuous stimulation area (dashed rectangles). B) Time course. The *stimulation* and *control* conditions were identical, except for the presence of the stimulus. Saccades were initiated by the repositioning of the fixation target. Upon detection of the saccade by an eye-tracker, the target was blanked for 100 ms in order to distinguish perisaccadic response modulations from confounding activity evoked by the fixation target. This was necessary as in some cases the RFs were close to the fovea and an undershoot of the primary saccades brought them close to the saccade target.
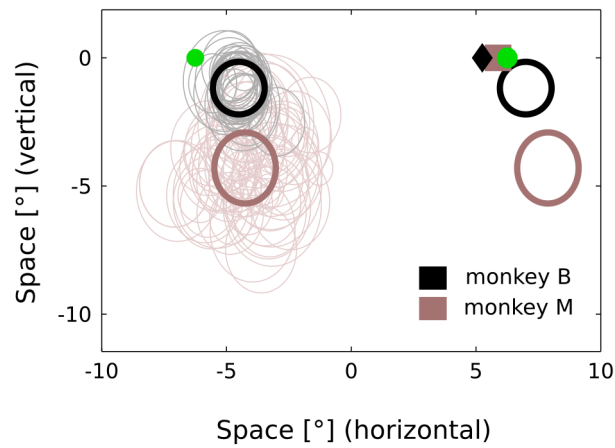
Figure 2. Receptive field positions. The positions of the RFs, recorded in monkey M (brown) and monkey B (black), are illustrated for fixation of the initial fixation point (left).Thin lines represent the RFs of individual recording sites, bold lines the population average. The coordinates (horizontal, vertical) of the average RF centers relative to the fovea were: $(1.9°, 4.5°)$ (monkey M) and $(1.1°, 1.2°)$ (monkey B). On the right, the postsaccadic RF positions after a primary saccade of average amplitude are presented. Average saccade amplitudes were $12.1°$ (monkey M, square) and $11.9°$ (monkey B, diamond).
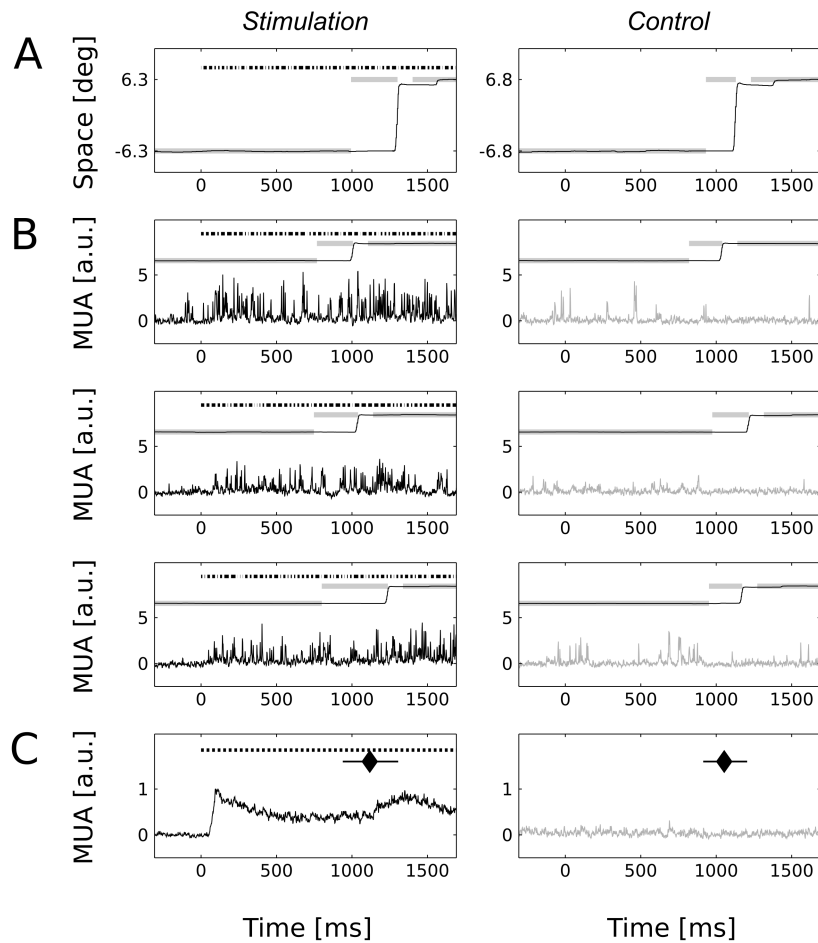
Figure 3. Example recordings of the *stimulation* (left) and *control* (right) conditions. All data from the same recording site, aligned on stimulation onset. A) Example eye traces (gray: fixation target, thin black: eye position, interrupted black: stimulation (schematic)). B) Single trial examples of the recorded multi-unit activity (MUA). The diagrams in the upper part mark the time course of the respective trial. Same conventions as in A). C) Trial-averaged MUA (*stimulation* : 150 trials, *control* : 50 trials). Diamonds mark the average saccade onset time, error bars: 95% confidence interval of the mean.
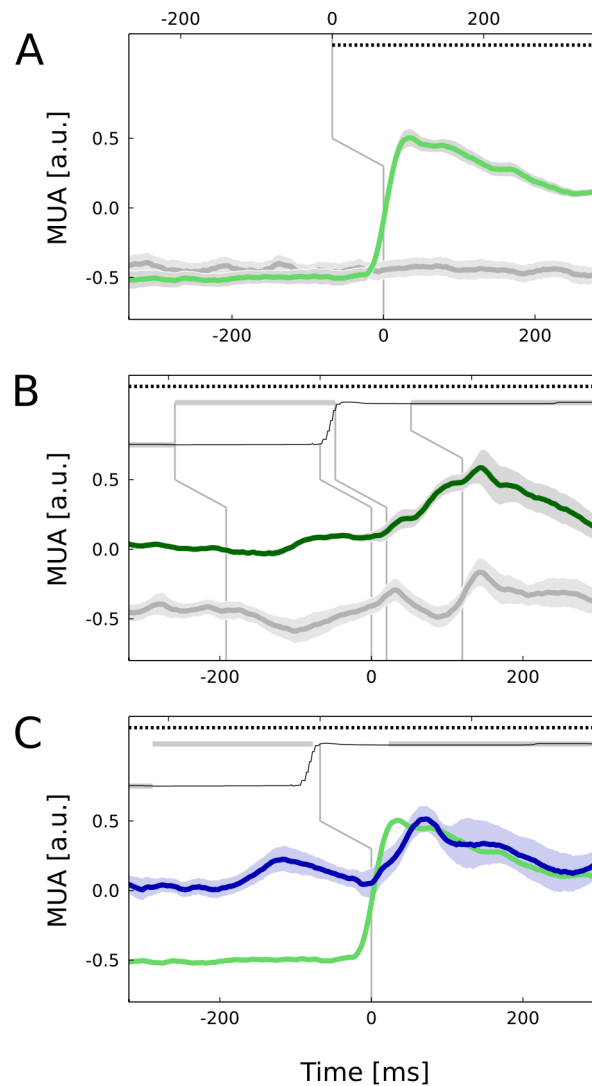
Figure 4. Population averaged MUA. A) Stimulation onset response (green) and corresponding data from the control condition (gray). Shaded areas correspond to the 95% confidence interval (CI) of the mean. The bottom axis takes the neuronal latency (halfmax) into account, marked by the flexed gray line ('shifted time', cf. Materials and methods). B) Perisaccadic response modulations triggered. The diagram in the upper part illustrates the typical time course of the trials. The marked events are (from left to right): displacement of the saccade target, saccade onset, target blanking, and target reappearance. Data are triggered on saccade onset; event times of the other events are averages. C) Comparison of the onset response (green, triggered on stimulation begin) with the perisaccadic activity (blue, triggered on saccade offset) corrected for non-stimulus driven activity also present in the control condition ('differential activity'; cf. Materials and methods).
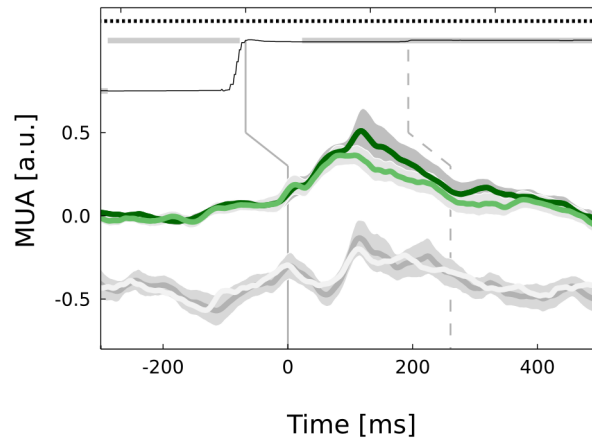
Figure 5. The role of corrective saccades. Perisaccadic population MUA from trials with (darker tones) and without corrective saccades (lighter tones). Conventions are the same as in Figure 4B, but trigger is saccade offset. The confidence interval for the control condition without corrective saccades is omitted for graphical reasons; it is comparable to the condition with corrective saccades. Corrective saccade onsets were on average 260 ms after saccade offset (dashed line).
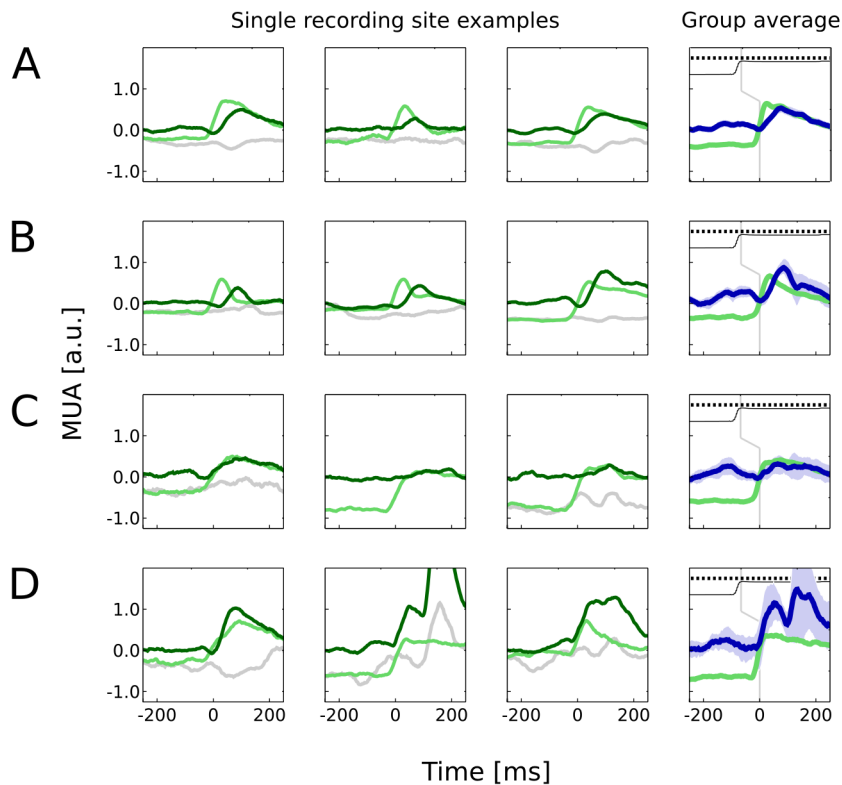
Figure 6. Examples of individual recording sites. The signals of individual recording sites, averaged over trials, were classified into four groups (plotted in different rows). The first three panels in each row present examples of group members, the last panel the group average. A) 'Early suppression' group. Compared to the onset response, the postsaccadic activity during the first 75 ms was smaller than expected by the onset response. B) 'Early suppression, late enhancement'. Similar to A), but the following activity exceeded the onset response. C) 'Match'. Onset response and postsaccadic activity were similar. This included cases that showed no clear postsaccadic enhancement and no neuronal adaptation C) 'Early enhancement'. The postsaccadic activity exceeded the onset response.
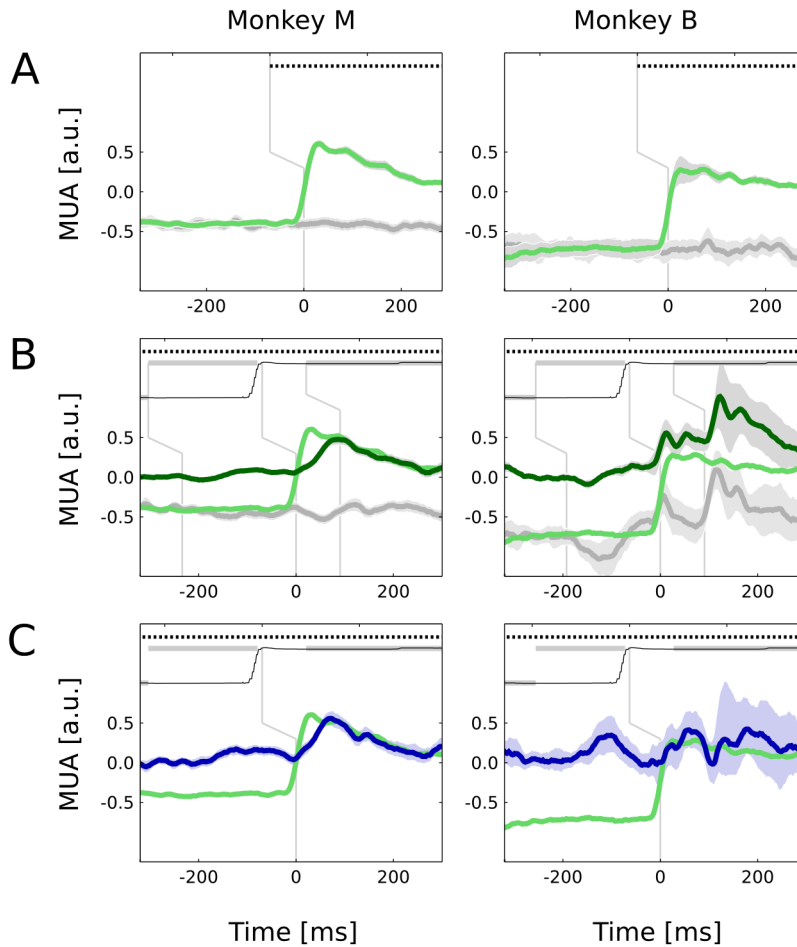
Figure 7. Average MUA separately analyzed for the two animals. Similar conventions as in Figure 4; data are aligned on stimulation onset (in A) and saccade offset (in B and C). The recorded RF in monkey B (right column) were more foveal than in monkey M (left column, cf. Figure 2). The stimulus onset responses recorded at the more eccentric positions in monkey M were significantly more transient than those of the more foveal RF positions in monkey B (transiency index: 2.8, CI: 2.5 to 3.0 and 1.8, CI: 1.6 to 2.1, respectively). The postsaccadic activity (B) as well as the differential activity (C) of the peripheral sites (left) showed a significant reduction in activity compared to the onset response during the first 52 ms. For the more foveal RFs (right), the time courses of the postsaccadic activity and the onset response did not differ significantly.

References

Armstrong KM, Moore T (2007) Rapid enhancement of visual cortical response discriminability by microstimulation of the frontal eye field. Proc Natl Acad Sci U S A 104(22):9499–9504

Azzopardi P, Jones KE, Cowey A (1999) Uneven mapping of magnocellular and parvocellular projections from the lateral geniculate nucleus to the striate cortex in the macaque monkey. Vision Res 39(13):2179–2189

Bichot NP, Rossi AF, Desimone R (2005) Parallel and serial neural mechanisms for visual search in macaque area v4. Science 308(5721):529–534

Bremmer F (2000) Eye position effects in macaque area v4. Neuroreport 11(6):1277–1283

Bremmer F, Kubischik M, Hoffmann KP, Krekelberg B (2009) Neural dynamics of saccadic suppression. J Neurosci 29(40):12,374–12,383

Clifford CWG, Webster MA, Stanley GB, Stocker AA, Kohn A, Sharpee TO, Schwartz O (2007) Visual adaptation: neural, psychological and computational aspects. Vision Res 47(25):3125–3131

Diamond MR, Ross J, Morrone MC (2000) Extraretinal control of saccadic suppression. JNeurosci 20:3449–3455

Ditchburn RW, Ginsborg BL (1952) Vision with a stabilized retinal image. Nature 170(4314):36–37

Eckhorn R, Krause F, Nelson JI (1993) The rf-cinematogram. a cross-correlation technique for mapping several visual receptive fields at once. Biol Cybern 69(1):37–55

Efron B (1979) Bootstrap methods: Another look at the jackknife. The Annals of Statistics 7:1–26

Einhäuser W, Mundhenk TN, Baldi P, Koch C, Itti L (2007) A bottom-up model of spatial attention predicts human error patterns in rapid scene recognition. J Vis 7(10):6.1–613

Ferrera VP, Nealey TA, Maunsell JH (1992) Mixed parvocellular and magnocellular geniculate signals in visual area v4. Nature 358(6389):756–761

Ferrera VP, Nealey TA, Maunsell JH (1994) Responses in macaque visual area v4 following inactivation of the parvocellular and magnocellular lgn pathways. J Neurosci 14(4):2080–2088

Fischer B, Boch R (1981a) Enhanced activation of neurons in prelunate cortex before visually guided saccades of trained rhesus monkeys. Exp Brain Res 44(2):129–137

Fischer B, Boch R (1981b) Selection of visual targets activates prelunate cortical cells in trained rhesus monkey. Exp Brain Res 41(3-4):431–433

Gallant JL, Connor CE, Essen DCV (1998) Neural activity in areas v1, v2 and v4 during free viewing of natural scenes compared to controlled viewing. Neuroreport 9(9):2153–2158

Gawne TJ, Woods JM (2003) The responses of visual cortical neurons encode differences across saccades. Neuroreport 14(1):105–109

Gee AL, Ipata AE, Goldberg ME (2010) Activity in v4 reflects the direction, but not the latency, of saccades during visual search. J Neurophysiol 104(4):2187–2193

Glasser DM, Tsui JMG, Pack CC, Tadin D (2011) Perceptual and neural consequences of rapid motion adaptation. Proc Natl Acad Sci U S A 108(45):E1080–E1088

Gouras P (1968) Identification of cone mechanisms in monkey ganglion cells. J Physiol 199(3):533–547

Hamker FH (2005) The reentry hypothesis: the putative interaction of the frontal eye field, ventrolateral prefrontal cortex, and areas v4, it for attention and eye movement. Cereb Cortex 15(4):431–447

Han X, Xian SX, Moore T (2009) Dynamic sensitivity of area v4 neurons during saccade preparation. Proc Natl Acad Sci U S A 106(31):13,046–13,051

References

Hubel DH, Livingstone MS (1990) Color and contrast sensitivity in the lateral geniculate body and primary visual cortex of the macaque monkey. J Neurosci 10(7):2223–2237

Ibbotson MR, Cloherty SL (2009) Visual perception: saccadic omission–suppression or temporal masking? Curr Biol 19(12):R493–R496

Ibbotson MR, Price NSC, Crowder NA, Ono S, Mustari MJ (2007) Enhanced motion sensitivity follows saccadic suppression in the superior temporal sulcus of the macaque cortex. Cereb Cortex 17(5):1129–1138

Ibbotson MR, Crowder NA, Cloherty SL, Price NSC, Mustari MJ (2008) Saccadic modulation of neural responses: possible roles in saccadic suppression, enhancement, and time compression. J Neurosci 28(43):10,952–10,960

Ito J, Maldonado P, Singer W, Grün S (2011) Saccade-related modulations of neuronal excitability support synchrony of visually elicited spikes. Cereb Cortex 21(11):2482–2497

Itti L, Baldi P (2005) A principled approach to detecting surprising events in video. Proc IEEE conference on computer vision and pattern recognition pp 631–637

Kagan I, Gur M, Snodderly DM (2008) Saccades and drifts differentially modulate neuronal activity in v1: effects of retinal image motion, position, and extraretinal influences. J Vis 8(14):19.1–1925

Kleiser R, Seitz RJ, Krekelberg B (2004) Neural correlates of saccadic suppression in humans. CurrBiol 14:386–390

Kohn A (2007) Visual adaptation: physiology, mechanisms, and functional benefits. J Neurophysiol 97(5):3155–3164

Krekelberg B, Boynton GM, van Wezel RJA (2006) Adaptation: from single cells to bold signals. Trends Neurosci 29(5):250–256

Lee D, Malpeli JG (1998) Effects of saccades on the activity of neurons in the cat lateral geniculate nucleus. J Neurophysiol 79(2):922–936

Leopold DA, Logothetis NK (1998) Microsaccades differentially modulate neural activity in the striate and extrastriate visual cortex. Exp Brain Res 123(3):341–345

Lisberger SG (1998) Postsaccadic enhancement of initiation of smooth pursuit eye movements in monkeys. J Neurophysiol 79(4):1918–1930

Lisberger SG, Movshon JA (1999) Visual motion analysis for pursuit eye movements in area mt of macaque monkeys. J Neurosci 19(6):2224–2246

Martinez-Conde S, Macknik SL, Troncoso XG, Dyar TA (2006) Microsaccades counteract visual fading during fixation. Neuron 49(2):297–305

Maunsell JH, Gibson JR (1992) Visual response latencies in striate cortex of the macaque monkey. J Neurophysiol 68(4):1332–1344

Mazer JA, Gallant JL (2003) Goal-related activity in v4 during free viewing visual search. evidence for a ventral stream visual salience map. Neuron 40(6):1241–1250

Merigan WH, Maunsell JH (1993) How parallel are the primate visual pathways? Annu Rev Neurosci 16:369–402

Moore T, Armstrong KM (2003) Selective gating of visual signals by microstimulation of frontal cortex. Nature 421(6921):370–373

Moore T, Tolias AS, Schiller PH (1998) Visual representations during saccadic eye movements. Proc Natl Acad Sci U S A 95(15):8981–8984

Motter BC (2006) Modulation of transient and sustained response components of v4 neurons by temporal crowding in flashed stimulus sequences. J Neurosci 26(38):9683–9694

Müller JR, Metha AB, Krauskopf J, Lennie P (1999) Rapid adaptation in visual cortex to the structure of images. Science 285(5432):1405–1408

Priebe NJ, Lisberger SG (2002) Constraints on the source of short-term motion adaptation in macaque area mt. ii. tuning of neural circuit mechanisms. J Neurophysiol 88(1):370–382

Ramcharan EJ, Gnadt JW, Sherman SM (2001) The effects of saccadic eye movements on the activity of geniculate relay neurons in the monkey. VisNeurosci 18:253–258

Ranganath C, Rainer G (2003) Neural mechanisms for detecting and remembering novel events. Nat Rev Neurosci 4(3):193–202

Reppas JB, Usrey WM, Reid RC (2002) Saccadic eye movements modulate visual responses in the lateral geniculate nucleus. Neuron 35:961–974

Riggs F L Aand Ratliff (1952) The effects of counteracting the normal movements of the eye. Journal of the Optical Society of America 42:872–873

Ross J, Morrone MC, Goldberg ME, Burr DC (2001) Changes in visual perception at the time of saccades. Trends Neurosci 24:113–121

Royal DW, Sáry G, Schall JD, Casagrande VA (2006) Correlates of motor planning and postsaccadic fixation in the macaque monkey lateral geniculate nucleus. Exp Brain Res 168(1-2):62–75

Schiller PH, Malpeli JG (1978) Functional specificity of lateral geniculate nucleus laminae of the rhesus monkey. J Neurophysiol 41(3):788–797

Seo HJ, Milanfar P (2009) Static and space-time visual saliency detection by self-resemblance. J Vis 9(12):15.1–1527

Thiele A, Henning P, Kubischik M, Hoffmann KP (2002) Neural mechanisms of saccadic suppression. Science 295:2460–2462

Tolias AS, Moore T, Smirnakis SM, Tehovnik EJ, Siapas AG, Schiller PH (2001) Eye movements modulate visual receptive fields of v4 neurons. Neuron 29:757–767

Vinje WE, Gallant JL (2000) Sparse coding and decorrelation in primary visual cortex during natural vision. Science 287(5456):1273–1276

Wurtz RH (2008) Neuronal mechanisms of visual stability. Vision Res 48(20):2070–2089

Yu S, Lee T (2000) What do v1 neurons tell us about saccadic suppression? Neurocomputing 32-33:271–277

2.6 Perisaccadic receptive field dynamics in area V4 of the macaque monkey during saccade adaptation

Abstract

The oculomotor system is capable of rapidly adjusting the amplitudes of saccadic eye movements to avoid movement inaccuracies caused by fatigue or changes in oculomotor conditions due to injury or growth of the eyeball. From psychophysical experiments it is known that this effect, called saccade adaptation, as well as saccades by themselves challenge perceptual stability: Stimuli presented briefly before, during, or after the eye movement are subject to characteristic mislocalization effects, some of them occur specifically during saccade adaptation. On the neuronal level, saccade-related changes in the receptive fields (RFs) of neurons have been observed in multiple areas of the macaque brain ('remapping'). These mechanisms are discussed to support perceptual stability across saccades and, when confronted with brief stimuli, to cause perisaccadic mislocalization effects. In this study, we investigated the influence of saccades and saccade adaptation on the RF structure in visual area V4 of the macaque monkey.

Specifically, we recorded multi-unit activity (MUA) and used a random noise stimulation technique to map the spatio-temporal RFs. In a visually guided saccade paradigm as well as during different stages of saccade adaptation, we compared RFs during fixation to those immediately before or after the eye movement. Saccade adaptation was elicited by a perisaccadic displacement of the saccade target against the movement direction ('backward adaptation').

In contrast to an earlier study (Tolias et al., 2001) and to the predictions of a recent model on remapping in V4 (Zirnsak et al., 2010), we found that the perisaccadic RFs of area V4 were remarkably stable in with respect to the fovea, i.e. we found no evidence for a saccadic remapping in this area. This was also true for the majority of the recordings sites during saccade adaptation. However, in a subpopulation of the recording sites with RFs close to the position of the adaptation step, we observed a small but consistent modulation of the postsaccadic RFs. During the first 50 ms following saccade offset the RFs were slightly distorted in shape and shifted against the direction of the adaptation step.

Taken together, our results challenge the view of V4 as an area subject to extensive perisaccadic remapping processes. If at all, RF modulations in this area seem to be small and confined to certain regions of the visual field. This suggests that perisaccadic mislocalization effects are probably not to be explained by RF

modulations in area V4.

Introduction

Despite of frequent saccadic eye movements, we perceive a continuous, stable visual environment. The mechanisms underlying this phenomenon, however, are not well understood to date. While theories on saccadic suppression and saccade induced visual masking focus on the question, why the retinal motion caused by the eye movement escapes perception, others emphasize the spatial aspect of the problem: The projection of an object that is stable in the visual scene is shifted to a different part of the retina with every change in gaze direction. The underlying question here is, if and how the pre- and postsaccadic retinal images are combined and transformed to the world-centered representation that corresponds to our percept and allows us to interact with the physical world. This problem, usually referred to as spatial updating, is often assumed to be related to a phenomenon called 'remapping' of receptive fields (RFs): Prior to or shortly after saccades ('perisaccadically'), neurons in many areas of the visual system dynamically change their spatio-temporal response profile. As an example, a subpopulation of the neurons in the lateral intraparietal area (LIP) of the macaque monkey has been reported to predictively (i.e. prior to the saccade) shift their RF to their postsaccadic position ('predictive remapping'): These neurons started to respond to stimulation outside of their classical RF, if an impending saccade later on brought their RF to the position of the presaccadic stimulus (Duhamel et al., 1992). Remapping processes with similar characteristics have since been reported in other cortical areas including the frontal eye fields (FEF; Sommer and Wurtz, 2006; Umeno and Goldberg, 1997, 2001), earlier extrastriate areas (V3A,V3,V2; Nakamura and Colby, 2002) as well as in the superior colliculus (SC; Walker et al., 1995). In ventral area V4, a different remapping pattern has been described: The RFs of about half of the recorded neurons shrank in size and were shifted in position towards the saccade target ('shift & shrink remapping', Tolias et al., 2001). Recently, the seemingly different remapping characteristics observed in different areas have been suggested to be caused by a common mechanism: focal attention that is directed towards the position of the saccade target (Zirnsak et al., 2010). This notion is based on a physiologically inspired model that predicts a detailed topography of the presaccadic remapping process in area V4. Specifically, the model predicts that for certain regions of the visual field, the remapping of V4 neurons conforms more to the predictive remapping scheme (i.e. a displacement of the RFs according to the saccade vector), while in other regions shift & shrink remapping is to be observed. Specifically, during horizontal saccades, predictive

remapping is postulated by the model for RFs positioned above or below the fixation point. On the other hand, the model predicts shift & shrink remapping for RFs close to the saccade target (cf. figures 7 and 8 in Zirnsak et al., 2010).

An interesting experimental design to study spatial updating is saccade adaptation. In saccade adaptation paradigms, the saccade target is perisaccadically displaced by a small amount from its initial position. As this displacement is accomplished while the eyes are in motion the target displacements typically escape perceptual awareness (Bridgeman et al., 1975; Klingenhoefer and Bremmer, 2011). The oculomotor system, however, gradually adapts the gain of the initial targeting saccades such that, after several trials ($\sim$50 trials in humans, $\sim$500 trials in monkeys), they will reach the displaced target position without corrective saccades (McLaughlin, 1967, see Hopp and Fuchs, 2004, for a review). In the context of spatial updating the saccade adaptation paradigm is of interest as it distorts a potentially established mapping between the pre- and post-saccadic visual input. For example, in the predictive remapping scheme described above, the question arises to which position the RF will be shifted: to where it would have been without adaptation (i.e. according to the vector of the intended saccade) or to the actual postsaccadic position (according to the vector of the adapted saccade). To our knowledge, the influence of saccade adaptation on the perisaccadic RF structure has not yet been investigated.

The goals of this study were twofold: we aimed at further investigating the topography of RF remapping in area V4. In particular, we were interested to see, if we could find evidence in support of the model recently described by Zirnsak et al. (2010). In addition, we aimed at determining the influence of saccade adaptation on the spatio-temporal RFs. We recorded multi-unit activity (MUA) in area V4 of the macaque monkey and mapped perisaccadic RFs in a visually guided saccade paradigm as well as in a saccade adaptation paradigm. We analyzed the RFs at different times relative to saccade execution as well as during different stages of the adaptation process.

Materials and methods

The results presented in this paper are partly based on the same experiments described in an accompanying paper (Klingenhoefer and Bremmer, 2012). For details on the experimental setup, animal preparation, and data acquisition, the reader is referred to this paper. Here, the focus of the analysis was on the spatial response properties. In addition, we report the results of a saccade adaptation paradigm tested in the same recording sessions.

Receptive field mapping and behavioral paradigms

We recorded multi-unit activity (MUA) in area V4 of two head-fixed macaque monkeys (animal M and B). The animals were trained to fixate a green circular target and to follow displacements of this target with their gaze. A liquid reward was given in trials in which the animals fixated the target correctly throughout the trial and responded to the dimming of the target by the release of a lever. The animals performed a visually guided saccade paradigm (*saccade*) and subsequently a saccade adaptation paradigm (*adaptation*). In the *saccade* condition, the animals performed horizontal saccades in response to a displacement of the fixation target (12.5° amplitude; animal B, always rightwards; in animal M, right- or leftwards changed on a daily basis). Upon detection of the eye movement by an eye tracking system (infrared camera system running at 240 Hz, Thomas Recording GmbH, Germany), the saccade target was blanked for 100 ms and then reappeared at the same position (Fig. 1A, top). The *adaptation* paradigm was similar to the *saccade* paradigm, except that the target did not reappear at the same position. Instead, the reappearance position was displaced by 1.9° (i.e. 15% of the saccade amplitude) against the direction of the saccade ('backward adaptation') (Fig. 1A, bottom). In addition to the primary saccades in response to the 12.5° target step, saccades of smaller amplitude were tested in the *saccade* paradigm: 500 ms after detection of the primary saccade, the fixation target was displaced again by an amplitude of 1.9°. The direction of this target step was randomly chosen to be either in or against the direction of the primary saccade. In both conditions, the horizontal extent of the receptive fields (RFs) was mapped throughout the trials using random noise stimulation. More specifically, two vertical luminance bars (75 cd/m^2, typical size: 4.5° (height) and 0.4° (width)) were repositioned horizontally at a frequency of 100 Hz. Positions of the two bars were independent of each other and randomly chosen within two adjacent regions forming a continuous area that covered the RF positions prior to, during, and after the saccade (Fig. 1B).

Data analysis

Receptive field analysis   The main goal of this study was to establish whether RFs in macaque area V4 are were dynamically modulated prior to or briefly after saccades. To this end, the continuous stream of stimuli was analyzed on a frame by frame basis to calculate the spatial response properties along the axis of the saccade vector and at different times relative to the saccade. In order to obtain data with signal-to-noise ratios appropriate for the analysis, the temporal sampling relative to the execution of the saccade was confined to time bins of 50 ms duration: We selected all stimuli that were presented during the same time bin and averaged

the post-stimulus activity following their presentation. We denote these time bins as 'windows' and use the convention that negative values represent times prior to saccade onset (e.g. -50 ms to 0 ms: the last 50 ms interval prior to saccade onset, Fig. 1C), and positive values refer to times after saccade offset (e.g. 0 ms to 50 ms: the first 50 ms interval after saccade offset, Fig. 1C). For each time window we calculated an 'activity map' which included the spatio-temporal RFs of a recording site and which consists of the averaged multi-unit activity following the presentation of a stimulus as a function of stimulus position in eye-centered coordinates (i.e. gaze position was subtracted from the stimulus position on the monitor). These three-dimensional activity maps are displayed as two-dimensional heat maps (stimulus position [deg] x time after stimulation [ms]) with different levels of activity represented by different colors.

In addition to the analysis of the activity maps as a function of the time relative to the saccade, we also investigated the activity maps during the course of saccade adaptation while retaining the perisaccadic temporal sampling. For this purpose, we pooled the data of 150 consecutive trials and calculated the full set of perisaccadic activity maps during the 150 trials of the *saccade* paradigm as well as during different 'epochs' of the *adaptation* paradigm (first adaptation epoch: trials 1 to 150, second: trials 151 to 300, third 300 to 450, Fig. 1C).

Population averaging Prior to the calculation of the perisaccadic activity maps, we additionally calculated two types of maps: the 'reference map' and (multiple) 'fixation control maps'. For these maps, longer integration times were used to obtain estimates of the RF less affected by noise. Fixation control maps were used for statistical testing, described below. A reference map was calculated for each recording site based on all trials of the *saccade* condition by pooling the data of all stimuli presented during the first 500 ms following stimulation onset. This map was used to establish the inclusion of a recording site in the analysis. To this end, the peak activity value of the reference map was determined. To make this estimate more robust against outliers, the map was slightly smoothed by convolution with a two dimensional Gaussian kernel (sigma: 0.5°). Unless otherwise noted, all other analyses used unsmoothed data. Then, the peak signal-to-noise ratio of the reference map was calculated. The signal noise of the reference maps was defined as the standard deviation of the activity map in a 'control region' (4° wide x 100 ms duration, positioned 4° away from the response peak). Recording sites with reference maps yielding a ratio greater than 5 (z-score) were included in the analysis. All activity maps of the included recording site were mean centered using the activity of the control region of the reference map; afterwards, the activity maps were normalized by division through the response peak of the

reference map. Further, the spatial dimension of all maps of a recording site was centered on the position of the response peak of the reference map, i.e. the spatial coordinates of the peak of the reference map were subtracted from the spatial coordinates of the activity maps. The spatial coordinates of the final activity maps thus correspond to positions relative to the RF center in the reference map. This centering and normalization procedure allowed us to pool and average different recording sites in order to investigate systematic changes in the receptive field structure on the population level.

Statistics   To analyze the spatial structure of the RFs in detail, we separately calculated spatial cross sections through the response peak of all activity maps of the individual recording sites. We averaged time slices of 10 ms centered around the time of the peak response in the reference map. The population mean of the spatial cross sections was calculated by averaging the individual cross sections. To test the perisaccadic RFs for significant modulations, we compared the cross sections of the perisaccadic activity maps to cross sections obtained from corresponding fixation control maps. The fixation control maps were obtained by pooling data from presaccadic time windows ranging from -450 ms to -200 ms. Thus, we calculated just one reference map for a single recording site (using data of the *saccade* paradigm), but multiple fixation control maps, a separate one for every adaptation epoch (including the *saccade* condition).

Statistical significant differences between two conditions were assessed by testing whether the bootstrapped 95-% confidence interval (CI) of the mean difference included zero (no significant difference) or not (significant difference). In particular, to test whether the spatial RF in a certain time window was significantly modulated, we tested whether the sample of cross sections of the respective time window differed from the sample of the corresponding fixation control. In these tests, all spatial sampling positions were tested independently; to correct for multiple testing, an effect was only considered significant if at least five adjacent positions (monitor pixels) differed significantly.

Results

We analyzed the perisaccadic receptive field (RF) dynamics during visually guided saccades as well as during different stages of saccade adaptation. We first report the RF dynamics as a function of the time relative to saccade execution; the results of the *adaptation* paradigm will be presented thereafter.

Perisaccadic receptive field dynamics

In order to investigate the RF structure as a function of the time relative to the saccade, we binned data from temporal 'windows' of 50 ms duration and calculated 'activity maps' representing the post-stimulus multi-unit activity as a function of stimulus position in retinal coordinates (relative to the position of the RF during fixation obtained from a 'reference map'; cf. Materials and methods). We included the data of n=128 recording sites, yielding signal-to-noise ration better than 5 (z-score), in the analysis. Saccades were slightly hypometric in comparison to the target displacement of 12.5° (average saccade amplitude: 12.1°); the average saccade latency was 186 ms.

The left column in Figure 2 presents the activity maps, averaged over the population of the recording sites, for different pre- and postsaccadic time windows. The classical RF of the population average is reflected in the circular areas of high activation near the reference position (at 0°) in the different maps. The neuronal latency of the peak response was 64 ms (time to half peak). In addition to the activity elicited by stimulation of the RF, a spatially non-selective increase in activity occurred after the saccade. This effect was caused by a general modulation of the activity level and was analyzed in detail in an accompanying paper (Klingenhoefer and Bremmer, 2012). To correct the activity maps for spatially non-selective changes of the general activity level, we subtracted, at each sampling time point of a map, the average activity level outside the classical RF from all data points (the activity outside the RF was averaged over a region 4° to 8° away from the center of the reference RF). The resulting maps show that both the position and the size of the population RF remained constant at all perisaccadic time windows (Fig. 2, right). Similarly, the response amplitudes remained at a comparable activity level during the presaccadic times; postsaccadically, they appeared slightly reduced.

To analyze the RF structure quantitatively, we compared spatial cross sections through the RF peaks, calculated by averaging time slices beginning 5 ms before the response peak of a map to 5 ms after the peak (Fig. 3). In particular, we tested whether the cross sections of the time windows immediately preceding and following a saccade differed significantly from those obtained from the fixation control maps. Prior to saccade onset the mean cross sections, averaged over all recording sites, did not differ significantly from the fixation control, neither in response amplitude nor in RF position or shape. Postsaccadically, the peak amplitudes were slightly reduced compared to the presaccadic fixation control. The effect was significant for all, except for the time window ranging from 50 to 100 ms (bootstrap test, cf. Materials and methods; data of later time windows

not shown). The spatial structure of the RFs was not altered postsaccadically.

An earlier study reported changes in RF size and position prior to saccades (Tolias et al., 2001); the effects in this study were most pronounced for RFs near the endpoint of the saccade. In our experiments described above the distance between the RFs and the saccade target was rather large ($\mathrm{\dot{c}}$ 10°). In order to test whether the RFs were modulated when they were positioned near the saccade target, we analyzed the data obtained later during the saccade paradigm, when the fixation target was displaced by 1.9° either in or against the direction of the RF positions (*towards* or *away* condition, respectively). The coordinates of the average RF centers relative to the fovea were: (1.1° , -1.3°) monkey B and (1.9° , -4.2°) monkey M (horizontal, vertical; positive values pointing to the right and upwards, respectively) Figure 4 presents the presaccadic activity maps and spatial cross sections for these cases. The average latency of these saccades was 169 ms. The uncorrected presaccadic activity maps showed a spatially unspecific increase in activity that lasted for the same time (cf. Fig 4, left column, middle panel); this activity was evoked by the fixation target that stimulated those RFs that lay close to the horizontal meridian (the RFs of monkey B) during the saccadic latency period. When the activity maps were, similar to as described above, corrected for changes in the general activity level, we did not observe any significant modulations of the RFs neither pre- nor postsaccadically (Fig. 4, right column; postsaccadic data not shown). This was also the case, when the RFs of monkey B, which lay at or very close to the target in the *towards* condition (distance between saccade target and center of average RF: 0.8° horizontal, 1.2° vertical), were analyzed separately (data not shown).

Receptive field dynamics during saccade adaptation

Similar to the analysis presented above, we investigated the perisaccadic RF dynamics during different epochs of the saccade adaptation paradigm; each epoch included 150 consecutive trials. In the *adaptation* paradigm, the saccade target was perisaccadically displaced by 1.9° against the direction of the saccade, corresponding to a shortening of the initial displacement amplitude from 12.5° to 10.6° . This manipulation lead to a progressive shortening of the saccade amplitude (Fig. 5). During the first adaptation epoch (trials 1 to 150) the average saccade amplitude was reduced by 1.1° compared to the initially given target repositioning (12.5°); in comparison to the average amplitude observed in the *saccade* condition this corresponded to a reduction in amplitude by -0.7° . The respective values of the following epochs were -1.6° , -1.7° , -2.1° (relative to the initially given target repositioning).

114

The adapted oculomotor behavior did not lead to any significant changes of the spatial RF structure in the activity maps. As an example, we present the spatial cross sections obtained during the first three postsaccadic time windows of the first three adaptation epochs (Fig. 6). Similar to the results of the *saccade* paradigm, the only significant effects detectable were small reductions in peak amplitude in the postsaccadic time windows.

We presumed that any potential RF modulations due to saccade adaptation would be strongest for RFs in the vicinity of the perisaccadic target displacement and for data obtained during sessions in which the animals had shown a clear adaptation effect. The first criterion was fulfilled by the RFs in monkey B. These RFs lay only slightly below the horizontal meridian (-1.2°) at an average horizontal excentricity of 1.1°. Consequently, these RFs were postsaccadically positioned next to or even covered the position the saccade target had initially been presented at (i.e. the position prior to the perisaccadic displacement). The second criterion, however, was only partially met in monkey B. Visual inspection of the adaptation courses of this animal revealed peculiar adaptation behavior in 30 of 53 cases (Fig. 7A): Upon beginning of the adaptation task, the animal had immediately decreased saccade amplitudes to compensate almost perfectly for the target displacement. In the remaining 23 sessions, the animal also showed a suspiciously large reduction in saccade amplitude already at the start of the adaptation paradigm; in these sessions, however, a further reduction in saccade amplitude was visible in later trials (Fig. 7B). In this data population, the average saccade amplitudes in the *saccade* paradigm were 11.7°. During the first three adaptation epochs the respective values were 10.9°, 10.4°, and 10.5°, corresponding to further reductions in amplitude by 0.8°, 1.3°, and 1.2° relative to the actual amplitude in the *saccade* paradigm. When the spatial cross sections of these sessions were analyzed separately, small modulations of the RFs could be observed in the first postsaccadic time windows of the adaptation epochs: The response peaks were slightly deformed in the direction against the adaptation step (Fig. 8). This effect was consistently visible during all adaptation epochs and reached significance in the first and third epoch. In all later postsaccadic time windows no significant modulations were detectable. To get an estimate of the effect size during the first postsaccadic time window, we pooled the data of the first three adaptation epochs (Fig. 8, top right panel). In the resulting cross section, the response peak was shifted by 0.3° compared to the corresponding data of the fixation control; the two curves differed significantly over a 0.5°-wide area of which the center was shifted by 0.5° relative to the peak of the fixation control cross section.

Discussion

In our present experiments, we investigated the influence of saccadic eye movements on the receptive field structure of neurons in area V4 of the macaque monkey. In retinal coordinates, the receptive fields were remarkably stable, perisaccadically as well as during saccade adaptation. The only exception were small but consistent modulations that occurred during the first 50 ms after saccade offset during saccade adaptation: Receptive fields near the fovea, and thus near the position of the intrasaccadic target displacement, were slightly distorted and shifted against the adaptation direction.

Remapping in V4?

An earlier study, in which the presaccadic receptive fields (RFs) in area V4 of the macaque monkey were mapped, reported shifting RFs towards the saccade target and a shrinkage of the RF size ('shift & shrink remapping', Tolias et al. (2001)). We could not reproduce these findings. This raises the question on the differences of the experiments. Tolias et al. (2001) found a significant increase in presaccadic activity that started to build up about 50 ms before the eyes started to move in 37 of 80 neurons. This effect is comparable to what we have observed in an analysis of the continuous perisaccadic activity, reported elsewhere (Klingenhoefer and Bremmer, 2012) using the same data of the *saccade* condition as used here. In this analysis, we found a presaccadic increase in activity in 30/90 neurons; the effect reached significance 64 ms prior to saccade onset. Tolias et al. confined their further analysis of the RFs to the subpopulation of those neurons, in which significant changes in perisaccadic activity were detected. In contrast, we included all recording sites in our analysis. However, we think it is unlikely that this different pooling strategy is responsible for the diverging results. In the analysis of the continuous perisaccadic activity, we followed the same strategy as here and could easily detect the contributions of the 33% of the neurons showing an enhancement effect in the population average. Further, the effect sizes reported by Tolias et al. were in the order of magnitude of several degrees (mean shift size: 4.3°). Given the high accuracy of our RF estimates, such clear effects, even if only present in a small subpopulation, would have been detectable in the population average. In our opinion, the most likely reason for the discrepancy of the results is to be found within the different RF mapping strategies. Tolias et al. presented one stable stimulus of long duration (> several hundred milliseconds) per trial and varied the stimulus position only between trials. We used a highly dynamic stimulus pattern, with single stimuli changing on a frame by frame basis. Tolias et al. found the clearest effects for RFs that were positioned near the saccade target. It

is conceivable, that the shift & shrink remapping reflects an interaction effect that only occurs when a salient stimulus, as the single probe stimulus on an otherwise blank screen in the experiments of Tolias et al. certainly must have been, is presented near the saccade target. Alternatively, shift & shrink could be the default remapping scheme in V4 that occurs in natural vision; then, the generality of the results obtained by using brief transient stimuli is to be questioned.

Indeed, it is known, that spatial stability on the perceptual level breaks down, when tested with brief stimuli; such stimuli are subject to characteristic mislocalization effects (Dassonville et al., 1992; Honda, 1989; Morrone et al., 1997). Zirnsak et al. (2010) presented a computational model that predicts the topography of RF remapping in V4 in detail. Initially, the parameters of this model were adjusted to explain the so called perisaccadic compression effect (Hamker et al., 2008): Under certain experimental conditions, perisaccadically presented brief stimuli are mislocalized towards the position of the saccade target (Ross et al., 1997). Once the model was calibrated by the behavioral data, the simulated neurons revealed remapping characteristics comparable in some parts of the visual field to the observed shift & shrink remapping; for other parts the model revealed predictive remapping as observed for example in area LIP (Duhamel et al., 1992). The model of Zirnsak et al. thus connects the results obtained in localization experiments using brief stimuli to shift & shrink remapping; this challenges the above mentioned hypothesis on different RF dynamics depending on the the mapping methods. Given the current experimental evidence, we can not resolve this issue. We believe, however, it is unlikely that, as proposed by the model, perisaccadic compression is to be explained by focal spatial attention directed towards the representation of the saccade target in V4. Unlike predicted by the model of Zirnsak et al., neither Tolias et al. nor we observed any evidence for predictive remapping in V4, even though some RFs in our experiments were positioned within regions for which the model showed predictive remapping (cf. their figures 7 and 8). This is accumulating evidence that predictive remapping is stronger in areas more directly linked to the oculomotor system (Nakamura and Colby, 2002). We therefore think it is unlikely that predictive remapping is the result of the same attentional mechanism known to improve perception at the saccade target (which might well be related to the presaccadic response characteristics in V4 Armstrong and Moore, 2007; Moore and Armstrong, 2003). However, given the striking explanatory power of the model concerning the results of the psychophysical localization experiments, we think it should not be completely dismissed; instead, it might be worth to consider and experimentally test its applicability to those areas already known to exhibit predictive remapping. We also suggest to rethink the causality of the involved processes. In the current interpretation

of the model, remapping is a consequence of an attentional process of which the function is to improve perception at the saccade target prior to the actual saccade. Such perceptual benefits at the saccade target have indeed been observed in a number of psychophysical experiments (Deubel et al., 1996; Kowler et al., 1995). The reported effects, however, are usually rather small, and it should be noted that only briefly after the presaccadic enhancement, namely once the saccade is accomplished, the full resolution and processing capacity of foveal vision is at the disposal of the former target region. It thus has to be questioned, whether a head start in processing at the saccade target is of behavioral relevance. On the other hand, although not finally proven, predictive remapping might be crucial for the maintenance of perisaccadic perceptual stability (Wurtz, 2008). The model of Zirnsak et al. implements a plausible mechanism that shows remapping. So it might be worth to consider the possibility that the signal driving the remapping process in the model of Zirnsak et al. is not of attentional nature as initially assumed, but that it is actually the same signal as the one known in the neurophysiological literature as corollary discharge, i.e. an internal copy of the motor command (von Holst, 1950; Sperry, 1950), known to cause RF remapping (Sommer and Wurtz, 2006). In this notion, enhanced presaccadic performance at the saccade target would not be the cause but the consequence of predictive remapping.

The effect of saccade adaptation

From psychophysical experiments, it is known that saccade adaptation can influence spatial perception (Awater et al., 2005; Bahcall and Kowler, 1999; Collins et al., 2007, 2009; Georg and Lappe, 2009; Klingenhoefer and Bremmer, 2011). In most of the experiments, stimuli that were presented prior to the saccade were mislocalized (Awater et al., 2005; Bahcall and Kowler, 1999; Collins et al., 2007, 2009; Georg and Lappe, 2009). We did not observe any changes of the RFs in presaccadic time windows related to saccade adaptation. One might consider this as evidence that the neural correlate of the above mentioned mislocalization effects is probably not to be found in the RF structure of V4. However, it has to be kept in mind, that the presaccadic mislocalization effects were reported either for the saccade target itself (Bahcall and Kowler, 1999; Collins et al., 2009) or for positions close to it (Awater et al., 2005; Georg and Lappe, 2009). The positions of the RFs in our experiments were separated from the position of the saccade target by more than $10°$. Given this geometry, we think it is unlikely that we would have detected any presaccadic spatial reorganization processes that might take place near the saccade target.

Instead, our experimental design certainly favored the detection of adaptation induced postsaccadic RF changes. We indeed observed such changes in a sub-population of the recording sites: The spatial response profile of RFs that were postsaccadically positioned close to the adaptation zone were slightly distorted immediately after saccade offset. The effect was quite small though, and it has to be asked whether it represents a true modulation of the RF structure. We believe that this might actually be the case. The effect was consistently present during all adaptation epochs (although only significant in two out of three cases); it is therefore unlikely to be caused by signal noise present in the RF maps. The quality of the eye position signal is another critical factor to consider as the RF maps were all determined in eye-centered coordinates. We did our best to eliminate signal delays between the eye tracker and the MUA recording system as well as to maintain an accurate calibration of gaze position throughout the adaptation sessions. But still, the accuracy of any camera based eye tracker (typically $> 0.5°$) is, at best, of similar magnitude as the observed effect size ($0.3°$ - $0.5°$). For this reason, it is important to note that the effect we observed occurred only for the first postsaccadic time window and was not present at later times; this rules out a calibration offset of the eye tracker. In addition, the effect was also not present in the *saccade* condition which excludes a delay between the eye-tracker and the MUA recording system as a potential confounding factor. Finally, the effect size might not be as small as it might appear at first glance. The reduction in saccade amplitude relative to the hypometric saccades (amplitude: 11.7) in the *saccade* paradigm were on average $1.1°$. The observed shift of the RF peak of $0.3°$ thus corresponds to an effect size of about 30% of the behavioral change; the center of the significant area lay $0.5°$ to the right of the reference position which corresponds to an effect size of about 45%.

Evidence for postsaccadic RF modulations during saccade adaptation might also arise from the psychophysical literature: Klingenhoefer and Bremmer (2011) assessed detection thresholds in human subjects for a displacement of the saccade target, accomplished during the eye movement. During backward saccade adaptation, the displacement detection thresholds for the saccade target were higher in the region near the adaptation step than during unadapted saccades. This can be seen as evidence for a spatial distortion in the region near the adaptation step; specifically, the effect can be interpreted in such a way that the adapted and the unadapted target positions were harder to distinguish, or, in other words, that the space between these positions was perceptually fused to some extend. At the neuronal level, such an effect could manifest itself in an expansion of RFs or the shift of some RFs from one position towards the other position. This seems to be consistent with the RF distortions we observed. However, Klingenhoefer and Bremmer

(2011) observed the described effect only in a paradigm in which the saccade target was not blanked postsaccadically; the data of a blanking paradigm, as applied here, did not show the effect. One possible reason for this discrepancy might be that Klingenhoefer and Bremmer (2011) tested perception during late adaptation epochs when adaptation had reached a steady state. Assuming that the perceptual effect vanishes after a while once adaptation is established, it is possible that the same effect observed for the non-blanking paradigm was also present during earlier adaptation epochs in the blanking paradigm, but was not detectable during late epochs: It might have decayed quicker in the blanking paradigm than in the non-blanking paradigm.

Taken together, our data presented here are evidence that the RFs in area V4 of the macaque monkey are rather unaffected by saccadic eye movements; instead, they are stable in eye-centered coordinates. This challenges the view that remapping processes in this area are the neural correlate of perisaccadic mislocalization effects observed psychophysically. We found some evidence for RF modulations related to saccade adaptation; however, given the small effect size, more experiments will certainly be needed to confirm our observation. It would be especially interesting to study the RF dynamics during saccade adaptation in frontal area FEF as well as in parietal area LIP as both areas are known to be closely involved in saccade generation and to show strong remapping effects. As these areas are also anatomically connected to V4 (Ungerleider et al., 2008), the adaptation induced effect we observed might suggest that in these areas remapping is partially directed towards the unadapted target position.
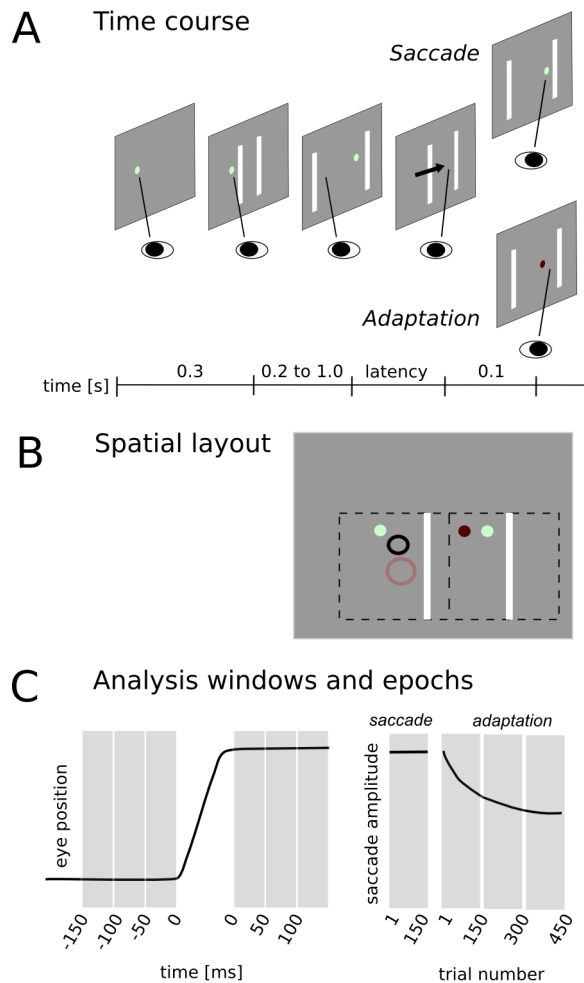
Figure 1. Experimental design (not drawn to scale; fixation targets are differently colored for illustration purposes only). A) Time course of the trials. The animals performed visually guided saccades in two paradigms: *saccade* and *adaptation*. In both paradigms a visually guided saccade was initiated by the repositioning of a fixation target by an amount of $12.5°$. Upon detection of the eye movement by an eye tracker the saccade target faded for 100 ms. In the *saccade* paradigm it then reappeared at the same position (upper panel); in the *adaptation* paradigm it was displaced by $1.9°$ against the direction of the saccade (lower panel). In the *saccade* paradigm, 500 ms after detection of the primary saccade, the fixation target was displaced again (amplitude: $1.9°$), either in or against the direction of the primary saccade (not included in the diagram). B) Spatial layout. In both conditions two luminance bars, which were independently and randomly repositioned every 10 ms within two subdivisions of a continuous stimulation area (dashed rectangles) were presented to map the receptive fields throughout the trials.

The approximate positions of the RFs of the two animals, obtained in an initial two dimensional RF mapping are illustrated by circles. The coordinates of the horizontal and vertical components of the center of the average RFs relative to the fovea were: (1.9°, -4.5°) (monkey M, light red) and (1.1°, -1.2°) (monkey B, black). C) Temporal analysis. To investigate the RF properties as a function of the time relative to the execution of a saccade, we analyzed the data separately for temporal 'windows' of 50 ms duration. Negative values represent times prior to saccade onset; positive values, times after saccade offset. In addition, we compared the perisaccadic RF dynamics during different stages of the adaptation process by pooling data from 'epochs' of 150 trials.

A *pre*

B *post*

T relative to saccade [ms]

Space relative to reference position [deg]
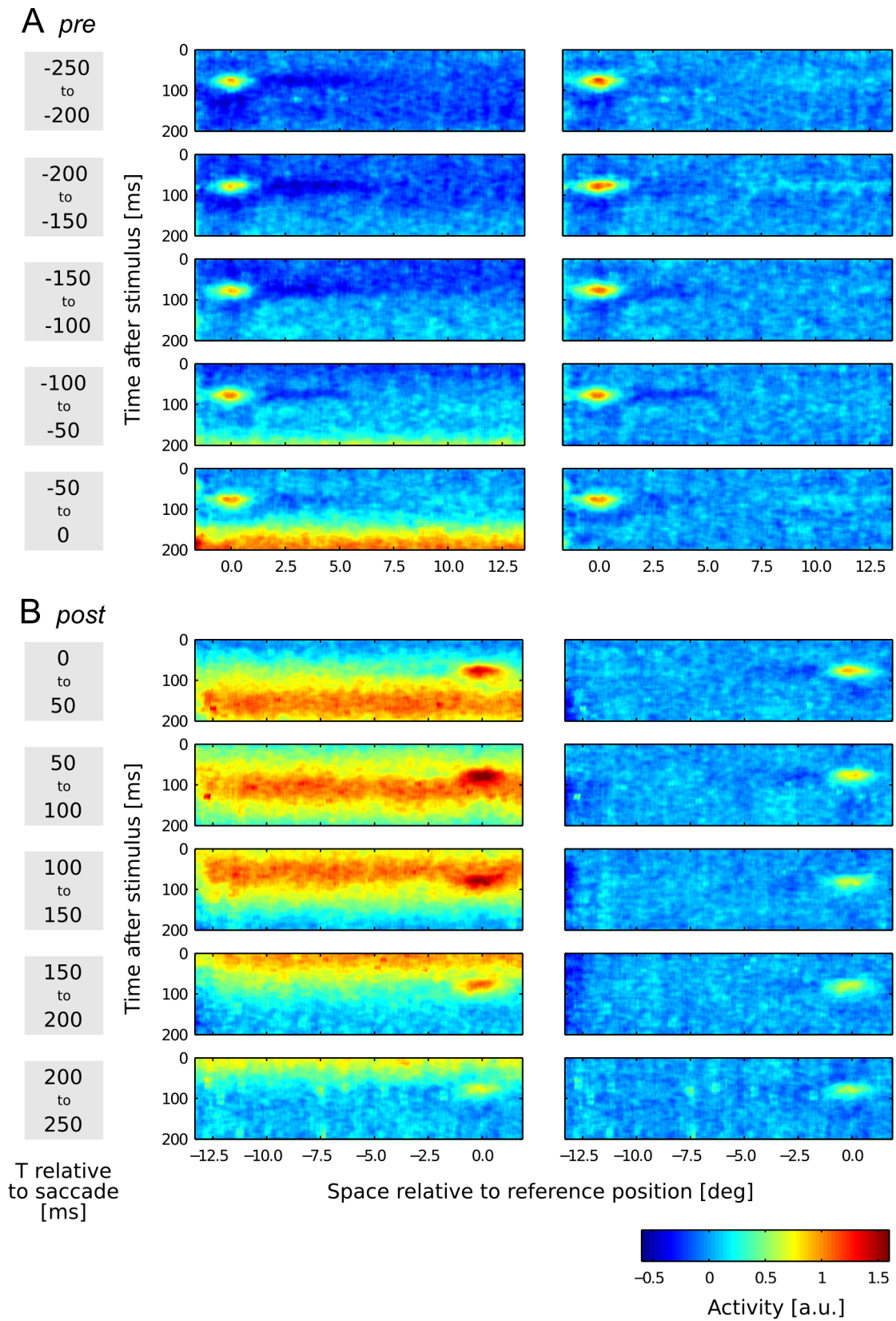
Activity [a.u.]

Figure 2. Activity maps obtained in the saccade paradigm. Different rows represent different time windows of stimulus presentation relative to the saccade. Multi-unit activity (color coded), averaged over the population of all recording sites of both monkeys, is presented as a function of post stimulation time and stimulus position. Stimulus position is given in eye-centered coordinates and relative to the position of the RF in a reference map (not shown), obtained during fixation using stimuli presented during the first 500 ms after stimulation onset (cf. Materials and methods). A) Presaccadic time windows. B) Postsaccadic time windows. Left column: Activity values in all panels were mean centered and normalized according to the reference map (cf. Materials and methods). Right column. In all maps, the activity values of every time slice were individually mean centered by subtraction of the average background activity of the respective time slice (averaged over a region 4° to 8° away from the RF center).
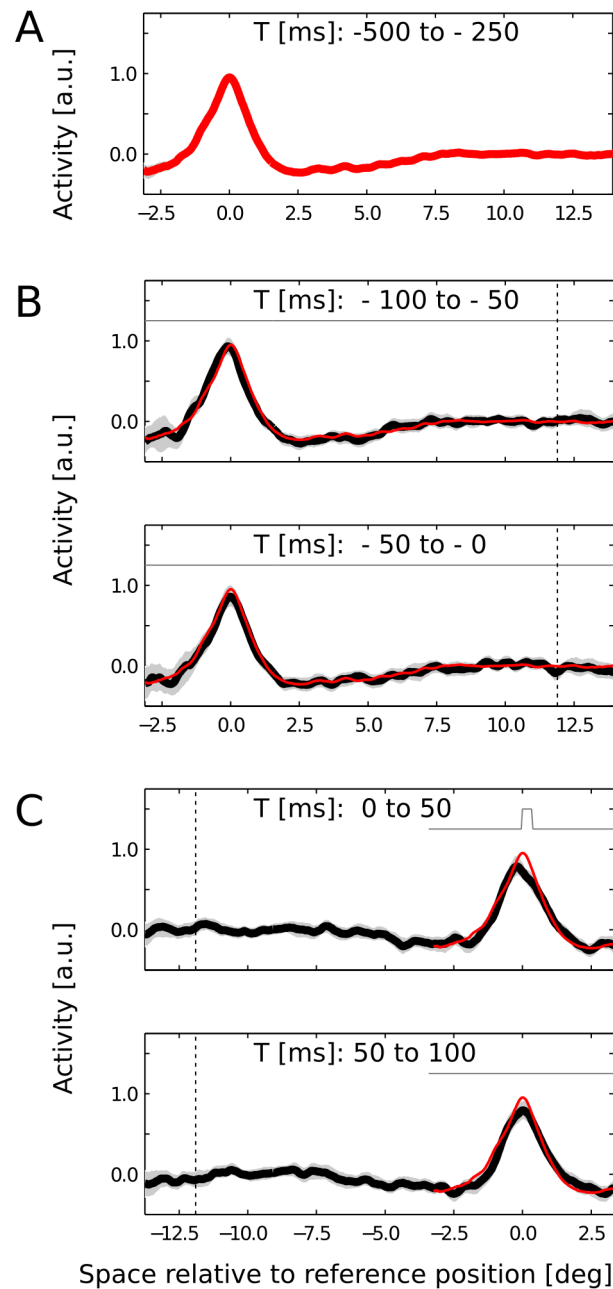
Figure 3. Spatial cross sections through the RFs at different time windows of the saccade paradigm. Errors bands represent the 95% confidence interval of the mean; if not visible, they are smaller than the line width. A) Cross section through the RF of the fixation control map used as comparison in significance testing (cf. Methods). B) Cross sections from presaccadic time windows (black). For comparison, the mean of the fixation control cross section is plotted in red. Significant differences between control and perisaccadic data are marked by positive deflections of the horizontal line presented in the upper part of each panel. The dotted vertical line marks the amplitude of the average saccade vector (12.1°). C) Data of the first two postsaccadic time windows.
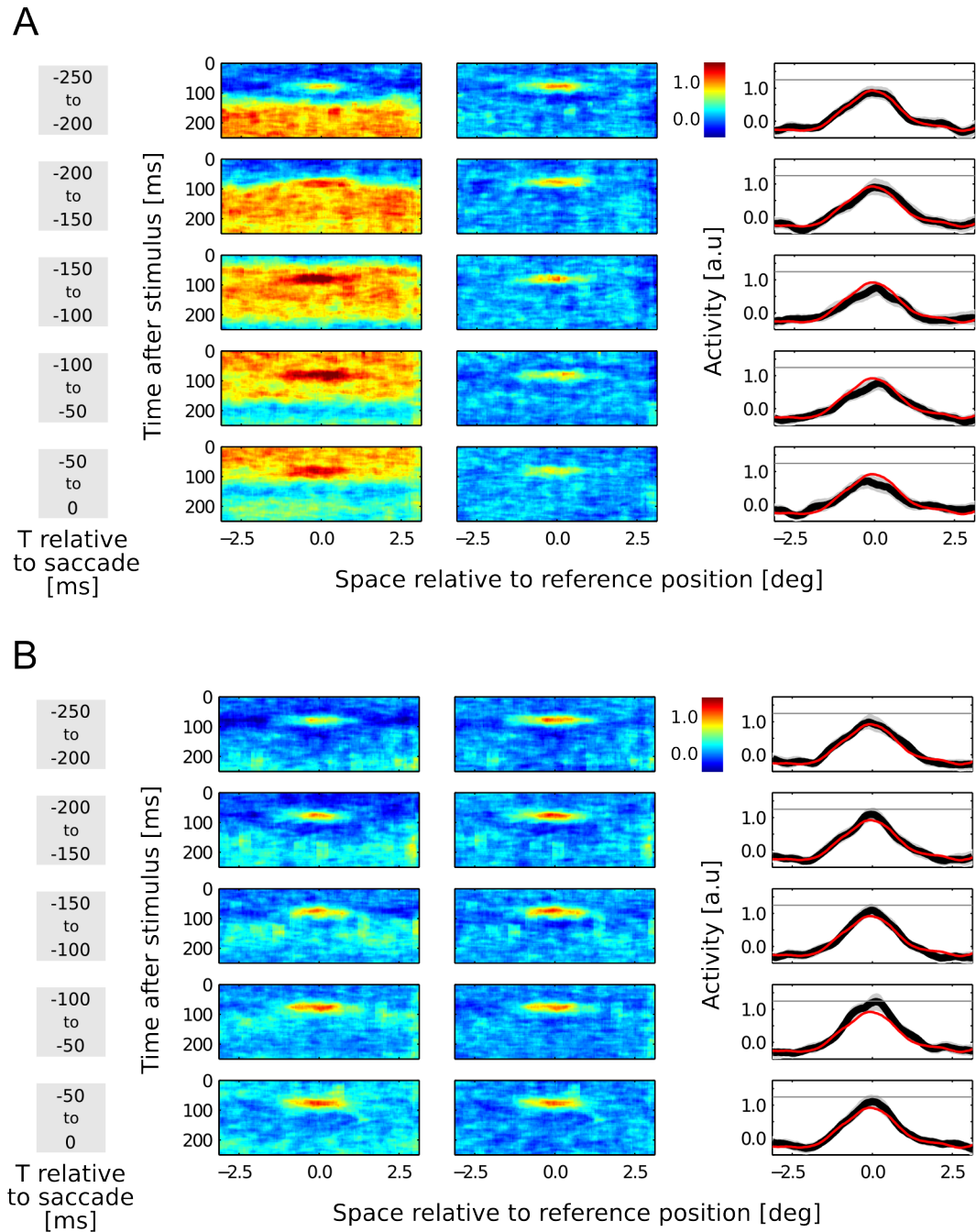
125

Figure 4. Presaccadic activity maps and cross sections in case of saccades towards or away from the RFs. Same conventions as in Fig. 2 and Fig. 3. In the *saccade* paradigm, the fixation point was displaced for a second time 500 ms after the initial saccade; the amplitude of this displacement was 1.9°; the direction was A) towards the positions of the RFs, or B) in the opposite direction. In A) the RFs recorded in monkey B (average coordinates: 1.1° (horizontal), -1.2° (vertical)) were stimulated during the latency period of the saccade (169 ms) by the saccade target. The average RF coordinates in monkey M were 1.9° (horizontal), -4.2° (vertical).
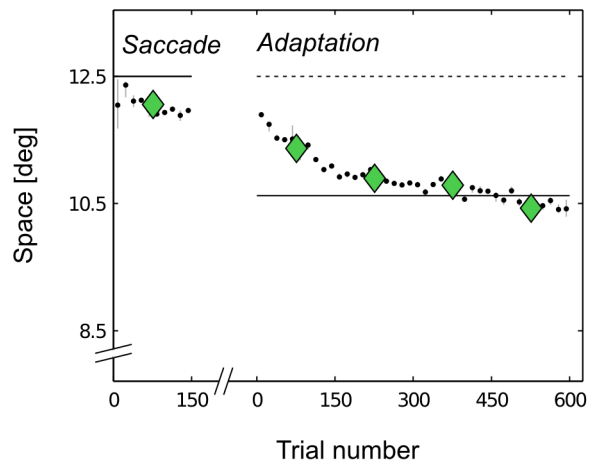
Figure 5. Saccade amplitudes in the *saccade* and *adaptation* paradigms. Error bars correspond to 95% confidence interval of the mean. Green diamonds represent mean values obtained for the different analysis epochs (including data of 150 trials); black dots, represent data binned over 15 trials.
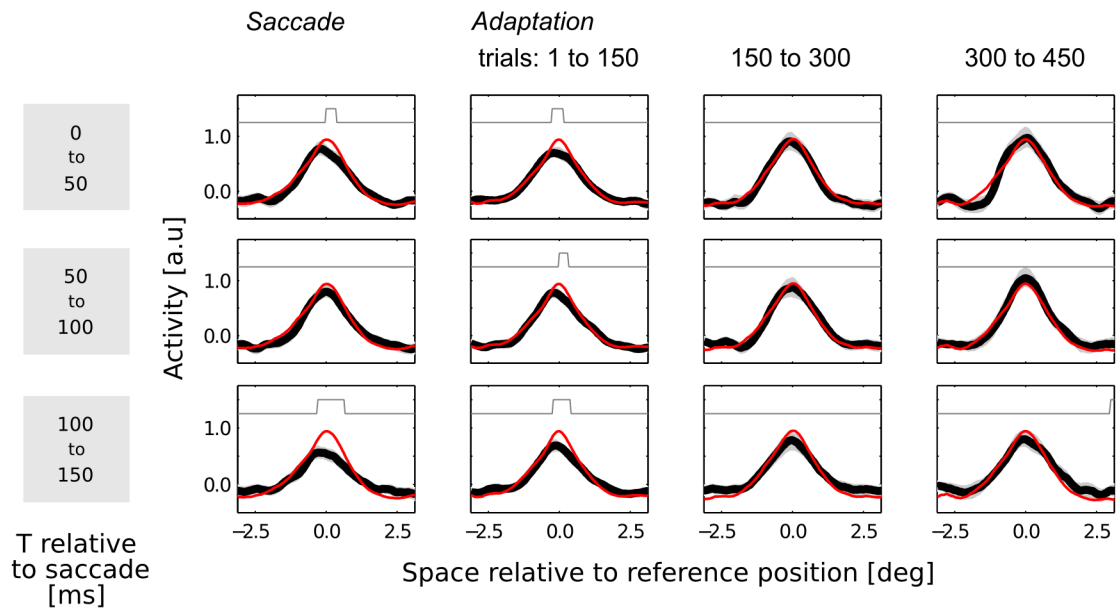
Figure 6. Spatial cross sections of the postsaccadic RFs during different epochs of saccade adaptation. Same conventions as in Fig. 3. Different columns, represent different epochs of the adaptation process. Red lines correspond to cross sections through the RF of the fixation control map of the respective epoch.
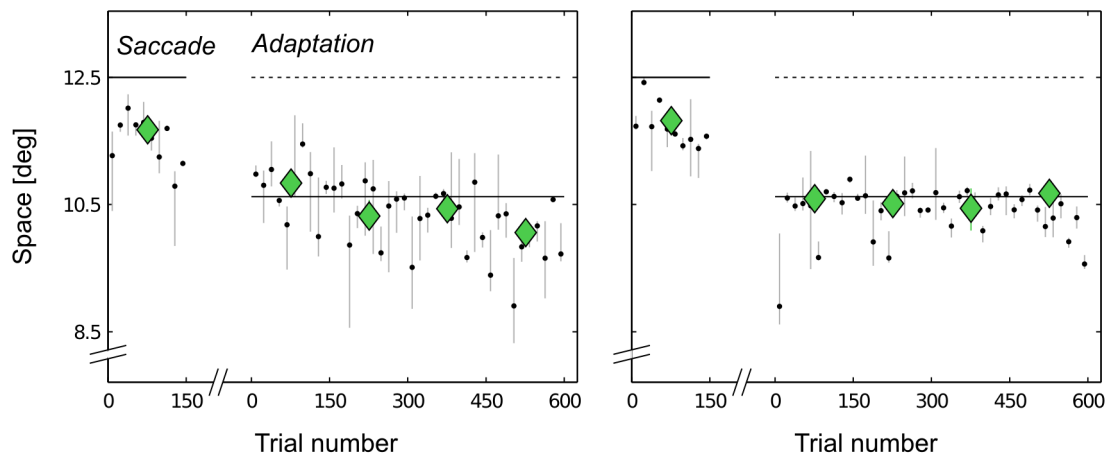
Figure 7. Divergence in oculomotor behavior of monkey B in the saccade adaptation paradigm. Same conventions as in Fig. 5. The data of this animal showed suspicious adaptation courses in 30 of 53 cases. For further analysis, we separated the data obtained from sessions during which a gradual decrease in saccade amplitude was visible (left panel) or was absent (right panel).
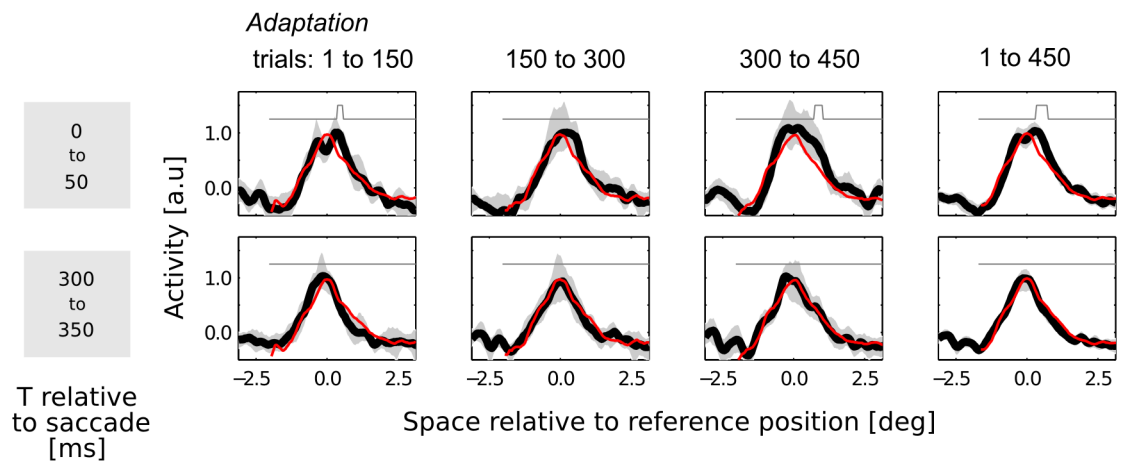
Figure 8. The influence of saccade adaptation on the postsaccadic RFs in monkey B. Only data from sessions in which a gradual change in saccade amplitude was visible were included (cf. Fig. 7). Same conventions as in Fig. 3. Data from the first postsaccadic time window and, for comparision, from a later time window are presented (top and bottom row, respectively). In the rightmost panels, data from the first three adaptation epochs were averaged.

References

Armstrong KM, Moore T (2007) Rapid enhancement of visual cortical response discriminability by microstimulation of the frontal eye field. Proc Natl Acad Sci U S A 104(22):9499–9504

Awater H, Burr D, Lappe M, Morrone MC, Goldberg ME (2005) Effect of saccadic adaptation on localization of visual targets. J Neurophysiol 93(6):3605–3614

Bahcall DO, Kowler E (1999) Illusory shifts in visual direction accompany adaptation of saccadic eye movements. Nature 400(6747):864–866

Bridgeman B, Hendry D, Stark L (1975) Failure to detect displacement of the visual world during saccadic eye movements. Vision Res 15(6):719–722

Collins T, Doré-Mazars K, Lappe M (2007) Motor space structures perceptual space: evidence from human saccadic adaptation. Brain Res 1172:32–39

Collins T, Rolfs M, Deubel H, Cavanagh P (2009) Post-saccadic location judgments reveal remapping of saccade targets to non-foveal locations. J Vis 9(5):29.1–29.9

Dassonville P, Schlag J, Schlag-Rey M (1992) Oculomotor localization relies on a damped representation of saccadic eye displacement in human and nonhuman primates. VisNeurosci 9:261–269

Deubel H, Schneider WX, Bridgeman B (1996) Postsaccadic target blanking prevents saccadic suppression of image displacement. Vision Res 36:985–996

Duhamel JR, Colby CL, Goldberg ME (1992) The updating of the representation of visual space in parietal cortex by intended eye movements. Science 255:90–92

Georg K, Lappe M (2009) Effects of saccadic adaptation on visual localization before and during saccades. Exp Brain Res 192(1):9–23

Hamker FH, Zirnsak M, Calow D, Lappe M (2008) The peri-saccadic perception of objects and space. PLoS Comput Biol 4(2):e31

von Holst H E Mittelstaedt (1950) Das reafferenzprinzip. wechselwirkungen zwischen zentralnervensystem und peripherie. Naturwissenschaften 37:464–476

Honda H (1989) Perceptual localization of visual stimuli flashed during saccades. PerceptPsychophys 45:162–174

Hopp JJ, Fuchs AF (2004) The characteristics and neuronal substrate of saccadic eye movement plasticity. Prog Neurobiol 72(1):27–53

Klingenhoefer S, Bremmer F (2011) Saccadic suppression of displacement in face of saccade adaptation. Vision Res 51(8):881–889

Klingenhoefer S, Bremmer F (2012) Perisaccadic response modulations in area v4 of the macaque monkey. In preparation

Kowler E, Anderson E, Dosher B, Blaser E (1995) The role of attention in the programming of saccades. Vision Res 35(13):1897–1916

McLaughlin S (1967) Parametric adjustment in saccadic eye movements. Percept Psychophys 2:359–362

Moore T, Armstrong KM (2003) Selective gating of visual signals by microstimulation of frontal cortex. Nature 421(6921):370–373

Morrone MC, Ross J, Burr DC (1997) Apparent position of visual targets during real and simulated saccadic eye movements. JNeurosci 17:7941–7953

Nakamura K, Colby CL (2002) Updating of the visual representation in monkey striate and extrastriate cortex during saccades. Proc Natl Acad Sci U S A 99(6):4026–4031

Ross J, Morrone MC, Burr DC (1997) Compression of visual space before saccades. Nature 386:598–601

Sommer MA, Wurtz RH (2006) Influence of the thalamus on spatial visual processing in frontal cortex. Nature 444(7117):374–377

Sperry RW (1950) Neural basis of the spontaneous optokinetic response produced by visual inversion. J Comp Physiol Psychol 43(6):482–489

Tolias AS, Moore T, Smirnakis SM, Tehovnik EJ, Siapas AG, Schiller PH (2001) Eye movements modulate visual receptive fields of v4 neurons. Neuron 29:757–767

Umeno MM, Goldberg ME (1997) Spatial processing in the monkey frontal eye field. i. predictive visual responses. JNeurophysiol 78:1373–1383

Umeno MM, Goldberg ME (2001) Spatial processing in the monkey frontal eye field. ii. memory responses. J Neurophysiol 86(5):2344–2352

Ungerleider LG, Galkin TW, Desimone R, Gattass R (2008) Cortical connections of area v4 in the macaque. Cereb Cortex 18(3):477–499

Walker MF, Fitzgibbon EJ, Goldberg ME (1995) Neurons in the monkey superior colliculus predict the visual result of impending saccadic eye movements. JNeurophysiol 73:1988–2003

Wurtz RH (2008) Neuronal mechanisms of visual stability. Vision Res 48(20):2070–2089

Zirnsak M, Lappe M, Hamker FH (2010) The spatial distribution of receptive field changes in a model of peri-saccadic perception: predictive remapping and shifts towards the saccade target. Vision Res 50(14):1328–1337

3 General discussion and outlook

In this thesis different aspects of the phenomenon of visual perceptual stability across saccadic eye movements and its potential neural correlates were investigated. As described in detail in the introduction, the problem of transsaccadic perceptual stability can be subdivided into a spatial aspect (saccadic updating) and the phenomenon of saccadic omission.

The 'world centered' hypothesis

An common experimental paradigm to study saccadic updating are localization experiments. It is well known that brief stimuli presented shortly before, during or after a saccade are subject to characteristic mislocalization effects (e.g. Honda, 1991; Matin and Pearce, 1965; Ross et al., 1997). In study 1 and study 2 of this thesis we investigated whether these effects are confined to visual localization in the fronto-parallel plane, or whether they are manifestations of a more general phenomenon. In study 2 we could show that during saccades localization in depth is also prone to strong systematic errors. Localization of auditory targets, on the other hand, was rather stable (study 1). These results suggest that mislocalization occurs when visual but not auditory spatial information has to be combined with fast changing eye-position signals.

One theory of transsaccadic perceptual stability relies on a world-centered neural representation of external space (cf. 1.4). Taking this idea one step further, it could be hypothesized that such a world-centered representation also integrates the signals across multiple modalities. The reported properties of area VIP neurons, coding visual and auditory information in a common, in many cases an extra-retinal reference frame (Schlack et al., 2005), could be considered as a step towards such a representation. The lack of cross-modal transfer of perisaccadic mislocalization found in study 2 of this thesis, however, argues against such a single, modality-independent representation of space.

The role of remapping receptive fields in perisaccadic mislocalization

In study 6 we investigated the neural basis of another widespread account of transsaccadic perceptual stability: the remapping of RFs. From physiological

studies it is well known that the RF structure in certain areas of the visual system of the monkey is perisaccadically subject to dynamic changes ('remapping', cf. 1.4). Currently, a direct link between RF remapping and perceptual stability still has to be shown. However, a connection between remapping and perisaccadic mislocalization, specifically 'perisaccadic compression', was recently proposed in a computational model presented by Zirnsak et al. (2010). This model predicted various RF remapping effects in area V4 of the macaque monkey (including 'predictive remapping'; cf. 1.4) as the basis of perisaccadic compression. In study 6, we tested this hypothesis in a physiological experiment. Our results clearly show that the RFs in area V4 are perisaccadically stable and remain at the same retinal position as during fixation. This is strong evidence for the hypothesis that the response properties of neurons in area V4 are not the neural correlate of perisaccadic compression as proposed by Zirnsak et al. (2010). As elaborated in more detail in the discussion of the respective study, our results give a restriction on the anatomical location of the effect (not V4), but it does not exclude the possibility that RF remapping in other, 'higher' cortical areas causes mislocalization. Another study, conducted in area MT of the dorsal stream, came to the same conclusions as we did (Hartmann et al., 2011): In area MT, which is considered to be located at a comparable processing stage as V4, the RF positions were not modulated by eye movements (specifically, the slow phase during optokinetic nystagmus). If perceptual mislocalization effects are caused by RF remapping, then the involved areas are probably located at higher processing stages than V4 or MT. This will have to be determined in future studies.

The representation of eye position

Besides changes in the neural representation of space, the second possible source of behavioral mislocalization of stimuli in an external (head-centered) reference frame is the neural representation of eye position. Study 3 of this thesis, a modeling study, followed this approach. The model presented in study 3 evolved based on earlier work (Dassonville et al., 1992; Honda, 1991; Pola, 2004). In all of these models two signals are combined to give an estimate of stimulus position in an external reference frame. One signal represents the stimulus position in retinal coordinates, the other an eye position signal (relative to the external reference frame). In earlier models the parameters were adjusted such that the psychophysical mislocalization results were reproduced; this approach, however, also predicts mislocalization for continuously present stimuli, not only for brief flashes. In other words, these models predict brief perisaccadic disruptions of perceptual stability. This is the decisive point wherein our model differs from earlier variants: We

built in the assumption of transsaccadic perceptual stability for stimuli that *are* actually stable, i.e. those that are permanently present at the same location in the outside world. Under this assumption, we were able to show, that the model could nevertheless reproduce the known mislocalization effects for flashed stimuli using physiologically plausible parameters. Probably the most remarkable point of our results is, that perceptual stability can be achieved by the combination of two erroneous signals: delayed and sluggish representations of eye and stimulus position.

Interestingly, there is by now neurophysiological evidence for such an erroneous eye position signal (Morris et al., 2012). It has been known for a while that eye position related signals are present in many areas of the brain (Andersen and Mountcastle, 1983; Bremmer, 2000; Bremmer et al., 1997a,b; Galletti and Battaglini, 1989). But only recently Morris et al. were able to decipher the perisaccadic dynamics of such eye position signals (in areas MT, MST, LIP, and VIP of the monkey). They found a striking congruency between the dynamics of the cortical eye position signal and the one postulated by earlier studies (Dassonville et al., 1992; Honda, 1991). This signal, notably obtained from recordings in the monkey, has already been used to reproduce the behavioral mislocalization data of human subjects; it is therefore probably the most convincing account of perisaccadic shift at the moment. It would be even more interesting to see, though, if this signal could be integrated into the modeling approach followed by us. In this case, the observed physiological signal would not only account for perisaccadic shift but also for transsaccadic perceptual stability.

Our model makes use of reafferent information (i.e. the optic flow produced during the saccade) to establish transsaccadic stability. The use of this source has received only few attention in the literature; probably because it is assumed that visual input during saccades is blocked by saccadic suppression. Watson and Krekelberg (2009) could show, however, that even those stimuli that go unnoticed because of saccadic omission are processed by the visual system. In line with this finding, we could show in study 5 that visual perisaccadic stimuli are not generally blocked from visual processing; they can at least reach the processing stage of V4. These results might be taken as motivation to further investigate the role of reafferent input during saccades.

The influence of saccade adaptation on space perception and its neuronal representation

The model presented in study 3 was based on the stability of the external world. In studies 4 and 6 we experimentally manipulated this fact: During the ongoing

eye movement, the saccade target was displaced by a small amount to a different position, consistently and over and over again during many trials (saccade adaptation paradigm). The reaction of the oculomotor system to this paradigm was as predicted by previous studies (e.g. McLaughlin, 1967): Saccade amplitudes gradually adapted and consequently the saccade endpoints approached the displaced target position. In study 4, we tested an aspect of spatial perisaccadic stability in this adaptation paradigm: we interspersed trials in which the performance of human subjects to detect target steps of different directions and amplitudes was assessed by psychophysical measures. The most prominent effect we observed was that psychophysical curves shifted during adaptation according to the change in oculomotor behaviour. The authors of a related study that used a comparable paradigm and found similar results interpreted this behavior as a mislocalization effect (Bahcall and Kowler, 1999). In the discussion of study 4 we pointed out that this conclusion is perfectly valid. However, we also offered a slightly different perspective on the effect, not considering it as a shortcoming of spatial perception but rather emphasizing the underlying functionality that perception adapts according to the changes in oculomotor behavior. We point out that, related to the reasoning in study 3, the results can be explained if the visual system relies on a) the stability of the external world and b) the accuracy of the oculomotor system by assuming that saccades will bring their targets near the fovea. More specific, in this account, spatial congruency in the sense of no perceived displacement between a pre- and a postsaccadic target will be established if the saccade brings the target close to the fovea. In study 3 we discuss in detail, why the two different viewpoints might be based on different neural mechanisms.

In study 6 we investigated the RF structure in V4 during saccade adaptation. On the population level, we could not detect any modulation of the pre- or postsaccadic RFs during adaptation; the RFs were fixed in eye-centered coordinates. This is in line with our interpretation of the behavioral data from study 4; the above mentioned mechanism relies on the postsaccadic target position relative to the fovea. But again, our observation in V4 does not exclude the possibility that at other, later processing stages saccade adaptation might have different effects.

In addition to the shifting psychometric functions during adaptation, we observed a broadening of the psychometric curve (i.e. subjects became more insensitive concerning the detection of target displacements) in the 'non-blank' backward adaptation condition in study 4. This effect might be related to the postsaccadic RF modulation we observed on the neuronal level. In the subpopulation of the recording sites for which the postsaccadic RF fell close to the initial (i.e. the unadapted) position of the saccade target, we observed a slight deformation of the postsaccadic RF against the adaptation step. Although we did not quantify the

size of the postsaccadic RF in this case, the deformation seems to include a broadening of the peak of the RF. An increase in RF size corresponds to a decrease in spatial resolution and might therefore explain the decreased sensitivity to detect target displacements (study 4). It would be interesting to characterize the RFs in areas FEF and LIP during saccade adaptation; we think it is conceivable that the RF deformation we observed in V4 might be mediated via top-down feedback from these areas. Both areas are anatomically connected to V4 (Ungerleider et al., 2008) and are known to exhibit prominent RF remapping, including pre- but also postsaccadic effects (e.g. Duhamel et al., 1992; Umeno and Goldberg, 1997). In the FEF it has been shown that the remapping relies on a signal that represents the vector of the upcoming saccade (Sommer and Wurtz, 2006). This signal, usually called 'corollary discharge', arises in the superior colliculus (SC) (Sommer and Wurtz, 2004). The neural site where saccade adaptation takes place is probably located at or downstream of the SC (Frens and Opstal, 1997; Melis and van Gisbergen, 1996, also cf. section 1.2). Depending on the exact site of adaptation it is therefore possible that RF remapping in the FEF might rely on a signal that represents the vector of the intended (i.e. the unadapted) and not the actual saccade. In this case the RFs would be remapped to their unadapted position. In an eye-centered reference frame, these unadapted positions appear postsaccadically to be displaced against the direction of the adaptation step. A fragment of this effect might be conveyed to V4 via top-down connections. Similar arguments might also hold true for area LIP. Though anatomically not implausible by current knowledge, it has to be noted that this potential mechanism is highly speculative at the moment; it could be tested by a characterization of the RFs during saccade adaptation in areas FEF and LIP. The specific prediction following this argumentation is that in these areas RFs are (partially) remapped to their unadapted positions.

The neuronal basis of saccadic omission

In study 5 we investigated the neural basis of saccadic omission by recording stimulus driven activity during fixation as well as during saccades in area V4 of the monkey. We did not find evidence for saccadic suppression in this area, but we could relate the strong postsaccadic increase in activity that we observed to the activity following stimulation onset. Specifically, we argued that the postsaccadic increase in activity reflected a release from neuronal adaptation caused by the saccade. A potential role of this relationship in visual masking induced by the saccade as well as further implications for perceptual stability during natural vision are discussed in detail in the respective manuscript. Here,

I would like to add one further comment concerning the generality of our results. The LGN is a central structure of the early visual pathway through which the vast majority of the signals that reach the visual cortex are relayed. Due to this prominent anatomical position, detailed knowledge of the response characteristics of this structure are of great interest as they can strongly influence the responses at later processing stages. In study 5 we hypothesized that the postsaccadic increase in LGN activity reported by Reppas et al. (2002), might also reflect a release from neuronal adaptation; the applied stimulation is likely to have caused neuronal adaptation. This hypothesis seems to be supported by a comparison of the time course of the postsaccadic activity reported by Reppas et al., cf. their figure 2 with the response pattern of LGN neurons following the onset of a static stimulus as observed by McLelland et al. (2009, cf. their figure 3): The signals seem to be largely overlapping. The fact that a the postsaccadic activity observed by Reppas et al. (2002) could indeed reflect a release from neuronal adaptation is intriguing because this study used full-field stimulation and consequently the release from adaptation could not be explained as a consequence of retinal blur caused by the saccade. Instead, it would have to be concluded that saccades can actively release neuronal adaptation.

Closing words

Transsaccadic perceptual stability has fascinated generations of researchers since centuries. Every generation has provided new insights and new ideas. My current impression of the field is that there are quite some promising approaches to solve the problem and that a bigger picture slowly starts to evolve from the many pieces that have been discovered. This thesis has provided some new pieces to the puzzle, and it has also shown that some seemingly established ones might need some refinement. If, at the very end of this thesis, I would have to give advise on how research in the field should proceed, my answer would be that the plasticity of the visual system should be further investigated. I believe that visual perceptual stability during saccades is maintained by adaptive, dynamic mechanisms.

References

Andersen RA, Mountcastle VB (1983) The influence of the angle of gaze upon the excitability of the light-sensitive neurons of the posterior parietal cortex. J Neurosci 3(3):532–548

Bahcall DO, Kowler E (1999) Illusory shifts in visual direction accompany adaptation of saccadic eye movements. Nature 400(6747):864–866

Bremmer F (2000) Eye position effects in macaque area v4. Neuroreport 11(6):1277–1283

Bremmer F, Distler C, Hoffmann KP (1997a) Eye position effects in monkey cortex. ii. pursuit- and fixation-related activity in posterior parietal areas lip and 7a. JNeurophysiol 77:962–977

Bremmer F, Ilg UJ, Thiele A, Distler C, Hoffmann KP (1997b) Eye position effects in monkey cortex. i. visual and pursuit-related activity in extrastriate areas mt and mst. JNeurophysiol 77:944–961

Dassonville P, Schlag J, Schlag-Rey M (1992) Oculomotor localization relies on a damped representation of saccadic eye displacement in human and nonhuman primates. VisNeurosci 9:261–269

Duhamel JR, Colby CL, Goldberg ME (1992) The updating of the representation of visual space in parietal cortex by intended eye movements. Science 255:90–92

Frens MA, Opstal AJV (1997) Monkey superior colliculus activity during short-term saccadic adaptation. Brain Res Bull 43(5):473–483

Galletti C, Battaglini PP (1989) Gaze-dependent visual neurons in area v3a of monkey prestriate cortex. J Neurosci 9(4):1112–1125

Hartmann TS, Bremmer F, Albright TD, Krekelberg B (2011) Receptive field positions in area mt during slow eye movements. J Neurosci 31(29):10,437–10,444

Honda H (1991) The time courses of visual mislocalization and of extraretinal eye position signals at the time of vertical saccades. Vision Res 31:1915–1921

Matin L, Pearce DG (1965) Visual perception of direction for stimuli during voluntary saccadic eye movements. Science 148:1485–1488

McLaughlin S (1967) Parametric adjustment in saccadic eye movements. Percept Psychophys 2:359–362

McLelland D, Ahmed B, Bair W (2009) Responses to static visual images in macaque lateral geniculate nucleus: implications for adaptation, negative afterimages, and visual fading. J Neurosci 29(28):8996–9001

Melis BJ, van Gisbergen JA (1996) Short-term adaptation of electrically induced saccades in monkey superior colliculus. J Neurophysiol 76(3):1744–1758

Morris AP, Kubischik M, Hoffmann KP, Krekelberg B, Bremmer F (2012) Dynamics of eye-position signals in the dorsal visual system. Curr Biol 22(3):173–179

Pola J (2004) Models of the mechanism underlying perceived location of a perisaccadic flash. Vision Res 44:2799–2813

Reppas JB, Usrey WM, Reid RC (2002) Saccadic eye movements modulate visual responses in the lateral geniculate nucleus. Neuron 35:961–974

Ross J, Morrone MC, Burr DC (1997) Compression of visual space before saccades. Nature 386:598–601

Schlack A, Sterbing-D'Angelo SJ, Hartung K, Hoffmann KP, Bremmer F (2005) Multisensory space representations in the macaque ventral intraparietal area. J Neurosci 25(18):4616–4625

Sommer MA, Wurtz RH (2004) What the brain stem tells the frontal cortex. i. oculomotor signals sent from superior colliculus to frontal eye field via mediodorsal thalamus. J Neurophysiol 91(3):1381–1402

Sommer MA, Wurtz RH (2006) Influence of the thalamus on spatial visual processing in frontal cortex. Nature 444(7117):374–377

Umeno MM, Goldberg ME (1997) Spatial processing in the monkey frontal eye field. i. predictive visual responses. JNeurophysiol 78:1373–1383

Ungerleider LG, Galkin TW, Desimone R, Gattass R (2008) Cortical connections of area v4 in the macaque. Cereb Cortex 18(3):477–499

Watson TL, Krekelberg B (2009) The relationship between saccadic suppression and perceptual stability. Curr Biol 19(12):1040–1043

Zirnsak M, Lappe M, Hamker FH (2010) The spatial distribution of receptive field changes in a model of peri-saccadic perception: predictive remapping and shifts towards the saccade target. Vision Res 50(14):1328–1337

Declaration of the author's contribution to the studies

This thesis comprises six studies which have been conducted in collaborative work. For the sake of simplicity I have always referred to this work in the plural throughout this thesis. The contributions of the individual authors are listed below:

Study 1: SK 90%, FB 10%.
SK and FB planned the experiments, SK setup and conducted the experiments, did the data analysis, and wrote the manuscript. FB proofread the manuscript. Part of the data were included in the diploma thesis of SK. During the phd time, the data on the memory guided saccades were collected, all data were reanalyzed, the manuscript was written.

Study 2: TT 65%, SK 25%, TW 5%, FB 5%.
TT and SK planned the experiments, TT and SK setup and conducted the experiments, TT did the data analysis, TT wrote the manuscript, the other authors proofread the manuscript. The study was also part of the dissertation of TT

Study 3: TT 65%, SK 25%, TW 5%, FB 5%.
TT and SK conceptualized the model, TT implemented the model and wrote the manuscript, the other authors proofread the manuscript.

Study 4: SK 90%, FB 10%.
SK and FB planned the experiments, SK setup and conducted the experiments, did the data analysis, and wrote the manuscript. FB proofread the manuscript.

Study 5: SK 75%, MW 15%, TW 5%, FB 5%.
SK and FB planned the experiments, SK and MW setup the experiments, SK conducted them, did the data analysis, and wrote the manuscript. FB proofread the manuscript.

Study 6: SK 75%, MW 15%, TW 5%, FB 5%.
SK and FB planned the experiments, SK and MW setup the experiments, SK conducted them, did the data analysis, and wrote the manuscript. FB proofread the manuscript.

Initials: FB: Prof. Dr. Frank Bremmer, SK: Steffen Klingenhoefer, MW: Markus Wittenberg, TT: Dr. Tobias Teichert, TW: PD Dr. Thomas Wachtler

Erklärung

Ich versichere gemäß §10(c) der Promotionsordnung, dass ich meine Dissertation

    Perceptual stability during saccadic eye movements

selbstständig, ohne unerlaubte Hilfe angefertigt und mich dabei keiner anderen als der von mir ausdrücklich bezeichneten Quellen und Hilfen bedient habe. Ich habe alle vollständig oder sinngemäß übernommenen Zitate als solche gekennzeichnet sowie die Dissertation in der vorliegenden oder einer ähnlichen Form noch bei keiner anderen in- oder ausländischen Hochschule anlässlich eines Promotionsgesuchs oder zu anderen Prüfungszwecken eingereicht.

Marburg, 24.08.2012

                                    (Steffen Klingenhöfer)

Danksagung

An dieser Stelle möchte ich mich herzlich bei all denjenigen bedanken, die auf verschiedenste Art und Weise zu dieser Arbeit beigetragen haben.

Besonderer Dank gilt Frank Bremmer für seine Unterstützung auf verschiedensten Ebenen. Auch dafür, daß er mir Freiheit gelassen hat eigene Gedanken zu verfolgen - auch wenn sie nicht in dieser Art am Ende eines Satzes stehen dürfen ;-)

Ohne meine Kollegen Markus, Tobias und Thomas wäre diese Arbeit in ihrer jetzigen Form nicht möglich gewesen. Gleiches gilt auch für Berti und Mao.

Allen aktuellen und ehemaligen Mitgliedern der AG Neurophysik gilt auch ein herzliches Dankeschön, ganz besonders den fleißigen Korrekturlesern meiner Arbeit, sowie Alexander Platzner und Sigrid Thomas für ihre hervorragende Unterstüzung. Ohne die ausgezeichnete Unterstützung durch die Feinmechanik- und Elektronikwerkstatt des Fachbereichs Physik hätten sich die von mir durchgeführten Experimente nicht umsetzen lassen können.

Vielleicht am wichtigsten zu erwähnen sind meine Freunde und Familie, die mir immer wieder zeigen, dass es auch ein Leben außerhalb der Wissenschaft gibt.